

Cloning and characterisation
of the *HMA3* gene and its promoter from
***Arabidopsis halleri* (L.) O'KANE and AL'SHEHBAZ and**
***Arabidopsis thaliana* (L.) HEYNHOLD**

DISSERTATION

in fulfilment of the requirements
for the academic degree of
doctor rerum naturalis
(Dr. rer. nat.)

submitted to the
Faculty of Mathematics and Natural Sciences
University of Potsdam

by
Toni Hoffmann

Potsdam, March 2007

This work is licensed under the Creative Commons Attribution-Noncommercial-No Derivative Works 2.0 Germany License. To view a copy of this license, visit <http://creativecommons.org/licenses/by-nc-nd/2.0/de/> or send a letter to Creative Commons, 171 Second Street, Suite 300, San Francisco, California, 94105, USA.

Elektronisch veröffentlicht auf dem
Publikationsserver der Universität Potsdam:
<http://opus.kobv.de/ubp/volltexte/2007/1525/>
urn:nbn:de:kobv:517-opus-15259
[<http://nbn-resolving.de/urn:nbn:de:kobv:517-opus-15259>]


The work presented in this thesis was carried out between October 2002 and January 2006 in the Metal Homeostasis group of Dr. habil. Ute Krämer at the Max-Planck-Institute of Molecular Plant Physiology, Potsdam, Germany.

- 1st Examiner Prof. Dr. Bernd Müller-Röber, Institute of Biology and Biochemistry,
University of Potsdam, Potsdam, Germany
- 2nd Examiner Dr. Lorraine E. Williams, School of Biological Sciences, University of
Southampton, Southampton, UK
- 3rd Examiner Dr. Pierre Berthomieu, UMR de Biochimie et Physiologie Moléculaire
des Plantes, Centre National de la Recherche Scientifique, Université
Montpellier 2, France

*“Within walnuts and trees and other plants
vast treasures will be found,
which lie hidden there and well guarded”*

Leonardo da Vinci in 'Prophecies', 1293

Danksagung

ie vorliegende Arbeit entstand am Max-Planck-Institut für Molekulare Pflanzenphysiologie in Potsdam in der Metallhomöostase-Arbeitsgruppe von Dr. Ute Krämer. Dr. Ute Krämer gilt an erster Stelle mein besonderer Dank für die Bereitstellung des interessanten Themas, die geduldige Betreuung, ihre stetige Diskussionsbereitschaft und dafür, dass sie mir die Möglichkeit gab, diese Arbeit zu vollenden.

Weiterhin möchte ich mich bei Prof. Dr. Mark Stitt und Prof. Dr. Bernd Müller-Röber dafür bedanken, dass sie als Betreuer und Gutachter meiner Doktorarbeit zur Verfügung standen und mir viele hilfreiche Ratschläge gaben. Weiterhin bedanke ich mich bei Dr. Lorraine E. Williams und Dr. Pierre Berthomieu für die externe Begutachtung meiner Arbeit.

Für die ausgesprochen freundliche und gute Arbeitsatmosphäre, für die Hilfsbereitschaft bei fachlichen und praktischen Fragen möchte ich mich bei allen ehemaligen und derzeitigen Mitgliedern der Arbeitsgruppe von Dr. Ute Krämer bedanken. Im Speziellen danke ich Toralf Senger, Marc Hanikenne, Ina Talke und Len Krall für viele anregende Diskussionen zu den verschiedensten Themen sowie Katrin Voigt und Stéphanie Arrivault für ihren erfrischenden Humor.

Ebenso danke ich allen Mitarbeitern des Max-Planck-Institutes für Molekulare Pflanzenphysiologie für das überaus angenehme familiäre Arbeitsklima und insbesondere dem „Green-Team“ für die gärtnerische Betreuung der Pflanzenexperimente.

Von ganzem Herzen danke ich meinen Eltern, ohne deren uneingeschränkte Unterstützung mein Studium und diese Arbeit nicht möglich gewesen wären. Und schließlich danke ich Claudia, für die verlässliche und liebevolle Person die sie ist sowie ihrer Familie.

Und natürlich auch an alle ungenannten guten Freunde: Dankeschön!

Summary

Being living systems unable to adjust their location to changing environmental conditions, plants display homeostatic networks that have evolved to maintain transition metal levels in a very narrow concentration range in order to avoid either deficiency or toxicity. Hence, plants possess a broad repertoire of mechanisms for the cellular uptake, compartmentation and efflux, as well as for the chelation of transition metal ions.

A small number of plants are hypertolerant to one or a few specific transition metals. Some metal tolerant plants are also able to hyperaccumulate metal ions. The Brassicaceae family member *Arabidopsis halleri* ssp. *halleri* (L.) O'KANE and AL'SHEHBAZ is a hyperaccumulator of zinc (Zn), and it is closely related to the non-hypertolerant and non-hyperaccumulating model plant *Arabidopsis thaliana* (L.) HEYNHOLD. The close relationship renders *A. halleri* a promising emerging model plant for the comparative investigation of the molecular mechanisms behind hypertolerance and hyperaccumulation. Among several potential candidate genes that are probably involved in mediating the zinc-hypertolerant and zinc-hyperaccumulating trait is *AbHMA3*. The *AbHMA3* gene is highly similar to *AtHMA3* (AGI number: At4g30120) in *A. thaliana*, and its encoded protein belongs to the P-type IB ATPase family of integral membrane transporter proteins that transport transition metals. In contrast to the low *AtHMA3* transcript levels in *A. thaliana*, the gene was found to be constitutively highly expressed across different Zn treatments in *A. halleri*, especially in shoots.

In this study, the cloning and characterisation of the *HMA3* gene and its promoter from *Arabidopsis halleri* (L.) O'KANE and AL'SHEHBAZ and *Arabidopsis thaliana* (L.) HEYNHOLD is described. Heterologously expressed *AbHMA3* mediated enhanced tolerance to Zn and to a much lesser degree to cadmium (Cd) but not to cobalt (Co) in metal-sensitive mutant strains of budding yeast. It is demonstrated that the genome of *A. halleri* contains at least four copies of *AbHMA3*, *AbHMA3-1* to *AbHMA3-4*. A copy-specific real-time RT-PCR indicated that an *AbHMA3-1* related gene copy is the source of the constitutively high transcript level in *A. halleri* and not a gene copy similar to *AbHMA3-2* or *AbHMA3-4*.

In accordance with the enhanced *AtHMA3* mRNA transcript level in *A. thaliana* roots, an *AtHMA3 promoter-GUS* gene construct mediated GUS activity predominantly in the vascular tissues of roots and not in shoots. However, the observed *AbHMA3-1* and *AbHMA3-2* promoter-mediated GUS activity in *A. thaliana* or *A. halleri* plants did not reflect the constitutively high expression of *AbHMA3* in shoots of *A. halleri*. It is suggested that other factors e.g. characteristic sequence inserts within the first intron of *AbHMA3-1* might enable a constitutively high expression. Moreover, the unknown promoter of the *AbHMA3-3* gene copy could be the source of the constitutively high *AbHMA3* transcript levels in *A. halleri*. In that case, the *AbHMA3-3* sequence is predicted to be highly homologous to *AbHMA3-1*.

The lack of solid localisation data for the *AbHMA3* protein prevents a clear functional assignment. The provided data suggest several possible functions of the *AbHMA3* protein: Like *AtHMA2* and *AtHMA4* it might be localised to the plasma membrane and could contribute to the efficient translocation of Zn from root to shoot and/or to the cell-to-cell distribution of Zn in the shoot. If localised to the vacuolar membrane, then a role in maintaining a low cytoplasmic zinc concentration by vacuolar zinc sequestration is possible. In addition, *AbHMA3* might be involved in the delivery of zinc ions to trichomes and mesophyll leaf cells that are major zinc storage sites in *A. halleri*.

Zusammenfassung

Pflanzen sind lebende Systeme, die nicht in der Lage sind ihren Standort sich ändernden Umweltbedingungen anzupassen. Infolgedessen weisen Pflanzen homöostatische Netzwerke auf, welche die Mengen an intrazellulären Übergangsmetallen in einem sehr engen Konzentrationsbereich kontrollieren um somit Vergiftungs- oder Mangelerscheinungen zu vermeiden. Pflanzen besitzen daher ein breites Spektrum an Mechanismen für die zelluläre Aufnahme, die Kompartimentierung und die Abgabe sowie für die Chelatisierung von Übergangsmetallionen.

Eine kleine Anzahl von Pflanzen ist hypertolerant gegenüber einem oder mehreren Übergangsmetallen. Einige wenige dieser metalltoleranten Pflanzen sind fähig Übergangsmetalle in beträchtlichen Mengen zu speichern, sprich zu hyperakkumulieren, ohne Vergiftungserscheinungen zu zeigen. Die hallersche Schaumkresse (*Arabidopsis halleri* ssp. *halleri* (L.) O'KANE und AL'SHEHBAZ) aus der Familie der Kreuzblütler (Brassicaceae) ist ein solcher Hyperakkumulator für Zink (Zn). Sie ist sehr nah verwandt mit der Modellpflanze Ackerschmalwand (*Arabidopsis thaliana* (L.) HEYNHOLD), die jedoch nicht-hypertolerant und nicht-hyperakkumulierend für Übergangsmetalle ist. Diese nahe Verwandtschaft macht *A. halleri* zu einer vielversprechende Modellpflanze für vergleichende Studien der molekularen Mechanismen, die Hypertoleranz und Hyperakkumulation zu Grunde liegen. Mehrere Kandidatengene wurden gefunden, die möglicherweise von Bedeutung für die Zink-hypertoleranten and -hyperakkumulierenden Eigenschaften von *A. halleri* sind. Zu diesen Kandidatengen gehört *AbHMA3*, ein Gen mit großer Ähnlichkeit zu *AtHMA3* (AGI number: At4g30120) aus *A. thaliana*. Es kodiert ein Protein aus der Familie transmembraner Übergangsmetall-Transportproteine, den P-type IB ATPasen. Im Gegensatz zu den niedrigen *AtHMA3* Transkriptmengen in *A. thaliana* wird das *AbHMA3* Gen in *A. halleri* in Gegenwart verschiedener Zn Konzentrationen konstitutiv hoch exprimiert, insbesondere im Spross der Pflanze.

Diese Arbeit beschreibt die Klonierung und Charakterisierung des *HMA3* Gens und seines Promoters aus *A. halleri* und *A. thaliana*. Es wurde gezeigt, dass heterolog exprimiertes *AbHMA3* Protein in metallsensitiven Hefestämmen eine erhöhte Toleranz gegenüber Zink und zu einem geringen Grad gegenüber Kadmium (Cd) jedoch nicht gegenüber Kobalt (Co) vermittelt. Weiterhin wurden im Genom von *A. halleri* mindestens vier *AbHMA3* Genkopien, *AbHMA3-1* bis *AbHMA3-4*, nachgewiesen.

Eine Genkopie-spezifische Echtzeit-RT-PCR (*real-time* RT-PCR) deutete darauf hin, dass eine *AbHMA3-1* und nicht eine *AbHMA3-2* ähnliche Genkopie die Quelle der konstitutiv hohen Transkriptmengen in *A. halleri* ist. Die *AbHMA3-4* Genkopie wurde mittels eines *AbHMA3-2* spezifischen Primerpaares auf zwei BAC Klonen nachgewiesen und wird daher vermutlich ebenfalls nicht hoch exprimiert.

In Übereinstimmung mit erhöhten mRNS Transkriptmengen in Wurzeln von *A. thaliana*, vermittelte ein *AtHMA3* Promoter-GUS (β -Glucuronidase) Genkonstrukt GUS-Aktivität hauptsächlich in

den Leitgeweben der Wurzeln jedoch nicht des Sprosses. Die vermittelte GUS-Aktivität durch Promoterfragmente von *AbHMA3-1* und *AbHMA3-2* in *A. thaliana* oder *A. halleri* Pflanzen spiegelte nicht die konstitutiv hohe *AbHMA3* Expression im Spross von *A. halleri* wieder. Es wird vermutet, dass andere Faktoren die konstitutiv hohe Expression ermöglichen wie zum Beispiel die gefundenen kopiespezifischen Sequenzinsertionen innerhalb des ersten *AbHMA3-1* Introns. Weiterhin ist es denkbar, dass der unbekannte Promoter der *AbHMA3-3* Genkopie die Quelle der konstitutiv hohen *AbHMA3* Transkriptmengen ist. In diesem Fall wird eine sehr hohe Ähnlichkeit zwischen den Sequenzen von *AbHMA3-3* und der *AbHMA3-1* vorhergesagt.

Der Mangel deutlicher Ergebnisse zur intrazellulären Lokalisierung des *AbHMA3* Proteins verhindert eine exakte Einordnung seiner Funktion. Die ermittelten Ergebnisse schlagen mehrere mögliche Funktionen für *AbHMA3* vor: Ähnlich *AtHMA2* und *AtHMA4* könnte *AbHMA3* in der Plasmamembran der Zelle sitzen und dort zur effizienten Translokation von Zink aus der Wurzel in den Spross und/oder zur Zell-zu-Zell Verteilung von Zn im Spross beitragen. Falls *AbHMA3* in der Membran der Vakuole sitzt, könnte es eine Rolle bei der Aufrechterhaltung niedriger zytoplasmatischer Zinkkonzentrationen durch vakuoläre Zinksequestrierung spielen. Zusätzlich ist es denkbar, dass *AbHMA3* an der Abgabe von Zinkionen an Trichome und Blattmesophyllzellen beteiligt ist, die die Haupteinlagerungsorte für Zink in *A. halleri* darstellen.

Contents

Contents	I
List of Figures	VII
List of Tables	VIII
Acronyms	IX
I Introduction	1
1 Introduction	2
1 Where do metals come from?	2
2 What is the role of metals in life? Past and Present.	3
3 What is the role of zinc in biology?	4
4 What is known on the metal homeostasis in plants?	6
4.1 Zinc/Transition metal hyperaccumulating plants	6
5 What are the components of metal homeostasis in plants?	9
5.1 Metal chelation	9
5.1.1 Phytochelatins	10
5.1.2 Metallothioneins	10
5.1.3 Organic and amino acids	10
5.1.4 Metallochaperones	11
5.2 Protein families involved in zinc transport	12
5.2.1 ZIP family: ZRT-, IRT-like proteins	12
5.2.2 CDF - cation diffusion facilitators	13
5.2.3 NRAMPs	13
5.2.4 ABC transporters	14
5.2.5 P-type ATPases	15
6 What are P-type ATPases?	15
6.1 P-type I ATPases - K^+ , transition metal pumps	17
6.1.1 The Menkes disease	17
6.1.2 The Wilson disease	18
6.2 P-type II ATPases - Ca^{2+} , Na^+/K^+ and H^+ -ATPases	18
6.3 P-type III ATPases - H^+ and Mg^{2+} pumps	18
6.4 P-type IV ATPases - aminophospholipid ATPases	19
6.5 P-type V ATPases	19
7 What are metal transporting P-type IB ATPases in plants?	19
7.1 The Cu/Ag cluster of P-type IB ATPases in plants	21

7.1.1	HMA6 and HMA8	21
7.1.2	HMA7	22
7.1.3	HMA5	23
7.2	The Zn/Cd/Co/Pb cluster of P-type IB ATPases in plants	23
7.2.1	HMA4 and HMA2	23
7.2.2	HMA3	24
7.2.3	HMA1	24
7.3	Mechanisms of regulation of P-type IB ATPases	25
7.3.1	Mechanisms of metal-dependent regulation in plants	26
2	Motivation and aims of the thesis	27
1	<i>HMA3</i> , a gene possibly involved in metal homeostasis in <i>Arabidopsis halleri</i> (<i>A. halleri</i>)	27
2	Motivation and aim of the thesis	28
II	Materials and Methods	29
3	Materials and Methods	30
1	Standard molecular biology techniques	30
2	Plasmids	30
2.1	<i>E. coli</i> expression vectors	30
2.1.1	pASK-IBA3 (<i>ptetA-cDNA:Strep-Tag</i>)	30
2.2	Yeast expression vectors	31
2.2.1	pFL61GW (<i>pPGK1-cDNA</i>)	31
2.3	Plant expression vectors	31
2.3.1	pBI101, pBI101.2, and pBI101.3 (<i>promoter:GUS</i>)	31
2.3.2	pMDC83 (<i>p35S-cDNA:GFP6</i>)	31
2.3.3	pBKSGWGUS (<i>promoter:GUS</i>)	32
2.3.4	pB735SGW (<i>p35S-cDNA</i>)	32
2.3.5	pK7GWIWG2(I) (<i>p35S-cDNA:itron:VNCI²</i>)	32
3	Culture conditions	33
3.1	Media and Supplements	33
3.1.1	Luria-Bertani media for <i>E. coli</i> cultivation	33
3.1.2	YEB media for <i>A. tumefaciens</i> cultivation	33
3.1.3	Media for yeast and plant cultivation	33
3.1.4	Transition metal salts	33
3.1.5	Antibiotics	33
3.1.6	Additional Supplements	33

4	Techniques related to DNA	34
4.1	Gateway® technology and PCR	34
4.1.1	Gateway® technology	34
4.1.2	Polymerase chain reaction (PCR)	37
4.1.3	Inverse PCR	39
4.1.4	Real-time RT-PCR	40
4.2	Detection of nucleic acids via hybridisation	42
4.2.1	Preparation of radioactive probes	42
4.2.2	DNA:DNA-Hybridisation (according to Southern, 1975)	42
5	Techniques related to proteins	44
5.1	Protein extractions and quantification	44
5.1.1	Total protein extraction from yeast cultures for SDS PAGE	44
5.1.2	Total protein extraction from plants for SDS PAGE	44
5.1.3	Denaturing-gel electrophoresis and Western Blotting	44
5.2	Protein expression and -purification with <i>Strep-Tag® II</i> -System	45
5.2.1	Cell growth, induction of expression and cell harvest	45
5.2.2	Breaking of cells and obtaining raw extract by ultrasonification	45
5.2.3	Affinity purification by <i>StrepTactin®</i> sepharose	46
6	Enzyme assays	46
6.1	Analysis of β -glucuronidase activity	46
6.1.1	Histochemical staining	46
6.1.2	Fluorometric GUS activity assay	47
7	Yeast experiments	47
7.1	Yeast strains	47
7.2	Transformation of <i>Saccharomyces cerevisiae</i>	47
7.2.1	Preparation of competent frozen yeast cells	47
7.2.2	Transformation and selection of yeast	48
7.3	Complementation assays	48
7.3.1	Drop test experiment	48
7.3.2	Liquid culture experiment	49
7.4	Metal ion accumulation assays	49
8	Techniques related to plants	49
8.1	Plant material and plant transformation	49
8.1.1	Transient expression in <i>Arabidopsis</i> suspension culture cells	50
8.1.2	Stable transformation of <i>Arabidopsis thaliana</i>	51
8.1.3	Stable transformation of <i>Arabidopsis halleri</i>	51
8.2	Growth conditions	53

8.2.1	Plant growth on soil	53
8.2.2	Plant growth on plates	53
8.2.3	Hydroponical plant growth	54
8.3	Analysis of transgenic plants	55
8.3.1	GFP analysis by confocal microscopy	55
8.3.2	Characterisation of homozygous transgenic lines	55
8.3.3	Metal tolerance assays	55
III Results		57
4 Characterisation of <i>HMA3</i> and the encoded protein		58
1	Genomic organisation, function and localisation	58
1.1	Characterisation of <i>HMA3</i> at the genomic and mRNA level	58
1.1.1	Copy Number of <i>AbHMA3</i>	58
1.1.2	Analysis of a BAC library	59
1.1.3	Sequence analysis and Exon-intron-structure of <i>HMA3</i>	61
1.1.4	Polymorphism in <i>AtHMA3</i> among <i>A. thaliana</i> ecotypes	66
1.1.5	Analysis of 5' and 3' untranslated regions of <i>AbHMA3</i>	67
1.1.6	Reevaluation of copy number and BAC library analysis	72
1.1.7	Summary - Characterisation of <i>HMA3</i> at the genomic and mRNA level	75
1.2	Functional characterisation	76
1.2.1	Functional expression of <i>AbHMA3</i> in yeast mutants	76
1.2.2	Functional expression and purification of <i>AbHMA3</i> in <i>E. coli</i> mutants	79
1.2.3	Functional characterisation of <i>HMA3</i> in <i>A. thaliana</i>	81
1.2.4	Summary - Functional characterisation	84
1.3	Subcellular localisation of <i>HMA3</i> in <i>A. thaliana</i>	85
1.3.1	<i>In silico</i> prediction of subcellular localisation	85
1.3.2	Expression of an <i>AbHMA3</i> :GFP6 fusion protein in <i>A. thaliana</i>	86
1.3.3	Summary - Subcellular localisation	86
2	Analysis of <i>HMA3</i> expression in <i>Arabidopsis</i>	87
2.1	<i>In silico</i> analysis of <i>AtHMA3</i> expression	87
2.1.1	<i>Digital in-situ</i> expression mapping in root tissue	89
2.2	Quantitative real-time RT-PCR	92
2.2.1	Expression analysis of <i>HMA3</i> in different ecotypes	92
2.2.2	Copy-specific expression analysis of <i>AbHMA3</i>	92
2.3	Summary - Analysis of <i>HMA3</i> expression in <i>Arabidopsis</i>	97

5	Cloning and characterisation of <i>HMA3</i> promoter regions	99
1	Cloning and characterisation of the promoter <i>pAbHMA3-1</i> and <i>pAtHMA3</i>	100
1.1	GUS activity under control of <i>pAtHMA3</i> and <i>pAbHMA3-1</i>	100
1.1.1	GUS activity in <i>pHMA3-GUS</i> lines of <i>A. halleri</i>	102
1.2	Regulation of <i>HMA3</i> promoter activity in <i>A. thaliana</i>	102
1.2.1	Quantitative analysis of GUS activity in <i>pHMA3-GUS</i> lines	102
1.2.2	Quantitative analysis of <i>pHMA3-GUS</i> activity in protoplasts	104
2	Cloning and characterisation of a second <i>AbHMA3</i> promoter, <i>pAbHMA3-2</i>	109
2.1	Obtaining additional <i>AbHMA3</i> promoter sequences from a BAC library	109
2.1.1	Inverse PCR	109
2.2	GUS activity of the second <i>AbHMA3</i> promoter, <i>pAbHMA3-2</i>	110
2.2.1	GUS activity after exposure to CuSO_4	111
2.2.2	GUS activity in <i>pAbHMA3-2-GUS</i> lines of <i>A. halleri</i>	112
2.3	Quantitative analysis of GUS activity in protoplasts	112
3	Summary - Cloning and characterisation of <i>HMA3</i> promoter regions	114
IV	Discussion	117
6	Discussion	118
1	Basic characteristics of metal homeostasis, hypertolerance and - accumulation	118
2	What is the role of <i>HMA3</i> and its encoded protein in hypertolerance and -accumulation in <i>A. halleri</i> ?	119
2.1	<i>HMA3</i> mediates enhanced Zn(Cd) tolerance in metal-sensitive yeast mutant strains	119
2.1.1	Model of Zn detoxification by <i>AbHMA3</i> and its regulation	120
2.2	The role of <i>HMA3</i> in metal homeostasis of <i>A. thaliana</i> and <i>A. halleri</i>	123
2.2.1	Functional redundancy of <i>HMA2</i> , <i>HMA4</i> and <i>HMA3</i> in <i>A. thaliana</i>	123
2.2.2	The role of <i>HMA3</i> in <i>A. halleri</i>	126
2.2.3	Potential functions of <i>HMA3</i> in metal homeostasis	132
2.3	Conclusions and summary	135
V	Bibliography and indices	i
	Bibliography	ii
VI	Appendices	A
A	Supplementary data	B

A.1	2D topology model of <i>AbHMA3</i>	B
A.2	Sequence alignment of 23 P-type IB ATPases	C
A.3	Sequence alignment of <i>HMA3</i> cDNA sequences	I
B	Eidesstattliche Erklärung	O
C	Curriculum Vitæ	Q

List of Figures

1	RNA code wheel	XIV
1.1	Phylogenetic relationships among different Brassicaceae species and <i>Populus</i>	9
1.2	The Post-Albers-Cycle	16
1.3	Phylogenetic tree of the P-type ATPase superfamily	17
1.4	Topology model of P-type IB ATPases	21
1.5	Phylogenetic tree of the P-type IB ATPase family	22
2.1	Comparison of <i>HMA3</i> expression level in <i>A. halleri</i> and <i>A. thaliana</i>	28
3.1	Principles of Gateway [®] technology	36
3.2	Schematic of the inverse PCR procedure	40
3.3	Capillary transfer	43
4.1	Southern blot analysis. Determination of <i>HMA3</i> copy number	59
4.2	PCR analysis of BAC DNA from <i>A. halleri</i>	61
4.3	Southern blot analysis of BAC clones	62
4.4	Analysis of genomic <i>HMA3</i> sequences	65
4.5	Single base pair deletion in <i>AtHMA3</i> of the accession Columbia	66
4.6	Alignment of 5'-RACE products	67
4.7	Alignment of 3'-RACE products	68
4.8	Single-nucleotide profile of the 3'-UTR	71
4.9	Alignment fingerprint and restriction sites of genomic <i>HMA3</i> and related promoter sequences	74
4.10	Heterologous expression of <i>AbHMA3</i> cDNA in yeast mutant strains	78
4.11	Zinc accumulation in yeast cells	79
4.12	Immunoblot analysis of epitope-tagged, heterologously expressed <i>AbHMA3</i> protein in the <i>Saccharomyces cerevisiae</i> (<i>S. cerevisiae</i>) mutant strain $\Delta zrc1 \Delta cot1$	80
4.13	Root elongation in a <i>HMA3</i> knockout line and wildtype plants	82
4.14	Root elongation in <i>HMA3</i> overexpressing lines and wildtype plants	83
4.15	Expression pattern of <i>AtHMA3</i> determined by GeneAtlas (Genevestigator Database)	88
4.16	Comparison of expression patterns of <i>HMA1</i> to <i>HMA7</i> determined by GeneAtlas (Genevestigator Database)	89
4.17	<i>A digital in-situ</i>	91
4.18	Expression analysis of <i>HMA1</i> to <i>HMA4</i> in different accessions of <i>Arabidopsis</i>	93
4.19	Copy-specific expression analysis of <i>AbHMA3</i>	96

5.1	Schematic comparison of <i>HMA3</i> promoter regions from <i>A. halleri</i> and <i>A. thaliana</i> . . .	101
5.2	Histochemical detection of GUS activity in seedlings	105
5.3	GUS activity in roots of <i>pAtHMA3-GUS</i> and <i>pAbHMA3-1-GUS</i> lines	106
5.4	GUS activity under control and zinc extrasupply conditions	107
5.5	GUS activity under control and zinc/iron extrasupply conditions	108
5.6	Schematic comparison of <i>AbHMA3</i> promoter regions from <i>A. halleri</i>	110
5.7	Histochemical detection of GUS activity in Arabidopsis seedlings	111
5.8	GUS activity in <i>A. thaliana</i> protoplasts transiently transformed with reporter constructs containing various <i>HMA3</i> promoter fragments	113
1	2D topology model of <i>AbHMA3</i>	B
2	Alignment of 23 P-type IB ATPases	H
3	Alignment of cDNA nucleotide sequences	M
4	Variant-specific features of genomic <i>HMA3</i> sequences	N

List of Tables

1.1	Selected zinc enzymes	5
1.2	Examples of metal hyperaccumulating plants	7
3.1	Stock solutions and final concentrations of applied antibiotics	34
3.2	Stock solutions and final concentrations of additional supplements	34
3.3	Applied primers	37
3.4	Yeast strains	48
3.5	Zinc contents in various agars	54
4.1	Confirmed <i>HMA3</i> positive clones and assigned numbers	60
4.2	Comparison of exon and intron regions of <i>HMA3</i>	64
4.3	Observed and predicted sizes of <i>AbHMA3</i> specific restriction fragments in genomic DNA	73
4.4	Observed and predicted sizes of <i>AbHMA3</i> specific restriction fragments in BAC DNA	73
4.5	Summary of the characterisation of <i>AbHMA3</i> at the genomic and mRNA level	75
4.6	<i>In silico</i> prediction of subcellular localisation of <i>AtHMA3/AbHMA3</i>	85

Acronyms

2,4-D	2,4-dichlorophenoxy acetic acid
3xHA	triple hemagglutinin epitope tag
4-MU	4-methylumbelliferone
4-MUG	4-methylumbelliferyl β -D-glucuronide
aa	amino acid
ABC	ATP-binding-cassette
AGI	Arabidopsis gene identifier
AHT	anhydrotetracycline
AMOZ	Arabidopsis medium “ <i>ohne Zucker</i> ” (sugar free)
BA	6-benzyladenine
BAC	bacterial artificial chromosome
BAP	6-benzylaminopurine
bHLH	basic helix-loop-helix
C	carbon
C-	carboxy
CaMV	cauliflower mosaic virus
CDF	cation diffusion facilitator
Cys	cysteine
DMSO	dimethyl sulfoxide
DNA	deoxyribonucleic acid
d.w.	dry weight
ECL	enhanced chemiluminescence
e. g.	<i>exempli gratia</i> (Latin = for example)

ER	endoplasmic reticulum
<i>et al.</i>	<i>et alii</i> (Latin = and others)
<i>etc.</i>	<i>et cetera</i> (Latin = and so on)
GABI-Kat	<i>Genomanalyse im biologischen System Pflanze - Kölner Arabidopsis T-DNA</i> lines
GFP	green fluorescent protein
GUS	β -glucuronidase
Gyr	giga year = 10^9 years
H	hydrogen
H⁺	proton
HBED	N,N'-di-(2-hydroxybenzoyl)-ethylenediamine-N,N'-diacetate
He	helium
His	histidine
HMA	heavy metal associated
IAA	indolyl-3-acetic acid
ICP-OES	inductively coupled plasma optical emission spectroscopy
i. e.	<i>id est</i> (Latin = that is to say)
IRT	iron regulated transporter
K	Kelvin
kDa	kilodalton
MAP	mitogen-activated protein
MPI-MP	Max-Planck-Institute for Molecular Plant Physiology
MPSS	massively parallel signature sequencing
MSH	membrane spanning helix
MT	metallothionein
MTP	metal transporting protein

Myr	Mega year = 10 ⁶ years
N-	amino
NA	nicotianamine
NAA	α -naphthaleneacetic acid
NAS	nicotianamine synthase
NASC	Nottingham Arabidopsis Stock Center
NOS	nopaline synthase
NRAMP	natural resistance associated macrophage protein
PC	phytochelatin
PCR	polymerase chain reaction
PPT	DL-phosphinotricin
PS	phytosiderophore
QTL	quantitative trait loci
RACE	rapid amplification of cDNA ends
RT	room temperature
SR	sarcoplasmic reticulum
TIGR	The Institute for Genomic Research
TMD	transmembrane domain
UV	ultraviolet
X-Gluc	5-bromo-4-chloro-3-indolyl- β -D-glucuronide
ZIP	ZRT-, IRT-like protein
ZRT	zinc regulated transporter

species names

A. eutrophus	<i>Alcaligenes eutrophus</i> , renamed in <i>R. metallidurans</i> , later in <i>C. metalliurans</i>
A. halleri	<i>Arabidopsis halleri</i>
A. lesbiacum	<i>Alyssum lesbiacum</i>
A. lyrata	<i>Arabidopsis lyrata</i>
A. thaliana	<i>Arabidopsis thaliana</i> (thale cress)
A. tumefaciens	<i>Agrobacterium tumefaciens</i>
B. napus	<i>Brassica napus</i> (rape)
C. elegans	<i>Caenorhabditis elegans</i>
C. merolae	<i>Cyanidioschyzon merolae</i>
C. metallidurans	<i>Cupriavidus metallidurans</i> , formerly known as <i>R. metallidurans</i> or <i>A. eutrophus</i>
C. reinhardtii	<i>Chlamydomonas reinhardtii</i>
E. coli	<i>Escherichia coli</i>
G. max	<i>Glycine max</i> (soybean)
H. sapiens	<i>Homo sapiens</i> (modern human)
H. vulgare	<i>Hordeum vulgare</i> (barley)
M. trunculata	<i>Medicago trunculata</i> (barrel medic)
M. jannaschii	<i>Methanococcus jannaschii</i>
N. tabacum	<i>Nicotiana tabacum</i> (common tobacco)
O. sativa	<i>Oryza sativa</i> (rice)
R. metallidurans	<i>Ralstonia metallidurans</i> , renamed in <i>C. metallidurans</i>
S. bicolor	<i>Sorghum bicolor</i> (sorghum)
S. cerevisiae	<i>Saccharomyces cerevisiae</i> (yeast)
S. pombe	<i>Schizosaccharomyces pombe</i> (fission yeast)
T. aestivum	<i>Triticum aestivum</i> (common wheat)

T. arvense	<i>Thlaspi arvense</i> (field penny cress)
T. caerulescens	<i>Thlaspi caerulescens</i> (alpine penny cress)
T. goesingense	<i>Thlaspi goesingense</i>
T. weissflogii	<i>Thalassiosira weissflogii</i>
Z. mays	<i>Zea mays</i> (maize)

Part I

Introduction

Chapter 1

Introduction

1 Where do metals come from?

The currently most accepted theory about the beginning of the universe starts with the Big Bang, an extremely hot and dense singular event that erupted approximately 15,000 million years (15 giga years (Gyr)) ago to form all space and matter. During the following period the universe began to rapidly expand and cool. After about 400,000 years this first phase resulted in the formation of electrically neutral hydrogen (H) and helium (He) atoms that condensed from the hot plasma. The abundance of 73% hydrogen and 25% helium that we can observe today throughout the visible universe comes from that condensation period. The remaining 2% of elements heavier than helium were produced later in stars (Weinberg, 1993).

As these clouds of hydrogen and helium were drifting through space they were contracted by their own gravitational forces. This contraction warmed up the clouds. When the temperature reached a few million Kelvin (K), nuclear reactions began. This marked the birth of the first protostars. These protostars were the first factories for more massive elements (CPEP, 2003).

Sun-like stars burn hydrogen into helium for most of their lifetime. When the hydrogen is exhausted, the core contracts and heats up until the fusion of three ^4He into one ^{12}C (carbon) begins. With their relatively low mass, stars like the Sun are unable to sustain higher internal temperatures than 10^8 K. Such temperatures are necessary to allow the fusion of carbon with helium in order to generate oxygen and to release energy. Stars of at least ten solar masses provide the environment to successively fuse low-mass nuclei into higher mass nuclei. At the end of a high mass star's life, atomic nuclei are fused to form the iron-peak metals. Those are all elements with an atomic number of 21 to 30, already including some transition metals¹ like iron, cobalt, nickel, copper and zinc. Once an iron

¹Metals are mainly malleable elements with a high electrical and thermal conductivity and a metallic lustre. About three-fourth of the 92 naturally occurring elements are therefore metals. Heavy metals are often defined as elements with a higher density than 5 g/cm^3 . Both definitions include many elements with no biological relevance. Transition metals are elements with incompletely filled 3d orbitals but entirely filled 4s orbitals that allow different oxidation states, i. e. in iron as Fe^{2+} or Fe^{3+} (Christen, 1988). These properties make them interesting partners for catalytic functions in biochemical reactions. In the periodic table of the elements they are found in subgroup 3 to 12, including all biologically relevant metals.

core is formed, it is no longer possible to release energy through fusion. Thus, the fusion reaction stops. Unable to sustain the necessary internal pressure to resist gravity, the star's core collapses, and the resulting shockwave forms a supernova, the explosion of a star. At this moment, heavier elements are formed through iron-peak elements capturing neutrons. The star explosion disperses the new elements into interstellar space. These clouds of star remains have been ever since the seeds for new generations of stars and their planets like our own Solar System and the Earth (CPEP, 2003).

2 What is the role of metals in life? Past and Present.

The Solar System and the planet Earth began to form approximately 5 to 6 Gyr ago; transition metals inclusive. About 3.8 Gyr ago the temperature of the planet's surface allowed water to stay liquid, and the heavier meteorite bombardments decreased. It appears that life occurred as soon as it was possible (Wald, 1964; Nisbet and Sleep, 2001).

The first living systems on Earth encountered transition metals almost everywhere and had to cope with them in order to replicate successfully. However, it might be possible that the relationship of life and transition metals started the other way round: life could probably not have occurred without transition metals. For instance, one presumed prerequisite step for the development of self-replicating systems was the polymerisation of monomeric organic compounds. This reaction is more likely with the aid of metal catalysis (Nriagu, 2003).

Interestingly, the RNA-world hypothesis postulates that the first replicating systems could have been RNA-like molecules (Gilbert, 1986). Nowadays, some descendent RNA molecules, called ribozymes, still possess enzyme-like activity without any known protein co-factor (Cech *et al.*, 1981; Kruger, 1982; Guerrier-Takada *et al.*, 1983). The structural stability and catalytic competence of the ribozymes depend on certain metal ions (Grosshans and Cech, 1989; Pyle, 1996; Weinstein *et al.*, 1997). For example, a ribozyme of *Tetrahymena thermophyla* needs Mg^{2+} for its catalytic function, but divalent cations like Mn^{2+} and Zn^{2+} may contribute to the stabilization of the tertiary RNA structure (Piccirilli *et al.*, 1993; Pyle, 2002)

A further indication of the importance of transition metals for the evolution of early biochemical reactions and living entities is the abundance of transition metals in housekeeping enzymes as well as in many other proteins (see page 9 and Table 1.1), lipids and cofactors. It has been estimated that probably about a quarter (Horton *et al.*, 2002) to one-third (Finney and O'Halloran, 2003) of all known enzymes require a particular metal ion for function.

Transition metals were not only present in the early days of life, but in certain locations on Earth, life had to face higher concentrations of transition metals in its environment than elsewhere. One such place were hydrothermal systems at mid ocean-ridges where warm, metal-rich and sulphuric water emerged (Nisbet and Sleep, 2001). For example, about 3.2 Gyr old filamentous microfossils in

In this thesis, the term "transition metal" is preferred over "heavy metal".

metal enriched rocks containing for instance Cu, Zn and Pb from precambrian deep-sea hydrothermal vents (*black smokers*) are witnesses of these times (Rasmussen, 2000). It may be possible that the first life forms originated from those hot submarine environments that were more abundant than today.

Today, transition metals are required for life in small amounts (see page 3 and Table 1.1). The quantity and variety of enzymes that depend on transition metals might still reflect at least in part the origin of the first life forms.

For example, essential trace elements especially cobalt, copper, iron, manganese, molybdenum, nickel, and zinc, play a central role as cofactors of enzymes. Superoxide dismutases can contain copper, manganese, iron, or zinc. Copper can also be found in plastocyanin and cytochrome c oxidase. Iron is part of enzymes involved in desoxyribonucleic acid (DNA) and hormone synthesis (e. g. ethylene in plants; Bouzayen *et al.*, 1991), nitrogen fixation and respiration. Cobalt occurs in vitamin B12 (cobalmin), a complex molecule with a cobalt-containing corrin ring synthesised only by bacteria (Porter, 1957; Stabler and Allen, 2004). Nickel is more common in proteins of anaerobic bacteria and archaeobacteria than in higher eukaryotes. In plants, only the enzyme urease from *Canavalia ensiformis* (jack bean) is known to be nickel-dependent (Marschner, 1986). Beside others, manganese is essential for the oxygen evolving complex of photosystem II (Rutherford, 1989; Minagawa and Takahashi, 2004), isocitrate dehydrogenase (citric acid cycle; Yasutake *et al.*, 2003) and glutamate synthetase (Suzuki and Knaff, 2005). Cadmium is not considered as an essential trace element. So far, it only appears to be a cofactor for a carbonic anhydrase expressed under Zn deficiency in the diatom *Thalassiosira weissflogii* (Lane and Morel, 2000; Lane *et al.*, 2005).

Deficiency in the mentioned essential elements often results in the disruption of important metabolic processes because the function of metal dependent enzymes is impaired. An excess of any of these metals can damage the organism. Hence the pressure of selection resulted in the formation of homeostatic networks to tightly control intracellular transition metal quantity and availability (Clemens, 2001).

3 What is the role of zinc in biology?

Zinc plays a prominent role among the essential transition metals. It can act as a cofactor with structural or catalytical function. For a steadily growing number of enzymes, recently more than 300, zinc is indispensable (Coleman, 1998; Eide, 1998). Keilin and Mann (1940) described the first zinc enzyme: a carbonic anhydrase from mammalian erythrocytes. Beside carbonic anhydrases, also alkaline phosphatase, carboxypeptidase, Cu/Zn superoxide dismutases and proteases contain zinc ions in their active sites. Zn can also help to stabilise biological membranes (Chvapil, 1973).

Furthermore, the importance of zinc is underscored by the fact that for example cells of *Escherichia coli* (*E. coli*), that have grown in the presence of about 100 nM Zn^{2+} , contained approximately 2000 times more zinc than the culture medium (Outten and O'Halloran, 2001). Remarkably, inside bacte-

ria, virtually no free zinc ions are present. Therefore, nearly all zinc ions have to be present in bound state.

As a structural component, zinc is important in the formation of the zinc finger, an essential protein domain for the function of many transcription factors. These are regulatory proteins that affect the expression of one or several genes (Takatsuji, 1999, 1998). Beside the zinc finger domains, Zn is also a constituent of zinc cluster, RING finger domains and numerous other similar domains involved in protein-protein or protein-DNA interactions. In the yeast *S. cerevisiae* and the worm *Caenorhabditis elegans* (*C. elegans*), about 2-3% of all encoded proteins contain typical zinc binding domains (Böhm *et al.*, 1997; Clarke and Berg, 1998; Eide, 1998; Fox and Guerinot, 1998). Examples of zinc dependent enzymes and proteins are listed in Table 1.1.

Table 1.1: Selected zinc enzymes.

type of protein/enzyme	function	present in plants?
Hydrolases (use Zn activated H ₂ O as direct nucleophile in hydrolyses or hydrations)		
carbonic anhydrase	CO ₂ + H ₂ O ⇌ HCO ₃ ⁻ + H ⁺ , also esterase & aldehyde hydration activity	yes
alcohol dehydrogenase	NAD ⁺ + C ₂ H ₅ OH ⇌ NADH ⁺ + CH ₃ CHO + H ⁺	yes
Phosphatases		
alkaline phosphatase	nonspecific phosphomonoesterase	yes
phospholipase C (PLC)	phosphodiesterase	yes
endonuclease P1	phosphodi- & monoesterase, yield 3'-hydroxyl & 5'-phosphoryl groups	fungi
Peptidases/Proteases (cleavage of peptide bond at carbonyl residue)		
HEXXH-Z ^a metalloproteases	contain HEXXH motif	pro-/eukaryotes
aminopeptidases		yes
carboxypeptidase G ₂	hydrolyses carboxy-terminal glutamate from folic acid and its analogs	yes
β-lactamase	hydrolyses the amid bond of the β-lactam ring ^b	pseudomonads bacteria
nucleic acid synthesis		
aspartate transcarbamylase	nucleic acid synthesis	yes
reverse transcriptase	DNA synthesis	yes
DNA polymerases	DNA synthesis	yes
RNA polymerases	RNA synthesis	yes
(type I, II & III)		yes
cytoplasmic tRNA synthase	transfer RNA synthesis	yes
zinc as structural component		
Cu/Zn superoxide dismutase	zinc stabilises, copper is the functional cofactor conversion of superoxide radicals to hydrogen peroxides	yes
Zinc finger proteins	transcription factors (binding to promoter sequences)	yes
Zinc cluster proteins	transcription factors	yes
RING ^c finger proteins	transcriptional regulation, targeted proteolysis	yes

^athere are 3 types of HEXXH-Z-metalloproteases, classified by the third (Z) protein ligand that can be glutamic acid(E), a histidine (H) or an yet unknown ligand

^bcause of the resistance of many microorganisms to β-lactam antibiotics

^cThe name derives from the first RING finger sequenced: Really Interesting New Gene 1 (*RING1*)

4 What is known on the metal homeostasis in plants?

Being living systems, plants possess homeostatic networks to maintain metal levels in a very narrow concentration range in order to avoid either deficiency or toxicity. Like other organisms, plants have a broad repertoire of mechanisms for the cellular uptake, compartmentation and efflux, as well as for the chelation of metal ions. Intracellular metal ion concentrations are regulated by modifying the uptake, storage and efflux rates in response to external and internal stimuli (Williams *et al.*, 2000; Clemens, 2001; Cobbett and Goldsbrough, 2002; Clemens *et al.*, 2002b; Meharg, 2005; Krämer and Clemens, 2005).

Usually, plants first come into contact with metals like zinc at the root-soil interphase. Here, the secretion of chelators or organic acids increases the biological availability of the metal ions by molecular binding, chelation, or acidification of the rhizosphere. Subsequently, chelated or hydrated metal ions are taken up and enter the root symplasm by various plasma membrane uptake systems. In parallel, solutes including metal ions also enter the root tissue by the apoplastic pathway that is the continuous system of cell walls and intercellular spaces in plant tissues. However, the apoplastic passage is only accessible until the Casparian strip². Here, at the latest, metal ions have to enter the symplastic pathway. In the cytoplasm of the cell, hydrated metal ions are chelated, and excess metal is sequestered in the vacuole in order to protect the cytoplasm from toxic concentrations. Before the transition metal ions can be transported from the root to the shoot, they have to be exported from the root symplasm into the apoplastic xylem either as hydrated ions, or as chelate-metal complexes. In the leaves, metals are delivered to different leaf cell types by various membrane transporters and moved intercellularly via plasmodesmata or by cellular export and re-uptake. Inside shoot and root cells, the distribution of essential transition metals, called metal trafficking, is done by specific metallochaperones, which deliver metal ions to target proteins or to endomembranous transporters (Kochian, 1993; Fox and Guerinot, 1998; Clemens *et al.*, 2002b). The molecular components of this metal homeostasis network are introduced in Section 5 on page 9.

Research on metal homeostasis in plants has been done primarily in the model organism *Arabidopsis thaliana*³ (Cobbett *et al.*, 2003), in crop plants like *Hordeum vulgare* (Higuchi *et al.*, 1999; Kim *et al.*, 2005), *Oryza sativa* (Takahashi *et al.*, 1999; Koike *et al.*, 2004), *Nicotiana tabacum* (Vögeli-Lange and Wagner, 1990; Arazi *et al.*, 1999), *Zea mays* (von Wiren *et al.*, 1994; Curie *et al.*, 2001), as well as on plant species that are particularly good in storing zinc (see next Section).

4.1 Zinc/Transition metal hyperaccumulating plants

A small number of plants are hypertolerant to one or a few specific transition metals. Some metal tolerant plants are also able to hyperaccumulate metal ions (Baker and Brooks, 1989). According to

²A thin, waxy, impermeable band of suberin- or lignin-like deposition in the radial and transverse walls between adjacent cells of the root endodermis. The Casparian strip blocks the flow of water and other solutes across the apoplast.

³for common English species names look up the *Acronyms* Section on page XII

Baker and Brooks, 1989, hyperaccumulation is defined by metal concentrations higher than 1 mg/g dry weight (d.w.) (0.1%) in any above ground tissue or organ. Manganese and Zinc hyperaccumulating plants are characterised by more than 10 mg/g d.w. (1%) and for Cd and As by more than 0.1 mg/g d.w. (0.01%). There is some evidence to suggest that hyperaccumulation is based on a high uptake rate of the metal ions from the soil into the root system, an efficient translocation from roots to shoots and efficient sequestration/detoxification of transition metals in suitable cells and subcellular compartments of the shoot (Lasat *et al.*, 2000). Presently, about 440 hyperaccumulating plant species in 45 families are described, which are mostly unrelated, including about 350 hyperaccumulators of nickel and 18 of zinc (Baker and Brooks, 1989; Baker *et al.*, 2000). Some examples are listed in Table 1.2.

Table 1.2: Examples of metal hyperaccumulating plants.

metal and species	metal concentration ^a [mg/g d.w.]	cited location
Zn		
<i>Thlaspi caerulescens</i>	27.3 [♣] , < 40 [◇]	Germany, Belgium
<i>Arabidopsis halleri</i>	13.6 [♣] , > 20 [♣]	Germany
	32.0 [‡] , 1.9 - 15.7 [§]	
<i>Nocca eburneosa</i>	10.5 [♣]	Switzerland
<i>Haumaniastrum katangense</i>	19.8 [♣]	Zaire
<i>Viola calaminaria</i>	10.0 [♣]	Germany
Cd		
<i>Thlaspi caerulescens</i>	10 [†] , < 4 [‡]	Belgium, France
<i>Arabidopsis halleri</i>	0.25 [♣] , 2.7 [‡]	France, Germany
Cu		
<i>Haumaniastrum katangense</i>	8.4 [♣]	Zaire
<i>Ipomoea alpina</i>	12.3 [♣] , 10 [◇]	Zaire
Co		
<i>Haumaniastrum robertii</i>	10.2 [♣]	Zaire
<i>Cyanotis longifolia</i>	4.2 [♣]	Zaire
Ni		
<i>Thlaspi goesingense</i>	12.0 [♣]	Austria
<i>Streptanthus polygaloides</i>	14.8 [♣]	Western USA
<i>Alyssum cypricum</i>	23.6 [♣]	Cyprus
<i>Alyssum lesbiacum</i>	23.6 [♣]	Lesvos
<i>Psychotria douarrei</i>	47.5 [♣]	New Caledonia
<i>Sebertia acuminata</i>	17.8 [♣] , 260 ^b	New Caledonia

^athe symbols refer to the citation source: ♣ Baker and Brooks, 1989; ♠ Dahmani-Muller *et al.*, 2000; ◇ Grill and Zenk, 1989; ‡ Küpper *et al.*, 2000; † Lombi *et al.*, 2000; ‡ Jiang *et al.*, 2005; ‡ Zhao *et al.*, 2000; § Bert *et al.*, 2002

^bnickel content in dried latex, the milk-like sap of the tree (Strasburger *et al.*, 1991)

The Brassicaceae family member *Arabidopsis halleri* ssp. *halleri* (L.) O'KANE and AL' SHEHBAZ (O'Kane and Al-Shehbaz, 1997; Al-Shehbaz and O'Kane, 2002), previously known as *Cardaminopsis halleri* (L.) HAYEK, is a hyperaccumulator of Zn (Ernst, 1968; Brooks, 1998; Dahmani-Muller *et al.*,

2000; Sarret *et al.*, 2002). According to Bert *et al.* (2000), *A. halleri* is a perennial, stoloniferous, mainly allogamous species that is pollinated by a broad range of insects. It flowers from April to October. Leaves of hydroponically grown *A. halleri* are able to accumulate about 32 mg Zn g⁻¹ d.w. (3.2%; Zhao *et al.*, 2000). Dahmani-Muller *et al.* (2000) and Bert *et al.* (2002) reported that healthy, field-grown *A. halleri* contain up to 2.2% Zn in shoot dry biomass. Like all other hyperaccumulators, *A. halleri* possesses naturally selected Zn hypertolerance.

Küpper *et al.* (2000) reported that hydroponically cultured *A. halleri* also hyperaccumulate Cd in the shoot tissues when treated with non-toxic Cd concentrations. However, cadmium hyperaccumulation is only described for some *A. halleri* populations in their natural habitat (Dahmani-Muller *et al.*, 2000).

In the field, *A. halleri* belongs to the *Galmei* flora⁴ of central and western Europe (Punz, 1995). Being associated with metal enriched soils, *A. halleri* is used as an indicator of heavy metal contamination (Brooks, 1998).

The model species of plant genetics *Arabidopsis thaliana* (*A. thaliana*) (L.) HEYNHOLD (Heynhold, 1842; Al-Shehbaz and O'Kane, 2002) is neither a hypertolerant nor a hyperaccumulating plant, although it is closely related to *A. halleri* (Figure 1.1). There is a wealth of information and established experimental methods on *A. thaliana*. Furthermore, the complete genomic sequence of *A. thaliana* is available (The Arabidopsis Genome Initiative, 2000). Within known coding regions of the genome, *A. halleri* and *A. thaliana* share an identity of about 93% at the nucleotide level (Becher *et al.*, 2004; see Section 1.1.3 on page 61). The close relationship, but the different behaviour in zinc accumulation and tolerance compared to *A. thaliana* renders *A. halleri* a promising emerging model plant for the comparative investigation of the molecular mechanisms behind hypertolerance and hyperaccumulation.

In 2004, Becher *et al.* and Weber *et al.* published results from cross-species microarray hybridisations on AFFYMETRIX Arabidopsis⁵ GeneChips[®] by which they identified *A. halleri* gene transcripts that are differentially expressed compared to *A. thaliana* after a treatment with various Zn concentrations. Those genes, which were termed candidate genes, may be functionally involved in hypertolerance and hyperaccumulation. Weber *et al.* (2004) found two genes that showed the highest expression in roots. These are the *NAS* gene, encoding nicotianamine (NA) synthase (see page 11) and *ZIP4*, encoding a putative Zn²⁺ uptake system (see page 12). The work of Becher *et al.* (2004) was focused on the expression of genes in shoot tissues. The identified candidate genes encode proteins that are similar to the putative cellular Zn uptake transporter ZIP6 (see page 12), the putative metal

⁴A distinct form of transition metal plant communities occurring on soils that contain elevated levels of zinc minerals ZnCO₃ (rare *Galmei*, smithsonite) and Zn₄(OH)₂Si₂O₇·H₂O (*common Galmei*, hemimorphite (Schröter *et al.*, 1979)). Besides Zn, those soils often contain high levels of Pb and Cd.

⁵The ISPMB (The International Society for Plant Molecular Biology) established that the name *arabidopsis* is vulgar like i. e. tomato or coconut, and thus it should not be written capitalised and in italics. *Arabidopsis* is equivalent with *Arabidopsis thaliana*. However, in accordance to the still common use in scientific publications, 'arabidopsis' will be written capitalised in this document. Italicised *Arabidopsis* encompasses other species of the genus *Arabidopsis*, mainly *A. thaliana* and *A. halleri*.

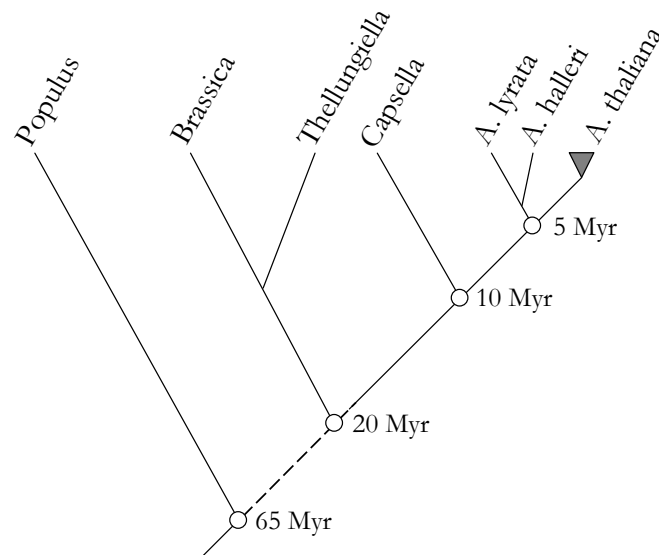


Figure 1.1: Phylogenetic relationships among different Brassicaceae species and *Populus*.

The Figure is taken from Weigel *et al.* (2006) and based on Koch *et al.* (2001) and Yang *et al.* (1999a,b). Approximate divergence times are in millions of years (Myr) before present. The triangle for *A. thaliana* indicates different wild strains that are being resequenced.

pumping P-type ATPase HMA3 (see page 24), the cation diffusion facilitator ZAT/CDF1 (see page 13), and the nicotianamine synthase NAS3 of *A. thaliana*.

5 What are the components of metal homeostasis in plants?

Two mechanisms of metal detoxification are common in all plants. One is the chelation of metal ions by specific high-affinity ligands, the other is the transport of metal ions out of the cytoplasm either into intracellular compartments or the apoplast. Vacuolar detoxification of metals is described in several plant species (Lasat *et al.*, 2000). The sequestration of transition metals into the endoplasmic reticulum (ER) has only been observed for manganese in developing embryos of *A. thaliana* (Otegui *et al.*, 2002). Not in plants but in the yeast *Schizosaccharomyces pombe* (*S. pombe*), Clemens *et al.* (2002a) described a zinc storage in the ER that is mediated by SpZHF1 (Zn homeostasis factor), a member of the CDF protein family (see page 13).

5.1 Metal chelation

Certain peptides, organic acids, and single amino acids can chelate metal ions. In plants, two major classes of metal chelating peptides are known to exist: phytochelatins (PCs) and metallothioneins (MTs).

5.1.1 Phytochelatins

Phytochelatin (PCs) are low molecular peptides that consist of [γ -Glu-Cys]₁₋₁₂-Gly units (Grill *et al.*, 1985). The enzymatic synthesis is catalysed by the PC synthase (Grill *et al.*, 1989; Rauser, 1999; Cobbett and Goldsbrough, 2002). In plants, these peptides form complexes mainly with Cd and Cu through the formation of thiolates with sulfhydryl groups of the cysteines (Cys). In yeast and plants, the PC-metal complexes are sequestered in the vacuole. Yeast and plant knockout mutants of PC synthase show a reduced tolerance to Cd (Howden *et al.*, 1995b; Clemens *et al.*, 1999).

Beside its contribution to the detoxification of Cd through the synthesis of PCs, Vatamaniuk *et al.* (1999) observed that in *A. thaliana*, the PC synthase itself can bind Cd²⁺ ions.

Glutathione Glutathione (GSH), a γ -Glu-Cys-Gly tripeptide, is the substrate of the PC synthase (Cobbett, 2000; Rauser, 1995; Zenk, 1996; Rauser, 1999). Accordingly, it could be shown that *S. pombe* and *A. thaliana* mutants with a deficiency in GSH biosynthesis are PC deficient and more sensitive to Cd (Mutoh and Hayashi, 1988; Howden *et al.*, 1995a).

In *S. cerevisiae* GSH forms a complex with Cd that is sequestered in the vacuole by a specific ABC transporter, YCF1 (Gaedeke *et al.*, 2001; Li *et al.*, 1996). More details can be found in the ABC transporter Section 5.2.4 on page 14.

Like PCs, GSH can bind and detoxify metal ions in plants.

5.1.2 Metallothioneins

In contrast to PCs, metallothioneins (MTs) are not enzymatically synthesised but encoded by a family of genes (Robinson *et al.*, 1993). Normally, these low molecular polypeptides contain two metal binding, cysteine (Cys)-rich domains. Based on the Cys pattern, MTs are grouped in three classes. Class I MTs are common in vertebrates and possess 20 highly conserved Cys residues. Class II MTs, including all plant, fungi, and some nonvertebrate MTs do not possess any strict arrangements of their Cys residues. Although of different origin than MTs, PCs were originally addressed as class III metallothioneins (Cobbett and Goldsbrough, 2002).

Plant MTs possess a high affinity to Cu and the expression is Cu inducible (Murphy *et al.*, 1997; Zhou and Goldsbrough, 1995).

5.1.3 Organic and amino acids

Cellular compounds other than peptides are also able to chelate metals and contribute to a higher metal tolerance. These are organic acid and single amino acids.

Organic acids Organic acids, like citrate, malate, oxalate or acetate were proposed to be involved in metal chelation due to the affinity of metal ions for carboxylic side chains. To date, only for aluminium (Al) tolerance, the formation of extracellular metal complexes with organic acids like citrate or malate

has been shown to play a functional role in plant metal tolerance. For example in *Triticum aestivum* (*T. aestivum*), increased Al tolerance is caused by an Al inducible efflux of malate from root tips (Ryan *et al.*, 1995a,b; Delhaize and Ryan, 1995). Larsen *et al.* (1998) observed an increased efflux of organic acids in roots of Al resistant mutants of *A. thaliana*. However, aluminium is a light metal not a transition metal. Until today, no involvement of organic acids in the chelation of transition metals has been observed.

Amino acids A large pool of free histidine binds Ni^{2+} ions in root and shoot tissue as well as in the xylem sap of *Alyssum lesbiacum* (*A. lesbiacum*), a nickel tolerant Ni hyperaccumulator (Krämer *et al.*, 1996) (Table 1.2). Liao *et al.* (2000) found a correlation between xylem sap concentrations of Cu and histidine (His), suggesting an involvement of His in the chelation of copper ions in the xylem sap of chicory (*Cichorium intybus*) and tomato (*Lycopersicon esculentum*).

Nicotianamine (NA) is a non-proteinaceous amino acid in plants. The synthesis of NA by nicotianamine synthase (NAS) (Higuchi *et al.*, 1999; Takahashi *et al.*, 1999) from three molecules of S-adenosylmethionine is accompanied by the release of three molecules of 50-S-methyl-50-thioadenosine. It can form complexes with various divalent metal ions including Cu, Ni, Co, Zn, Fe, and Mn (Stephan and Scholz, 1993; Stephan *et al.*, 1996).

Becher *et al.* (2004) and Weber *et al.* (2004) showed that NA might be involved in metal hyperaccumulation or hypertolerance in *A. halleri*. Their experiments revealed that the NA synthase is constitutively highly expressed at the transcript level in roots and shoots of *A. halleri* compared to *A. thaliana* under various conditions. Roots of *A. halleri* also show a higher NA synthase protein level associated with higher NA levels than those of *A. thaliana*.

The expression of different NA synthase isoforms complements the Zn hypersensitive phenotype of mutant yeast strains of *S. cerevisiae* and *S. pombe* (Becher *et al.*, 2004; Weber *et al.*, 2004). Wildtype cells of *S. cerevisiae* expressing a NA synthase are Ni resistant through the binding of Ni to NA (Vacchina *et al.*, 2003).

Phytosiderophores In graminaceous plants, NA is the precursor for phytosiderophores (PS), a complex group of plant metal ligands. Graminaceous plants are so called strategy II plants that secrete chelating phytosiderophores to effectively solubilise inorganic Fe(III) by the formation of Fe(III) phytosiderophores. The Fe(III)-PS complexes are taken up on the root plasmalemma by specific transporters (Römheld and Marschner, 1986; Curie and Briat, 2003; Callahan *et al.*, 2006).

5.1.4 Metallochaperones

Metallochaperones are an essential part of the intracellular metal trafficking. Metallochaperones are soluble metal binding proteins that can also contribute to the protection of the cytoplasm from toxic metal concentrations, although their main purpose is to direct a metal to its destination.

In *Saccharomyces cerevisiae* three metallochaperones have been described. Copper is delivered by CCS1 (copper chaperone for superoxide dismutase) into the active site of cytosolic Cu/Zn superoxide dismutase (Hall *et al.*, 2000), by COX17 (cytochrome c oxidase assembly protein) to the mitochondrial cytochrome c oxidase (Glerum *et al.*, 1996) and by ATX1 (antioxidant) to the P-type ATPase CCC2 (cross-complements Ca^{2+} phenotype of the *csg1* yeast mutant), located in a post-Golgi compartment (Lin and Culotta, 1995; Lin *et al.*, 1997). In *A. thaliana*, yeast metallochaperone homologs have been described (Abdel-Ghany *et al.*, 2005a; Balandin and Castresana, 2002; Himelblau *et al.*, 1998). Based on yeast two-hybrid experiments, Andrés-Colás *et al.* (2006) suggest an interaction of AtHMA5, a putative copper pumping P-type ATPase, with an ATX1-like chaperone of *A. thaliana*.

So far, only Cu and Ni metallochaperones have been described, but the existence of yet unidentified chaperones for Zn and Fe is expected (Clemens, 2001; Clemens *et al.*, 2002b).

5.2 Protein families involved in zinc transport

Members of various protein families are involved in metal uptake, metal efflux, or in metal detoxification by transporting metal ions out of the cytoplasm either into the vacuole or the apoplast of plant cells.

5.2.1 ZIP family: ZRT-, IRT-like proteins

The ZRT-, IRT-like protein (ZIP) family was named after its two founding members, ZRT1, a zinc transporter of *S. cerevisiae* and IRT1, an iron transporter of *A. thaliana* (Gaither and Eide, 2001). ZIP related genes are found in a wide range of organisms, including archaea, bacteria, fungi, plants and animals. Members of the ZIP family contain eight putative membrane spanning helices (MSHs) and can mediate the influx of metal ions into the cytoplasm. Some ZIPs are known to efflux metal ions from intracellular compartments into the cytoplasm like the yeast ScZRT3 that mobilises Zn by transporting it out of the vacuole into the cytoplasm (MacDiarmid *et al.*, 2000).

Arabidopsis thaliana possesses fifteen ZIP genes (Mäser *et al.*, 2001). AtZIP1 to AtZIP4 are involved in cellular Zn uptake (Guerinot, 2000; Gaither and Eide, 2001; Hall and Williams, 2003), AtIRT1 and AtIRT2 play a role in iron uptake into the roots (Vert *et al.*, 2001, 2002, 2003). Although AtIRT1 has a high affinity for Fe^{2+} ions it can also transport Mn, Zn, Cd and Co (Eide *et al.*, 1996; Korshunova *et al.*, 1999).

The genes ZIP6 and ZIP9 are among the genes that are constitutively highly expressed in the Zn hyperaccumulator *A. halleri*. It is proposed that ZIP9 mediates an elevated cellular Zn uptake in the roots and ZIP6 in the shoots of *A. halleri* (Becher *et al.*, 2004; Weber *et al.*, 2004).

5.2.2 CDF - cation diffusion facilitators

The cation diffusion facilitator (CDF) family was described first by Nies and Silver (1995). One of the first identified member, CzcD was found in *Cupriavidus metallidurans* strain CH34 (Vandamme and Coenye, 2004) formerly known as *Ralstonia metallidurans* and *Alcaligenes eutrophus*, a gram-negative beta-proteobacterium that encodes a multitude of metal-resistance systems on two large megaplasmids (Anton *et al.*, 1999; Nies *et al.*, 1989). All known CDFs possess six putative MSHs and are common in archaea, bacteria, and eukaryotes where they transport mainly Zn, Cd, and Co (Paulsen and Saier, 1997; Gaither and Eide, 2001; Nies, 2003; Hall and Williams, 2003).

The genome of *A. thaliana* is predicted to encode twelve CDF proteins, named metal tolerance protein *AtMTP1* to *AtMTP12* (Mäser *et al.*, 2001; Delhaize *et al.*, 2003). The CaMV 35S promoter-controlled expression of *AtMTP1*, first described as ZAT (Zn transporter of *A. thaliana*), increased Zn tolerance and root Zn accumulation in *A. thaliana* (van der Zaal *et al.*, 1999). *AtMTP3*, like *AtMTP2* closely related to *AtMTP1*, is probably involved in Zn and Co detoxification in *A. thaliana* (Arrivault, 2005; Arrivault *et al.*, 2006).

A gene that encodes a member of the CDF family, *AhMTP1*, was found to display constitutively high transcript levels in the Zn hyperaccumulator *A. halleri* compared to the non-hyperaccumulator *A. thaliana* (Becher *et al.*, 2004; Dräger *et al.*, 2004). *MTP1*-like transcript levels were also found to be elevated in the Zn hyperaccumulator *Thlaspi caerulescens* (*T. caerulescens*) (Assunção *et al.*, 2001) and the Ni hyperaccumulator *Thlaspi goesingense* (*T. goesingense*) (Persans *et al.*, 2001). The MTP1 proteins are involved in the detoxification of Zn by compartmentalising Zn ions into the vacuole (van der Zaal *et al.*, 1999; Bloss *et al.*, 2002; Dräger *et al.*, 2004; Kobae *et al.*, 2004).

There are five CDF proteins in *S. cerevisiae*. Among these, ZRC1 (zinc resistance conferring; Kamizono *et al.*, 1989) and COT1 (cobalt toxicity; Conklin *et al.*, 1992) efflux Zn (Cd/Co) from the cytoplasm across the vacuolar membrane into the vacuole. The *zrc1 cot1* double mutant is hypersensitive to zinc, and to a much lesser degree, to cobalt (MacDiarmid *et al.*, 2000).

5.2.3 NRAMPs

Another family of metal ion transporters comprises the natural resistance associated macrophage proteins (NRAMPs). Like CDFs, NRAMPs appear to be evolutionarily conserved and are present in prokaryotes and eukaryotes. They contain twelve predicted MSHs. The genome of *A. thaliana* encodes six NRAMP proteins (Mäser *et al.*, 2001). Studies with plant NRAMPs in yeast mutants suggest a role in the transport of divalent cations like Fe^{2+} , Mn^{2+} , Cd^{2+} , and Zn^{2+} (Mäser *et al.*, 2001; Hall and Williams, 2003).

Transgenic *A. thaliana* plants that overexpress the *AtNRAMP3* gene showed a downregulation of the expression of the Fe transporter IRT1 and the ferric chelate reductase FRO2 (ferric reductase oxidase). This suggested an involvement of *AtNRAMP3* in Fe homeostasis. Furthermore, knockout

plants of *AtNRAMP3* accumulated Mn and Zn in the roots. *AtNRAMP3* fused to the green fluorescent protein (GFP), was localised to the vacuolar membrane. Based on these observations, it was proposed that *AtNRAMP3* plays a role in the intracellular remobilisation of vacuolar metal pools and thus, supporting the root-to-shoot translocation of metal ions (Thomine *et al.*, 2003; see also pages 12 and 26). Lanquar *et al.* (2005) showed that the remobilisation of vacuolar Fe stores by *AtNRAMP3* and *AtNRAMP4* plays an essential role in early plant development and is required for seed germination on low iron concentrations.

Weber *et al.* (2004) observed a higher expression level of *AbNRAMP3* in roots of *A. halleri* relative to *A. thaliana* suggesting a possible role in the metal homeostasis of metal hyperaccumulators.

5.2.4 ABC transporters

The superfamily of ATP binding cassette (ABC) transporters is a large and diverse family of membrane proteins. It exists in all three kingdoms of life. Members of the ABC transporter family are known to transport a wide range of substrates like alkaloids, amino acids, antibiotics, lipids, peptides and peptide conjugates, pigments, sugars and sugar conjugates, as well as metal chelates (Higgins, 1992; Martinoia *et al.*, 2002; Holland, 2003; Rea *et al.*, 2003). The transport is driven by the hydrolysis of ATP.

In *S. cerevisiae*, the double mutant YYA4 is Cd-sensitive (Gaedeke *et al.*, 2001; Li *et al.*, 1996). The phenotype of YYA4 is caused by the loss of YCF1, a vacuolar glutathione S-conjugate ABC transporter and the loss of YHL035, a protein that is strongly similar to YCF1 but with an unassigned biological function. The mutant has a reduced ability to detoxify Cd by sequestering Cd-glutathione complexes in the vacuole (Li *et al.*, 1996, 1997).

Up to now, no plant ABC transporter has unequivocally been confirmed to play a role in the transport of metals. However, in *S. pombe*, a member of the half-size ABC transporter subfamily, *SpHMT1* (heavy metal tolerance 1), has been shown to transport phytochelatin-Cd complexes into the vacuole (Ortiz *et al.*, 1992, 1995). It has been suggested that also in plants ABC transporters might mediate the transport of phytochelatin-Cd complexes across the tonoplast (Rea *et al.*, 1998).

Interestingly, among the transcripts that were increased by high Zn in *A. thaliana*, there was an ABC transporter of the multidrug-resistant protein subfamily, *AtMRP2* (Becher *et al.*, 2004). *AtMRP2* localises to the vacuolar membrane and has been shown to transport glutathione and glucuronate conjugates when heterologously expressed in yeast (Liu *et al.*, 2001). Dräger *et al.* (2005) showed that the transcript levels of *AbPDR11* in *A. halleri* are slightly induced after exposure to high metal concentrations. PDRs comprise the pleiotropic drug resistance subfamily and confer resistance to a multitude of toxins and organic acids (Decottignies and Goffeau, 1997; Piper *et al.*, 1998). However, the transport of phytochelatin or glutathione conjugates has not been described for this subfamily.

5.2.5 P-type ATPases

A detailed overview of this superfamily of membrane transport proteins is given below.

6 What are P-type ATPases?

The P-type adenosine triphosphatases (ATPases) are of ancient evolutionary origin and form one of the largest superfamily of integral membrane proteins (Pedersen and Carafoli, 1987). They are found in archaea, prokaryotes and eukaryotes. Substrates of P-type ATPases include K^+ , Na^+ , H^+ , Mg^{2+} , Ca^{2+} , various transition metal cations and aminophospholipids (Axelsen and Palmgren, 1998; Palmgren and Axelsen, 1998; Baxter *et al.*, 2003; Hertogh *et al.*, 2004)

Suggesting that the membrane potential in nerve cells of crabs (*Carcinus maenas*) is generated by a K^+ -stimulated ATPase, Skou (1957)⁶ was the first to describe a member of this family, now known as Na^+/K^+ -ATPase.

The best known members of the P-type ATPase superfamily are the nerve Na^+/K^+ -ATPase (Skou, 1957), the sarcoplasmic Ca^{2+} -ATPase (Hasselbach and Makinose, 1961), and the yeast plasma membrane H^+ -ATPase (Dufour and Goffeau, 1978). The first X-ray structure of a P-type ATPase was obtained for the calcium pump of the sarcoplasmic reticulum (Toyoshima *et al.*, 2000)

The name P-type ATPase refers to the formation of an aspartylphosphate catalytic intermediate during the reaction cycle, called Post-Albers cycle (Post *et al.*, 1972; Albers, 1967) (Figure 1.2). The transport is driven by the hydrolysis of ATP that binds to an ATP binding domain in the protein. With it, the enzyme becomes phosphorylated at an invariant aspartate (D) residue of the highly conserved sequence DKTGT (Solioz and Vulpe, 1996; Axelsen and Palmgren, 1998). The phosphorylation results in a transition from the conformational state E1 into E2 (de Meis and Vianna, 1979). A phosphatase domain dephosphorylates the aspartylphosphate and the enzyme shifts back into the E1 state. The conformational change is accompanied by the translocation of one to three ions across the membrane.

The members of the P-type ATPase superfamily are mostly single catalytic units that differ greatly in length. The smallest known P-type ATPase is 642 aa long (an ATPase from *Synechocystis* PCC6803), and the largest has 1956 amino acids (an ATPase from *Plasmodium falciparum*) resulting in molecular weights between 70 and 215 kilodalton (kDa). This difference is mainly caused by variations in the lengths of the amino (N-) and carboxy (C-) terminal domains. Despite this diversity in length, all P-type ATPases share common features (Figure 1.4 on page 21). They possess six to twelve MSHs. Both, the N-terminal and the C-terminal ends, are on the cytoplasmic side of the membrane. A small cytoplasmic loop and a large cytoplasmic loop, which are separated by two MSHs, form the common conserved core region (Axelsen and Palmgren, 1998). This core region contains eight highly conserved domains, three in the small cytoplasmic loop, one in the second membrane spanning helix (MSH),

⁶In 1997, he was honoured with the Nobel prize for this work

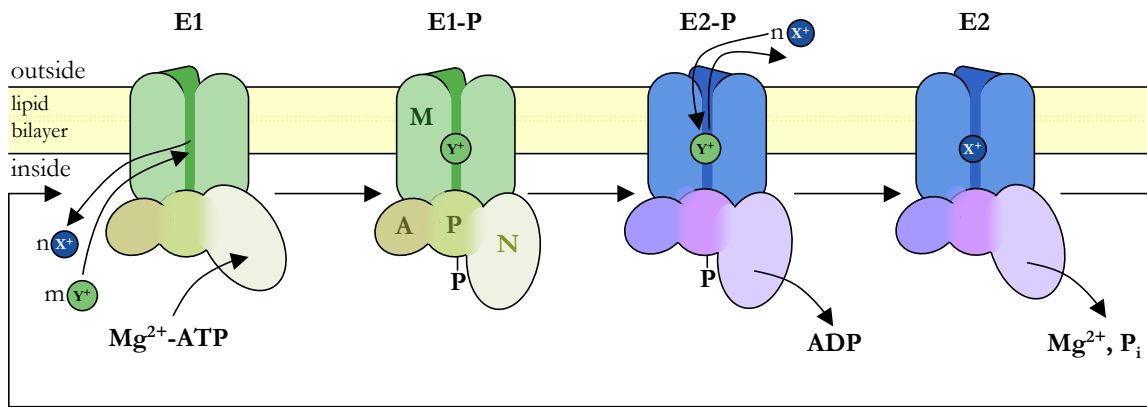


Figure 1.2: The Post-Albers-Cycle.

A general scheme for the reaction cycle of P-type ATPases. Cation Y^+ (green) from the inside of the cell binds to a high affinity site in the ATPase E1 state. The binding initiates the phosphorylation of the protein by Mg^{2+} -ATP that results in the phosphorylated E1-P state. This state is followed by E2-P state with a reduced affinity to cation Y^+ . Thus, the Y^+ ion is released to the outside. X^+ (blue) from the outside is bound. Subsequent hydrolysis of the aspartylphosphate transforms the protein into the E2 state accompanied with the release of X^+ to the inside and the binding of another Y^+ from the inside. Now, the cycle can start again with the phosphorylation of the ATPase E1 state.

The labels n and m stand for natural numbers from 1 to 3, e.g. the sarcoplasmic reticulum calcium ATPase pumps two Ca^{2+} (X^+) ions out of muscle cells into the lumen of the SR per ATP, in exchange for two or three H^+ (Y^+) ions (Kühlbrandt, 2004).

M marks the **m**embrane domain, A the **a**ctuator-, P the **p**hosphorylation- and N the **n**ucleotide binding domain.

and four in the large cytoplasmic loop (Figure 2 in the *Appendix* Section). Together with the N-terminal end, the small cytoplasmic loop is also called actuator domain and might play a role in sensing and regulation of the enzyme activity (Kühlbrandt, 2004). The last MSH, labeled with “VI” in Figure 1.4, before the large cytoplasmic loop contains an invariant proline, probably involved in ion translocation. The nucleotide binding domain is found in the large cytoplasmic loop, which also includes the phosphorylation site motif DKTGT mentioned above (Kühlbrandt, 2004).

The number of different P-type ATPase genes per organism can vary a lot. The genome of some parasitic bacteria encodes only a few P-type ATPases. Free living bacteria possess usually seven to nine P-type ATPases, *S. cerevisiae* contains sixteen and *A. thaliana* remarkably forty-six (Palmgren and Axelsen, 1998). The genomes of only a few organisms are known not to contain any P-type ATPases, for example the parasitic bacterium *Borrelia burgdorferi* (Fraser *et al.*, 1997) or the archaea *Pyrococcus horikoshii* (Axelsen and Palmgren, 2001).

Based on a dataset containing 159 different sequences of P-type ATPases, Axelsen and Palmgren (1998) constructed a phylogenetic tree, showing that the superfamily can be divided into five main branches of monophyletic origin, including a number of minor families (Figure 1.3). These five groups are named I (including IA and IB), II (A, B, C, D), III (A,B), IV and V.

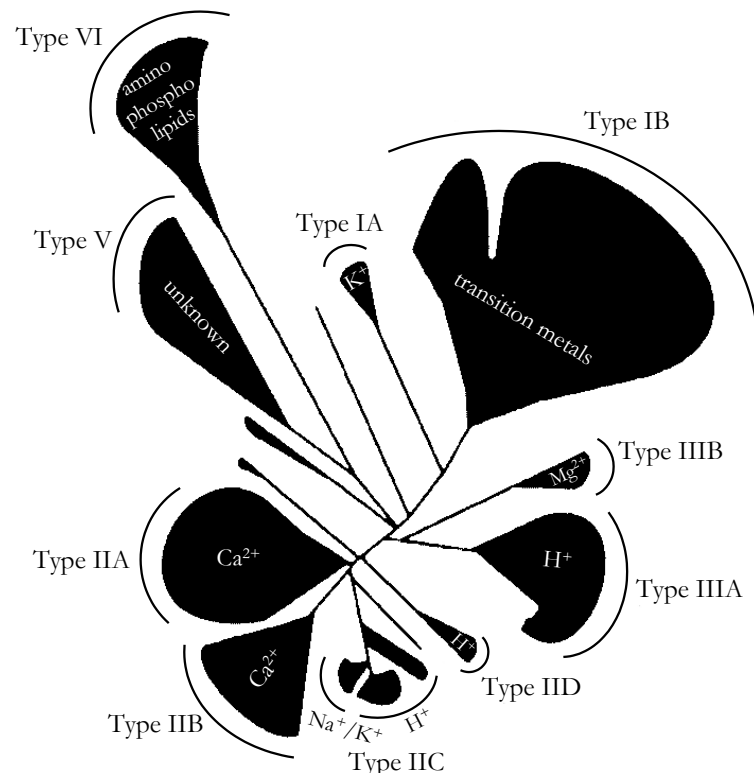


Figure 1.3: Phylogenetic tree of the P-type ATPase superfamily (modified from Axelsen and Palmgren, 1998).

The tree was produced from a dataset containing 159 different sequences of P-type ATPases. Hatched areas indicate major families including known substrate specificities.

6.1 P-type I ATPases - K^+ , transition metal pumps

Only a few bacterial enzymes form a family of their own, called P-type IA ATPases. These primitive and probably ancestral pumps transport K^+ ions, for example the Kdp (K^+ -dependent) complex from *E. coli* (Burrman *et al.*, 1995; Altendorf *et al.*, 1998).

The majority of enzymes in this main branch belongs to the IB family of P-type ATPases that transport transition metals. This family will be discussed with a focus on plant members in Section 7 on page 19.

Two inherited human disorders are caused by mutated forms of IB P-type ATPases. The Menkes and Wilson diseases in *Homo sapiens* are caused by the disruption of copper homeostasis.

6.1.1 The Menkes disease

In Menkes disease patients, the gene *ATP7A*, encoding a copper transporting P-type IB ATPase, is mutated. It is expressed in most tissues except in liver (Vulpe *et al.*, 1993; Chelly *et al.*, 1993; Davies, 1993). The X chromosome linked disease results in a defective intestinal copper transport accompanied by an ineffective mobilisation of the little copper that is absorbed. The failure of copper delivery

to other tissues leads to a copper deficiency.

6.1.2 The Wilson disease

Patients with the autosomal recessive Wilson disease possess a mutated form of the *ATP7B* gene that is closely related to *ATP7A*. Affected organs, particularly the liver, are unable to export Cu effectively and thus accumulate Cu (Bull *et al.*, 1993; Chelly *et al.*, 1993; Tanzi *et al.*, 1993). The decreased liver copper export results in copper induced chronic liver disease and damages the brain, kidneys and eyes (Danks, 1989).

6.2 P-type II ATPases - Ca^{2+} , Na^+/K^+ and H^+ -ATPases

ATPases that belong to this main branch are thought to be involved largely in the transport of Ca^{2+} . The Ca^{2+} -pumping members are divided into two families⁷, IIA and IIB. The mammalian sarcoplasmic reticulum (SR) Ca^{2+} ATPase (Hasselbach and Makinose, 1961; Lee, 2002; Stokes and Green, 2003) belongs to family IIA, and plasma membrane Ca^{2+} pumps are part of family IIB (Geisler *et al.*, 2000; Harper, 2001).

The genome of *A. thaliana* encodes four IIA members, *AtECA1* to *AtECA4* (endoplasmic reticulum calcium ATPase). Based on yeast experiments, it has been suggested that *AtECA* proteins can transport Ca^{2+} , Mn^{2+} , and Zn^{2+} ions. The analysis of *AtECA1* knockout mutants of *A. thaliana* showed that *ECA1* probably pumps Ca^{2+} and Mn^{2+} into the endoplasmic reticulum (Hong *et al.*, 1999; Wu *et al.*, 2002).

Ten IIB members are found in *A. thaliana*, *AtACA1* to *AtACA10* (autoinhibited calcium ATPase). *AtACA2*, *AtACA4*, and *AtACA8* have an N-terminal, calmodulin-regulated autoinhibitory domain (Malmström *et al.*, 1997; Harper *et al.*, 1998; Bonza *et al.*, 2000; Geisler *et al.*, 2002). They localise to a variety of cellular membranes, i. e. to the plasma membrane, to the tonoplast or to the ER membrane (Harper *et al.*, 1998; Geisler *et al.*, 2002; Bonza *et al.*, 2000).

Two other minor families are not known to be present plants. The IIC family is represented by Na^+/K^+ and H^+/K^+ -ATPases in animal systems (Kaplan, 2002; Jorgensen *et al.*, 2003). P-type IIC ATPases are hetero-oligomers consisting of the catalytic ATPase α -subunit and a β -subunit, apparently important for assembly and membrane insertion. Type IID ATPases, Na^+ ATPases, are formed by a few fungal species.

6.3 P-type III ATPases - H^+ and Mg^{2+} pumps

Two families comprise branch III, IIIA and IIIB. Members of IIIA are H^+ pumping plasma membrane ATPases, almost exclusively restricted to plants and fungi. Only a single IIIA H^+ -ATPase was detected

⁷Together with P-type IIIA ATPases they are important for the generation and maintenance of membrane potentials of cells. The result of their activity is the often observed significantly different ion concentration on either side of the membrane.

in the genome of the archaea *Methanococcus jannaschii* (*M. jannaschii*) (Morsomme *et al.*, 2002). *Arabidopsis* contains eleven P-type IIIA ATPases, *AtAHA1* to *AtAHA11* (*Arabidopsis* H⁺ ATPase). It is thought that most *AtAHA* proteins are plasma membrane pumps, but only for two members the plasma membrane localisation has been confirmed (DeWitt *et al.*, 1996). Several AHAs, i. e. AHA2 appears to be activated by the binding of 14-3-3 proteins, a process that depends upon phosphorylation of the conserved penultimate threonine (Thr) residue (Palmgren *et al.*, 1991; Baunsgaard *et al.*, 1998; Palmgren, 2001; Arrango *et al.*, 2003; Fuglsang *et al.*, 2003) (see also page 25).

The IIIA family group together with a small class of bacterial Mg²⁺ translocating pumps of the type IIIB family.

6.4 P-type IV ATPases - aminophospholipid ATPases

This group, so far only detected in eukaryotes, contains the most recently discovered members of the P-type ATPase family. Auland *et al.* (1994) and Tang *et al.* (1996) described some of them as aminophospholipid translocating ATPases. They are thought to carry the molecules from the outer to the inner leaflet of, for example, the plasma membranes of red blood cells (Daleke, 2003) or *S. cerevisiae* (Pomorski *et al.*, 2003).

The genome of *Arabidopsis* encodes twelve P-type IV ATPases, *AtALA1* to *AtALA12* (aminophospholipid ATPases). To date, only one member (*AtALA1*) has been analysed, and its downregulation by antisense suppression was found to reduce the cold tolerance of *A. thaliana* plants (Gomes *et al.*, 2000).

6.5 P-type V ATPases

Like the type IV branch, the fifth branch includes only eukaryotic ATPases. Only a single member of P-type V ATPases is encoded in *A. thaliana* (Axelsen and Palmgren, 2001). So far, the substrate specificity is unknown. These ATPases share a characteristic amino acid motif, PPxxP, often found in the fourth MSH. There are speculations that this family might be involved in the transport of anions (Gerencser, 1996; Gerencser and Purushotham, 1996). Experiments in *S. cerevisiae* on SPF1/COD1, one of two P-type V ATPase in yeast, did not reveal a substrate specificity but hint to a functional role in lipid biogenesis, pathogen response and general ion homeostasis and a localisation at the endoplasmic reticulum membrane (Cronin *et al.*, 2002; Vashist *et al.*, 2002; Suzuki, 2004; Ando and Suzuki, 2005).

7 What are metal transporting P-type IB ATPases in plants?

All members of type IB ATPases are thought to be involved in the transport of transition metal cations. To date, it is unknown if one, several, or any at all counter ions are transported for each pumped transition metal ion. Eight P-type IB ATPases are encoded in the genome of *A. thaliana*

(Axelsen and Palmgren, 2001; Baxter *et al.*, 2003). Phylogenetically, the eight P-type IB ATPases of *A. thaliana* cluster into two groups. One group is related with monovalent Cu/Ag ion transporting ATPases, and the other group is more similar to divalent Zn/Cd/Co/Pb ion transporting ATPases (see Figure 1.5). HMA1 to HMA4 belong to the Zn/Cd/Co/Pb cluster and HMA5 to HMA8 are members of the Cu/Ag cluster (Axelsen and Palmgren, 1998, 2001; Baxter *et al.*, 2003; Williams and Mills, 2005).

Because of a distinctive N-terminal sequence, the heavy metal associated (HMA) motif, all type IB ATPases in plants are named HMAs. The HMA motif was first described in bacteria and suggested to play a role in metal binding (Silver *et al.*, 1989). In 1994, the conserved core sequence GMTCxxC, located in the N-terminal cytoplasmic domain, was termed heavy metal associated motif (HMAM) (Bull and Cox, 1994). The HMAM is embedded in a heavy metal associated domain (HMAD) of about 30 aa. This HMAD is referred to as HMA_1 pattern at the PROSITE database (PS01047). The database contains also a HMA_2 profile (PS50846) of about 70 aa that contains the HMA_1 pattern (Hulo *et al.*, 2006; www.expasy.org/prosite). For the characterisation of the HMA proteins from plants, the description of HMA sequences follows the characterisation of Williams and Mills (2005).

In P-type IB ATPases, the HMA_2 profile can occur in repetitions. Two copies are found in HMA5 and HMA7 (RAN1, responsive to antagonist 1). HMA6 (PAA1, P-type ATPase of Arabidopsis 1) and HMA8 (PAA2) possess only one copy. The proteins HMA2 to HMA4 do contain a variation of the HMA_2 profile in which the GMTCxxC residues are replaced by a GICC(T/S)E motif. In addition, HMA2, HMA3 and HMA4 possess cysteine-cysteine (Cys-Cys, CC) dipeptide and histidine (His, H)-rich motifs in their C-terminal cytoplasmic domain. One exceptional HMA protein that does not contain any HMA profile is HMA1. Instead, it features N-terminal consecutive histidine residues and CC dipeptides. All those sequences, the HMA and CC or His-rich loci could be involved in metal ion binding (Silver *et al.*, 1989; Solioz and Vulpe, 1996; Williams *et al.*, 2000).

Beside the mentioned putative metal binding sites and other P-type ATPase specific features (see page 6), P-type IB ATPases share several features that distinguish them from other ATPases. They possess eight MSHs with a small cytoplasmic loop between MSH IV and V and a big loop containing the phosphorylation domain between MSH VI and VII. The sixth MSH contains a highly conserved CPx (Cys-Pro-x) motif (Figure 1.4). Hence, P-type IB ATPases are also referred to as CPx-type ATPases (Solioz and Vulpe, 1996). The x in this motif is usually a cysteine (Cys) but sometimes it is substituted by a histidine (His) like in CopB of *Enterococcus hirae* or a serine (Ser) like an unnamed pump of *Helicobacter pylori* (Argüello, 2003). In only a few known exceptions, the CPx is even changed into an APC (e. g. in *Mycobacterium tuberculosis*, *Legionella pneumophila*), TPC (e. g. in *Corynebacterium spec.*, *Rhizobium spec.*, *Streptomyces coelicolor*) or SPC (e. g. in AtHMA1) motif (Argüello, 2003). In all P-type IB ATPases the proline (Pro) is invariant. It appears that the CPx motif is of particular importance for the transport of transition metal ions. The equivalent sequence motifs, for example in Ca²⁺ and Na⁺/K⁺-ATPases are IPE and VPE, respectively. Thus the CPx motif is a characteristic feature

that allows to identify P-type IB ATPases among other P-type ATPases. Furthermore, this particular motif is believed to be involved in the translocation of the metal ion through the membrane pore (Solioz and Vulpe, 1996). Another distinguishing motif is a conserved cytoplasmic histidine-proline dipeptide (HP) that follows the CPx/SPC motif at a distance of about 34 to 43 amino acids. The precise function of this motif is still unknown but a frequent mutation in Wilson's disease patients (see page 17) is a substitution of the histidine for glutamic acid (H714E) that inactivates the mammalian copper P-type IB ATPase ATP7B (see page 17).

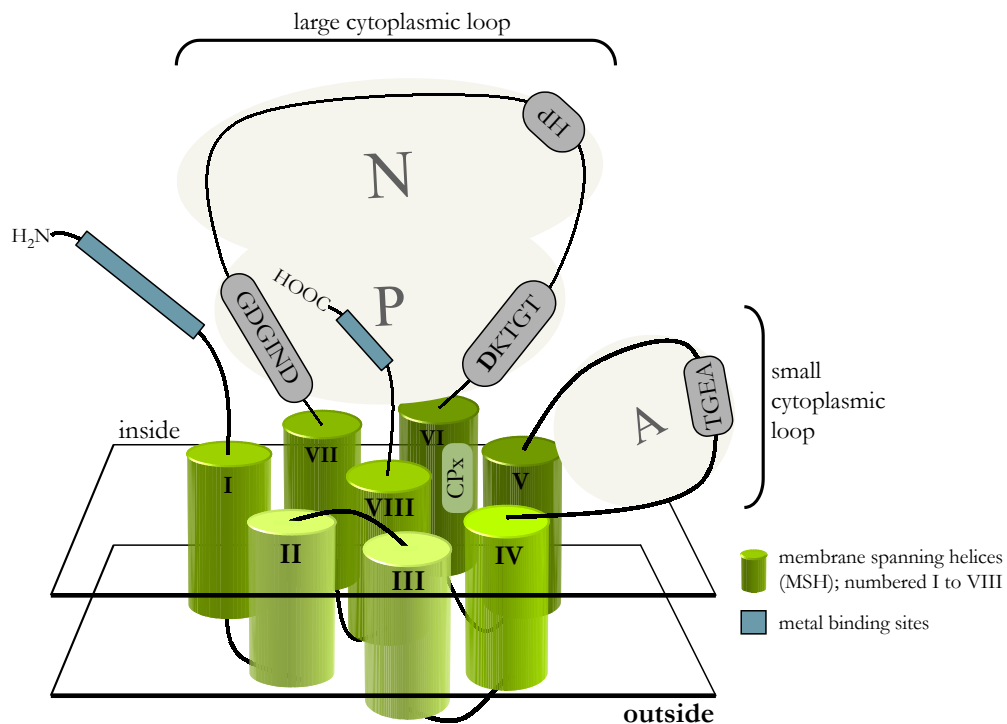


Figure 1.4: Topology model of P-type IB ATPases (modified after Camakaris *et al.*, 1999).

P-type IB ATPases possess 8 MSHs with a small cytoplasmic loop between MSH IV and V that forms the phosphatase or actuator (A) domain and a large cytoplasmic loop between MSH VI and VII containing the phosphorylation (P) and the nucleotide binding (N) domain. The large cytoplasmic loop contains the highly conserved **DKTGT** motif, the site of phosphorylation during the reaction cycle. The conserved **HP** and **GDGIND** motifs are of unknown function. The sixth MSH contains a highly conserved **CPx** (Cys-Pro-x) motif.

The functions of some HMA ATPases have been determined in recent years.

7.1 The Cu/Ag cluster of P-type IB ATPases in plants, HMA5 to HMA8

7.1.1 HMA6 and HMA8

HMA6 and HMA8, also referred to as PAA1 and PAA2, have a role in delivering copper to Cu-requiring proteins in the chloroplast (Shikanai *et al.*, 2003; Abdel-Ghany *et al.*, 2005b). PAA1 localised in the plastid envelope supplies the stromal Cu/Zn superoxide dismutase (AtCSD2) with Cu. As an enzyme of the thylakoid membrane, PAA2 transports the Cu from the stroma into the lumen

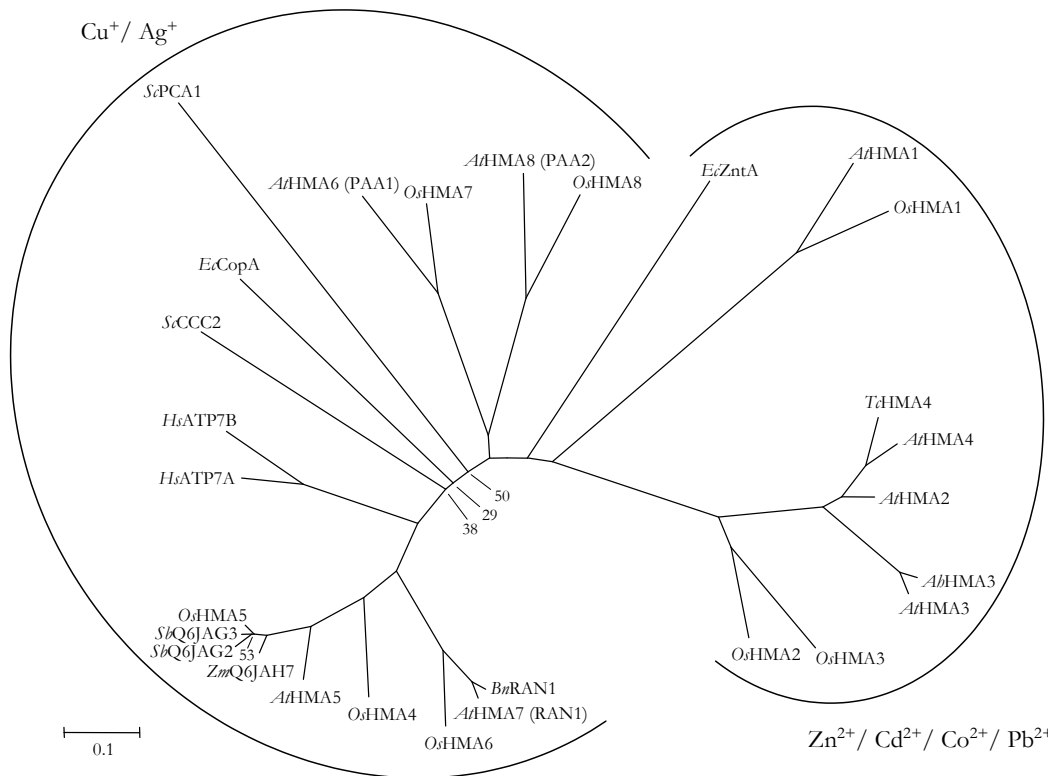


Figure 1.5: Phylogenetic tree of the P-type IB ATPase family.

Neighbour joining tree produced by using the *MEGA* application version 3.1 (Kumar *et al.*, 2004, default parameters). The tree is based on a ClustalW (Chenna *et al.*, 2003) alignment of conserved P-type ATPase core sequences, extracted from eight *A. thaliana* (*At*), eight *O. sativa* (*Os*), one *A. halleri* (*Ah*), two *S. bicolor* (*Sb*), one *T. caerulea* (*Tc*), one *Z. mays* (*Zm*), one *B. napus* (*Bn*), two *S. cerevisiae* (*Sc*), two *H. sapiens* (*Hs*) and two *E. coli* (*Ec*) P-type IB ATPases. The tree was bootstrapped 1000 times. The percentage of times that a certain branch occurred is given for branches that were present in less than 60% of the produced trees. The bottom scale measures evolutionary distances in substitutions per amino acid.

of the thylakoids. There it is required for the formation of holoplastocyanin that functions in the photosynthetic electron transport chain. Contrary to PAA1, but in agreement with its function, PAA2 is only found in shoots (Abdel-Ghany *et al.*, 2005b). In shoots of the Zn hyperaccumulator *A. halleri*, *HMA6* transcript levels are increased compared to *A. thaliana* shoots (Talke *et al.*, 2006).

7.1.2 HMA7

HMA7, a pump that became known as RAN1, was demonstrated to play a role in the ethylene signalling pathway. It is suggested that RAN1 pumps Cu ions across a post-Golgi-compartment membrane, thus supplying Cu ions to an ethylene receptor (ETR1) (Alonso *et al.*, 1999; Hirayama and Alonso, 2000). Besides, the rosette-lethal phenotype of the *ran1-3* mutant might point to another additional function of HMA7/RAN1 affecting cell expansion (Woeste and Kieber, 2000).

7.1.3 HMA5

Recently, Andrés-Colás *et al.* (2006) presented data of yeast two-hybrid experiments that hints to an interaction of the metal-binding domains of HMA5 and *A. thaliana* proteins similar to ATX1, a metallochaperone of *S. cerevisiae* that delivers Cu ions to the P-type ATPase CCC2, located in a post-Golgi compartment (Lin and Culotta, 1995; Lin *et al.*, 1997). Furthermore, the authors localised the copper inducible expression of *HMA5* primarily in roots. The two analysed *A. thaliana* mutants, *hma5-1* and *hma5-2*, are hypersensitive to Cu but not to Fe, Zn, or Cd. They accumulate Cu to a higher extent than the wildtype under excess of Cu. Andrés-Colás *et al.* (2006) propose that HMA5 plays a role in Cu compartmentalisation and detoxification.

7.2 The Zn/Cd/Co/Pb cluster of P-type IB ATPases in plants, HMA1 to HMA4

7.2.1 HMA4 and HMA2

Expression of *AtHMA4* in bacteria conferred increased tolerance to Zn but not Cu. *AtHMA4* expression in *S. cerevisiae* increased the tolerance to Cd (Mills *et al.*, 2003). Two years later, Mills *et al.* (2005) and Verret *et al.* (2005) demonstrated that *AtHMA4* expression in metal sensitive mutants of *S. cerevisiae* also increased Zn and Pb tolerance. Surprisingly, Verret *et al.* (2005) observed a slightly enhanced sensitivity to Co. In a recent study, the HMA4 ATPases from *A. thaliana* and *A. halleri* were shown to similarly complement the Zn or the Cd sensitive phenotype of two yeast mutants (Talke *et al.*, 2006).

In *A. thaliana* *HMA4* transcript levels are increased in response to high concentrations of Zn and Mn in the medium, and downregulated following exposure to Cd (Mills *et al.*, 2003; Verret *et al.*, 2005). Overexpression of *AtHMA4* in *A. thaliana* increased the tolerance of the plants to Zn, Cd, and Co, predominantly apparent at the root level. Furthermore, at toxic concentrations, more Zn and Cd was translocated to the shoot than in wild-type plants (Verret *et al.*, 2004). The authors suggested that the translocation of metals into the shoots might render the plant more tolerant as the shoot represents the bulk of the plant biomass containing much more vacuolar space for metal sequestration than roots.

The *A. thaliana* *hma2 hma4* double mutant is Zn deficient, chlorotic, and has a stunted appearance. Compared to wild-type plants, the Zn content is higher in roots and reduced in shoots. An oversupply of Zn is able to rescue the phenotype (Hussain *et al.*, 2004). The single insertional mutants of *hma2* and *hma4* do not show any phenotypes (Hussain *et al.*, 2004; Verret *et al.*, 2004) suggesting at least a partial functional redundancy of both pumps. Based on *promotor-GUS* (β -glucuronidase) and *cDNA:GFP* fusion studies, Hussain *et al.* (2004) and Verret *et al.* (2004) showed that HMA2 and HMA4 are expressed in the vascular tissue of roots, stems, and leaves and localise to the plasma membrane. Moreover, HMA2 and HMA4 were found to be expressed in shoot phloem tissue, developing anthers and at the base of developing siliques. Based on these data, it is thought that under Zn sufficient con-

ditions HMA2 and HMA4 could play a role in translocating Zn^{2+} ions from the root to the shoot via loading into the xylem. Thus, they provide the shoot with the essential metal. A similar role was indicated by functional analysis for *TcHMA4*, a homologue of *AtHMA4* from the Zn hyperaccumulator *T. caerulescens* (Papoyan and Kochian, 2004). At higher metal concentrations, HMA2 and HMA4 are probably involved in $Zn^{2+}/Cd^{2+}/Co^{2+}/Pb^{2+}$ detoxification by protecting the root cells from excess metal accumulation.

Recently, *HMA4* was included in a published list of 18 putative metal homeostasis genes that were found in a comparison of the Zn hyperaccumulator *A. halleri* and the non-hyperaccumulator *A. thaliana* using genome-wide cross-species microarray analysis and real-time RT-PCR (Talke *et al.*, 2006). It was shown that *HMA4* transcript levels are constitutively high in roots of *A. halleri* under various conditions and slightly inducible in *A. halleri* shoots under Zn deficiency (Talke *et al.*, 2006).

7.2.2 HMA3

AtHMA3, which is closely related to HMA2 and HMA4 at the amino acid sequence level, has been shown to increase tolerance to Cd and Pb but not to Zn when expressed in metal sensitive *S. cerevisiae* mutants. The authors report that *AtHMA3* localises to the vacuolar membrane of yeast, although the evidence provided is not convincing (Gravot *et al.*, 2004). Hussain *et al.* (2004) could show that the *HMA3* gene of the Columbia (Col) accession of *A. thaliana* contains a single base pair deletion. This deletion leads to a frame shift and subsequently to a truncation of the encoded protein after amino acid 542. The predicted protein is lacking the essential nucleotide binding domain (N-domain) and is likely to be non-functional. In the Wassilewskija (Ws) accession of *A. thaliana* such a deletion was not detected. It is unlikely that *AtHMA3* has an essential role in *A. thaliana*.

Some P-type IB ATPases were identified to possibly play a role in metal hyperaccumulation and hypertolerance by comparing hyperaccumulating with non-hyperaccumulating plant species using microarray transcript profiling techniques. The *HMA3* gene showed a constitutively high expression in shoots of the Zn hyperaccumulator *A. halleri* compared to the non-hyperaccumulating *A. thaliana* (Becher *et al.*, 2004; Talke *et al.*, 2006). Another study compared the shoot transcriptomes of the Zn hyperaccumulator *T. caerulescens* and the non-hyperaccumulator *Thlaspi arvense* (*T. arvense*) (Hammond *et al.*, 2006). In this study, homologues of *AtHMA3* and *AtHMA4* were more highly expressed in shoots of *T. caerulescens* than in *T. arvense*.

7.2.3 HMA1

AtHMA1 forms a subcluster with other P-type IB ATPases from *O. sativa*, *Hordeum vulgare* (*H. vulgare*), *Glycine max* (*G. max*), the algae *Chlamydomonas reinhardtii* (*C. reinhardtii*) and *Cyanidioschyzon merolae* (*C. merolae*) and bacteria (Williams and Mills, 2005). One special feature these P-type IB ATPases share is the motif SPC, instead of the more common CPx in the MSH VI. The only functional data of a SPC containing P-type IB ATPase comes from the cobalt transporter CoaT of the

cyanobacteria *Synechocystis* PCC6803 (Rutherford *et al.*, 1999). Williams and Mills (2005) indicate that *AtHMA1* can transport Cd in yeast. Very recently, Seigneurin-Berny *et al.* (2006) reported that *AtHMA1* localises to the chloroplast envelope. Furthermore, expression in yeast cells suggest a transport of Cu and Zn ions. Contrary to *AtHMA6* (PAA1) but similar to *AtHMA8* (PAA2), *AtHMA1* appears to be mainly expressed in green tissue. Seigneurin-Berny *et al.* (2006) conclude that *AtHMA1* could play a distinct role in supplying copper to chloroplasts, despite having a partial functional redundancy with *AtHMA6* (PAA1). Still, the contradictory information concerning the physiological function of *AtHMA1* does not allow a clear assignment. In Talke *et al.* (2006), *HMA1* transcript levels were shown to be increased in *A. halleri* shoots compared to shoots of *A. thaliana*.

7.3 Mechanisms of regulation of P-type IB ATPases

Only a few data are available about the regulation of plant P-type IB ATPases. On the transcriptional level it has been shown that some P-type IB ATPase transcripts are regulated by metals. Mills *et al.* (2003) concluded from RT-PCR experiments that the *A. thaliana HMA4* expression in roots is slightly enhanced by Zn or Mn and reduced by Cd. In contrast to this, Bernard *et al.* (2004) could not demonstrate that Cd affects the expression of *AtHMA4*. The homologous gene transcript in the Zn and Cd hyperaccumulator *T. caerulescens*, *TcHMA4*, is slightly upregulated in roots and shoots at higher Cd concentrations (Bernard *et al.*, 2004) and upregulated in roots under Zn-deficient and high Zn or Cd conditions as shown by Northern blot analyses (Papoyan and Kochian, 2004).

Becher *et al.* (2004) described a slight upregulation of the *HMA3* transcript in roots of *A. thaliana* and a more pronounced upregulation in roots of *A. halleri* at high levels of Zn. Interestingly, *AtHMA3* is strongly upregulated in Fe-deficient roots of *A. thaliana* and this regulation seems to depend mainly on FIT1, the Fe-deficiency induced transcription factor 1. FIT1 regulates the iron uptake response in Arabidopsis. In *fit1* mutant plants, *AtHMA3* transcript levels are not enhanced under Fe-deficient conditions (Colangelo and Gueriot, 2004).

It is unknown if any plant P-type IB ATPase is regulated at the post-transcriptional or post-translational level. However, when these plant pumps are aligned to homologous bacterial proteins, one distinguishing feature is an extended cytoplasmic C-terminal end. One might speculate that this domain is of special importance for the function of these pumps in plants. The C-terminus is important for the function of *AtHMA4*. Mills *et al.* (2005) observed that the ability of *AtHMA4* to confer an enhanced Zn/Cd resistance in yeast is not impaired when its full 457 amino acid (aa) C-terminus is deleted. Verret *et al.* (2005) reported that the deletion of a 11 histidine long C-terminal stretch inactivates the Cd/Zn transport activity.

In this context, the described post-translational regulation of the H⁺ pumping P-type IIIA ATPase AHA2 by its autoinhibitory C-terminal domain is noteworthy. In *A. thaliana*, protons are pumped across the plasma membrane from the cytoplasm to the plant cell exterior by the P-type ATPase AHA2 (see page 18). In order to activate the proton pumping, a membrane bound protein-kinase

phosphorylates the threonine (T) in a YTV motif at the C-terminal end of AHA2. Subsequently a 14-3-3 protein can bind and trigger the proton pumping activity by displacing the C-terminal autoinhibitory domain from the functional domain (Palmgren *et al.*, 1991; Baunsgaard *et al.*, 1998). One could imagine similar regulatory mechanisms in P-type IB ATPases.

7.3.1 Mechanisms of metal-dependent regulation in plants

Other well-studied mechanisms of metal regulation may offer insights into possible regulatory mechanisms of P-type IB ATPases. One example is the response of plants to different iron conditions, especially to Fe-deficiency.

Cis-acting promoter elements Potential *cis*-acting elements, i. e. nucleotide sequences located in proximity to the regulated gene, that are important to drive the iron-regulated expression of plant genes were described by a few authors. The promoter regions of the phytoferritin genes from *Z. mays* and *A. thaliana* contain iron-dependent regulatory sequence (IDRS) elements (Petit *et al.*, 2001) and the soybean ferritin gene promoter possess an iron regulatory element (FRE) (Wei and Theil, 2000). Phytoferritins are iron storage proteins. The discovered *cis*-acting elements are needed to derepress the expression of phytoferritin genes in response to iron overload. In 2003, Kobayashi *et al.* reported two homologous iron-deficiency responsive elements, IDE1 and IDE2, common in the promoter regions of many iron-deficiency-responsive genes, like *AtFRO2* and *AtIRT1*.

Transcriptional regulation FIT1 plays a major role in the regulation of the iron deficiency response in *A. thaliana*. The mRNA of this putative basic helix-loop-helix (bHLH) transcription factor is accumulated in the outer cell layers of the root under Fe-deficient conditions. The expression of at least 40 % of iron-regulated genes depends directly on FIT1 as shown by microarray analysis of wild-type and *fit1* mutant plants (Colangelo and Guerinot, 2004). Among these genes are the genes encoding the Fe(III) chelate reductase FRO2 and, as mentioned above, the P-type IB ATPase *AtHMA3*. The reduction of the corresponding mRNAs in *fit1* mutant plants under Fe deficiency indicates a control by FIT1 at the mRNA level.

Posttranslational regulation Interestingly, in the *fit1* mutant plants mentioned above, the protein level of IRT1, a high affinity Fe(II) transporter and member of the ZIP family (see page 12), is depleted but the *IRT1* mRNA level is not affected. This indicates that FIT1 or a protein acting downstream of FIT1 might control IRT1 at the level of protein accumulation. Colangelo and Guerinot (2004) speculate that FIT1 could negatively regulate a factor that is important for ubiquitin-mediated protein turnover of IRT1 proposed by Curie and Briat (2003). The ubiquitination and endocytosis was described for the IRT1 homolog ZRT1, a zinc transporter in *S. cerevisiae* (Gitan *et al.*, 1998; Gitan and Eide, 2000).

Chapter 2

Motivation and aims of the thesis

1 *HMA3*, a gene possibly involved in metal homeostasis in *A. halleri*

The initial motivation for the project of this thesis came from experiments that proposed a possible role of *HMA3* in the metal homeostasis network of *A. halleri*, a Zn hyperaccumulating and Zn hyper-tolerant plant that is closely related to the non-hyperaccumulator model plant *A. thaliana* (see page 6). Transcript profiles were generated by hybridisation of AFFYMETRIX Arabidopsis GeneChips® by Becher *et al.* (2004). Total leaf mRNA of *A. thaliana* and *A. halleri* was used. The experiments identified several potential candidate genes which are differentially regulated between *A. halleri* and *A. thaliana* (Figure 2.1 A). One of the identified candidate genes in *A. halleri* was *AbHMA3*, which is highly similar to *HMA3* in *A. thaliana* (Arabidopsis gene identifier (AGI) number: At4g30120; see Section 7 on page 19).

The high expression of *AbHMA3* in *A. halleri* was confirmed by real-time RT-PCR (Becher *et al.*, 2004; Figure 2.1 B). Transcript levels of *HMA3* in shoots and roots of *A. thaliana* and *A. halleri* were compared under low and high zinc conditions. The *A. halleri* shoots showed a constitutively high expression of *AbHMA3* across different Zn treatments. The expression of *HMA3* in the roots was also constitutively higher in *A. halleri* than in *A. thaliana*, but lower than in *A. halleri* shoots. *AbHMA3* expression was slightly inducible by Zn in *A. halleri* roots. In *A. thaliana*, the relative transcript level was much lower than in *A. halleri*. Contrary to the situation in *A. halleri*, there was a higher expression in the roots compared to the shoots.

A

Chip id.	MIPS/AGI code	Annotation	Name	Average ratio low Zn	$P < 0.05$	Average ratio high Zn	$P < 0.05$
19521_s_at	At2g27880	Argonaute (AGO1)-like protein	AGO5	218.9	*	18.2	*
19296_at	At4g30120	Cd ²⁺ -transporting P-type ATPase-like protein (3.A.3)	HMA3	175.2	*	124.1	*
17762_s_at	At2g14580	Putative pathogenesis-related protein-like (PR1)	PR1-like	110.0	*	121.6	*
14385_at	At2g45830	Unknown protein		52.5	*	20.3	*
19045_at	At2g46950	Putative cytochrome P450	CYP709B2	44.8	*	32.6	*

B

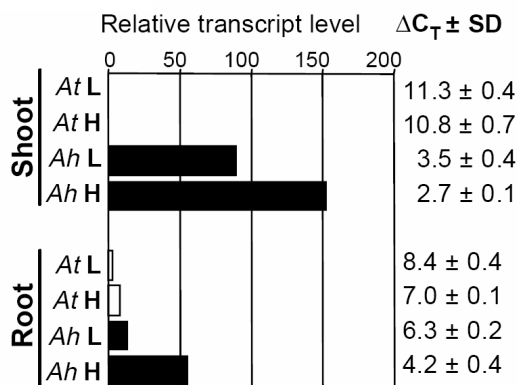


Figure 2.1: Comparison of HMA3 expression level in *A. halleri* and *A. thaliana* using Affymetrix Arabidopsis GeneChip® hybridisations (A) and real-time RT-PCR (B) (Becher *et al.*, 2004).

(A) Analysis of AFFYMETRIX Arabidopsis Genechip® data. Genes expressed at higher levels in *A. halleri* than in *A. thaliana* after 4 days of growth under low Zn supply. Only the top 5 genes are listed. Values are average ratios of normalised signals of *A. halleri* versus *A. thaliana*, which were calculated using the GENESPRING™ software. Asterisk symbols (*) indicate a significant difference in expression between *A. halleri* and *A. thaliana* at $P < 0.05$.

(B) Transcript levels were analysed in shoots and roots of six-week old plants of *A. halleri* (black) and *A. thaliana* (white) after a four-day exposure to low and high Zn concentrations in the culture medium. The given relative transcript level means a relative fold expression compared to the C_T of *EF1 α* /1000. For a detailed description please refer to Becher *et al.* (2004).

2 Motivation and aim of the thesis

While many studies have been done on prokaryotic P-type IB ATPases and their importance for metal homeostasis, little information is available on P-type IB ATPases in plants, especially in metal hyperaccumulators. The functional characterisation of the P-type IB ATPase HMA3 could broaden the understanding of the molecular mechanisms enabling certain plants to hyperaccumulate and hypertolerate transition metal ions.

The objective of this study was to solve questions that arose from the first results described above: What is the role of *HMA3* in zinc homeostasis of *A. halleri*? How and to which extent does *HMA3* contribute to the observed zinc hypertolerance and -accumulation in *A. halleri*? Where is HMA3 localised? How is the expression of *HMA3* regulated in *A. halleri* and *A. thaliana*?

Part II

Materials and Methods

Chapter 3

Materials and Methods

1 Standard molecular biology techniques

Standard techniques, such as transformation and culture of *E. coli*, plasmid extraction, plasmid digestion with restriction enzymes, dephosphorylation of vectors by alkaline phosphatase, precipitation of RNA and DNA, ligation of DNA fragments or DNA extraction from plants were performed as described (Sambrook and Russel, 2001).

Plasmids and PCR products that needed to be sequenced and DNA fragments from agarose gels were extracted, prepared and purified using commercial kits according to the manufacturer's instructions unless indicated otherwise (QIAGEN GmbH, Hilden, Germany; Invitrogen, Karlsruhe, Germany).

2 Plasmids

2.1 *E. coli* expression vectors

2.1.1 pASK-IBA3 (*ptetA-cDNA:Strep-Tag*)

The pASK plasmids are included in the *Strep-Tag*^{®II}-System (Institut für Bioanalytik (IBA), Göttingen, Germany) for protein expression and purification. It is based on the stringent regulated expression of a protein under the control of the tetracycline promoter (*tetA* promoter; Skerra, 1994) and the selective binding of the *Strep-Tag*^{®II} peptide (NH₂-WSHPQFEK-COOH) during the purification on *StrepTactin*[®]. The cloning of the recombinant gene into the pASK-IBA3 vector fuses the N-terminus of the protein with the *Strep-Tag*^{®II} peptide after expression. Transformed *E. coli* cells were selected with carbenicillin on LB media (see page 33 and Table 3.1).

pASK-IBA7GW (*ptetA-Streptag:cDNA*) The plasmid pASK-IBA7GW is a modified pASK-IBA7 vector that is adapted for the use with the Gateway[®] system. For this purpose, the Gateway[®] cassette A (GW-A) was inserted into the pASK-IBA7 vector. The resulting vector pASK-IBA7GW was used to

fuse a *Strep-Tag*^{®II} peptide to the C-terminus of a recombinant protein. Transformed *E. coli* cells were selected with carbenicillin on LB media (see page 33 and Table 3.1).

2.2 Yeast expression vectors

2.2.1 pFL61GW (*pPGK1-cDNA*)

The multi-copy vector pFL61GW (A.-G. Desbrosses-Fonrouge, not published) is a Gateway[®] adapted version of the vector pFL61 (Minet *et al.*, 1992). It contains the replication origin of the yeast 2 μ m plasmid, the *URA3* gene, and the promoter and terminator of the yeast phosphoglycerate kinase I gene (*PGK1*) for the heterologous expression of cDNA in *S. cerevisiae*. Transformed *E. coli* cells were selected with carbenicillin on LB media (see page 33 and Table 3.1).

pFL613GW (*pPGK1-3xHA:cDNA*) The vector pFL613GW (Dräger *et al.*, 2004) is a modified pFL61GW that generates a translational fusion of the encoded protein with an N-terminal triple hemagglutinin epitope tag (3xHA).

2.3 Plant expression vectors

2.3.1 pBI101, pBI101.2, and pBI101.3 (*promoter:GUS*)

The binary vector pBI101 (Clontech Laboratories, Mountain View, CA, USA) contains the *GUS* gene that encodes the reporter enzyme β -glucuronidase (GUS) (Jefferson *et al.*, 1987) and derived from the *uidA* locus of *E. coli* (Novel and Novel, 1973). The vector is used to analyse the activity of a cloned promoter sequence. Selection is carried out with kanamycin in *E. coli*, *Agrobacterium tumefaciens* (*A. tumefaciens*) and plants (see page 33 and Table 3.1).

The vectors pBI101.2 and pBI101.3 are variations of pBI101 and contain one and two additional base pairs in the multiple cloning site, respectively. Thus creating different reading frames.

2.3.2 pMDC83 (*p35S-cDNA:GFP6*)

The binary vector pMDC83 (Curtis and Grossniklaus, 2003) is designed for translational fusion of an encoded protein to the N-terminus of the histidine-tagged GFP6. This vector contains the cauliflower mosaic virus (CaMV) 35S promoter (Odell *et al.*, 1985) and the nopaline synthase (NOS) terminator of *A. tumefaciens* (Hellens *et al.*, 2000) and is adapted for Gateway[®] cloning. Selection is performed in *E. coli* and *A. tumefaciens* strains with kanamycin and in plants with hygromycin (see page 33 and Table 3.1).

Direct cloning of *AbHMA3* in pMDC83 (*p35S-cDNA:GFP6*) *AbHMA3* was amplified from a pENTR[™]-*AbHMA3* template with the primers AhHMA3-SpeI-F and AhHMA3-KpnI-R (see Table 3.3 on page 37). The PCR product was digested with *SpeI* and *KpnI*, and subcloned into the *SpeI*

and *KpnI* sites of pMDC83 to produce the plasmid pMDC83-*AbHMA3:GFP*. After transformation in *E. coli* and selection for kanamycin resistance, positive clones with the correct sequence were obtained. Two of those positive pMDC83-*AbHMA3:GFP* constructs were independently transformed in *A. tumefaciens* followed by the infiltration of *A. thaliana*.

2.3.3 pBKSGWGUS (*promoter:GUS*)

The binary vector pBKSGWGUS is a gatewayised pBLUESCRIPT vector (pBKS(+)). It was generated by amplifying the *Gateway:GUS* cassette of the pMDC163 vector (Curtis and Grossniklaus, 2003) and subsequently cloning it into the *XhoI* site of pBKS(+) (Marc Hanikenne, group of Dr. Ute Krämer; personal communication). The purpose of that procedure was to obtain a small *GUS* reporter plasmid that should show a higher transformation efficiency in protoplasts than other larger plasmids. The vector is used to analyse the activity of a cloned promoter sequence in transiently transfected protoplasts. Transformed *E. coli* cells were selected with carbenicillin on LB media (see page 33 and Table 3.1).

(Karimi *et al.*, 2002) contains the promoter and terminator of the cauliflower mosaic virus (CaMV) (Odell *et al.*, 1985) to overexpress a cDNA in plants and is adapted for Gateway® cloning. Selection is performed in *E. coli* and *A. tumefaciens* strains with spectinomycin and in plants with DL-phosphinotricin (PPT) (see page 33 and Table 3.1).

2.3.4 pB735SGW (*p35S-cDNA*)

The binary vector pB735SGW (Karimi *et al.*, 2002) contains the promoter and terminator of the CaMV (Odell *et al.*, 1985) to overexpress a cDNA in plants and is adapted for Gateway® cloning. Selection is performed in *E. coli* and *A. tumefaciens* strains with spectinomycin and in plants with DL-phosphinotricin (PPT)(PPT, Duchefa, Harlem, The Netherlands) (see page 33 and Table 3.1).

2.3.5 pK7GWIWG2(I) (*p35S-cDNA:intron:VNQ²*)

The Gateway® adapted binary vector pK7GWIWG2(I) (Karimi *et al.*, 2002) contains the promoter and terminator of the CaMV (Odell *et al.*, 1985) to overexpress a cDNA:intron:VNQ² loop construct in plants in order to silence the expression of the gene that is homologous to the cloned cDNA fragment. Selection is performed with kanamycin in bacteria and in plants (see page 33 and Table 3.1).

3 Culture conditions

3.1 Media and Supplements

3.1.1 Luria-Bertani media for *E.coli* cultivation

Luria-Bertani (LB) medium (Sambrook and Russel, 2001) was used for the cultivation of *E. coli* strains during cloning processes. One liter $\text{H}_2\text{O}_{\text{bidest}}$ contains 10 g bacto-trypton, 5 g yeast extract, and 5 g NaCl. The pH is adjusted to 7.0 with NaOH. To obtain plates, 15 g agar was added to the medium.

3.1.2 YEB media for *A.tumefaciens* cultivation

For the cultivation of *A. tumefaciens* strains, YEB media was used. A liter of YEB contains (5 g/l bacto-tryptone, 1 g/l bacto-yeast-extract, 1 g/l bacto-peptone, and 5 g/l sucrose in H_2O . To obtain plates, 15 g agar was added to the medium.

3.1.3 Media for yeast and plant cultivation

Media used for the cultivation of yeast strains and plants are described as part of the experimental protocols in the corresponding section on techniques related to yeast (see page 47) and to plants (see page 49).

3.1.4 Transition metal salts

The transition metal salts CdSO_4 , CoSO_4 , and ZnSO_4 were prepared as aqueous stock solutions of 0.1 M and 1 M, respectively. The stock solutions were diluted in sterile medium to obtain the described final concentrations.

3.1.5 Antibiotics

Stock solutions of antibiotics were prepared according Ausubel *et al.* (1993) and stored at -20°C . In Table 3.1, the final concentrations in sterile media are listed.

3.1.6 Additional Supplements

Table 3.2 lists the stock solutions and final concentrations in sterile media of additional supplements.

Table 3.1: Stock solutions and final concentrations of applied antibiotics.

antibiotic	stock solution	final concentration in media ^a
carbenicillin	100 g/l H ₂ O _{bidest}	100 mg/l
chloramphenicol	20 g/l Ethanol (96%)	20 mg/l
gentamicin	25 g/l H ₂ O _{bidest}	25 mg/l (<i>A. tumefaciens</i>)
hygromycin	10 g/l H ₂ O _{bidest}	10 mg/l (plants)
kanamycin	25 g/l H ₂ O _{bidest}	125 mg/l
	50 g/l H ₂ O _{bidest}	50 mg/l (plants)
DL-phosphinotricin, PPT	25 g/l H ₂ O _{bidest}	25 mg/l (plants)
Rifampicin	50 g/l in DMSO ^b	100 mg/l (<i>A. tumefaciens</i>)
spectinomycin	50 g/l in DMSO ^b	50 mg/l (<i>E. coli</i>)
		100 mg/l (<i>A. tumefaciens</i>)
streptomycin	150 g/l H ₂ O _{bidest}	100 mg/l

^aif no organism is mentioned, the given values refer to the selection of transformed *E. coli*

^bDMSO, dimethyl sulfoxide, (CH₃)₂SO

Table 3.2: Stock solutions and final concentrations of additional supplements.

supplement	stock solution	final concentration in media
AHT	2 g/l H ₂ O _{bidest}	200 µg/l
IPTG	200 g/l H ₂ O _{bidest}	40 mg/l
X-Gal	200 g/l dimethylformamide	48 mg/l

4 Techniques related to DNA

4.1 Gateway[®] technology and PCR

4.1.1 Gateway[®] technology

The Gateway[®] technology employs *in vitro* site-directed recombination instead of restriction and ligation to insert a DNA fragment of interest into a Donor Vector to obtain an Entry Vector containing the DNA fragment with its orientation and reading frame maintained. The DNA fragment can subsequently be subcloned into various Destination Vectors, for example to obtain Expression vectors ready to be used for expression in the appropriate host (Life technologies, 2000). The Gateway[®] technology is based on the well-characterised λ bacteriophage site-specific recombination system (Landy, 1989).

The DNA fragment of interest is amplified by the polymerase chain reaction (PCR). The fragment can be cloned into an Entry Vector using a forward primer that adds a CACC tetranucleotide to the 5'-end of the PCR product. In a subsequent TOPO[®] cloning reaction, the blunt-end PCR product is directionally inserted into a pENTR[™]-TOPO[®] vector (Figure 3.1 A). The reaction is mediated by the enzyme topoisomerase I (Shuman, 1991, 1994). The enzyme cleaves the phosphodiester backbone in one strand at the CACC site of the vector. The energy of the broken phosphodiester backbone is conserved by formation of a covalent bond between the 3'phosphate of the cleaved strand and a

tyrosyl residue of topoisomerase I. The GTGG overhang in the cloning vector invades the 5'-end of the PCR product, anneals to the added tetranucleotide, and stabilises the PCR product in the correct orientation. Then, the phosphotyrosyl bond between the DNA and the enzyme can be attacked by the 5'-hydroxyl of the attached PCR product. This reverses the reaction and releases the topoisomerase (Invitrogen, 2006).

An alternative method to obtain an Entry Vector containing the cloned gene is the use of primer pairs that contain two recombination sites, *attB1* and *attB2* at their 5'-ends that are added to the forward primer and the reverse primer, respectively (Figure 3.1 B). These 25 bp long *att* sites contain the binding sites for the proteins that mediate the recombination. The obtained PCR fragment is then cloned by a so-called BP reaction into a Donor Vector (Figure 3.1 B). The Donor Vector plasmid contains a selectable marker (for example kanamycin) and a Gateway® cassette consisting in two recombination sites (*attP1* and *attP2*) that flank a cassette containing a chloramphenicol resistance gene and a gene for negative selection, *ccdB*¹. The *ccdB* product reacts with an arginine at position 462 of the gyrase gene. Its expression is lethal in *E. coli* strains containing this residue. To amplify vector DNA of all vectors containing the *ccdB* gene, *E. coli* strains are used in which the arginine is replaced by a cysteine (DB3.1 strain; Invitrogen, Karlsruhe, Germany). The integration reaction (*attB* × *attP*) is mediated by the proteins integrase (Int) and host integration factor (IHF). The sequence differences between the *att1* and *att2* sites confer directionality and specificity of recombination, so that only *attB1* will react with *attP1* to form *attL1*, and *attB2* with *attP2* to form *attL2* (Figure 3.1 B).

The products of a BP reaction are the Entry Vector containing two newly generated sites flanking the integrated PCR fragment, *attL1* and *attL2*, with no loss of DNA sequence, and a by-product (the Gateway® cassette). The desired plasmid is under two forms of selection: positive antibiotic resistance (kanamycin) and negative selection against the Donor Vector containing the original Gateway® cassette (*ccdB* gene). The *E. coli* strain used after the recombination (DH5-α; Gibco, Karlsruhe, Germany) is sensitive to the *ccdB* gene product and therefore, any non-recombinant Entry Vector is eliminated. Inserted PCR fragments in the Entry Vector were sequenced.

The Entry Vector can be used to subclone the PCR fragment into a variety of Destination Vectors by a so-called LR reaction (Figure 3.1 C). These plasmids contain two recombination sites (*attR1* and *attR2*) that flank an array of a gene for negative selection, *ccdB*, and a selection marker different from the one in the Entry Vector (for example ampicillin). When integration occurs, two new sites are generated in the expression vector, *attB1* and *attB2*, flanking the integrated PCR fragment, with no loss of DNA sequence. The recombination sites confer directionality and specificity for recombination, so that only *attL1* will react with *attR1* to form *attB1*, and *attL2* with *attR2* form *attB2*. The product of these two recombination events is the expression vector containing the PCR fragment and

¹Together with *ccdA*, the *ccdB* gene is localised at the *ccd* locus of *E. coli* and was originally described as a system that couples cell division to plasmid replication by inhibiting division of cells with fewer than two plasmid copies (Ogura and Hiraga, 1983; Miki *et al.*, 1984). The *ccd* locus was shown later to mediate plasmid maintenance by postsegregational killing (PSK; Jaffé *et al.*, 1985; Hiraga *et al.*, 1986)

a by-product (labeled as the Donor Vector in Figure 3.1 B). The desired plasmid is under two forms of selection: positive antibiotic resistance (ampicillin) and negative selection against the Destination Vector containing the original Gateway® cassette (*ccdB* gene). Selecting for antibiotic resistance eliminates the starting vector (Entry Vector) and the by-product. The presence of the negative selection marker eliminates the Destination Vector and co-integrated molecules.

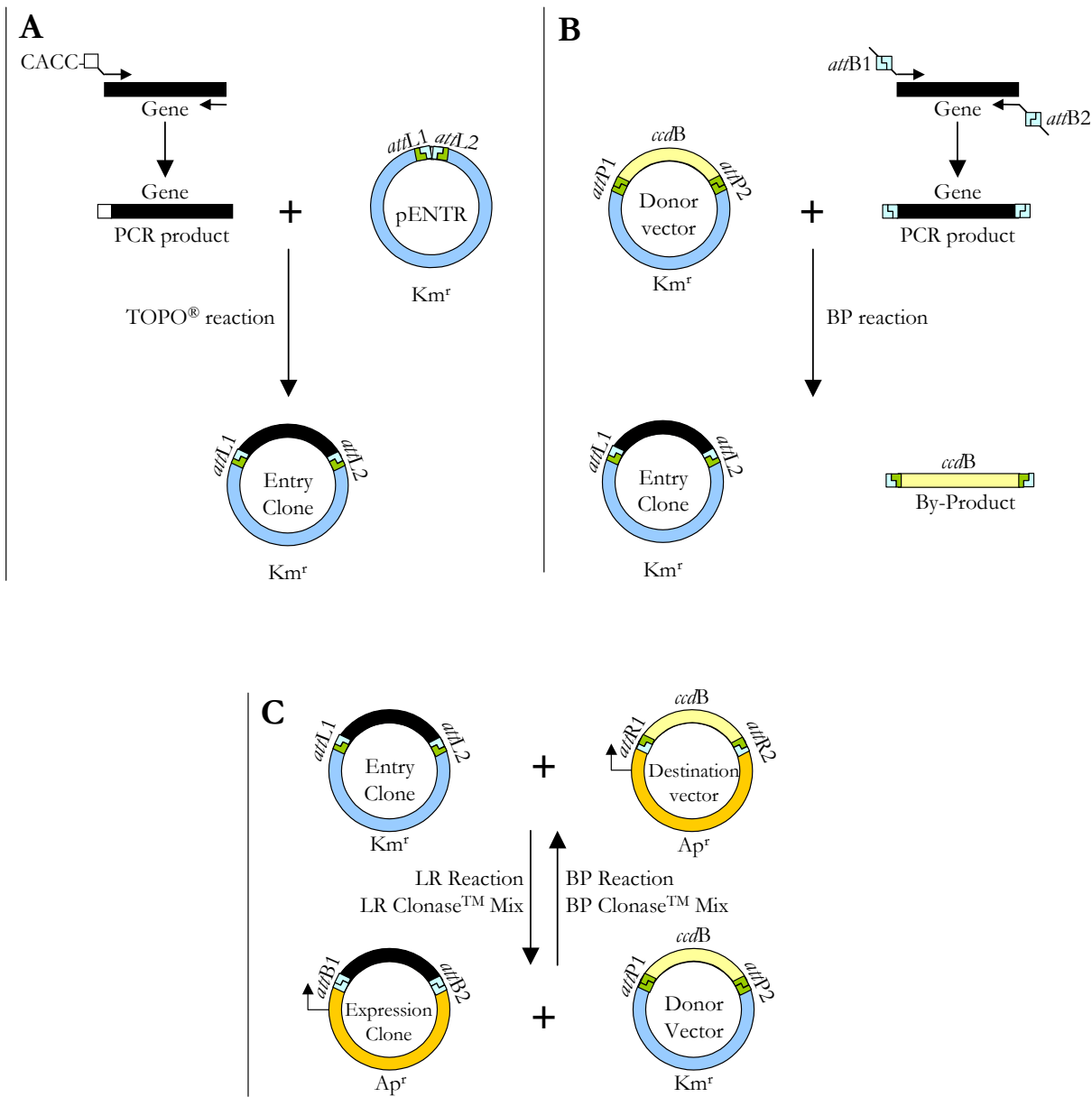


Figure 3.1: Principles of Gateway® technology (www.invitrogen.com, Karlsruhe, Germany). The DNA fragment of interest is amplified and integrated into an Entry Vector by directional TOPO™ cloning (A) or a recombination BP reaction with a Donor Vector (B). The Entry Clone can be used to insert the DNA fragment into a variety of Destination Vectors by site-directed recombination (LR and BP reaction, C).

4.1.2 Polymerase chain reaction (PCR)

Primer selection Based on known sequences, regular primers were designed with the help of the *Oligo Explorer* software (version 1.2, Gene Link, Hawthorne, NY, USA) and real-time RT-PCR primers with the *Primer Express* software (version 2.0, Applied Biosystems, Foster City, CA, USA). The oligonucleotides were ordered from AGOWA GmbH (Berlin, Germany) or Eurogentec (Liège, Belgium). The primers were diluted in sterile H₂O to a final concentration of 10 μM and stored at -20°C. An overview of all applied primers can be found in Table 3.3.

Table 3.3: Used primers.

primer name	orientation	sequence 5'→3' position ^a	description
Cloning of <i>HMA3</i> promoter			
Pt01 F	→	⁻²⁰⁰⁵ aagcaaaccagtcctatg	full promoter
Pt01 CACC F	→	cacc ⁻²⁰⁰⁵ aagcaaaccagtcctatg	<i>pHMA3-1</i>
Pt01 R	←	⁶⁶ gacgtcgaagtaacttgctg	
P50 F	→	⁻¹⁰⁰⁵ aagctttattctacaagtgtatgatg	2 nd <i>AbHMA3</i> promoter,
P50 CACC F	→	cacc ⁻¹⁰⁰⁵ aagctttattctacaagtgtatgatg	<i>pAbHMA3-2</i>
P50.1 F	→	⁻⁹⁵⁰ aaaggtccaccagtttcg	
Pt800 F	→	⁻⁴⁸⁸ gcccaataggctcttttct	medium sized promoter
Pt800 CACC F	→	cacc ⁻⁴⁸⁸ gcccaataggctcttttct	
Pt200 F	→	⁻¹⁸⁷ atctcagcattgaatttagaaa	small sized promoter
Pt200 CACC F	→	cacc ⁻¹⁸⁷ atctcagcattgaatttagaaa	
PLoop R	←	⁹⁵⁶ aagctcatcagtgatgacattacagt	full promoter
PLoop.1 R	←	⁹⁵⁴ gctcatcagtgatgacattacagt	including first MSHs
Cloning of <i>HMA3</i>			
AtHMA3 F	→	cacc ₁ atggcgaaggtgaagagt	full <i>AtHMA3</i> , M. Becher
ahhma3 F	→	₁ atggcgaaggtgaagaggc	full <i>AbHMA3</i>
V01 F	→	₁ atggcgaaggtgaagagg	full <i>AbHMA3</i>
V01 OA F	→	₄ gcggaaggtgaagaggcca	w/o ATG
V01 OS R	←	³⁰⁹⁸ ctttgttgattgtccttagggc	w/o TGA
V01 OS+T R	←	a ₃₀₉₈ ctttgttgattgtccttagg	w/o TGA, with T
V01 R	←	³¹⁰¹ tcactttgttgattgtccttagg	full <i>HMA3</i>
cloning of <i>AbHMA3</i> cDNA in pASK-IBA3 (<i>ptetA-cDNA:Streptag^{®II}</i>)			
H3ask3 F	→	atggtagaagacaa▼aatg...	introduces
		₁ atggcgaaggtgaagaggccaaga	<i>BbsI</i>
H3ask3 R	←	atggtagaagacaa▼gcgct...	restriction
		³⁰⁹⁸ ctttgttgattgtccttagggcc	sites
cloning of <i>AbHMA3</i> cDNA in pMDC83 (<i>p35S-cDNA:GFP6</i>)			
AhHMA3SpeI F	→	tctagaa▼ctagt...	introduces <i>SpeI</i>

continued on next page...

^aPositions of cloning relevant restriction sites that were introduced are underscored and black triangles (▼) mark the cleavage position. Restriction sites that are not underscored were not used for cloning procedures. Emphasised (**bold-faced**) nucleotides mark substitutions. Deep-placed numbers mark the nucleotide position in the genomic *AtHMA3*-sequence (GenBank accession NC_003075) relative to the transcriptional start (₁ATG).

Table 3.3 continued

primer name	orientation	sequence 5'→3' position ^a	description
AhHMA3KpnI R	←	<u>1</u> atggcagaagg ^g tgaagaggccaag tctaccggtac▼ ₃₀₉₈ ... ttttgttgattgctccttagggcc	and <i>KpnI</i> restriction sites
copy-specific cloning of <i>AhHMA3</i> cDNA			
AhHMA3-1 R	←	³¹⁷⁹ ctctggtttgaaacaagtaaccctc	binds in 3'-UTR
AhHMA3-2 R	←	³¹⁸³ ccctctctggtttgaaacaagtatatac	binds in 3'-UTR
cloning of truncated <i>HMA3</i> cDNA			
K01 MS R	←	tca ₂₉₃₆ ttcacgctcatcgcgta	with TGA
K01 R	←	²⁹³⁶ ttcacgctcatcgctagaa	w/o TGA
K01 +T R	←	a ₂₉₃₆ ttcacgctcatcgctagaa	w/o TGA, + T
sequence analysis of cloned <i>HMA3</i> cDNA			
hma302 F	→	⁷⁵⁰ tattctcagttgcagattggc	sequence analysis
hma3g02 F	→	⁵⁵⁵ tgcttcagtcacaaggttc	sequence analysis
HMA304 R	←	¹⁰¹⁶ ccaacctcatcaacatcaacttc	sequence analysis
hma3g03 F	→	¹¹¹⁹ atcattccctgtctccaac	sequence analysis
hma3g03 R	←	¹⁹⁷⁷ cttgcgtagtcaataagcg	sequence analysis
hma302 R	←	²⁶¹⁷ ccgtctcctaccatcattgta	sequence analysis
hma3g02 R	←	²⁶²⁰ agccatctctaccatc	sequence analysis
Site directed mutation of <i>HMA3</i>			
D397A F	→	¹⁷⁰⁸ caagattggtgcttttgcca... aaacaggaactattac	changes D ₃₉₇ KTGT in
D397A R	←	¹⁷⁴³ gtaatagttcctgtttgg... caaaagcaacaatcttg	A ₃₉₇ KTGT
Southern probe preparation for <i>HMA3</i>			
S01 F	←	²⁷³⁵ gattcctaaagggatgagac	3' probe
S01ENTR F	←	cacc ²⁷³⁵ gattcctaaagggatgagac	amplification
S01 R	→	³⁰⁶⁸ acaaccagagcaacaactc	
5probe F	→	¹⁰⁶ gtccacttgacggcgtcaaag	binds in 5' region of
5probe R	←	²⁰ ggcctcttcaccttctgcat	1 st exon, inverse PCR
Real-time RT-PCR primers			
<i>EF1α</i> -F (At5g60390)	→	tgagcacgctcttctgtcttca	constitutive control gene,
<i>EF1α</i> -R	←	ggtggtggcatccatctgtgtaca	Becher <i>et al.</i> , 2004
Ah/Athma1 F	→	cttgagaggttgcaaacgca	Becher <i>et al.</i> , 2004
Ah/Athma1 R	←	tcctctggctttaggttgacg	Becher <i>et al.</i> , 2004
Athma2 F	→	ggtttttgttcaagtcctgctg	I. Talke, L. Krall
Athma2 R	←	gcaatggctatcgctcttca	I. Talke, L. Krall
Ahhma2 F	←	ggttgtgttcaagtcctgctg	I. Talke, L. Krall
Ahhma2 R	←	gcaatgtccatcgctcttca	I. Talke, L. Krall
Ah/Athma3 F	→	²⁶²¹ taacgatgcccggcttta	Becher <i>et al.</i> , 2004
Ah/Athma3 R	←	²⁶⁹¹ ttgcaagtgtgaccctgaga	Becher <i>et al.</i> , 2004
hma3F (BAC Fb)	→	⁵⁸ ttggaatctgctgttcatcgg	universal <i>HMA3</i> primer
Ahhma3-1F (BAC7 F)	→	⁷³ catcggagggtttctatcgtcgg	<i>AhHMA3-1</i> specific
Ahhma3-2F (BAC6 F)	→	⁷³ catcggagggtttctatcgtcacc	<i>AhHMA3-2</i> specific
Ahhma3R (BAC R)	←	²⁰⁷ ccttgacgatttgaagcgga	universal <i>Ahhma3</i> primer

continued on next page...

^aPositions of cloning relevant restriction sites that were introduced are underscored and black triangles (▼) mark the cleavage position. Restriction sites that are not underscored were not used for cloning procedures. Emphasised (**bold-faced**) nucleotides mark substitutions. Deep-placed numbers mark the nucleotide position in the *AtHMA3*-sequence (GenBank accession NC_003075) relative to the transcriptional start (1stATG).

Table 3.3 continued

primer name	orientation	sequence 5'→3' position ^a	description
Athma4 F	→	agagagcacgaattgttccacg	Talke <i>et al.</i> , 2006
Athma4 R	←	gcctgataaccaccaagctagca	Talke <i>et al.</i> , 2006
Ahhma4 F	→	tgaaggtggtggtgattgca	Talke <i>et al.</i> , 2006
Ahhma4 R	→	tccacattgcccaacttcg	Talke <i>et al.</i> , 2006
RACE primers			
5'-RACE R	←	¹⁰⁵ ggagaacgctcggtgacgatagaaacc	
5'-RACEN01 R	←	⁸³ aacctccgatgaacagcagattccaacg	
5'-RACE01 R	←	¹³⁴ ggagaattctttgacgccgcaagtggac	
3'-RACE01 F	→	²⁸⁵⁸ ggcagctgttcttcagatgcaggaacttg	
3'-RACEN01 F	→	²⁹⁷⁴ cggtgaaacttgaggaggatgaagcagagg	
3' UTR R	←	³¹⁸⁶ ggctccctctctggttttgaa	L. Krall
3' UTR02 R	←	³²⁷⁸ cttgcatttcggttcaactc	
BAC primers			
BAC Fa	→	¹⁰⁹ cacttgacgcgctcaagaa	<i>AbHMA3</i> specific
BAC Fb	→	⁵⁸ ttggaatctgctgttcacg	<i>HMA3</i> specific
BAC R	←	²⁰⁷ ccttgacgatttgaagcgga	<i>AbHMA3</i> specific
BAC7 F	→	⁷³ catcggaggtttctatcgtcgg	<i>AbHMA3-1</i> specific
BAC7 02 F	→	⁷³ catcggaggtttctatcgtcgg	<i>AbHMA3-1</i> specific
BAC6 F	→	⁷³ catcggaggtttctatcgtcacc	<i>AbHMA3-2</i> specific
BAC7a R	←	³⁷⁴ agtctcgcttgattcagagccttg	<i>AbHMA3-1</i> specific
BAC6a R	←	³⁷⁴ agtcttgcttgattcaagccttg	<i>AbHMA3-2</i> specific
Other purpose primer			
GUS01 R	←	cacaggccgctcgagtttt	sequence analysis, binds app. 60 bp downstream of the ATG of the β -glucuronidase gene
M13 F(-20)	→	gtaaaacgacggccag	Invitrogen
M13 R	←	caggaaacagctatgac	Invitrogen
M13 F(59)	→	cacgacgttgtaaaacgac	T. Senger
M13 R(60a)	←	ggataacaatttcacacagg	T. Senger
pK7kan F	→	gaccttaggcgacttttgaacgc	analysis of
pK735S R	→	gcacctacaaatgccatcattgcg	pK7GWIWG2(I)
pK7Int F	→	gtctcataccaacaagtgccacc	(RNAi construct)
pK7Int R	←	ggtggcacttgttggtatgagac	Stéphanie Arrivault
MC83 35S F	→	gtaagggatgacgcacaatc	binds in the 35S region of the pMDC83 vector

^aPositions of cloning relevant restriction sites that were introduced are underscored and black triangles (▼) mark the cleavage position. Restriction sites that are not underscored were not used for cloning procedures. Emphasised (**bold-faced**) nucleotides mark substitutions. Deep-placed numbers mark the nucleotide position in the *AtHMA3*-sequence (GenBank accession NC_003075) relative to the transcriptional start (1ATG).

4.1.3 Inverse PCR

Inverse PCR (iPCR) allows to amplify rapidly unknown DNA sequences that flank a region of known sequence (Ochman *et al.*, 1988, 1990). The method uses the PCR, but it has the primers oriented in the reverse direction of the usual orientation. The template for the primers is a restriction fragment that has been ligated upon itself to form a circle (Figure 3.2). Here, the primers '5probe F' and '5probe

R' (Table 3.3) were used to amplify desired but unknown *AbHMA3* flanking promoter regions from self-ligated bacterial artificial chromosome (BAC) fragments.

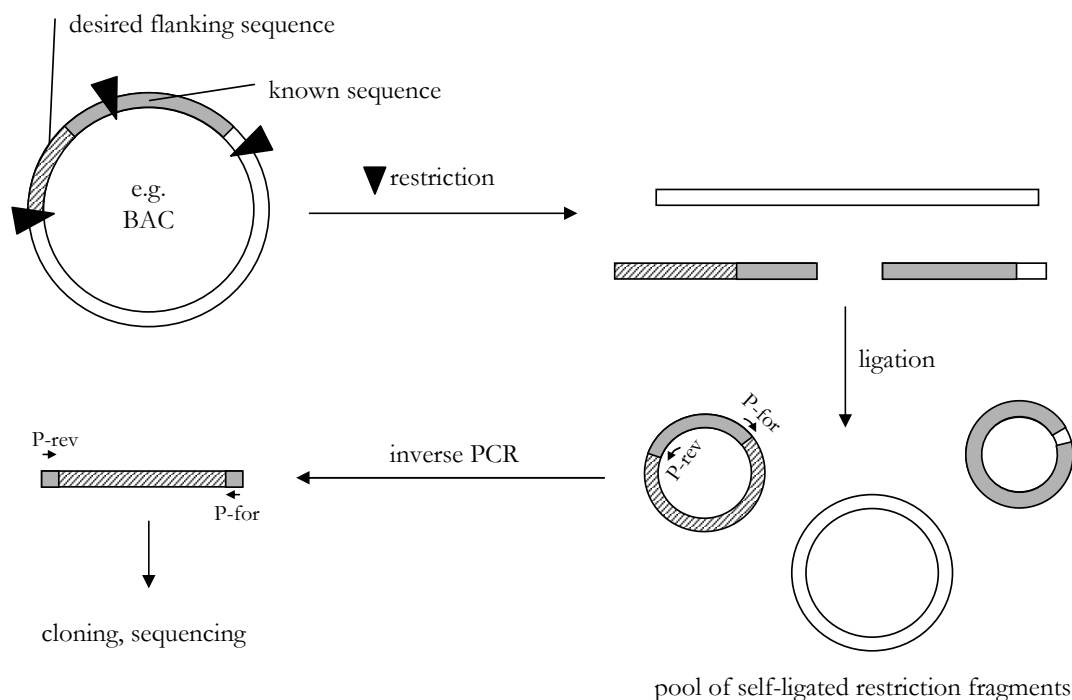


Figure 3.2: Schematic of the inverse PCR procedure.

Filled grey boxes represent the known core sequence. Hatched boxes depict the desired flanking regions. Here, BAC plasmid DNA was prepared from overnight cultures of *E. coli* BAC clones. DNA was digested with suitable restriction enzymes and separated by agarose gel electrophoresis. Restriction sites are marked with black triangles. The restriction fragments were circularised by ligation upon themselves and amplified using PCR with primers that are oriented in opposite directions (P-for and P-rev). Primers and the direction of DNA synthesis are given by arrows.

4.1.4 Real-time RT-PCR

RNA extraction and cDNA synthesis Total RNA was extracted using the QIAGEN RNeasy plant mini-RNA kit (QIAGEN, Hilden, Germany) from approximately 100 mg of frozen material. For each sample, three independent extractions were performed. Genomic DNA was removed using DNAase (DNA-free™, Ambion Europe Ltd., Huntingdon, UK) according to the manufacturer's instructions. The integrity of DNA-free RNA was checked by agarose gel electrophoresis. Equal amounts (1.5 µg) of RNA were reverse transcribed (Superscript™ kit; Invitrogen, Karlsruhe, Germany) with oligo-dT oligonucleotide primers to generate first strand cDNA in 20 µl H₂O_{bidest}. Absence of genomic DNA was checked by PCR using the *EF1α* primers pair chosen to span an intron. Prior to real-time RT-PCR, cDNAs were diluted 1:10 (v/v).

Real-time PCR primers All primers for real-time RT-PCR (Eurogentec, Liege, Belgium) were designed using *Primer Express* software (version 2.0, Applied Biosystems, Foster City, CA, USA) for amplicon lengths between 60 and 100 bp.

Primer sequences are presented in Table 3.3 on page 37. The primer pairs for the constitutively expressed control genes were preferentially chosen to span an intron. The constitutive control genes used in the real-time experiments are indicated in the corresponding figures in the *Results* Chapter of this thesis (Figure 4.18 on page 93 and Figure 4.19 on page 96).

Real-time reactions PCR reactions were performed in a 384-well plate with an Applied Biosystems ABI Prism 5700 Sequence Detection System, using SYBR® GreenI (Eurogentec, Cologne, Germany) to monitor cDNA amplification. For each PCR reaction, 4 µl of diluted cDNA were used. In addition, a PCR reaction contained 6 µl consisting of 5 µl of qPCR™ Mastermix SYBR® GreenI (Eurogentec, Liege, Belgium), 0.5 µl of a mix of the primer pair (10 µM each) and 0.5 µl water. PCR reactions without added template were used as negative controls.

The following standard thermal profile was used: 2 min at 50°C, 10 min at 95°C, followed by 40 cycles of 15 s at 95°C and 60 s at 60°C. Data were analysed using the *GENEAMP 5700 SDS* software (version 1.3, Applied Biosystems, Foster City, CA, USA) and the absence of genomic DNA and side-products of the PCR amplification were confirmed by analysis of dissociation curves and agarose gel electrophoresis of the PCR products.

Data analysis The values presented are mean $\Delta C_T \pm SD$ and mean relative transcript levels calculated from two technical replicates from one experiment representative of a total of two independent experiments. The ΔC_T values were calculated as follows:

$$\Delta C_T = C_T(\text{target gene}) - C_T(\text{constitutive control gene})$$

The C_T value corresponded to the cycle number at which SYBR® GreenI fluorescence, in a real-time RT-PCR, reached an arbitrary threshold value (set at 0.1) during the exponential phase of cDNA amplification. Relative transcript levels (RTL) were calculated as follows:

$$RTL = 1000 \cdot 2^{-\Delta C_T}$$

To calculate the reaction efficiency (R_{eff}) of primer pairs, the *LinRegPCR* software version 7.5 was used (Ramakers *et al.*, 2003). The program uses the fluorescence measured at the end of each cycles to calculate the slope of the curve. The reaction efficiency for each primer pair is determined by

$$R_{eff} = 10^{\text{slope}}$$

Relative transcript levels (RTL) were calculated as follows:

$$\text{RTL} = \frac{(\text{R}_{\text{eff}}^{C_T})_{\text{control gene}}}{(\text{R}_{\text{eff}}^{C_T})_{\text{target gene}}} \cdot 1000$$

The R_{eff} values were included in the calculation of relative transcript levels of *HMA3* copies (see page 92).

4.2 Detection of nucleic acids via hybridisation

4.2.1 Preparation of radioactive probes

Synthesis of DNA fragments A 334 bp fragment of the 3' end of *AbHMA3* was amplified by PCR from a pENTR™-TOPO® vector containing the *AbHMA3* coding sequence (primer 'S01 F' and 'S01 R', Table 3.3 on page 37). A 126 bp fragment of the 5'-end of *AbHMA3* was generated by the digestion of PCR amplified *AbHMA3* with the restriction enzyme *EcoRI*. The resulting fragment was purified by gel extraction (QIAquick Gel extraction Kit; QIAGEN GmbH, Hilden, Germany).

The 5'- and 3'-end fragments served as probes for the detection of *HMA3* specific nucleic acids. Both fragments were used to determine the genomic copy number of *HMA3* and to find suitable restriction enzymes for the digestion of BAC plasmid DNA fragments as a prerequisite step for the inverse PCR (see page 39).

DNA labeling The probe was labeled with radioactive α -³²P-dCTP using the Rediprime™ II random prime labeling system (Amersham Biosciences, Little Chalfont, UK). Different from the manufacturer's instructions, the final incubation step was carried out for 1 to 2 h instead of 10 min. Nick™ columns (Pharmacia, Milton Keynes, UK) were used for radioactive probe purification from residual nucleotides.

4.2.2 DNA:DNA-Hybridisation (according to Southern, 1975)

Gel electrophoresis and DNA blotting After overnight digestion with restriction endonucleases (5 units/μg DNA), 3 μg of genomic DNA was separated on an 1% (w/v) agarose gel. The gel was run at 80 V for at least 2 h in 1× TAE buffer (40 mM Tris, 1 mM EDTA, 20 mM acetic acid).

Subsequently, the gel was prepared for the DNA transfer as follows:

- depurination: 15 min in 0.25 N HCl
- washing: 3 times 5 min in H₂O
- denaturing: 30 min in denaturing solution (0.5 M NaOH, 1.5 M NaCl)
- neutralisation: 3 times 15 min in neutralisation solution
(0.5 M Tris-HCl pH 7.0, 1.5 M NaCl, 1 mM EDTA)

In the meantime, a Hybond™-N+ nylon transfer membrane (GE Healthcare, formerly Amersham Biosciences, Piscataway, NJ, USA) was cut to fit the gel. The membrane was washed in sterile H₂O and shortly soaked in 10× SSC [20× SSC (0.3 M Na-Citrat, pH 7.0, 1.5 M NaCl)]. The DNA transfer from the gel into the membrane was done by a capillary blot overnight (see Figure 3.3).

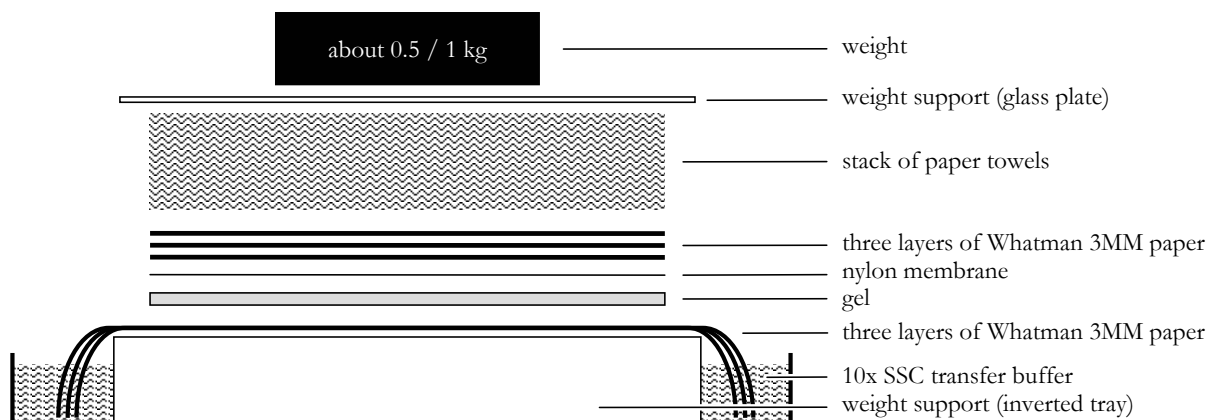


Figure 3.3: Set up of capillary transfer (based on Southern, 1975).

The capillary transfer system was set up by placing a tray filled with 10× SSC transfer buffer, inserting an inverted tray, and laying three layers of Whatman 3MM filter paper pre-wet in 10× SSC on top of the inverted tray. The filter paper stripes were long enough to immerse both ends in the transfer buffer and a bit wider than the gel. The gel was briefly rinsed in H₂O_{bidest} and placed on top of the filter paper with its bottom side facing up. The nylon membrane was moistened in 10× SSC and placed on top of the gel. The formation of air bubbles was avoided. Three sheets of filter paper (pre-soaked in 10×SSC) covered the membrane. Remaining air bubbles were squeeze out by rolling a glass test-tube over the filter paper. Then, a thick stack of dry paper towels was placed on top. A 0.5 to 1 kg weight on top of the transfer stack supported by a glass plate, enhanced the transfer.

On the next day, the position of the gel was marked on the membrane and the membrane was washed in 2× SSC for 15 min. The DNA was cross-linked to the membrane by a three-minute exposure to ultraviolet (UV) light on either side. At this step the membrane could be dried and stored between sheets of filter paper, or it was used directly for the hybridisation.

Prehybridisation and hybridisation The membrane with the cross-linked DNA was shortly rinsed in sterile water to remove salt residues. Then, the membrane was incubated in prehybridisation solution for 2 h at 65°C [Herby buffer: 0.25 M Na-phosphate buffer (Na₂HPO₄, NaH₂PO₄), 1 mM EDTA, 6.6% (w/v) SDS, 10 g/l BSA]. Meanwhile, the probe was radioactively labeled (see above on page 42).

The prehybridisation buffer was exchanged with new Herby buffer including the labeled probe. The membrane was washed after hybridisation (low stringency wash: 2 times 2 min at RT with 2 times SSC, 0.5% (w/v) SDS or if needed, high stringency wash: 2 times 15 min at 68°C with 0.5× SSC, 0.1% (w/v) SDS).

X-ray films were exposed to the membrane for varying amounts of time, depending on the signal

strengths.

5 Techniques related to proteins

5.1 Protein extractions and quantification

5.1.1 Total protein extraction from yeast cultures for SDS PAGE

For each transformant, a 5 ml overnight culture was centrifuged (14000 rpm; 2 min) and the pellet washed with 1 ml 50 mM Tris-HCl (pH 7.5). Glass beads and 30 μ l ESB extraction buffer [2% (w/v) SDS; 80 mM Tris, pH 6.8; 10% (v/v) glycerol; 1.5% (v/v) DTT; 0.1 mg/ml bromophenol blue] were added to the pellet. The ESB buffer was supplemented with a cocktail of protease inhibitors (EDTA-free protease inhibitor cocktail tablets, Roche Diagnostics, Mannheim, Germany). Extraction of total protein was carried out by vortexing 1 min followed by 1 min on ice, repeated four times. Then, 70 μ l ESB buffer were added to the protein extract and the samples denatured at 37°C for 1 h. Protein quantification was performed with the Bradford protein assay to standardise the extracts for protein concentration (Bradford, 1976; Bio-Rad, München, Germany; based on Coomassie®Brilliant Blue G-250 dye that shifts from 465 nm to 595 nm when binding to protein occurs).

5.1.2 Total protein extraction from plants for SDS PAGE

Plant tissues were ground with mortar and pestle in 100°C hot ESB extraction buffer in the presence of sea sand. The extracts were centrifuged at 14000 rpm for 10 min to remove debris and kept at -70°C until further utilisation. Protein quantification was performed with the Bradford protein assay (Bradford, 1976; Bio-Rad, München, Germany; based on Coomassie®Brilliant Blue G-250 dye that shifts from 465 nm to 595 nm when binding to protein occurs).

5.1.3 Denaturing-gel electrophoresis and Western Blotting

Proteins were separated on a 10% (v/v) denaturing SDS-polyacrylamide gel and subsequently transferred to polyvinylidene difluoride membranes (Immobilon™, Bedford, MA, USA) by electroblotting (Towbin *et al.*, 1979).

Membranes were blocked in 1× PBST [0.1% (v/v) Tween 20, 10 mM Tris, 0.9% (w/v) NaCl, pH 7.4] with 10% (w/v) non fat dry milk overnight at 4°C and then washed briefly in 1× PBST. Blots were probed for 2 h in 1× PBST and 1% (w/v) non fat dry milk either with a mouse monoclonal anti-HA antibody (Covance Research Products, Santa Clara, CA, USA; 1:5000) or with the specific rabbit polyclonal anti-AbHMA3 antibody (1:250). The anti-AbHMA3 antibody was raised in rabbits against a synthetic peptide. Antisera were collected and affinity purified (Eurogentec, Cologne, Germany). After incubation in solutions containing the primary antibody, the membranes were washed in 1× PBST and 1% (w/v) non fat dry milk three times for 10 min each. Membranes were incubated

with sheep anti-mouse-IgG or donkey anti-rabbit-IgG peroxidase-conjugated antibodies (Amersham Biosciences, Little Chalfont, UK; 1:10000) in 1× PBST and 1% (w/v) non fat dry milk followed by three washes for 10 min each in 1× PBST and 1% (w/v) non fat dry milk. Proteins were detected by enhanced chemiluminescence (ECL) using an ECL protein gel blot detection kit (Amersham Biosciences, Little Chalfont, UK) according to the manufacturer's instructions.

5.2 Protein expression and -purification with *Strep-Tag*[®] II-System

This *Strep-Tag*[®] II-system (Institut für Bioanalytik (IBA), Göttingen, Germany) allows the efficient expression and fast purification of recombinant proteins in *E. coli*. It is based on the stringent regulated expression of a protein under the control of the tetracycline promoter (*tetA* promoter, Skerra, 1994) and the selective binding of the *Strep-Tag*[®] II peptide (NH₂-WSHPQFEK-COOH) during the purification on *StrepTactin*[®]. The *Strep-Tag*[®] II peptide should neither influence the folding nor the function of the recombinant protein. The cloning of the recombinant gene into the *Strep-Tag*[®] vector fuses the protein with the *Strep-Tag*[®] II peptide after expression. The fused protein can be purified by affinity chromatography on immobilised *StrepTactin*[®]. The protein is eluted by specific competition with desthiobiotin.

5.2.1 Cell growth, induction of expression and cell harvest

The constructed plasmids were transformed into the host strain *E. coli* DH5 α . The main cultures were started from fresh cell material of a single colony and grown at room temperature or 30°C in 20 to 500 ml LB medium containing 125 μ g/l carbenicillin. The culture was grown to an OD₆₀₀ of about 0.5. Sometimes the main culture was started from a preculture that was grown over night in 3 ml LB medium at 37°C.

The *tetA* promoter was induced by supplying anhydrotetracycline (AHT) to the main culture. The maximum activity is reached with a final concentration of AHT of 200 μ g/l. The growth of the culture was monitored for 3 h. Samples of 200 μ l were taken after 0, 1, 2, and 3 h. In the end, the main culture was centrifuged at 5000 rpm and 4°C for 15 min (Hettich Universal 30 RF, Tuttlingen, Germany). The supernatant was removed carefully and the cell pellets were stored at -20°C.

5.2.2 Breaking of cells and obtaining raw extract by ultrasonification

The cell pellet was resuspended in 2 ml (per 50 ml culture) of ice chilled buffer W (100 mM Tris/HCl pH 8.0, 1 mM EDTA). Forty μ l of this suspension were taken for the analysis of the total cell protein by SDS-PAGE. The cells were ruptured by ultrasonification (Uniequip Laborgerätebau UW60, Martinsried, Germany) under constant cooling at a maximum output of 60 W and an impulse frequency of 1 Hz. The procedure was continued until the cell suspension became translucent. For the separation of cell debris, the suspension was centrifuged at 5000 rpm and 4°C for 20 min. Afterwards the

supernatant could be purified on a *StrepTactin*[®] column.

5.2.3 Affinity purification by *StrepTactin*[®] sepharose

A disposable column (polypropylene column 1 ml, QIAGEN, Hilden, Germany) was filled with 0.5 ml of immobilised *StrepTactin*[®] and equilibrated with 5 ml of buffer W (100 mM Tris/HCl pH 8.0, 1 mM EDTA). The column was loaded with clear raw extract. The used volume was chosen to allow the passing of about 40 mg total protein extract through the column at constant gravity. With it, the fusion protein binds to the *StrepTactin*[®]. Run-through sample volumes of 1 ml were collected in 1.5 ml reaction plastic tubes (Eppendorf, Hamburg, Germany) and stored on ice. Other proteins were removed by the following washing steps:

After the complete uptake of the sample into the column material, the column was washed 5 to 10 times with 1 ml of buffer W (optionally including 1 M NaCl). The run-through was collected in 1 ml fractions. The elution of the recombinant protein was done by adding 3 ml of buffer E (100 mM Tris/HCl, pH 8.0; 1 mM EDTA; 2.5 mM desthiobiotin). The eluate was collected in 0.5 ml fractions and stored on ice. The fractions were frozen at -20°C for long-term storage.

Column regeneration was done by washing 3 times with 5 ml of buffer R (100 mM Tris/HCl pH 8.0, 1 mM EDTA, 1 mM HABA). This changed the matrix colour from yellow-orange into red due to free binding sites. This change of colours indicates the regeneration process as well as the activity state of the column. Afterwards, buffer R was removed by washing twice with 4 ml of buffer W. This decoloured the column again. The *StrepTactin*[®] column was covered with 2 ml of buffer W and stored at 4°C until the next use.

6 Enzyme assays

6.1 Analysis of β -glucuronidase activity

6.1.1 Histochemical staining

Plant tissues were harvested, transferred into ice-cold 90% (v/v) acetone and incubated at room temperature for 20 min. Tissues were washed in staining buffer (0.2% (v/v) Triton X-100; 50 mM Na-PO₄ buffer, pH 7.2; 2 mM potassium ferrocyanide; 2 mM potassium ferricyanide) and transferred into staining buffer supplemented with 2 mM 5-bromo-4-chloro-3-indolyl- β -D-glucuronide (X-Gluc) (Duchefa, Harlem, The Netherlands).

Samples were infiltrated under vacuum for 20 min and stained at 37°C for several hours or overnight followed by an incubation in 30% (v/v) ethanol for 1 h, and in fixative solution for 30 min [50% (v/v) ethanol; 5% (v/v) formaldehyde; 10% (v/v) acetic acid]. Removal of the remaining chlorophyll was performed by successive incubations in 70% (v/v) and 90% (v/v) ethanol. Samples were kept in 90% (v/v) ethanol at 4°C until further utilisation. Digital images were recorded using a *Meta Imaging*

Series program (Universal Imaging Corporation, Puchheim, Germany).

6.1.2 Fluorometric GUS activity assay

Fluorometric assays were performed as described (Jefferson *et al.*, 1987), with some modifications. Fresh plant tissues (roots or shoots pooled from 5 to 7 *Arabidopsis* seedlings) were ground in 200 μ l extraction buffer [50 mM phosphate buffer, pH 7.4; 10 mM β -mercaptoethanol; 10 mM EDTA; 0.1% (w/v) SDS and 0.1% (v/v) Triton X-100]. The samples were centrifuged at 14000 rpm for 15 min at 4°C.

Ten μ l of supernatant were transferred to 300 μ l GUS assay buffer [1 mM 4-methyl umbelliferyl β -D-glucuronide (4-MUG) in extraction buffer]. After incubation at 37°C for 2 h, the reactions were stopped by addition of 300 μ l of 200 mM Na_2CO_3 . The fluorescence of 4-methylumbelliferone (4-MU) was determined with a sensitivity of 75. Protein concentrations in protein extracts were determined by a Bradford assay (Bradford, 1976; Bio-Rad, München, Germany; based on Coomassie® Brilliant Blue G-250 dye that shifts from 465 nm to 595 nm when binding to protein occurs) according to the manufacturer's instructions. Ten μ l of protein extract were diluted in 190 μ l assay solution. By testing a 200 μ l blank control that contained 10 μ l of the extraction buffer, it was ensured that the used SDS and Triton X-100 concentrations do not affect the Bradford assay. After calibration with the fluorescent product 4-MU, the fluorometric activity was expressed in fmol 4-MU/ μ g protein/min.

Fluorometric GUS activity assay using protoplast The following modifications were made to the protocol: 75 μ l of the prepared protoplast extract (see page 50) were mixed by pipetting with 75 μ l 2 \times GUS assay buffer and incubated for 3 h at 37°C. The reaction was stopped with 150 μ l 0.2 M Na_2CO_3 .

7 Yeast experiments

7.1 Yeast strains

Yeast strains that were used in experiments are listed in Table 3.4 below.

7.2 Transformation of *Saccharomyces cerevisiae*

Competent yeast cell preparation and transformation were carried out using a modified ethylene glycol method (Dohmen *et al.*, 1991).

7.2.1 Preparation of competent frozen yeast cells

A 5 ml culture was grown overnight in YPAD (10 g/l Bacto yeast extract; 20 g/l Bacto peptone; 20 g/l D-glucose; 100 mg/l adenine hemisulfate) and used to inoculate a 100 ml YPAD culture. When the OD_{600} reached 0.6, yeast cells were centrifuged (2400 rpm, 10 min), washed in 20 ml solution A

Table 3.4: Yeast strains.

strain	genotype	comment and reference
$\Delta zrc1 \Delta cot1$	Mat a, <i>zrc1::natMX3</i> , <i>cot1::kanMX4</i> , <i>his3Δ1</i> , <i>leu2Δ0</i> , <i>met15Δ0</i> , <i>ura3Δ0</i>	Dräger <i>et al.</i> , 2004
BY4741	Mat a, <i>his3Δ1</i> , <i>leu2Δ0</i> , <i>met15Δ0</i> , <i>ura3Δ0</i>	$\Delta zrc1 \Delta cot1$ parental wild type strain, Goldstein and McCusker, 1999
YYA4	Mat a, $\Delta ycf1::loxP-KAN-loxP$, $\Delta ybl035::HIS3$, <i>ade2-1</i> , <i>his3-11, -15</i> , <i>leu2-3</i> , <i>112 trp1-1</i> , <i>ura3-1</i> , <i>can1-100</i>	Gaedeke <i>et al.</i> , 2001
W303-1A	Mat a, <i>ade2-1</i> , <i>his3-11, -15</i> , <i>leu2-3</i> , <i>112 trp1-1</i> , <i>ura3-1</i> , <i>can1-100</i>	YYA4 parental wild type strain, Thomas and Rothstein, 1989

[10 mM bicine, pH 8.35; 1 M sorbitol, 3% (v/v) ethylene glycol], centrifuged and resuspended in 2 ml solution A. Aliquots (200 μ l) were made and stored until further utilisation at -70°C.

7.2.2 Transformation and selection of yeast

A total of 1 μ g plasmid and 50 μ g salmon sperm DNA denatured by boiling was added to the frozen cells. After thawing at 37°C for 5 min, 1 ml of solution B [200 mM bicine, pH 8.35; 40% (w/v) PEG 1000] was added and gently mixed for 1 h at 30°C. Yeast cells were then centrifuged (3000 rpm, 2 min), the pellet washed twice in 800 μ l solution C (10 mM bicine, pH 8.35; 150 mM NaCl) and finally resuspended in 100 μ l solution C. Transformants were selected on solid minimal medium (SC) lacking uracil (Sherman *et al.*, 1986) with 2% (w/v) D-glucose as carbon source.

7.3 Complementation assays

7.3.1 Drop test experiment

For each construct, two independent transformant colonies were grown overnight at 30°C in 2 ml SC-URA to early stationary phase ($OD_{600} \approx 1.0$). Yeast cells were washed twice in sterile water and resuspended in low sulphate/phosphate (LSP) medium (modified according to Conklin *et al.*, 1992). This media contains 80 mM NH_4Cl , 0.5 mM KH_2PO_4 , 2 mM $MgSO_4$, 0.1 mM $CaCl_2$, 2 mM NaCl, 10 mM KCl, trace elements (1.4 μ M $ZnSO_4$, 2.5 μ M $MnSO_4$, 8 μ M H_3BO_3 , 0.1 μ M $CuSO_4$, 0.6 μ M KI, 1.8 μ M $FeSO_4$, and 0.7 μ M NH_4MoO_4), vitamins (0.08 μ M biotin, 16.78 μ M D-pantothenic acid hemicalcium salt, 32.5 μ M nicotinic acid, 19.5 μ M pyridoxine HCl, 11.8 μ M thiamine, and 111 μ M inositol), 2% (w/v) D-glucose and is lacking uracil (URA). Twenty μ l of each of several dilutions of each cell suspension were spotted on agar plates (1.5% (w/v) agarose; Seakem, BMA, Rockland, ME, USA) containing control LSP-URA or LSP-URA supplemented with various concentrations of transition metal salts from sterile stock solutions of $ZnSO_4$ (0.1 M), $CoCl_2$ (0.1 M), $CdSO_4$ (1 M) or $FeSO_4$ (0.1 M), respectively. The plates were sealed with parafilm and incubated at 30°C for 3 days.

7.3.2 Liquid culture experiment

For each construct, six independent transformant colonies were grown overnight as described above. Then, yeast cells were washed once in water and resuspended in LSP-URA medium. A total volume of 3 ml control LSP-URA or LSP-URA supplemented with concentrations of ZnSO₄ between 0.25 mM and 10 mM was inoculated with yeast cells at a cell density of 0.3·10⁶ cells/ml. Cultures were incubated at 30°C with constant mixing in a culture wheel, and OD₆₀₀ values were measured after 72 h.

7.4 Metal ion accumulation assays

A total volume of 5 ml LSP-URA without supplements or with added 100 μM ZnSO₄ was inoculated with overnight-grown yeast cells at a cell density of 0.6·10⁶ cells/ml, and cultivation was performed as mentioned above. After 24 h of growth, the cells were collected by centrifugation (8000 rpm, 10 min) and resuspended in ice-cold 10 mM CaCl₂ to desorb loosely bound Zn. Cells were washed two more times with CaCl₂, finally once with deionised water and OD₆₀₀ values were measured again. Yeast cell pellets were dried overnight at 60°C, digested with 65% (v/v) HNO₃ using a microwave-accelerated-reaction-system (CEM Corporation, Matthews, NC, USA) and diluted in water. Metal concentrations of the samples were determined by Inductively Coupled Plasma Optical Emission Spectrometry (ICP-OES, ThermoFisher Scientific, Waltham, MA, USA).

8 Techniques related to plants

8.1 Plant material and plant transformation

Plant expression vectors were introduced by electroporation into *A. tumefaciens* strain GV3101 with the pMP90 plasmid unless indicated otherwise. *A. thaliana* (L.) HEYNHOLD (accession Columbia, Col-0) plants were transformed by floral-dip infiltration (Clough and Bent, 1998).

The T-DNA insertion line 274D12 (*AtHMA3* knockout, *hma3-a*³, Columbia ecotype) was obtained from the GABI-KAT collection (Genomanalyse im biologischen System Pflanze - Kölner Arabidopsis T-DNA lines; Rosso *et al.*, 2003).

For real-time RT-PCR experiments, cDNA was synthesised from total RNA of *A. thaliana* plants from the Wassilewskija (Ws) and the Brunn (Br) accessions in addition to total RNA from the Col-0 ecotype.

Arabidopsis halleri ssp. *halleri* (L.) O'KANE and AL'SHEHBAZ (O'Kane and Al-Shehbaz, 1997; Al-Shehbaz and O'Kane, 2002) plants derived from seeds of a single mother plant that was grown from seeds collected at Langelsheim, Germany (accession Langelsheim, Lan).

³Two T-DNA insertion lines are available at GABI-Kat (*Genomanalyse im biologischen System Pflanze - Kölner Arabidopsis T-DNA lines*), 274D12 (*hma3-a*) and 606H08 (*hma3-b*). However, the *hma3-b* line was not ordered because the T-DNA insertion is located 533 bp downstream of the transcriptional stop of *HMA3* and thus, is not considered to disrupt *HMA3* activity efficiently.

8.1.1 Transient expression in *Arabidopsis* suspension culture cells

The used suspension culture of *A. thaliana* cells was originally provided by Sébastien Thomine⁴ and prepared as described in Elzenga (1991) and Thomine *et al.* (1995).

Protoplast preparation Two times 40 ml of 2 to 5 day-old *Arabidopsis* cells (accession Columbia) were sedimented in 50 ml plastic tubes by centrifugation at 1500 rpm for 5 min. The supernatant was discarded. The cells were resuspended in 25 ml enzyme solution [1% cellulase (Serva), 0.2% macerozyme (Yakult Honsha, Tokyo, Japan); in B5-0.34 M GM] and filled to 50 ml with B5-0.34 M GM [B5 powder (Duchefa, Harlem, The Netherlands), 0.34 M glucose, 0.34 M mannitol, pH 5.5 with KOH]. The suspension was transferred to two large petri dishes and 25 ml of B5-0.34 M GM were added to each. Then, the suspension cultures were shaken gently for about 3 h while checking the release of protoplasts every hour under the microscope. Afterwards, the cells were transferred to two 50 ml plastic tubes and sedimented at 1500 rpm for 5 min. The supernatant was discarded, the cells were resuspended in 25 ml of B5-0.34 M GM and sedimented again at 1500 rpm for 5 min. After the supernatant was removed, the pellets were resuspended in 5 ml of B5-0.28 M S each [B5 powder (Duchefa, Harlem, The Netherlands), 0.28 M sucrose, pH 5.5 with KOH]. The suspended cells were combined in a 13 ml plastic tube and centrifuged at a maximum rate of 400 to 500 rpm for 5 min. Afterwards, the cells should float. If not, the spinning time was increased. The floating cells were transferred to a new 13 ml plastic tube and could be stored at 4°C. Cells were counted and checked for their quality under the microscope in a 1:100 dilution.

Protoplast transformation Five µg of each plasmid (max. 15 µg) in 15 µl H₂O were used. Fifty µl with 2·10⁵ cells were added and mixed with plasmid solution by tipping against the tube wall. Then, 150 µl PEG solution (25% PEG 6000, 0.45 M mannitol, 0.1 M Ca(NO₃)₂, pH 9.0 with KOH) was added immediately and mixed again by tipping against the tube. The mixture was incubated for 15 to 30 min at room temperature in the dark followed by a washing step with 2 times 0.5 ml of 0.275 M Ca(NO₃)₂. The tube was inverted several times and centrifuged at 250 rpm for 10 min. The supernatant was sucked using a vacuum pump and a glass pipette. For cultivation, 0.5 ml of B5-0.34 M GM was added.

Preparation of transformed protoplast for fluorometric GUS activity assay After transformation, the cells were centrifuged at 800 rpm (67 g) for 2 min. After removal of the medium, 200 µl of CCLR buffer (Cell Culture Lysis Reagent, Luciferase Assay System, Promega, Madison, WI, USA) was added. Then the solution was vortexed for 1 min and spun down at 13500 rpm for 5 min at 4°C. The supernatant was stored on ice and was used for a fluorometric GUS activity assay (see page 47).

⁴Institut des Sciences du Végétal, CNRS UPR 2355, 1 Avenue de la Terrasse, 91198 Gif-sur-Yvette Cedex, France

8.1.2 Stable transformation of *Arabidopsis thaliana*

Plant expression vectors were introduced by electroporation into *A. tumefaciens* strain GV3101 with the pMP90 plasmid unless indicated otherwise (Mersereau *et al.*, 1990). *A. thaliana* (L.) HEYNHOLD (accession Columbia, Col-0) plants were transformed by floral-dip infiltration (Clough and Bent, 1998).

Transformation of *A. tumefaciens* A 50 µl aliquot of competent *A. tumefaciens* cells were mixed with about 100 ng plasmid DNA on ice and transferred to a cooled 2 mm cuvette. The cuvette was dried and then inserted into the electroporation device (electroporation conditions: 400 Ω, 25 µF, 2.5 kV for 5 ms). In the next step, 1 ml YEB medium without antibiotics was added, mixed well, and transferred to precooled 1.5 ml plastic reaction tubes. For cell regeneration, the tubes were incubated for 2 to 4 h at 28 °C and about 180 rpm. After that time, 200 µl of the cells were plated on selective YEB plates and incubated for 2 to 3 days at 28 °C.

Floral-dip infiltration Ten ml of selective YEB medium were inoculated with a fresh colony of transformed *A. tumefaciens*. The medium was incubated overnight at 28 °C and 200 rpm. The culture was transferred into 400 ml selective YEB medium and cultivated overnight at 28 °C and 200 rpm. The cells were sedimented by centrifugation at 4000 rpm for 30 min at room temperature, and the supernatant was removed. The pellet was resuspended in 400 ml infiltration medium [5% (w/v) saccharose, 0.22% MS salt (Murashige and Skoog, 1962), 0.005% 2-(N-morpholino) ethanesulfonic (MES) acid buffer (Duchefa, Harlem, The Netherlands), 10 µl 6-benzylaminopurine (BAP) (1 mg/ml in dimethyl sulfoxide), pH 5.75 with KOH].

Two glass pots were each filled with 200 ml resuspended cells, 100 ml infiltration medium and 500 µl Silwet L-77 (Helena Chemical, Fresno, USA). The inflorescences of about six-week old *Arabidopsis* plants were immersed in this suspension for about 2 to 5 s. The plants were pulled out of the suspension, laid on filter paper and covered with a plastic hood. On the next day, the cover was removed, the plants were positioned upright and cultivated for seed production.

For seed sterilisation and further selection steps in plants see page 53 below.

8.1.3 Stable transformation of *Arabidopsis halleri*

Because of the self-incompatibility, a difficult flowering induction and the low amount of seeds (10-20) produced by *A. halleri*, the method of transformation by floral-dip infiltration (Clough and Bent, 1998) is not feasible in this species. Therefore, a stable transformation system based on the co-cultivation of root-callus pieces with transformed *A. tumefaciens* was established by Ina Talke (group of Ute Krämer, MPI-MP, Potsdam, Germany). The used hormone concentrations are based on a publication of Chateau *et al.* (2000).

Seed sterilisation and plant growth Seeds of *A. halleri* were sterilised as described (see page 53) and grown for 4 to 6 weeks in small glass pots containing sterile Arabidopsis medium “*ohne Zucker*” (sugar free) medium [AMTZ, sugar free 0.5× MS medium (Murashige and Skoog, 1962), 0.7% (w/v) Select agar (Invitrogen, Karlsruhe, Germany), adjusted to pH 5.7] supplemented with 1% (w/v) sucrose.

Callus induction of root tissue The plants were pulled out of the agar medium and the shoots were cut off. Then the roots were washed in liquid AMTZ medium and cut into small pieces of approximately 5 mm in length. Several root pieces were put in groups onto CIM medium [callus inducing 1× MS medium (Murashige and Skoog, 1962) with 2% (w/v) sucrose, 0.7% (w/v) select agar (Invitrogen, Karlsruhe, Germany), 1 mg/l 2,4-dichlorophenoxy acetic acid (2,4-D) and 0.5 mg/l kinetin] and were stored in the dark at room temperature for 7 to 8 days. The calli developed at the cut ends of root pieces and were visible after about a week.

Transformation using Agrobacteria Fresh colonies of transformed *A. tumefaciens* (see page 49) were incubated in 4 ml of selective YEB medium. Depending on the used strain, the cultures were incubated for 1.5 to 3 days at 30°C and then transferred into 50 ml selective YEB medium. After 1 to 2 days, the cultures were centrifuged at 3500 rpm for 5 min at 20°C. Cultures were harvested in the middle of their logarithmic growth phase. The pellets were washed twice with 20 ml 10 mM MgSO₄ and centrifuged in between for 10 min. In the end, the pellets were resuspended in 15 ml 1× MS containing 2% (w/v) sucrose. After the resuspension, the cultures were put back onto a shaker for 1 h in order to recover and thus increasing their infectionness.

About 5 to 10 ml Agrobacteria suspension was poured into small petri dishes. The root-callus pieces were bathed in that suspension for 10 min and then put on sterile filter paper to blot off excess liquid and bacteria. Then, the roots were put back onto CIM medium. The roots and Agrobacteria were co-cultivated on CIM for 2 to 3 days in the dark at RT.

Regeneration of transformed plants The calli were transferred onto SIM medium [shoot inducing 1× MS medium (Murashige and Skoog, 1962) with 2% (w/v) sucrose, 0.7% (w/v) select agar (Invitrogen, Karlsruhe, Germany), 1 mg/l 6-benzyladenine (BA) and 0.5 mg/l α -naphthaleneacetic acid (NAA); always supplemented with 125 mg/l β -bactyl to kill off the Agrobacteria]. The transfer was repeated weekly on new SIM plates gradually introducing selective antibiotics (1st week: without antibiotics, 2nd week: half concentrated antibiotics, 3rd week: full antibiotic concentration). The weekly change of medium was continued for several weeks until the induced shoots became bigger. Then they were moved into small plastic pots (80 mm diameter × 90 mm high) containing SIM medium.

Bigger shoots that were all green on selective SIM medium for several weeks were then transferred onto RIM medium [root inducing 1× MS medium (Murashige and Skoog, 1962) with 2% (w/v)

sucrose, 0.7% (w/v) select agar (Invitrogen, Karlsruhe, Germany), 1 mg/l indolyl-3-acetic acid (IAA), selective antibiotics and 125 mg/l β -bactyl] in small plastic pots (80 mm diameter \times 90 mm high). The clustered shoots had to be taken apart in order to ensure that single shoots are transferred. The roots needed about two weeks to develop. After 4 to 6 weeks the plants were developed enough to transfer one cutting in a big glass jar (100 mm diameter \times 147 mm high, 850 ml, Weck No.743; Weck Company, Wehr, Germany) with RIM medium and the rest of the plant with roots onto soil.

8.2 Growth conditions

8.2.1 Plant growth on soil

A. thaliana plants were grown on a mixture of 1:1 (v/v) standard soil (GS90) and vermiculite in a greenhouse (20°C day / 18°C night; 50% relative humidity day / 80% night; 16 h photoperiod at 250 μ mol/m²/s).

8.2.2 Plant growth on plates

Seed sterilisation and seeding Seeds of *A. thaliana* were surface sterilised for 3 min with 70% (v/v) ethanol in 1.5 or 2 ml plastic reaction tubes (Eppendorf, Hamburg, Germany). This step was followed by one wash for 10 min with bleach solution [3% (w/v) NaOCl, 0.05% (w/v) Tween 20, diluted in sterile H₂O_{bidest}] and four washes with sterile deionised water. For *A. thaliana*, sterile seeds were resuspended in sterile 0.1% (w/v) agarose and disposed one per one on square polyethylene plates (120 mm \times 120 mm \times 15 mm) containing approximately 50 ml of appropriate media with a seed microtiter pipette (Ultipipette, Agar, Germany).

This procedure is not applicable to seeds of *A. halleri* due to their larger size. Therefore, for selection of *A. halleri* plants, seeds were dried overnight on sterile filter paper (Whatman International, Maidstone, UK) and then spread on square polyethylene plates (120 mm \times 120 mm \times 15 mm) containing approximately 50 ml of appropriate media using a bent sterile glass pipette.

Plant growth media Sterile AMOZ medium corresponding to sugar free 0.5 \times MS (Murashige and Skoog, 1962) medium supplemented with 0.7% (w/v) select agar (Invitrogen, Karlsruhe, Germany) and adjusted to pH 5.7 was used. For selection of transformed plants, this medium was supplemented with 0.5% (w/v) sucrose and the appropriate antibiotic. Kanamycin (Sigma, Seelze, Germany) was used at a final concentration of 50 mg/l and DL-phosphinotricin at 25 mg/l (Duchefa, Harlem, The Netherlands). As a control of selection efficiency, wild-type seeds were subjected to the same selection.

The control 0.25-strength Hoagland medium (Hoagland and Arnon, 1938; Becher *et al.*, 2004) is a minimal medium used for metal ion treatments containing 0.28 mM KH₂PO₄, 1.25 mM KNO₃, 1.5 mM Ca(NO₃)₂, 0.75 mM MgSO₄, 5 μ M Fe-HBED [a complex of Fe(III) and N,N'-di-(2-hydroxybenzoyl)-ethylenediamine-N,N'-diacetate]; Strem Chemicals, Inc., Newburyport, MA, USA], 5 μ M

H₃BO₃, 5 μM MnSO₄, 1 μM ZnSO₄, 0.5 μM CuSO₄, 50 μM KCl and 5 μM Na₂MoO₄, 3 mM MES acid buffer (Duchefa, Harlem, The Netherlands), and buffered at pH 5.7 with KOH prior to autoclaving. In case of iron or zinc deficiency, Fe-HBED or ZnSO₄ were respectively omitted during preparation. For metal treatments, sterile seeds were germinated on plates containing control 0.25-strength Hoagland medium supplemented with 0.5% (w/v) sucrose, 0.9% (w/v) phytoagar (Sigma). Depending on the metal treatment, the medium was supplemented with metal from sterile stock solutions of ZnSO₄ (0.1 M), CoCl₂ (0.1 M), or FeHBED (0.5 M). To induce Zn deficiency, 0.25-strength Hoagland medium without ZnSO₄ was used, and Seakem agarose was chosen instead of phytoagar. Seakem agarose showed the lowest Zn content by ICP-OES analysis (see Table 3.5), among different agaroses and agars available. As a control, 0.25-strength Hoagland medium (1 μM ZnSO₄) and Seakem agarose were used in Zn deficiency experiments.

Table 3.5: Zinc contents in various agars.^a

	Seakem agarose	Noble agar	Phytoagar
Zn (μmol/g)	0.01	0.07	0.03

^aas measured by ICP-OES according Talke *et al.* (2005), unpublished data

Seedling growth conditions After seeding, square polyethylene plates (120 mm × 120 mm × 15 mm) plates were sealed with Leucopore tape (Beiersdorf, Hamburg, Germany), and kept horizontally at 4°C for 3 days for stratification. For subsequent determination of elemental contents, plates were then placed vertically for one month in a climate-controlled growth cabinet (20°C day / 16°C night; 60% relative humidity day / 75% night; 14 h photoperiod at a photon flux density of 120 μmol/m²/s; Percival, CLF Laborgeräte GmbH, Emersaker, Germany). For all other purposes, plates were placed vertically in a climate-controlled growth cabinet with the same parameters as described above but with a 16 h photoperiod. Antibiotic selection was carried out for 10 days, unless indicated otherwise. Depending on the purpose, seedlings were subsequently analysed or transferred onto soil or onto different plates for metal treatments. Durations of metal treatments used in this study are indicated in the *Results* Chapter.

8.2.3 Hydroponical plant growth

Plant seeds were placed on a layer of 0.8% (w/v) solidified Noble agar (Bio101, Vista, CA, USA) in clipped black 0.5 ml plastic tubes (Eppendorf, Hamburg, Germany), and germinated and cultivated in a modified 0.25-strength Hoagland solution (Hoagland and Arnon, 1938; Becher *et al.*, 2004; see above on page 53 for composition). After germination, solutions were exchanged weekly.

Plants were grown in a climate-controlled growth chamber (20°C day / 16°C night; 60% relative humidity day / 75% night; 14 h photoperiod at 120 μmol/m²/s; Percival, CLF Laborgerate GmbH,

Emersaker, Germany).

When plants were 6 weeks old, the hydroponic solutions were replaced by the experimental treatments as described in the corresponding *Results* Sections.

8.3 Analysis of transgenic plants

8.3.1 GFP analysis by confocal microscopy

Approximately 100 plants of the T1 generation and 20 selected lines of the T2 generation transformed with a *p35S-AhHMA3:GFP6* construct were selected for kanamycin resistance and tested for fluorescent GFP signals. Fluorescence were visualised by confocal laser scanning microscopy (Leica TCS SP2, Leica Microsystem, Wetzlar, Germany) with excitation at 488 nm. Green fluorescence of GFP was detected between 490 nm and 510 nm. Digital images were recorded using the confocal operating system software.

8.3.2 Characterisation of homozygous transgenic lines

A total of 100 seeds from the T2 generation were placed with a micropipette on appropriate selective media. After two weeks of growth in a cabin, the numbers of non-germinated seeds, tolerant and non-tolerant seedlings were counted. To determine if the transgenic lines were carrying T-DNA insertions at a single or at several loci, the following ratio was calculated for each independent line: tolerant seedlings/total germinated seedlings. Based on Mendelian genetics (Mendel, 1866), a ratio of approximately 0.75 tolerant seedlings per germinated seedlings corresponds to a single T-DNA insertion. Lines exhibiting this ratio ± 0.05 were kept and propagated to the T3 generation. Selection was performed on the T3 generation to find homozygous individuals showing a ratio of 1 tolerant seedling per germinated seedling.

8.3.3 Metal tolerance assays

Measurement of root elongation Ten to twenty seeds per selected individual and per selected line or wildtype were germinated in square polyethylene plates (120 mm \times 120 mm \times 15 mm) on approximately 50 ml MS medium supplemented with 0.7% (w/v) select agar and 0.5% (w/v) sucrose. Four days after germination, the seedlings were transferred onto 0.25-strength Hoagland medium containing 1, 10, 30, 60, 150 and 300 μ M ZnSO₄. Every third day, the root length was measured. In order to reduce the effect of minimal difference in the initial root lengths of control and knockout line on the day of transfer, the obtained data was normalised to the root length on day 7. The normalisation is based on day 7 instead of day 4 because the longer roots on day 7 allowed more accurate length measurements. The normalisation was performed by calculating a root elongation factor as the ratio of root length on the final day and day 7.

Part III

Results

Chapter 4

Characterisation of *HMA3* and the encoded protein

1 Genomic organisation, function and localisation

1.1 Characterisation of *HMA3* at the genomic and mRNA level

1.1.1 Copy Number of *AbHMA3*

A Southern hybridisation was chosen to gain insights into the organisation of the *HMA3* gene in the *A. halleri* genome. A ³²P-labeled 334 bp PCR fragment from the 3'-end of the transcribed region of *AbHMA3* served as a *HMA3* specific probe. The probe did not span an intron and none of the used enzymes cut within the probe sequence.

As expected, only one signal was detected after digestion of genomic DNA from the *A. thaliana* ecotype Columbia with the restriction enzymes *EcoRI*, *DraI*, or *EcoRV*, respectively. The *AtHMA3* containing fragments were detected at their predicted sizes (*EcoRI*: 5.2 kbp, *DraI*: 2.4 kbp, and *EcoRV*: 3.9 kbp; Figure 4.1). For genomic DNA of *A. halleri*, the digestion with the restriction enzyme *EcoRI* led to the detection of three signals in the individual 3.1 from the Langelsheim accession (Lan3.1) and of two signals in the individual Lan5. After digestion with *DraI*, three to four, and two signals were detected in Lan3.1 and Lan5, respectively. The use of the restriction enzyme *EcoRV* resulted in four *HMA3* specific signals in Lan3.1 and three signals for Lan5. It might be noted that there were always more signals detected on genomic DNA from individual Lan3.1 than from individual Lan5 (Figure 4.1).

The obtained data will be reevaluated later under consideration of more sequence information and in greater detail (see Section 1.1.6 on page 72). However, at this point, the preliminary conclusion is that the genome of *A. halleri* possesses a minimum of two and a maximum of four *HMA3* gene copies.

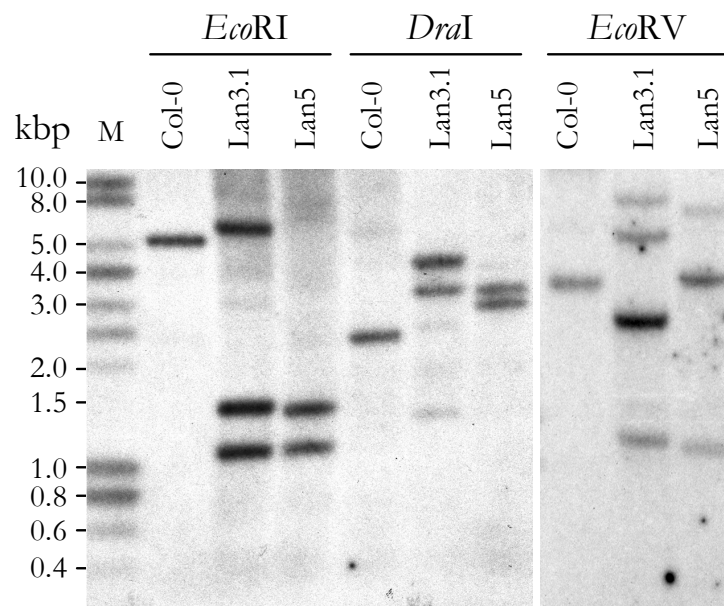


Figure 4.1: Southern blot analysis. Determination of *HMA3* copy number.

Genomic DNA was prepared from inflorescences of *A. thaliana* accession Columbia (Col-0) and *A. halleri* individuals from the Langelsheim location (Lan3.1 and Lan5). DNA was digested with *EcoRI*, *DraI* and *EcoRV* and separated by agarose gel electrophoresis. For detection of the *HMA3* gene, a ^{32}P -labeled 334 base pair PCR fragment from the 3'-end of *AhHMA3* was used as a probe for hybridisation. The probe does not span an intron and none of the used enzymes cuts within the probe sequence. The molecular size marker was loaded on lane M.

1.1.2 Analysis of a BAC library

For the further characterisation of the genomic organisation of *HMA3*, a BAC library of *A. halleri* (Rodacherbrunn and Stutenkamm accessions, Southern Thuringia, *Schiefergebirge*) was screened by Marc Hanikenne (postdoctoral researcher, group of Ute Krämer) in collaboration with Dr. Jürgen Kroymann at the MPI-CE (Max-Planck-Institute of Chemical Ecology, Jena, Germany). Eight *HMA3*-positive BAC clones were obtained and made available for this project for PCR analyses (Figure 4.2) and Southern hybridisations (Figure 4.3). Table 4.1 gives overview of the eight BAC clones and the assigned numbers.

PCR analysis A first analysis of the obtained eight BAC clones was done by PCR using primers that amplify the *AbHMA3* coding sequence. It could be shown that all BAC clones contained the full length *AbHMA3* coding sequence (Figure 4.2 A) in a genomic fragment of the predicted size of 3.1 kbp. When tested with primers that were designed based on the *A. thaliana* genome sequence and used for the cloning of full, medium and small size fragments of the promoter *pAbHMA3-1* (see Section 1 on 100), only BAC DNA of the clones No.1 and No.7 yielded PCR fragments (Figure 4.2 B, C, and D) of the expected sizes of 2.2 kbp, 0.8 kbp, and 0.2 kbp, respectively. During the course of the project, the BAC clones were also tested with primers specific to a second *AbHMA3* promoter (*pAbHMA3-2*). BAC clones No.5 and No.6 appeared to contain that second promoter sequence (data not shown).

Table 4.1: Confirmed *HMA3* positive clones and assigned numbers.

The column “signal” gives the strength of the hybridisation signal as determined by eye with an *AhHMA3* specific 3'-end probe.

original BAC No.	assigned No.	signal	<i>AbHMA3</i> group ^a
37	1	strong	-1c
42	2	medium	-3a
43	3	medium	-3b
44	4	strong	-2e
48	5	strong	-2d
50	6	strong	-2c
51	7	strong	-1b
53	8	strong	-3c

^aAssignment is based on similar sizes of *AbHMA3* specific BAC DNA fragments detected by Southern hybridisation and PCR analysis.

Lane 3, 4, and 5 of Figure 4.2 C and lane 4 of Figure 4.2 D also yielded a few PCR fragments. However, the yielded amount is very low compared to the high amount of PCR fragments amplified from BAC DNA of the other clones. Moreover, the fragments correspond to sizes of some of the control fragments. Thus, the weakly amplified fragments are likely to result from small contaminations.

Analysis by Southern hybridisation The eight BAC clones were further characterised using Southern hybridisation. This experiment aimed to reveal fragment patterns that would allow a grouping of the BAC clones according to the contained *HMA3* gene copies. For the later selection of *AbHMA3* containing fragments that are suitable for the cloning of additional promoter sequences (see Section 2 on page 109), a probe that hybridises to the 5'-end of *AbHMA3* was chosen. The probe was a ³²P-labeled fragment that is specific to the first 127 bp of *AbHMA3* and that does neither contain recognition sites for the used restriction enzymes nor span an intron (Figure 4.9 A). The BAC DNA was digested with the following enzymes: *EcoRI*, *AvaI*, *AccI*, *XbaI* or *HindIII*.

In most cases, a single *AbHMA3* specific signal was detected (Figure 4.3). Only the digestion with *EcoRI* resulted in several signals in certain BAC clones. There, the most prominent double signal was observed in BAC clones No.1 and 7. Weaker triple signals were detected in BAC clones No.2, 3 and 8. It remains to be investigated if the weak triple signals point to several *AbHMA3* gene copies.

Based on the observed sizes of detected *AbHMA3* specific fragments, it is possible to sort sort the eight BAC clones in three distinct groups. The first group with similar fragment sizes contains BAC clones No.1 and 7 (*AbHMA3-1*). A second group includes BAC clones No.4, 5, and 6 (*AbHMA3-2*). The remaining BAC clones No.2, 3, and 8 comprise the third group (*AbHMA3-3*). This grouping is particularly recognisable after the digestion with *AvaI* or *HindIII*, but also with *EcoRI* despite multiple

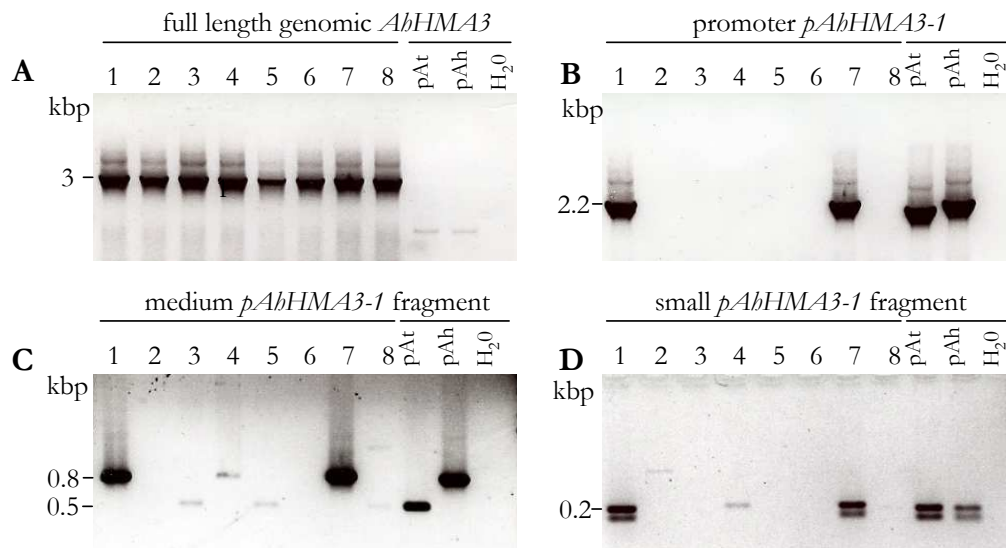


Figure 4.2: PCR analysis of BAC DNA from *A. halleri*.

BAC DNA was prepared from overnight cultures of *AhHMA3* positive *E. coli* BAC clones and used as template for the PCR using primers to amplify

A: full length *HMA3* (primers *AtHMA3* F & *V01* R)

B: full sized *pAtHMA3* and *pAhHMA3-1* promoter sequences (primers *Pt01* F & *Pt01* R)

C: medium sized *pAtHMA3* and *pAhHMA3-1* promoter sequences (primers *Pt800* F & *Pt01* R)

D: small sized *pAtHMA3* and *pAhHMA3-1* promoter sequences (primers *Pt200* F & *Pt01* R)

signals for single BAC clones (Figure 4.3).

In summary, one can conclude that the general grouping of the BAC DNA in three groups suggests the occurrence of at least three *AbHMA3* copies in the genome of *A. halleri*. Observed variations of band patterns within groups might reflect allelic sequence differences. The occurrence of two clear signals for *AbHMA3* on BAC DNA of clone No.1 and No.7 suggests the existence of two *AbHMA3* gene copies in proximity to each other. This second putative *AbHMA3* gene copy on clone No.1 and No.7 will be named *AbHMA3-4*. Multiple detected signals might indicate that the BAC clones No.2, 3, and 8 carry up to three gene copies of *AbHMA3*. However, the existence of up to five or even six *AbHMA3* gene copies is not supported by previously conducted Southern analyses of genomic DNA from *A. halleri* (Figure 4.1 on page 59).

1.1.3 Sequence analysis and Exon-intron-structure of *HMA3*

It is known that regulatory elements inside intron sequences can affect the transcriptional control of a gene. The *cis*-regulatory sequences located in the second intron of the floral homeotic gene *AGAMOUS* are a well documented example (Sieburth and Meyerowitz, 1997; Busch *et al.*, 1999; Deyholos and Sieburth, 2000; Hong *et al.*, 2003). For that reason it was important to compare the exon-intron structure and sequences of the *HMA3* genes from *A. halleri* and *A. thaliana*. Genomic sequences of

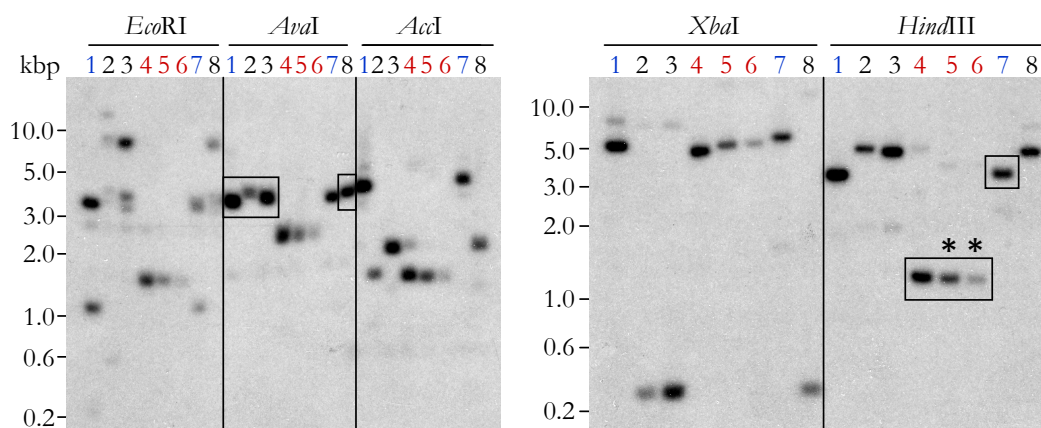


Figure 4.3: Southern blot analysis. Detection of *AhHMA3* specific fragments in BAC DNA.

BAC DNA was prepared from overnight cultures of *AhHMA3* positive *E. coli* BAC clones. DNA was digested with *EcoRI*, *AvaI*, *AccI*, *XbaI* and *HindIII* and separated by agarose gel electrophoresis. For detection of the *HMA3* gene, a ^{32}P -labeled 126 base pair PCR fragment from the 5'-end of *AhHMA3* was used for hybridisation. Digested DNA, framed in black boxes, was selected for later ligation and inverse PCR. An asterisk above a fragment marks a clone from which an *AhHMA3* specific sequence was obtained successfully by inverse PCR. Numbers of BAC clones with similar band sizes are coloured in blue, black or red.

A. halleri were obtained from Lan3.1 and Lan5 individuals of the Langelsheim accession and from clones of a BAC library (accession Rodacherbrunn and Stutenkamm, Southern Thuringia, *Schiefergebirge*; see Section 1.1.2 on page 59). The genomic *AhHMA3* sequence between translational start and translational stop codons was amplified. The sequences were compared to the *HMA3* sequence of *A. thaliana* ecotype Columbia (AGI number: At4g30120). The *AtHMA3* sequence and its annotated gene structure was obtained from the *TIGR* database (www.tigr.org).

A similarity fingerprint of the alignment is shown in Figure 4.4 A. All exon-intron boundaries are conserved between the *AtHMA3* and the cloned *AhHMA3* sequences. Table 4.2 shows the calculated amount of nucleotide differences in each exon or intron sequence. In general, most differences occurred inside intron sequences. Within introns, nucleotide divergence between *A. halleri* and *A. thaliana* was on average 24%. Between different *A. halleri* *HMA3* intron sequences, only 4.3% of the nucleotides were different. As expected, the protein coding exon sequences were more conserved. Here, the average interspecies divergence was about 6.0% and in an intraspecies comparison, *A. halleri* exon sequences differed in only 0.7% nucleotide positions on average.

Dissimilarities between *HMA3* coding regions were more evenly distributed over the length of the sequence (Table 4.2, Figure 4.4 B) than in intron sequences, in which more differences were found in the first three introns (Table 4.2, Figure 4.4 C). Most differences between *A. thaliana* and *A. halleri* occurred in exon I and VIII and intron 1 to 3. The *A. halleri* sequences varied mostly in exon I, II and V and in the introns 1 and 2.

Based on sequence similarity, the aligned *A. halleri* sequences were sorted into two groups, designa-

ted as *AbHMA3-1* and *AbHMA3-2*. Twelve clearly distinguishing features were found that separate the *AbHMA3-1* group (*AbHMA3* amplified and cloned from individual Lan5 (a), BAC No.7 (b) and No.1 (c)) from the *AbHMA3-2* group (*AbHMA3* amplified and cloned from two Lan3 individuals (a, b) and BAC clone No.6 (c)). The features are labeled with numbers from 1 to 12 in Figure 4.4 A. The feature containing *AbHMA3* regions can be seen in greater detail in Figure 4 in the *Appendix* Section on page N. Altogether, the twelve group characteristics comprised 46 nucleotides. Based on the amount of specific nucleotide differences, about 76% (35 of 46 nucleotides) of all differences between group 1 and group 2 *AbHMA3* sequences occurred in the first intron (Table 4.2, Figure 4.4 A). The first intron also included the most prominent feature (No.5), a 29 bp insertion that occurred in intron I of *AbHMA3-1* but is missing in *AbHMA3-2*. Seventeen of these 29 nt were present in *AtHMA3*. The second intron included also a dinucleotide insertion (feature No.7) in *AbHMA3-2* sequences. The fourth exon contained a *AbHMA3-2* specific triplet insertion (feature No.10). A group distinguishing AAC/GGT polymorphism was found in exon I.

The comparison of *AtHMA3* to all *AbHMA3* sequences revealed several *A. thaliana* specific characteristics. Already mentioned was a stretch that covered only 17 of the 29 bp insertion in *AbHMA3-1* sequences and that is completely missing in *AbHMA3-2* sequences. Besides minor nucleotide substitutions along the entire *HMA3* sequence, major dissimilarities between *A. halleri* and *A. thaliana* are found in the third intron.

The distinguishing features, especially in intron 1, 2 and 3 were queried for putative motifs with regulatory function. The following databases were used:

- PLACE (www.dna.affrc.go.jp/PLACE)
- TFSearch (www.cbrc.jp/research/db/TFSEARCH.html)
- Signal Scan (bimas.dcrn.nih.gov)
- PlantCARE (bioinformatics.psb.ugent.be/webtools/plantcare/html/)

None of the examined intron sequences received a significant high probability score for known motifs.

Table 4.2: Comparison of exon and intron regions of *HMA3*.

Given is the percentage nucleotide divergence. Compared are the genomic sequences of *HMA3* from *A. thaliana* (At) and *A. halleri* (*AhHMA3-1b*, BAC No.7; *AhHMA3-2c*, Bac No.6) in the exon and intron regions. Boxed in grey are particularly high values. For a graphical representation see Figure 4.4 B and C

gene region		sequence difference [%] ^a			special characteristics
exon	At/ <i>AbHMA3-1</i>	At/ <i>AbHMA3-2</i>	<i>AbHMA3-1</i> / <i>AbHMA3-2</i>		
I	8.4	10.9	2.5		group specific feature ^b 1, a GGT/ACC substitution
II	7.8	7.4	1.2		group specific features 8 and 9
III	4.1	4.1	0.0		
IV	6.6	6.3	0.4		group specific feature 11
V	3.0	3.0	1.5		group specific feature 12
VI	5.2	5.5	0.3		
VII	5.0	5.0	0.0		
VIII	8.4	8.4	0.0		
IX	4.1	3.9	0.2		
average	5.8	6.0	0.7		
intron					
1	17.4±0.4	26.8±3.2	24.9±3.6		group specific features 2 to 7; 29 bp insertion in <i>AbHMA3-1</i> sequences
2	38.8±1.3	37.0±0.3	5.9±0.1		
3	40.8±3.5	48.3±2.8	2.5±0.0		group specific feature 10, an AAC insertion in <i>AbHMA3-2</i> sequences
4	13.3±0.2	13.6±0.2	0.0±0.0		
5	13.1±0.1	13.3±0.1	0.0±0.0		
6	19.4±0.3	19.8±0.3	0.0±0.0		
7	18.6±1.0	20.0±1.0	0.0±0.0		
8	22.4±1.7	21.2±1.8	1.2±0.0		
average	23.0±1.1	25.0±1.2	4.3±0.5		

^aThe given standard deviation for the percentage (*PND*) of nucleotide divergence (*ND*) in intron sequences results from different lengths (*L*) of compared introns, i. e. for each compared intron region two percentage nucleotide divergences (*PND(A)* and *PND(B)*) are calculated, e. g. for intron I: $PND(A)_{intron I} = \frac{ND_{intron I}(AtHMA3 \text{ vs. } AhHMA3-1)}{L_{intron I}(AtHMA3)} \times 100$ and

$$PND(B)_{intron I} = \frac{ND_{intron I}(AhHMA3 \text{ vs. } AhHMA3-1)}{L_{intron I}(AhHMA3-1)} \times 100.$$

^ba feature that distinguishes the two found groups of *A. halleri* sequences, *AbHMA3-1* and *AbHMA3-2* (see Figure 4.4 A)

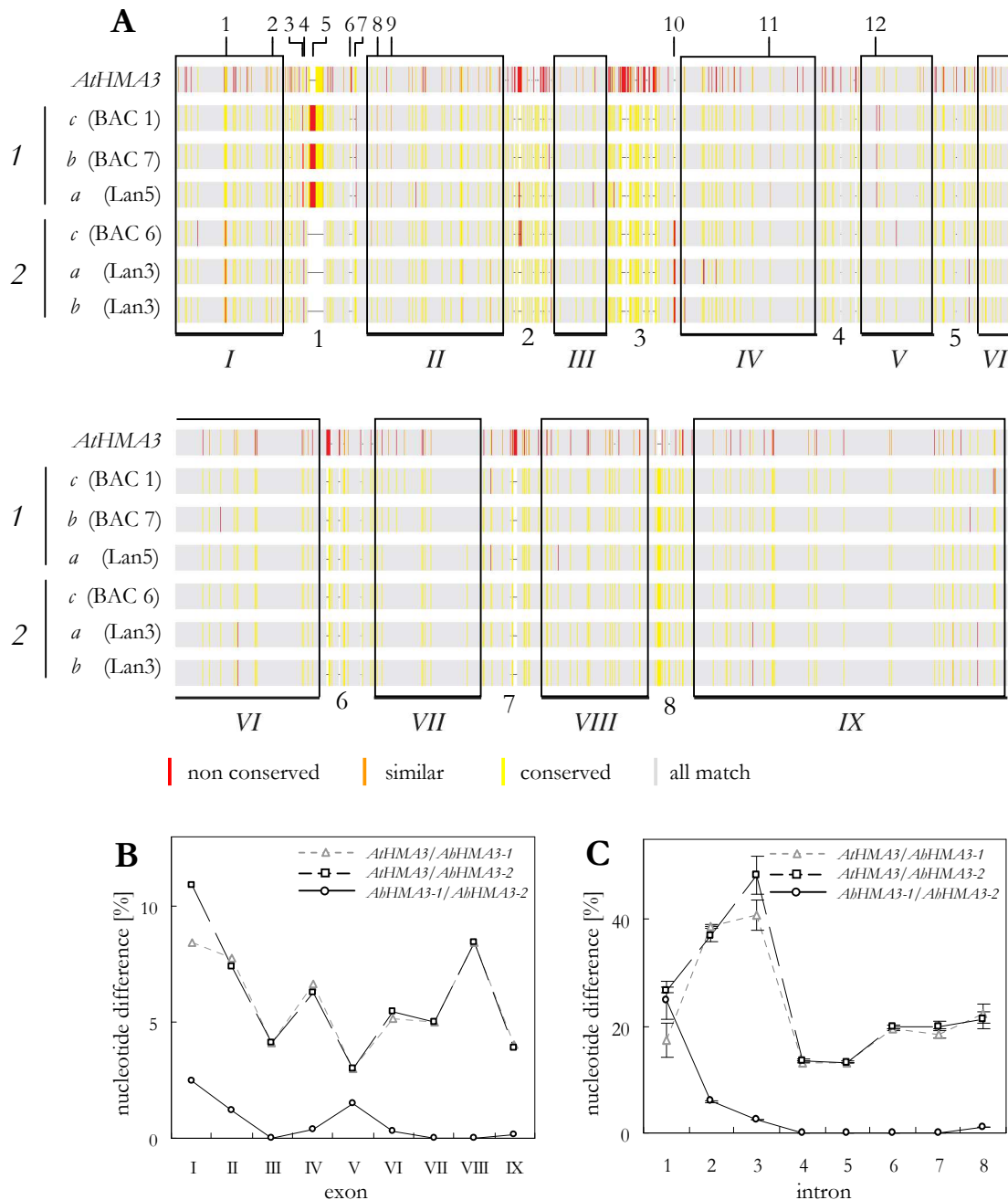


Figure 4.4: Analysis of genomic *HMA3* sequences.

A: An alignment fingerprint of genomic *HMA3* sequences from *A. thaliana* (*AtHMA3*) and *A. halleri* from translational start to translational stop codons. Genomic sequences of *A. halleri* were obtained from Lan3.1 and Lan5 individuals from the Langelsheim accession and from clones No.1, 6, and 7 of a BAC library (accession Rodacherbrunn and Stutenkamm, Southern Thuringia, *Schiefergebirge*; see Section 1.1.2 on page 59). The *AhHMA3* sequence was amplified by PCR using the primer pair V01 F & V01 R, cloned in the pCR2.1TOPO® vector and sequenced. The sequences are compared to the *HMA3* sequence of *A. thaliana*, accession Columbia (AGI number: At4g30120). The *AtHMA3* sequence and its annotated gene structure was obtained from the TIGR *A. thaliana* database (www.tigr.org). The gene structure of *AhHMA3* was determined by comparing genomic sequences with cDNA sequences.

Features that distinguish between *AhHMA3* variants are labeled with numbers on top. Black frames, labeled with roman numbers, mark the 9 exons of *HMA3*. Arabic numerals at the bottom number the 8 introns. The numbers “1” and “2” at the left side mark the two clearly distinct groups of *AhHMA3* sequences, designated *AhHMA3-1* and *AhHMA3-2*. The feature containing *AhHMA3* regions can be seen in greater detail in Figure 4 in the Appendix Section on page N.

B: The percentage of nucleotide differences in the 9 exons.

C: The percentage of nucleotide differences in the 8 introns.

The alignment file was produced using the MEGA application version 3.1 (Kumar *et al.*, 2004, default parameters) and the fingerprint was generated using TEXshade (Beitz, 2000a). Nucleotide positions are shaded as follows: ■ all match (100% identical nucleotides), ■ conserved (more than 50% identity); ■ similar (less than 50% identity but all are purine or pyrimidine nucleotides); ■ non conserved (less than 50% and mixed purine/pyrimidine)

1.1.4 Polymorphism in *AtHMA3* among *A. thaliana* ecotypes

One difficulty for further investigations was the discovery of a single base pair deletion in *AtHMA3* of the *A. thaliana* Columbia (Col-0) accession.

In 2004, it was shown that the *AtHMA3* gene of the Columbia accession contains a single base pair deletion (see Figure 4.5 below and the *Appendix* Section A.3 on page I). The deletion leads to a frameshift and consequently to a truncation of the encoded protein after amino acid 542. This predicted protein is lacking the ATP binding site and is likely to be non-functional with respect to metal transport. Such deletion was not detected in the Wassilewskija (Ws) accession of *A. thaliana* (Hussain *et al.*, 2004).

The described single base pair deletion could be confirmed in the *A. thaliana* ecotype Columbia used at the Max-Planck-Institute for Molecular Plant Physiology (MPI-MP) by amplifying and sequencing the relevant region from isolated genomic DNA in this study.

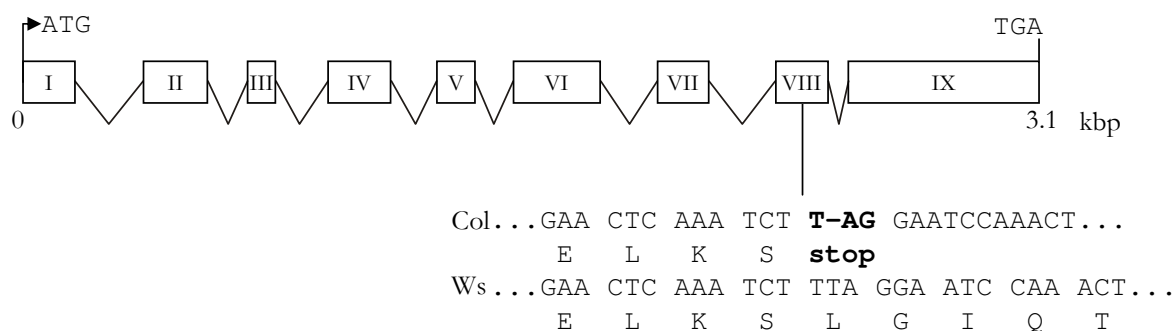


Figure 4.5: Single base pair deletion in *AtHMA3* of the accession Columbia.

Illustration modified from Hussain *et al.* (2004). A schematic illustration of the *HMA3* gene. Boxes indicate exon coding sequences and connecting lines indicate introns. The single base pair deletion polymorphism in *AtHMA3* in the accession Columbia (Col) is shown as well as the corresponding wildtype sequence of the accession Wassilewskija (Ws).

1.1.5 Analysis of 5' and 3' untranslated regions of *AbHMA3*

To analyse the 5' and 3' untranslated region (UTR) of *AbHMA3* and to search for potential alternative open reading frames, a rapid amplification of 5'- and 3'-cDNA ends (5'- and 3'-RACE) was performed. A 3'- and 5'-RACE library of *A. balleri* served as template. This method allows the amplification of nucleic sequences from a messenger RNA template between a defined internal site and unknown sequences at either the 3'- or the 5'-end of the mRNA.

Analysis of 5'-RACE products For the amplification of 5'-RACE products an internal primer was used that binds 105 bp downstream of the translational start of *AbHMA3*. After cloning and sequencing of the 5'-RACE products, the four obtained sequences differed from each other (Figure 4.6). However, three products (5' UTR-1.2, 1.4 and 1.5) could be assigned to the later cloned promoter *pAbHMA3-1* (see page 100) and the *AbHMA3-1*-like sequences. A single clone (5' UTR-2.4) appears similar to the later cloned promoter *pAbHMA3-2* (see page 109) and the *AbHMA3-2*-like sequences (see also Figure 4.4).

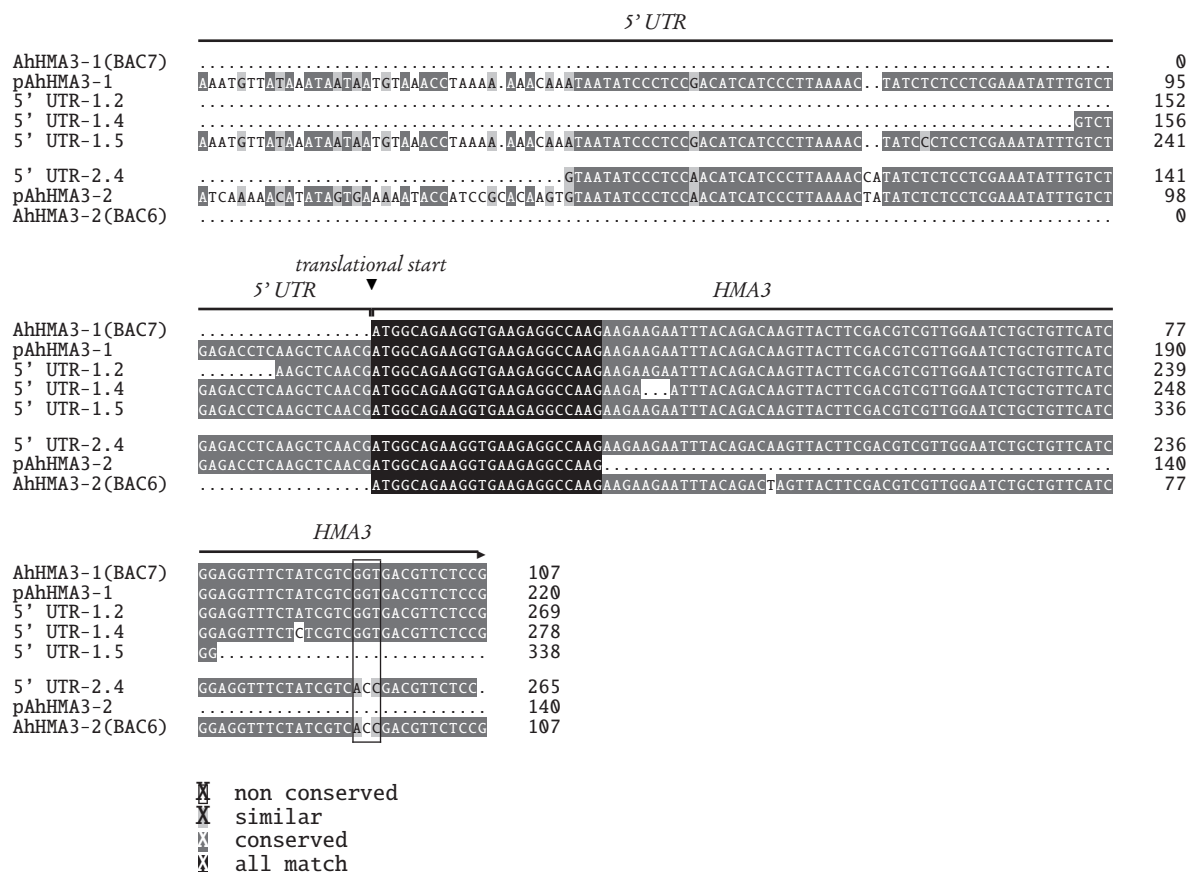


Figure 4.6: Alignment of 5'-RACE products.

Four 5'-RACE products aligned with partial sequences of the genes *AhHMA3-1b*, *AhHMA3-2c* and the promoters *pAhHMA3-1* and *pAhHMA3-2* are shown. The putative 5' UTR and the *AhHMA3* coding sequence is labeled on top. The characteristic GGT / ACC substitution between *AhHMA3-1* and *AhHMA3-2* is framed in black.

The alignment file was produced using the *MEGA* application version 3.1 (Kumar *et al.*, 2004, default parameters) and *TeXshade* (Beitz, 2000a).

Analysis of 3'-RACE products The 3'-RACE yielded 11 clones. The sequenced 3'-RACE products fall into three different groups based on sequence alignments. The largest group, including 7 clones, shares similarities with the *AbHMA3-1* sequence. In a second group, three clones are more similar to the *AbHMA3-2* sequence. The third group comprises two unusual 3'-RACE products that are about 110 bp longer than the other clones. Only the first 79 bp are similar to other 3'-RACE products. The remaining stretch of about 245 bp has no similarity to the other 3'-RACE products or known genomic sequences downstream of *AtHMA3* from *A. thaliana* (Figure 4.7).

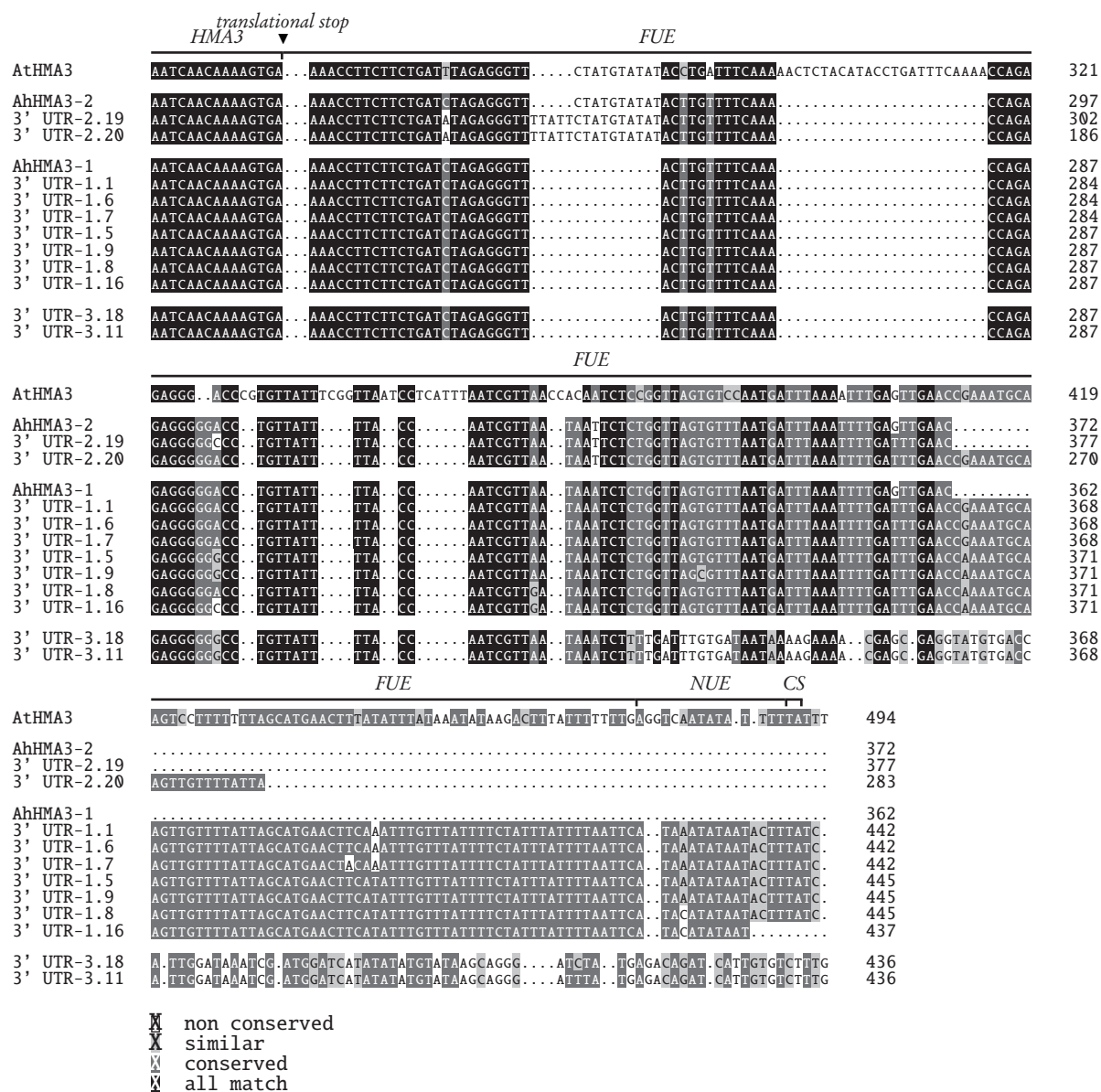


Figure 4.7: Alignment of 3'-RACE products.

Eleven 3'-RACE products aligned with partial sequences of the genes *AhHMA3-1* (BAC No.7), *AhHMA3-2* (BAC No.6) and the genomic sequence of *AtHMA3* (ecotype Columbia) are shown. The putative far upstream element (FUE), the near upstream element (NUE), and the cleavage site (CS) of *AtHMA3* are labeled on top. The alignment file was produced using the *MEGA* application version 3.1 (Kumar *et al.*, 2004, default parameters) and *TEXshade* (Beitz, 2000a).

For further characterisation, the 3'-RACE products were analysed for the occurrence of common

cis-signals required for the messenger RNA polyadenylation process. This crucial maturation step of most eukaryotic mRNA adds a polyadenine stretch to the 3'-end of a precursor mRNA (pre-mRNA). This poly(A) tail affects the stability, translatability and the nuclear-to-cytoplasmic export (Zhao *et al.*, 1999). In plants, poly(A) signals consist of three major elements: a far upstream element (FUE), a near upstream element (NUE; an AAUAAA-like element) and a cleavage sites (CS) followed by a cleavage element (CE) (Li and Hunt, 1997; Rothnie, 1996; Rothnie *et al.*, 2001; Loke *et al.*, 2005) (Figure 4.8 A). The FUE, a control or enhancing element upstream of the NUE, consists of ambiguous uracil-glycine (UG) motifs and/or an UUGUAA motif (Hunt, 1994). The A-rich NUE is located between 13 to 30 nucleotides (nt) upstream of the CS (referred to as position -13 to -30 nt) and spans about 6 to 10 nt. The CS is a cytosine-adenine (CA) or uracil-adenine (UA) dinucleotide embedded in an U-rich region. The uracil is represented as tyrosine (T) in RACE product sequences (Figure 4.7).

Following the publication of Loke *et al.* (2005), a single-nucleotide profile of representative 3'-RACE products was calculated in order to obtain an overview of the distribution of nucleotides in the 3' untranslated region of *AbHMA3*. Clone No.5 was chosen to represent the two related groups of 3'-RACE products. Clone No.18 was chosen to represent the third distinct group of 3'-RACE products. Loke *et al.* (2005) scanned the 3'-UTR sequences of about 17.000 independent genes of *A. thaliana* to identify common features by compiling an average single-nucleotide profile (Figure 4.8 A). Here, only single sequences are considered and analysed for the occurrence of the described common features of the 3'-UTR region. For that purpose, a single-nucleotide profile describing the nucleotide distribution of a 3'-RACE product was analysed using the EXCEL software application (Microsoft®, USA). The profile was calculated by counting the number of a certain nucleotide (A, T, G or C) in a sequence window of 10 nucleotides. For each datapoint, the window was shifted by 5 nucleotides along the clone sequence. The window size was chosen as a compromise between the necessary high nucleotide count to reduce the noise of the nucleotide background pattern and a sufficiently small nucleotide count that does not lose information on short sequence stretches.

The 3'-RACE product No.5 shows a similar distribution of single nucleotides in the 3'-UTR as the average single-nucleotide profile of 3'-UTRs in *A. thaliana* (Figure 4.8 B). The translational stop (TGA) of *AbHMA3* is followed by a primarily T-rich region with a high content of adenine between 200 and 40 nt upstream of the CS. This is typical for the FUE. Between about 18 and 35 nt upstream of the CS, an A-rich peak occurs in the profile similar to the NUE. The site contains an ATA(A/C)ATATAATA stretch that resembles the common NUE motif AAUAAA. The 3'-RACE product was amplified from mRNA that already contained a poly(A) tail. Therefore, the CS site can only be marked as the last TA or CA after 3 to 4 tyrosines before the poly(A) tail and not based on being embedded in a T-rich stretch. However, a TA dinucleotide embedded in a T-rich stretch is found in the homologous sequence of *A. thaliana* immediately downstream of the NUE.

In the sequence of the 3'-RACE clone No.18, only the first 79 nt downstream the translational stop were similar to clones of the two other groups. After that position the sequences diverged (Figure 4.7).

For this divergent sequence, no significant similarity to genomic sequences of higher plants was found using the *TAIR BLAST 2.2.8.* tool for querying the *TAIR* databases (www.arabidopsis.org/Blast/). The single-nucleotide profile did not allow a clear assignment to the general 3'-UTR profile found in *A. thaliana* (Figure 4.8). Although three T-rich peaks appeared between position -150 and -75 nt, the putative FUE stretch was not consistently rich in tyrosine and adenine as expected for the FUE. A putative NUE was found in clone No.18. But it was located at between position -39 and -57 nt, about 30 nt further away from the poly(A) sequence than expected. In the similar sequence of of the 3'-RACE clone No.11, this putative NUE appeared at position -5 to -23 but the expected 3 to 4 tyrosines preceding the CS site were missing.

In summary, the alignment of 5'-UTR sequences showed 2 groups of RACE products fragments (5' UTR-1, 5' UTR-2) that may belong to two different *HMA3* copies. The comparison of 3'-RACE products showed three groups of UTR fragments (3' UTR-1, 3' UTR-2 and 3' UTR-3). Two groups were in agreement with partially known 3' UTR regions of two different *AbHMA3* sequences from the BAC library (BAC No.6 and BAC No.7). A third group differed clearly and may correspond to a third group of BAC clones of which no sequence information was obtained. Based on obtained UTR sequence information, future investigations should attempt to amplify corresponding genomic sequences in order to validate the clone sequences.

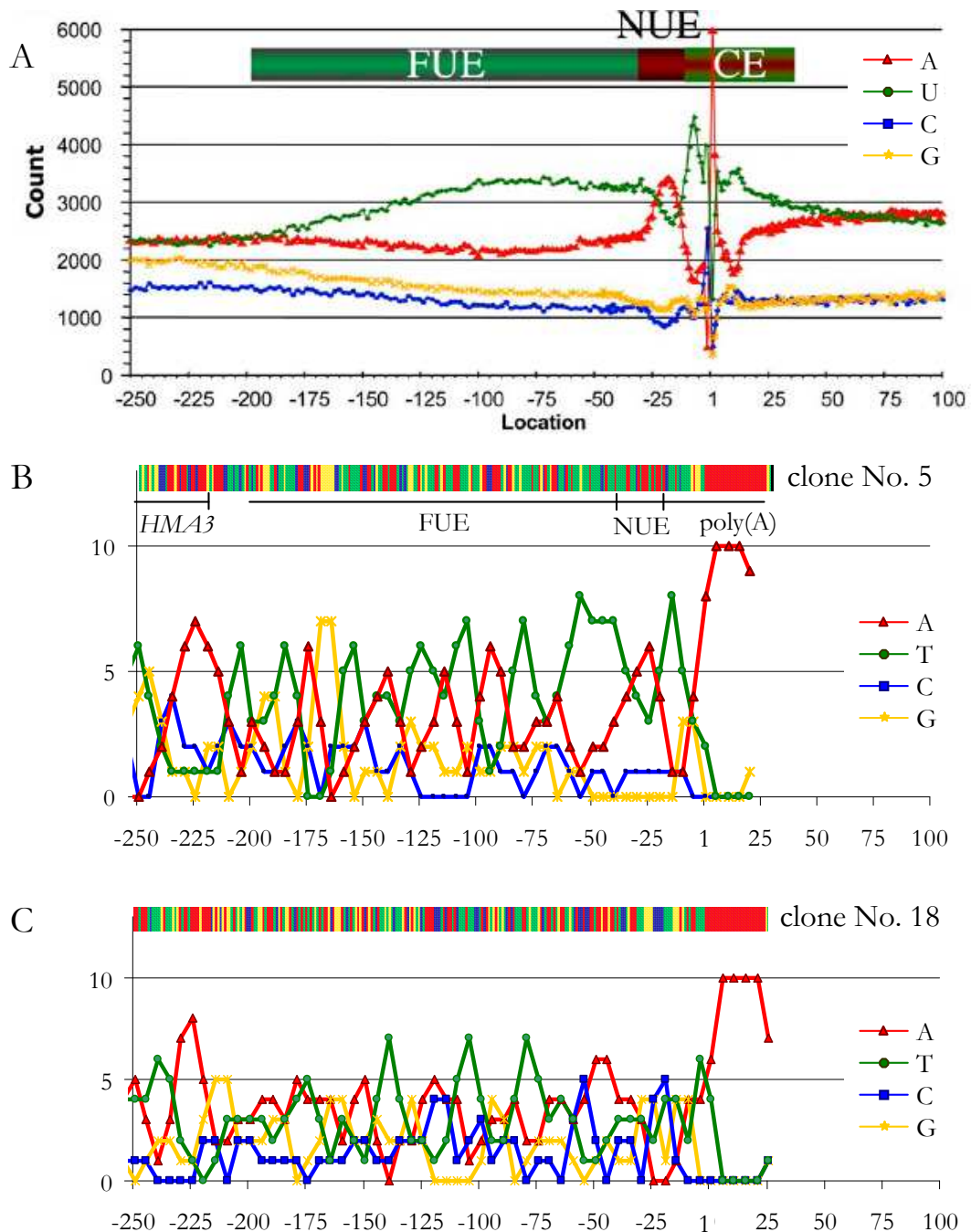


Figure 4.8: Single-nucleotide profile of the 3'-UTR of *A. thaliana* genes and the 3'-UTR of *A. halleri* *HMA3* genes. Marked are the *far upstream elements* (FUE), the *near upstream elements* (NUE) and the *cleavage element* (CE). Position 1 is the cleavage site (CS). Please note that in diagrams B and C, the CE site cannot be labeled because the profile of B and C are based on 3'-RACE products. Therefore, downstream of the start of poly(A)-tail, no sequence information is available. Diagram A does not include a poly(A) stretch because the used dataset is based on genomic sequence information (Loke *et al.*, 2005).

A: Single-nucleotide scan from positions -250 to +100 in the whole 3'-UTR + downstream region as published by Loke *et al.* (2005).

B: single-nucleotide profile of 3'-RACE *AhHMA3* clone No.5, resembling *AhHMA3-1* and *AhHMA3-2*

C: single-nucleotide profile of 3'-RACE *AhHMA3* clone No.18, resembling none of the cloned *AhHMA3* sequences

The single-nucleotide profile shown in diagram B and C was made using the EXCEL software application (Microsoft®, USA). Each datapoint represents the quantity of a certain nucleotide (A, G, C or T) in a sequence window of 10 nucleotides. For each datapoint, the window was shifted by 5 nucleotides along the sequence.

1.1.6 Reevaluation of copy number and BAC library analysis

Combining the data of genomic sequences of *AbHMA3* obtained from the BAC library (see page 61), the 5’-/3’-RACE products (see page 67), and from cloned promoter fragments (see page 99), it is possible to reevaluate and to summarise the conclusions regarding the *HMA3* copy number in *A. baumannii*. Figure 4.9 gives an overview on obtained *HMA3* sequences¹ and contained restriction sites that are relevant for the interpretation of Southern hybridisations.

Including the Southern hybridisations on genomic DNA of *A. baumannii* (see page 58), the new sequence information obtained by cloning genomic *AbHMA3* sequences and RACE-Analyses allows to predict minimum expectable fragment sizes (Table 4.3). Only in case of *DraI* restriction, one can make exact size predictions for certain combinations of promoter, 3’-UTR and *AbHMA3* sequences. Most detected *AbHMA3* specific fragments exceed the predicted minimum size. The only exception is a weak signal at about 1.3 kbp from genomic Lan3.1 DNA after digestion with *DraI*.

Predictions of the expected minimum size of *AbHMA3* fragments of digested BAC DNA were also performed (Table 4.4). Most of the detected fragment sizes exceeded the predicted minimum size. An exception was found for the BAC clones of the third group (No.2, 3 and 8) after treatment with the enzyme *XbaI*. The detected fragments of about 0.3 kbp were smaller than the expected size of at least 1.1 kbp. This points to the existence of an unknown promoter sequence containing an *XbaI* restriction site in between the first 170 kb upstream of the translational start of *AbHMA3*.

In summary, the obtained sequence information cannot explain entirely the observed fragment sizes and thus, indicates the existence of yet unknown sequences. Furthermore, it is not possible to clearly assign which promoter is located upstream of which *AbHMA3* copy. However, similarities in RACE products point to a possible connection between *pAbHMA3-1* and *AbHMA3-1* as well as *pAbHMA3-2* and *AbHMA3-2*.

¹Figure 4.9 contains sequence data that was obtained from different experiments described in the *Results* Section. To avoid confusion, a consistent nomenclature for *HMA3* of *A. baumannii* (*AbHMA3*) sequences is introduced at this point. *AbHMA3* sequences that were determined during the course of this thesis can be sorted into two groups that differ significantly from each other. They are designated as *AbHMA3-1* and *AbHMA3-2*. Each group consist of three *AbHMA3* variants of different origin and are marked by an additional small letter, i. e. *AbHMA3-1a*. During the description and discussion of results, I refer to different *AbHMA3* variants. If necessary, I refer to a single variant, i. e. *AbHMA3-2b* but if the mentioned result is valid for all *AbHMA3* sequences or a certain group, I only speak of *AbHMA3* or *AbHMA3-1*, *AbHMA3-2*, etc. A similar nomenclature is used for *AbHMA3* promoter fragments, i. e. *pAbHMA3-1* and cloned fragments of the 5’- and 3’ untranslated region (UTR), i. e. 5’ UTR-1. The last number express a similarity or a putative connection between different *AbHMA3* related sequences. But if not indicated otherwise, sequences with the same number do not necessarily belong together.

Table 4.3: Observed and predicted sizes of *HMA3* specific restriction fragments resulting from cleavage of genomic DNA.

	genomic DNA	<i>EcoRI</i>	<i>DraI</i>	<i>EcoRV</i>
observed	At Col	5.2	2.4	3.8
	Ah Lan3.1	1.1, 1.4, 5.5	1.3, 2.5, 3.4, 4.2	1.1, 3.0, 5.2, 8.0
	Ah Lan5	1.1, 1.4	3.0, 3.4	1.1, 3.9, 7.0
predicted	Col	5.23	2.42	3.99
	<i>A.balleri</i>	> 0.85 ^a > 0.66 ^b	> 4.39 ^{a1} > 4.15 ^{a2} > 4.18 ^{b1} 3.94 ^{b2} > 3.1 ^{c1} 2.90 ^{c2}	> 1.36 ^a > 1.17 ^b

^{a, b}based on *AbHMA3* + shortest (a) or longest (b) 3'-RACE product

^{a1, b1}based on promoter *pAbHMA3-2* and *AbHMA3-2* + longest (a1) or shortest (b1) 3'-RACE product

^{a2, b2}based on promoter *pAbHMA3-1* and *AbHMA3-2* + longest (a2) or shortest (b2) 3'-RACE product

^{c1, c2}based on AhHMA3-1 + longest (c1) or shortest (c2) 3'-RACE product

Table 4.4: Observed and predicted sizes of *HMA3* specific restriction fragments resulting from cleavage of BAC DNA.

	BAC No.	<i>EcoRI</i>	<i>AvaI</i>	<i>AccI</i>	<i>XbaI</i>	<i>HindIII</i>
observed	1	1.2, 3.8	3.9	4.2	5.0	3.1
	7	=	=	4.3	5.1	=
	4	1.7	2.6	1.7	4.7	1.2
	5	=	=	=	5.0	=
	6	=	=	=	=	=
	2	4.0, 8.0, > 10.0	4.0	1.7	0.3	4.5
	3	3.4, 3.8, 7.9	=	2.0	=	=
	8	3.6, 7.9	=	=	=	=
predicted		> 2.427 ^a > 1.133 ^b	> 3.559 ^a > 4.200 ^{a1} > 2.265 ^b > 2.906 ^{b1}	> 3.318 ^a > 2.024 ^b	> 2.448 ^a > 1.154 ^b	> 2.683 ^a > 1.389 ^b

^{a, b}based on sequences of the promoter *pAbHMA3-1* (a) or *pAbHMA3-2* (b) + genomic *AbHMA3*

^{a1, b1}based on sequences of the promoter *pAbHMA3-1* (a1) or *pAbHMA3-2* (b1) + AhHMA3-1c (BAC No.1)

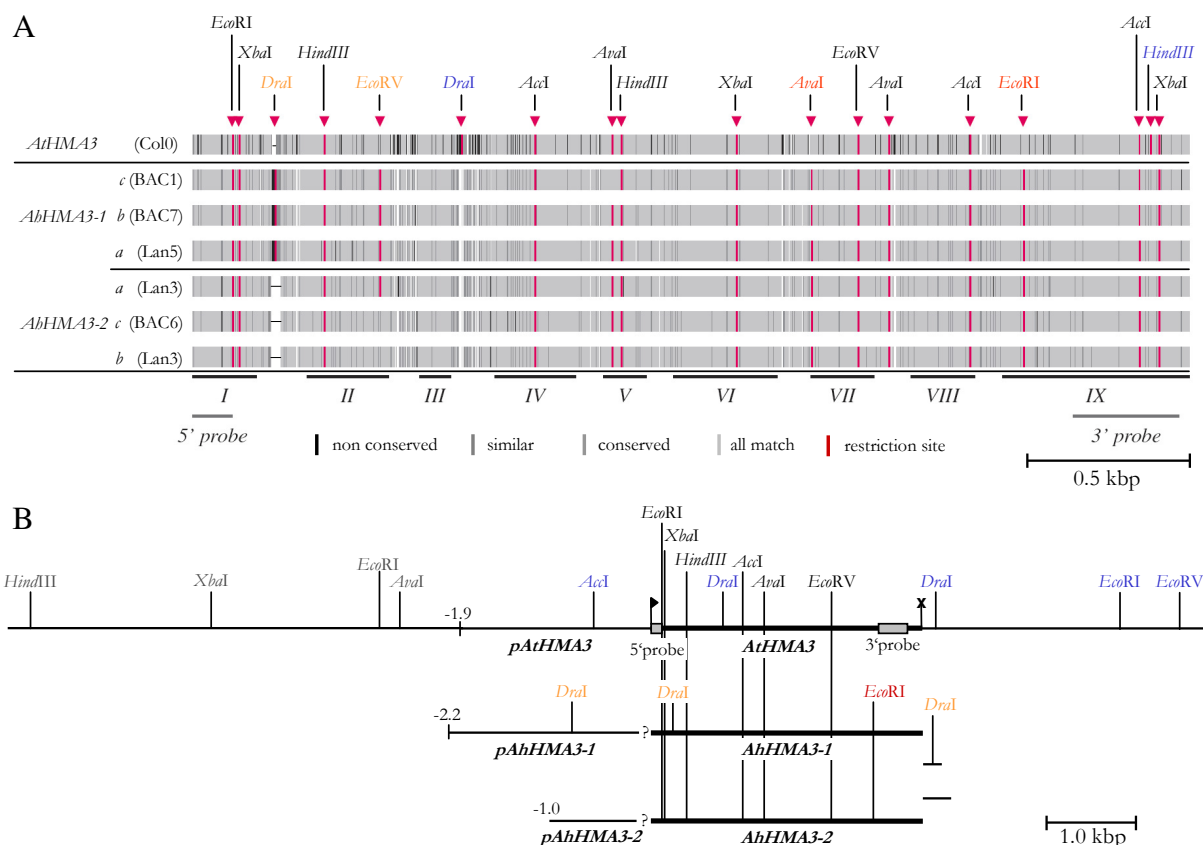


Figure 4.9: Alignment fingerprint and restriction sites of genomic *HMA3* and related promoter sequences.

A: The alignment of genomic *HMA3* coding sequences from *A. thaliana* (*AtHMA3*) and *A. halleri* (*AhHMA3-1a*, *b*, *c*; *AhHMA3-2a*, *b*, *c*) is shown as a fingerprint scheme. For *AhHMA3* nomenclature remarks see footnote 1 on page 72.

The *AtHMA3* sequence and its annotated gene structure was obtained from the *TIGR* database (www.tigr.org, At4g30120).

AhHMA3-1a was cloned from the individual Lan5, *AhHMA3-2a*, *b* from individual Lan3 of the Langelshelm accession of *A. halleri*. *AhHMA3-1b* and *c* were obtained from two different BAC clones, No.7 and No.1 (*A. halleri* BAC library: accession Rodacherbrunn and Stutenkamm, Southern Thuringia, *Schiefergebirge*; see Section 1.1.2 on page 59). *AhHMA3-2c* was obtained from BAC No.6 of the same BAC library.

Restriction sites are marked on top with red triangles and inside the fingerprint with corresponding red bands (■). Conserved restriction sites are labeled in black. Sites that are specific to *A. thaliana* are labeled in blue, *A. halleri* specific sites in red. Polymorphic restriction sites in *A. halleri* are labeled in orange. Black lines at the bottom, labeled with roman numbers, mark the 9 exons of *HMA3*. Horizontal dark grey bars mark the position of the 3'- and the 5'-probe that were used in Southern hybridisation.

The alignment file was produced using the *MEGA* application version 3.1 (Kumar *et al.*, 2004, default parameters) and the fingerprint was generated using *TpXshade* (Beitz, 2000a). Nucleotide positions are shaded as follows: ■ all match (100% identical nucleotides), ■ conserved (more than 50% identity); ■ similar (less than 50% identity but all are purine or pyrimidine nucleotides); ■ non conserved (less than 50% and mixed purine/pyrimidine).

B: Restriction sites that are relevant for the Southern hybridisation in known sequences of *HMA3* from *A. halleri* and *A. thaliana*. Black labeled restriction sites occur in all *HMA3* sequences. Blue labeled sites are specific for *A. thaliana*, Red sites do occur only in *AhHMA3* and orange sites are polymorphic in *AhHMA3* variants. For grey restriction sites no correlating *A. halleri* sequence is known. It cannot be concluded without doubt which of the two *AhHMA3* promoter sequences is upstream of which *AhHMA3* variant. The question mark (“?”) expresses that uncertainty. The black arrow (►) and the black (X) mark the translational start and translational stop of *HMA3*, respectively.

1.1.7 Summary - Characterisation of *HMA3* at the genomic and mRNA level

Analysis of digested genomic DNA from *A. balleri* by Southern hybridisation using a *HMA3* specific probe suggested the existence of at least 2 and at most 4 copies of *HMA3* in the genome of *A. balleri* (see Table 4.5).

Probing eight *HMA3* containing BAC clones by Southern hybridisation allowed the formation of three distinct groups of BAC clones, *AbHMA3-1*, *AbHMA3-2* and *AbHMA3-3*. Moreover, two clear signals for *AbHMA3* on BAC DNA of clone No.1 and No.7 suggested the existence of two *AbHMA3* gene copies in proximity to each other.

When genomic sequences of *HMA3* from *A. thaliana* were compared to sequences of *HMA3* from *A. balleri* that were obtained from genomic DNA and from BAC clones, two different sequence groups of *AbHMA3* were revealed. The two groups showed the lowest sequence similarity in the first three introns.

UTR sequences of the 5'- and 3'-ends of *AbHMA3* were obtained by RACE. The alignment of 5'-UTR sequences showed 2 groups of RACE products fragments (5'-UTR-1, 5'-UTR-2) that may belong to two different *HMA3* copies. The comparison of 3'-RACE products showed three types of UTR fragments (3'-UTR-1, 3'-UTR-2 and 3'-UTR-3). Two types correlated with known 3'-UTR sequences of two different *AbHMA3* sequences from the BAC library. A third group differed clearly.

Taken together, the obtained data showed the existence of at least three and possibly four *AbHMA3* gene copies that are encoded in the genome of *A. balleri*. The occurrence of more gene copies as has been previously suggested by Southern analysis of digested DNA of BAC clones was not supported by the additional data.

Table 4.5: Summary of the characterisation of *AbHMA3* at the genomic and mRNA level.

A putative grouping of different *AbHMA3* variants based on various experimental data is suggested.

Analysis of genomic DNA from		UTR analysis by RACE	
individual plants ^a	a BAC library ^b	5'-UTR	3'-UTR
Southern hybridisations 2 to 4 gene copies	Southern hybridisation 3 groups: <i>AbHMA3-1/AbHMA3-4</i> (BAC 1, 7) <i>AbHMA3-2</i> (BAC 4, 5, 6) <i>AbHMA3-3</i> (BAC 2, 3, 8)	2 groups: 5' UTR-1 (3 clones) 5' UTR-2 (1 clone)	3 groups: 3' UTR-1 (2 clones) 3' UTR-2 (7 clones) 3' UTR-3 (2 clones)
cloning 2 variants: <i>AbHMA3-1</i> (Lan5) <i>AbHMA3-2</i> (Lan3)	cloning 2 variants: <i>AbHMA3-1</i> (BAC 1, 7) <i>AbHMA3-2</i> (BAC 6)		

^aindividual No.3 and No.5 from the Langelsheim accession (Lan3, Lan5)

^baccession Rodacherbrunn and Stutenkamm, Southern Thuringia, *Schiefergebirge*

1.2 Functional characterisation

1.2.1 Functional expression of *AbHMA3* in yeast mutants

Before the start of this project, Ina Talke expressed *AbHMA3* in the Zn sensitive $\Delta zrc1 \Delta cot1$ double mutant of *S. cerevisiae*. These two genes mutated in this double mutant encode CDF proteins that efflux Zn (Cd/Co) from the cytoplasm into the vacuole. Therefore, the mutants are hypersensitive to Zn and to a lesser degree to Co (MacDiarmid *et al.*, 2000) (see also page 13 of the *Introduction*). In this study, the functional expression of *AbHMA3* in yeast was repeated, but using a different vector that fuses the protein with a N-terminal 3xHA tag. Furthermore, *AbHMA3* was expressed in the Cd-hypersensitive YYA4 yeast double mutant (Gaedeke *et al.*, 2001; Li *et al.*, 1996, 1997). The Cd-sensitive phenotype of YYA4 is caused by the loss of YCF1, a vacuolar glutathione S-conjugate pump and the loss of YHL035, a protein that is highly similar to YCF1 but with an unassigned biological function. The mutant is unable to detoxify Cd by sequestering Cd-glutathione complexes in the vacuole (see also page 14 of the *Introduction*).

Growth of the yeast mutant strains $\Delta zrc1 \Delta cot1$ and YYA4 transformed with *AbHMA3* cDNA

The $\Delta zrc1 \Delta cot1$ yeast mutant transformed with the empty vector (ev) pFL61 was able to grow on medium containing 150 μM Zn (data not shown) but not on medium with 300 μM Zn. When *AbHMA3* was expressed in the $\Delta zrc1 \Delta cot1$ yeast mutant, it exhibited growth at Zn concentration of up to 400 μM (Figure 4.10 A).

On medium containing 15 μM Cd, the YYA4 yeast mutant transformed with the empty vector could grow but stopped growing in the presence of 17.5 μM Cd. In contrast, YYA4 yeast mutants expressing *AbHMA3* were able to grow at 17.5 μM Cd (Figure 4.10 B) and stopped growing at concentrations above 20 μM (data not shown). The observed Cd tolerance conferred by *AbHMA3* expression was subtle but reproducible.

No difference in growth was observed on Co containing medium. The empty vector control and the *AbHMA3* expressing strain ceased to grow at Co concentration of 600 μM (Figure 4.10 C).

The observed differences in Zn and Cd tolerance between the empty vector control and yeast mutants expressing *AbHMA3* could be caused by the transport activity of *AbHMA3* or by a passive chelation of metal ions by the protein. One can distinguish between both possibilities by testing a nonfunctional *AbHMA3* protein in parallel. The nonfunctional *AbHMA3* was obtained by introducing an aspartate→alanine (D→A) mutation at the DKTGT phosphorylation site at position 397 of the *AbHMA3* peptide sequence. The aspartate (D) of this motif becomes phosphorylated during the transport cycle and has been demonstrated to be required for the function of P-type ATPases, i. e. in ZntA, a bacterial zinc-transporting ATPase (Okkeri *et al.*, 2002). Here, site-directed mutagenesis on the pFL613-*AbHMA3* vector changed the D encoding GAC triplet into an A encoding GCC triplet. The nonfunctional *AbHMA3* did neither complement the Zn nor the Cd sensitive phenotype of $\Delta zrc1$

$\Delta cot1$ or YYA4 yeast mutant (Figure 4.10 A, B).

P-type ATPases of plants possess a longer cytoplasmic C-terminal domain than their bacterial counterparts (see Figure 2 in the *Appendix* Section). Published experimental data suggest a regulatory function of the C-terminal domain of plant P-type ATPases. For example, for AHA2, a proton pump in the plasma membrane of *A. thaliana*, an autoinhibitory function is described (Palmgren *et al.*, 1991; Baunsgaard *et al.*, 1998). Further evidence for the importance of the C-terminus of P-type IB ATPases came from experiments on modified *AtHMA4* pumps (Mills *et al.*, 2005; Verret *et al.*, 2005) (see *Introduction* Section on page 25 for more details). A truncated *AbHMA3* was generated to test the influence of the C-terminus on the activity of the protein. For that purpose, *AbHMA3* was cloned with a premature stop at a position to generate a protein equivalent to homologous bacterial P-type IB ATPases that lack the C-terminal domain. The site of truncation is indicated in Figure 2 in the *Appendix* Section. The truncated *AbHMA3* (*AbHMA3* ΔC) did not affect the metal sensitive phenotype of the $\Delta zrc1 \Delta cot1$ or the YYA4 yeast mutant (Figure 4.10 A, B).

This result suggests that the C-terminal domain of *AbHMA3* is required for its transport function. However, the truncated protein may alternatively be unstable or mislocalised in yeast cells. This needs further investigations and will be discussed later (see *Discussion* on page 119).

Zinc accumulation in transformed yeast mutant cells The observed complementation of the Zn sensitive phenotype of $\Delta zrc1 \Delta cot1$ can be caused by either an efflux of Zn ions out of the cells into the surrounding medium or by an Zn transport into the vacuole. Therefore it should be possible to distinguish between a plasma membrane or an internal membrane localisation of *AbHMA3* in yeast cells by determining the cellular Zn content. For this purpose, transformed yeast cells were grown in the presence of 100 μM ZnSO_4 . Yeast mutant cells transformed with the empty control vector pFL61 were compared to cells transformed with pFL613-3xHA:*AbHMA3*. The Zn content was measured by inductively coupled plasma optical emission spectroscopy (ICP-OES). No significant difference in Zn content between the empty vector control and the *AbHMA3* expressing yeast cells was found. But it might be noted that the *AbHMA3* expressing yeast mutant tended towards a higher concentration of cell-associated Zn (Figure 4.11).

The collected data does not allow to distinguish between a plasma membrane or an internal membrane localisation of *AbHMA3* in yeast cells. Future investigations should include wildtype yeast cells transformed with the empty control vector pFL61 as a positive control. This could help to evaluate if the chosen method is sensitive enough to distinguish between cell-associated Zn concentrations in empty vector control and *AbHMA3* expressing yeast cells of the $\Delta zrc1 \Delta cot1$ double mutant.

Immunoblot analysis of heterologously expressed *AbHMA3* protein in yeast mutant strain $\Delta zrc1 \Delta cot1$ For the specific detection of heterologously expressed *AbHMA3*, total microsomal membrane fractions were prepared from yeast mutant cells transformed with the empty vector pFL61 or with the

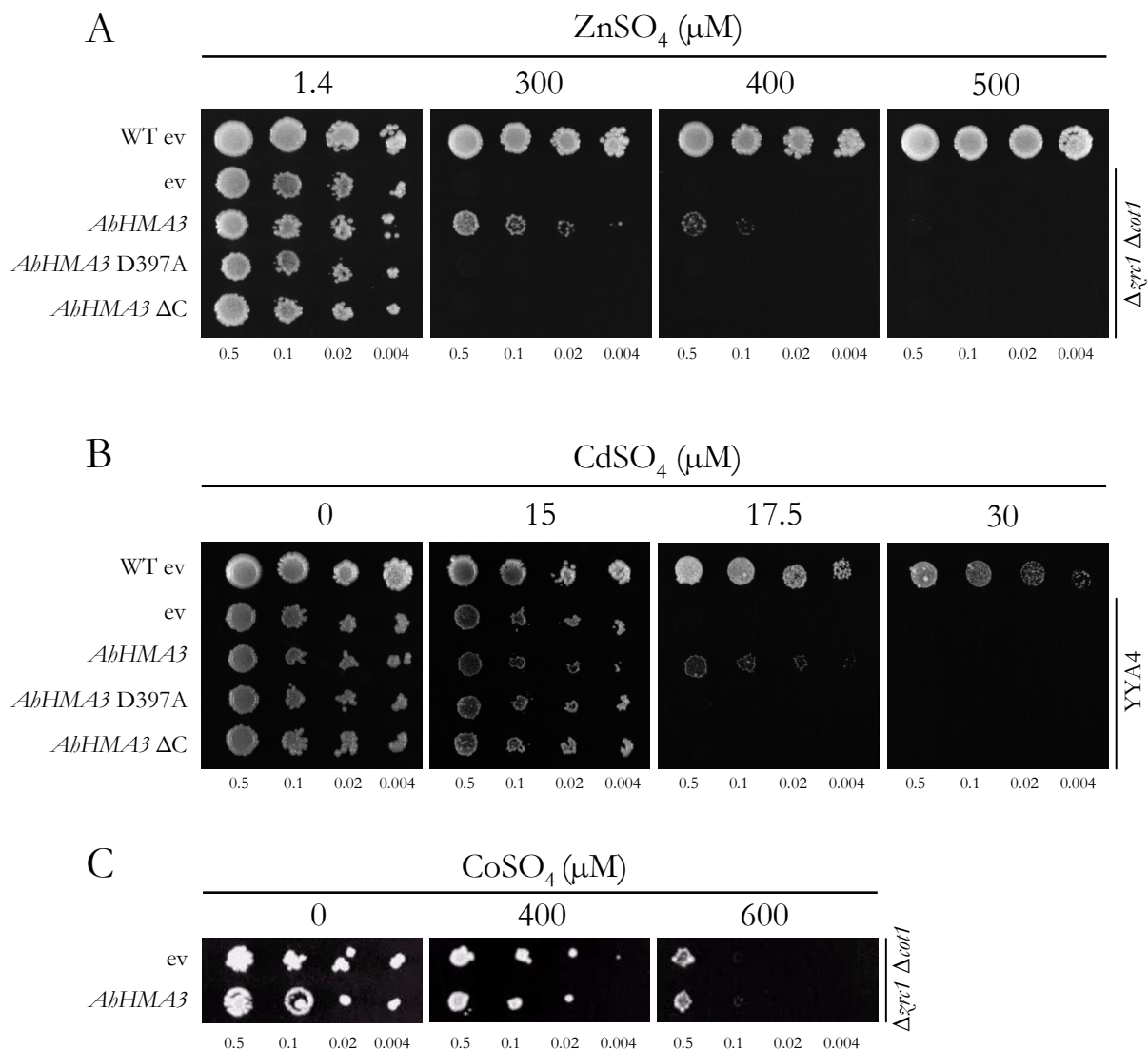


Figure 4.10: Heterologous expression of *AhHMA3* cDNA in the *S. cerevisiae* mutant strains $\Delta zrc1 \Delta cot1$ (A & C) and *YYA4* (B).

The *S. cerevisiae* mutants transformed with pFL61 or pFL613/*AhHMA3* recombinant vector were grown on LSP-URA medium overnight, adjusted to $OD_{600} = 0.5$ and serially diluted (5-fold in each column) in water. Ten μ l aliquots of each dilution were spotted onto LSP-URA medium containing increasing concentrations of (A) $ZnSO_4$, (B) $CdSO_4$ or (C) $CoSO_4$, and incubated for 5 days at 30 °C.

WT: *S. cerevisiae* strain BY4741

ev: pFL61

AhHMA3: pFL613-*AhHMA3*

AhHMA3 D397A: pFL613-*AhHMA3* with D→A mutation in the DKTGT phosphorylation site

AhHMA3 Δ C: pFL613-*emphAhHMA3* with deleted C-terminal end

pFL613-3xHA:*AhHMA3* recombinant vector (Figure 4.12). The prepared membrane fractions were separated on an 8% acrylamid gel by SDS-PAGE and electroblotted onto nitrocellulose membrane. The subsequent immunoblot analysis with an anti-3xHA mouse polyclonal IgG antibody and an anti-mouse IgG horseradish peroxidase-linked monoclonal antibody showed that an 3xHA containing

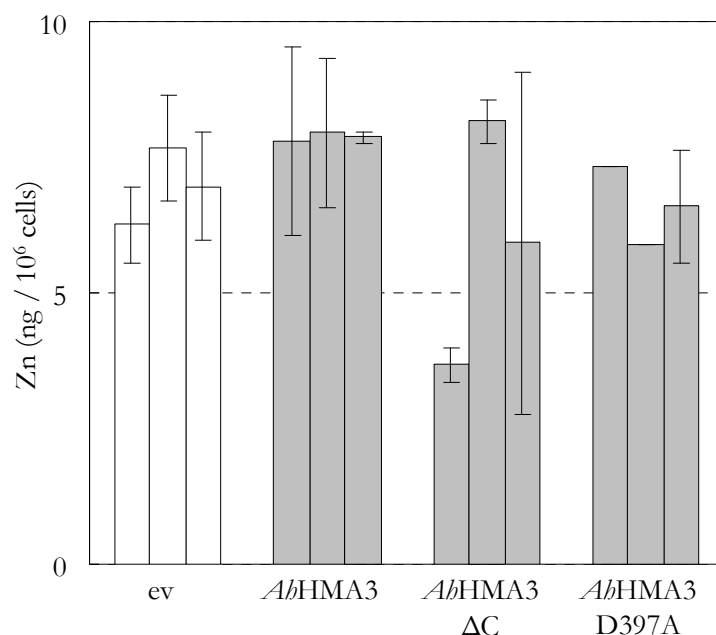


Figure 4.11: Zinc accumulation in yeast cells.

Values are average zinc contents in *S. cerevisiae* $\Delta zrc1 \Delta cot1$ cells transformed with the empty pFL61 vector, or transformed with pFL613-3xHA:AhHMA3, pFL613-3xHA:AhHMA3 ΔC or pFL613-3xHA:AhHMA3 D397A. Cultures were inoculated at an initial density of $0.1 \cdot 10^6$ cells ml⁻¹ and grown to an OD₆₀₀ of approximately 0.5 in LSP-URA medium supplemented with 100 μ M ZnSO₄. Zinc concentrations, analysed by ICP-OES, are expressed per one million yeast cells. Data are arithmetic means \pm standard deviation of three replicate cultures of one transformant. Shown are the values for three replicate independent transformants.

ev: pFL61
 AhHMA3: pFL613-AhHMA3
 AhHMA3 D397A: pFL613-AhHMA3 with D \rightarrow A mutation in the D₃₉₇KTGT phosphorylation site
 AhHMA3 ΔC : pFL613-AhHMA3 with deleted C-terminal end

protein with a molecular weight of about 80-85 kDa is present in yeast cells. The predicted molecular size of AhHMA3 is 86 kDa. However, the direct immunodetection of AhHMA3 with two polyclonal anti-AhHMA3 rabbit peptide antibodies failed, even at lower dilutions as suggested by experiences with another peptide antibody (Stéphanie Arrivault, MPI-MP, personal communication). Peptide antibodies are in general less robust in detection as antibodies directed against whole proteins. The folding of AhHMA3 might render the selected peptide inaccessible to the anti-AhHMA3 peptide IgG antibody.

1.2.2 Functional expression and purification of AhHMA3 in *E. coli* mutants

As an alternative system to investigate the function of HMA3 and furthermore to purify it, AhHMA3 was functionally expressed as a tagged protein in wildtype and mutant cells of *E. coli*. For this purpose, the Strep-Tag[®] II system (IBA, Göttingen, Germany) was chosen. The system allows the expression and fast purification of recombinant proteins in *E. coli* under the control of the stringent controlled tetracycline-promoter (tetA-promoter; Skerra, 1994; see page 45). The promoter is inducible by an-

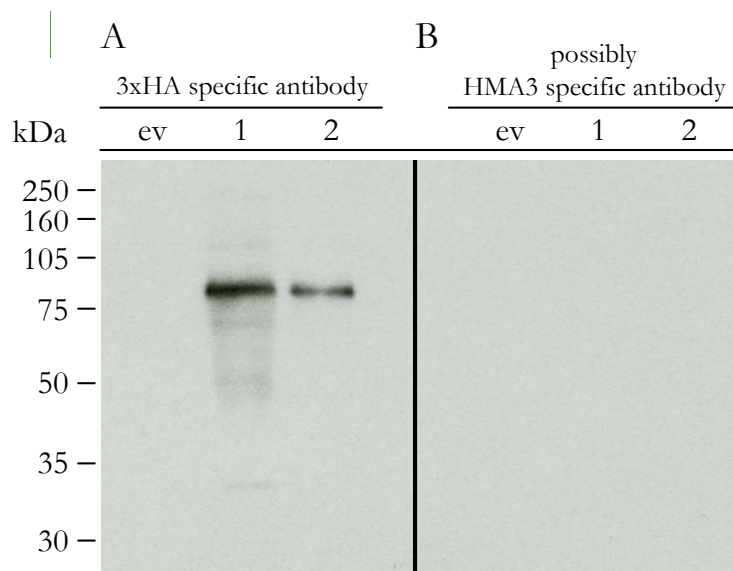


Figure 4.12: Immunoblot analysis of epitope-tagged, heterologously expressed *AhHMA3* protein in the *S. cerevisiae* mutant strain $\Delta zrc1 \Delta cot1$.

Membrane preparations containing approximately 10 μ g protein per lane from yeast cells transformed with pFL61 (empty vector control, **ev**) or pFL613-3xHA:*AhHMA3* recombinant vector (**1** and **2**) were separated in an 8% acrylamide gel by SDS-PAGE.

Heterologous protein was detected after electroblotting the gels onto nitrocellulose membranes and immunostaining with anti-3xHA mouse polyclonal IgG (1:3000 dilution) (**A**) or affinity-purified anti-HMA3 rabbit polyclonal IgG (1:500) (**B**), followed by anti-mouse or anti-rabbit IgG horseradish peroxidase-linked monoclonal antibody (1:5000), respectively (**A**, **B**).

Molecular weight in kDa is indicated on the left. Theoretical molecular weight of 3xHA-*AhHMA3* is 86 kDa.

hydrotetracycline (AHT). For convenience and because *AhHMA3* was already cloned into the Entry Vector of the Gateway[®] cloning system (Invitrogen, Karlsruhe, Germany), it was decided to gatewayise a pASK vector of the *Strep-Tag*[®] II system. The Gateway[®] cassette A (GW-A) was inserted into the pASK-7 vector followed by the integration of the *AhHMA3* sequence from the Entry Vector by a LR reaction (Figure 3.1 on page 36). The resulting recombinant plasmid encodes a N-terminal strep-tagged *AhHMA3* protein.

Only a few *E. coli* colonies positively transformed with this construct were obtained which were impaired in growth. The induction of expression by AHT, even at lower concentrations than recommended, killed the cells (data not shown). It may be that the presence of *HMA3* containing plasmids had toxic effects. The reduction of the incubation temperature (30°C or room temperature, instead of 37°C) neither increased the transformation rate nor the growth of the obtained colonies after transformation.

It is reported that in some cases the C-terminal fusion of the *Strep-Tag*[®] II to the target protein can solve the problem (A. Anton, ScilProt, Halle/Saale, personal communication). Thus, *AhHMA3* was cloned into the pASK-IBA3 vector. This time the cloning was not made via the Gateway[®] system, but instead by restriction and ligation procedures after the addition of flanking restriction sites to

AbHMA3 (see Table 3.3 in the *Materials and Methods* Section). This procedure reduced the amount of additional sequence stretches between the *Strep-Tag[®] II* and *AbHMA3*. The transformation of *E. coli* strains with the resulting pASK-3-*AbHMA3* did not improve the transformation rate or the growth of the cells.

Bacterial complementation experiments and the purification of the protein were no longer continued due to time constraints.

1.2.3 Functional characterisation of *HMA3* in *A. thaliana*

Analysis of a *AtHMA3* T-DNA insertion line The T-DNA insertion line 274D12 (*bma3-a²*, an *AtHMA3* knockout) was obtained from the GABI-Kat collection (Columbia ecotype, Rosso *et al.* (2003)). The given segregation ratio (about 77% sulfadiazine resistant plants) in the T2 generation is consistent with a single T-DNA insertion in the genome. According to the GABI-KAT information the T-DNA should be inserted into the 6th exon of the *AtHMA3* coding region. This corresponds to the 5th transmembrane domain of the protein. One would expect that this insertion causes a loss of *AtHMA3* transport activity. For further studies, progeny of three T2 individuals (No.1.3, 1.7 and 1.8) were selected which were completely resistant to sulfadiazine. The position of the insertion and homozygosity was verified by PCR using genomic DNA as a template (data not shown). The next step was to look for an altered phenotype in selected plants compared to wildtype plants of *A. thaliana* ecotype Columbia.

Four days after germination on MS media, seedlings were transferred onto Hoagland-based agarose media containing different Zn concentrations and root elongation was measured. At all tested Zn concentrations, root elongation in the knockout plants did not differ significantly from those of wildtype plants (Figure 4.13). One exception was observed once for the progeny of individual No.3 of the knockout line at 150 μ M Zn. These knockout plants appeared more sensitive to Zn than the wildtype plants (Figure 4.13 B). After repeating the assay, this phenotype could not be confirmed. Interestingly, when the plants were kept growing for a longer period, only the wildtype plants started to flower at higher Zn concentrations. Since this phenotype occurred only once on one plate, it was not reproducible and will not be considered further.

While conducting those experiments, Hussain *et al.* (2004) published data that shows that the Columbia ecotype of *A. thaliana* is a natural knockout of *AtHMA3*. In the Columbia ecotype a single base pair deletion leads to a subsequent truncation of the encoded *AtHMA3*. The mutation was confirmed in the *A. thaliana* ecotype Columbia used at the MPI-MP (see details on page 66). In the light of this data, further experiments on the mentioned T-DNA insertion line were discontinued. It might be noted that the predicted truncated protein in Columbia wildtype plants is 215 amino acids

²Two T-DNA insertion lines are available at GABI-Kat (*Genomanalyse im biologischen System Pflanze - Kölner Arabidopsis T-DNA lines*), 274D12 (*bma3-a*) and 606H08 (*bma3-b*). However, the *bma3-b* line was not ordered because the T-DNA insertion is located 533 bp downstream of the transcriptional stop of *HMA3* and thus, is not considered to disrupt *HMA3* activity efficiently.

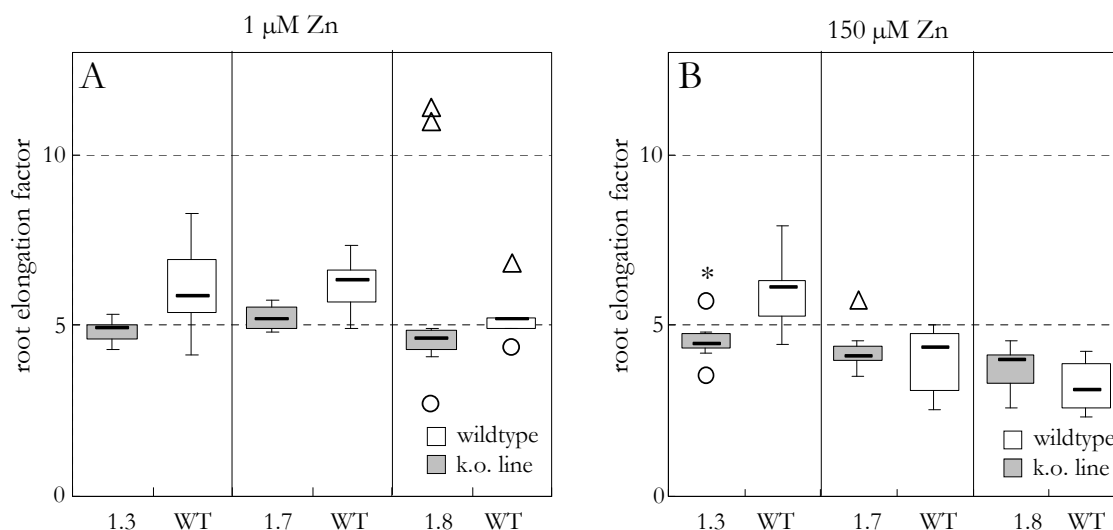


Figure 4.13: Root elongation in a *HMA3* knockout line and wildtype plants on $ZnSO_4$ containing medium.

The diagram shows average root elongation factors calculated as the ratio of root length at day 18 and day 7 of *A. thaliana* seedlings (ecotype Columbia) of wildtype plants and three homozygous *AtHMA3* T-DNA single-insertion lines (GABI-KAT No.274D12). The plants were germinated on MS medium supplemented with 0.7% (w/v) select agar and 0.5% (w/v) sucrose. Four days after germination, the seedlings were transferred onto 0.25-strength Hoagland medium containing 1, 10, 30, 60, 150 (A) and 300 μM (B) $ZnSO_4$. Data are arithmetic means of 10 seedlings from one experiment representative of a total of two independent experiments. Vertical bars represent interquartile ranges. The asterisk (*) indicates a statistically significant difference between means ($P < 0.05$) according to a one-way ANOVA, followed by a Tukey's test.

Circles (o) represent normal outliers, triangles (Δ) extreme outliers.

Normal outliers: do not lie between the "3rd quartile + ($1.5 \times IQR$)" and the "1st quartile - ($1.5 \times IQR$)" (IQR means interquartile range).

Extreme outliers: do not fit between the "3rd quartile + ($3 \times IQR$)" and the "1st quartile - ($3 \times IQR$)"

longer than in the T-DNA insertion line and additionally contains residues of the large cytoplasmic loop.

Ectopic overexpression of *AbHMA3* in *A. thaliana* The binary vector pB735SGW, containing the promoter and terminator of the Cauliflower Mosaic Virus (CaMV 35S) was used to overexpress *AbHMA3* in *A. thaliana* ecotype Columbia. The construct was generated by Martina Becher, a former PhD student in the group of Ute Krämer. After infiltration and seed harvest, only two resistant seedlings were obtained after selection on phosphinotrycin giving rise to line 1 and line 2. The T2 progeny of these two lines showed a 15:1 segregation ratio for phosphinotrycin resistance suggesting two independent T-DNA insertions in the genome. Based on Mendel's law, it was expected that 26.7% of the resistant T2 plants are heterozygous single insertions, i.e. 4 to 6 of 20 plants. Hence, the progeny of 20 T2 seedlings per line was analysed for a 3:1 segregation ratio. Three 3:1 segregating T3 populations per line were found and cultivated for seed production. Two T4 progenies per line (line 1.1, 1.9 and 2.5, 2.6) that showed a 100% resistance to phosphinotrycin were selected for root

elongation test on plates containing different Zn concentrations.

Four days after germination on MS media, seedlings were transferred onto Hoagland-based agarose media containing different Zn concentrations and root elongation was measured. Root elongation factors of the *35S-AhHMA3* plants did not differ significantly from those of wildtype plants (Figure 4.14). One exception was observed for line 2.6 at 150 μ M Zn. These *AhHMA3* overexpressing plants appeared to be more sensitive to Zn than the wildtype plants (Figure 4.14 B). However, the effect of *AhHMA3* overexpression on the root elongation of seedlings in the presence of different Zn concentrations was, if at all, only subtle. An explanation could be that overexpressed *AhHMA3* does not contribute substantially to the Zn detoxification of roots *in planta* because of the lack of equally overexpressed, functionally essential, interacting protein partners as will be discussed in the case of 14-3-3 proteins (see *Discussion* section 2.1.1 on page 121). It might also be that *in planta* *AhHMA3* is more specific to Cd than to Zn. A root elongation test on plates containing different Cd concentrations should help to investigate that possibility. Furthermore, it remains to be verified if *AhHMA3* transcript levels are enhanced in tested *35S-AtHMA3* T-DNA insertion lines e. g. by real-time RT-PCR or Northern blotting.

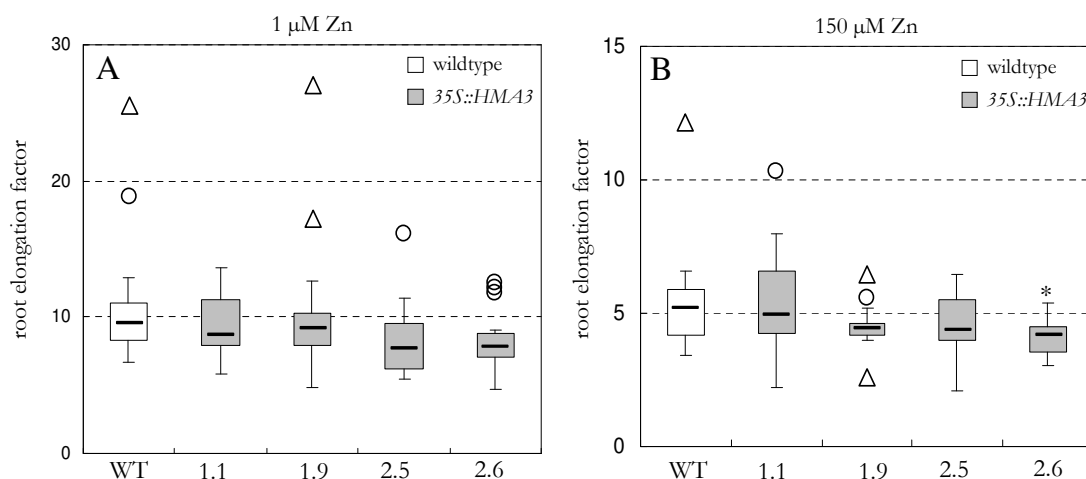


Figure 4.14: Root elongation in *HMA3* overexpressing lines and wildtype plants on $ZnSO_4$ containing medium.

The diagram shows average root elongation factors calculated as the quotient of root length at day 17 and day 7 of *A. thaliana* seedlings (ecotype Columbia) of wildtype plants and plants of 2 homozygous *35S-AtHMA3* T-DNA single-insertion lines. The plants were germinated on MS medium supplemented with 0.7% (w/v) select agar and 0.5% (w/v) sucrose. Seven days after germination, the seedlings were transferred onto 0.25-strength Hoagland medium containing 1 μ M $ZnSO_4$ (A) or 150 μ M $ZnSO_4$ (B). Data are arithmetic means of 20 seedlings from one experiment representative of a total of two independent experiments. Vertical bars represent interquartile ranges. The asterisk (*) indicates a statistically significant difference between means of a line and wildtype means ($P < 0.05$) according to a one-way ANOVA, followed by a Tukey's test.

Circles (o) represent normal outliers, triangles (Δ) extreme outliers.

Normal outliers: do not lie between the "3rd quartile + (1.5 \times IQR)" and the "1st quartile - (1.5 \times IQR)" (IQR means interquartile range).

Extreme outliers: do not fit between the "3rd quartile + (3 \times IQR)" and the "1st quartile - (3 \times IQR)"

1.2.4 Summary - Functional characterisation

In the $\Delta zrc1 \Delta cot1$ *S. cerevisiae* mutant, heterologously expressed *AbHMA3* partially complemented the Zn but not the Co hypersensitive phenotype. The Cd sensitive phenotype of the YYA4 yeast mutant was complemented to a minimal degree by *AbHMA3* expression. A nonfunctional *AbHMA3* mutated in the essential phosphorylation site **DKTGT**, did not show any complementation. The deletion of the C-terminal domain of *AbHMA3* did not affect the metal sensitive phenotype of the used yeast mutants, indicating that the C-terminal domain is required for *AbHMA3* function. The Zn content in *AbHMA3* expressing yeast cells and cells transformed with an empty vector did not differ significantly. Future investigations should include wildtype yeast cells transformed with the empty control vector pFL61 as a positive control in order to evaluate if the chosen method is sensitive enough to distinguish between cell-associated Zn concentrations in empty vector control and *AbHMA3* expressing metal-sensitive yeast cells. *AbHMA3* was not detected by a possibly anti-HMA3 polyclonal IgG antibody. The use of a 3xHA polyclonal IgG antibody confirmed, however, the expression of a protein in transformed yeast cells with a molecular size similar to *AbHMA3*.

The expression and purification of *AbHMA3* as a strep-tagged fusion protein in *E. coli* did not work due to a bad growth and viability of obtained bacterial clones, especially after induction of *AbHMA3* expression.

The analysis of root elongation of an *A. thaliana* (Columbia accession) *AtHMA3* T-DNA line and a *HMA3* overexpressing line on plates containing different Zn concentrations did not reveal an altered sensitivity to Zn compared to the wildtype. Considering the results of the T-DNA line analysis, it is important to know that Hussain *et al.* (2004) reported a single-site base pair deletion that renders the encoded *AtHMA3* nonfunctional in the Columbia accession that was the wildtype for the T-DNA line analysed here. The results reported here are therefore as expected based on Hussain *et al.* (2004).

Obtained data from *AbHMA3* overexpressing lines are only preliminary because *HMA3* transcript levels were not quantified in the generated lines. However, the data raised the possibility of a functionally important interaction of *AbHMA3* with an unknown component *in planta*, or to an altered metal specificity of *AbHMA3* when expressed *in planta*. Testing root elongation in response to high concentrations of Cd or other transition metals should help to investigate this possibility.

1.3 Subcellular localisation of HMA3 in *A. thaliana*

The subcellular localisation of HMA3 is important to understand its function. For a first hypothesis, *in silico* predictions can yield useful information.

1.3.1 *In silico* prediction of subcellular localisation

Based on known signal peptide sequences, several algorithms exist to calculate the probability for an unknown protein to be targeted to the chloroplast, mitochondria, nucleus, the endoplasmic reticulum (ER) or to the secretory pathway. Prediction algorithms for tonoplast localisation are not available. The probability values are often given in a range from 0 to 1 with 1 as the highest probability. A good online service that summarises the results from a query of nine different prediction algorithms can be found on the ARAMEMNON webpage (release 3.2, aramemnon.botanik.uni-koeln.de)

For *AtHMA3*, thirteen out of fifteen predictions show a maximum of less than 10% probability for the localisation to the highest-scoring subcellular compartment (Table 4.6). TargetP_v1 predicts *AtHMA3* to be localised to the secretory pathway with a probability of 16% and ChloroP_v1.1 shows a 44% likelihood for a chloroplastic localisation. For *AhHMA3*, the values do not differ much. Therefore, based on this *in silico* analysis, a clear prediction of the localisation of *HMA3* to the membranes of chloroplasts, mitochondria or the secretory pathway is not possible.

However, signal peptide predictions can only be used to generate a hypothesis concerning a possible localisation. Any predicted localisation has to be verified by experimental data. One way to obtain such data is the fusion of the investigated protein with a reporter protein, for example the green fluorescent protein (GFP).

Table 4.6: *In silico* prediction of subcellular localisation of *AtHMA3*/*AhHMA3*.

Shown are the results from the ARAMEMNON webpage (release 3.2, aramemnon.botanik.uni-koeln.de) for the *AtHMA3*. Values for *AhHMA3* were obtained separately for each given prediction tool. The given values are signal peptide probabilities in the range from 0 to 1 with 1 as the highest probability.

tool	<i>AtHMA3</i> / <i>AhHMA3</i>		
	chloroplast	mitochondria	secretory pathways
TargetP_v1.1	0.02 / 0.015	0.04 / 0.045	0.16 / 0.017
Predotar_v1	0.00 / 0.01	0.01 / 0.00	0.01 / 0.01
iPSort	0.00 / 0.00	0.00 / 0.00	0.00 / 0.00
ChloroP_v1.1	0.44 / 0.43		
PCLR_v0.9	0.04 / 0.015		
MitoProt_v2		0.04 / 0.015	
Mitopred		0.00 / 0.00	
SignalP_HMM_v3			0.00 / 0.049
SignalP_NN_v3			0.06 / 0.00

1.3.2 Expression of an *AbHMA3*:GFP6 fusion protein in *A. thaliana*

The histidine-tagged reporter protein GFP6 (Schuldt *et al.*, 1998) was fused to the C-terminus of *AbHMA3* because a N-terminal fusion could lead to a mislocalisation of the fusion protein. For that purpose, the Gateway® binary vector pMDC83 (Curtis collection, Curtis and Grossniklaus (2003)) was chosen. For a C-terminal fusion it was necessary to clone *AbHMA3* without a stop codon into the vector pENTR™/D-TOPO® (Section *Materials and Methods* on page 34). Similar problems as described for the cloning of *AbHMA3* for the expression in *E. coli* (page 79) occurred. The plated transformations did not result in a positive pENTR™-*AbHMA3* clone without a stop codon. After transformation and selection on kanamycin, the few obtained colonies had mutated sequences, often resulting in a frameshift and a premature translational stop codon. Also the reduction of the incubation temperature did not help to obtain positive clones with the desired sequence.

Hence, it was attempted to clone *AbHMA3* without stop directly into pMDC83 avoiding further subcloning steps. After transformation in *E. coli* and selection for kanamycin resistance, positive clones with the correct sequence were obtained (see *Materials and Methods* Section on page 31). In individuals of the T1 generation no GFP signal could be detected. For further analysis, about 30 T2 seedlings per line were tested for a 3:1 segregation ratio and GFP signals. No GFP signal was detectable. It is possible that the transcript of *AbHMA3* or the translated protein itself is stabilised by the presence of metal ions. In an attempt to enhance the putative GFP signal from a *AbHMA3*-GFP fusion protein, seedlings of all lines were transferred on plates containing 100 µM ZnSO₄ or 40 µM CuSO₄. No GFP signal was detected during a 5 day observation period.

1.3.3 Summary - Subcellular localisation

Based on *in silico* analysis, a prediction of the subcellular localisation is not possible.

A. thaliana was independently transformed twice with a *AbHMA3*:GFP construct. No GFP signal was detected in plants of the T1 generation and in 20 selected lines of the T2 generation. There are many possible reasons for the failed detection. In short, the aggregation and precipitation of *AbHMA3* in the cell as non-fluorescent inclusion bodies, or an unstable, misfolded, and rapidly degraded GFP fused HMA3 protein could serve as an explanation. Zinc plays an critical structural role and could also be important for the stabilisation and correct folding of HMA3. However, the adding of extra zinc to the growth medium did not enhance a potential fluorescence signal. This will be discussed later on page 125.

2 Analysis of *HMA3* expression in *Arabidopsis*

2.1 *In silico* analysis of *AtHMA3* expression

The expression of *HMA3* in *A. thaliana* was analysed *in silico* by querying the Geneinvestigator Database (geneinvestigator.ehz.ch; Zimmermann *et al.*, 2004). This database provides access to an extensive set of AFFYMETRIX Arabidopsis GeneChip® data. The experimental data and annotations are provided by the:

- Gruissem Laboratory (ETH Zurich)
(www.fgcz.ethz.ch)
- Functional Genomics Center Zurich (FGCZ)
(www.fgcz.ethz.ch)
- Arabidopsis Functional Genomics Network consortium (AtGenExpress)
(web.uni-frankfurt.de/fb15/botanik/mcb/AFGN/atgenex.htm)

and public repositories, namely the:

- Nottingham Arabidopsis Stock Centre Transcriptomics Service (NASCarrays)
(ssbdjc2.nottingham.ac.uk/narrays/experimentbrowse.pl)
- European Bioinformatics Institute (ArrayExpress)
(www.ebi.ac.uk/arrayexpress/)
- Gene Expression Omnibus at NCBI (GEO)
(www.ncbi.nih.gov/geo/)

The Geneinvestigator database features a function called GeneAtlas. This function was chosen to display the results of a query sorted by organ (Figure 4.15). The reported single-base pair deletion in *AtHMA3* from *A. thaliana* accession Columbia is likely to result in reduced *AtHMA3* transcript levels caused by non-sense mediated mRNA decay (Maquat, 2002; Hussain *et al.*, 2004; see section 1.1.4 on page 66). The Geneinvestigator database did not allow to exclude expression data from *A. thaliana* accession Columbia plants. Nonetheless, even if *HMA3* expression is reduced, the relative ratio between *HMA3* transcript levels in different plant organs should remain unchanged.

Based on the database query, *AtHMA3* is ubiquitously expressed in *A. thaliana*. The highest expression levels are reported for radicles of one-week-old seedlings, for roots of three-week-old plants and for senescent leaves (Figure 4.15).

The Geneinvestigator database also offers the possibility to compare the expression levels of several genes in different plant tissues by the provided Meta-Analyzer function. This was done for *AtHMA1* to *AtHMA7*. The expression pattern of *AtHMA8* is missing because it is not represented on AFFYMETRIX Arabidopsis GeneChips® (Figure 4.16). All data comes from *A. thaliana* plants of the Columbia accession.

Each *HMA* gene shows a distinct expression pattern with the exception of *AtHMA5* and *AtHMA7* (*RAN1*). The latter two genes share a similar expression pattern. Published data suggests a localisation

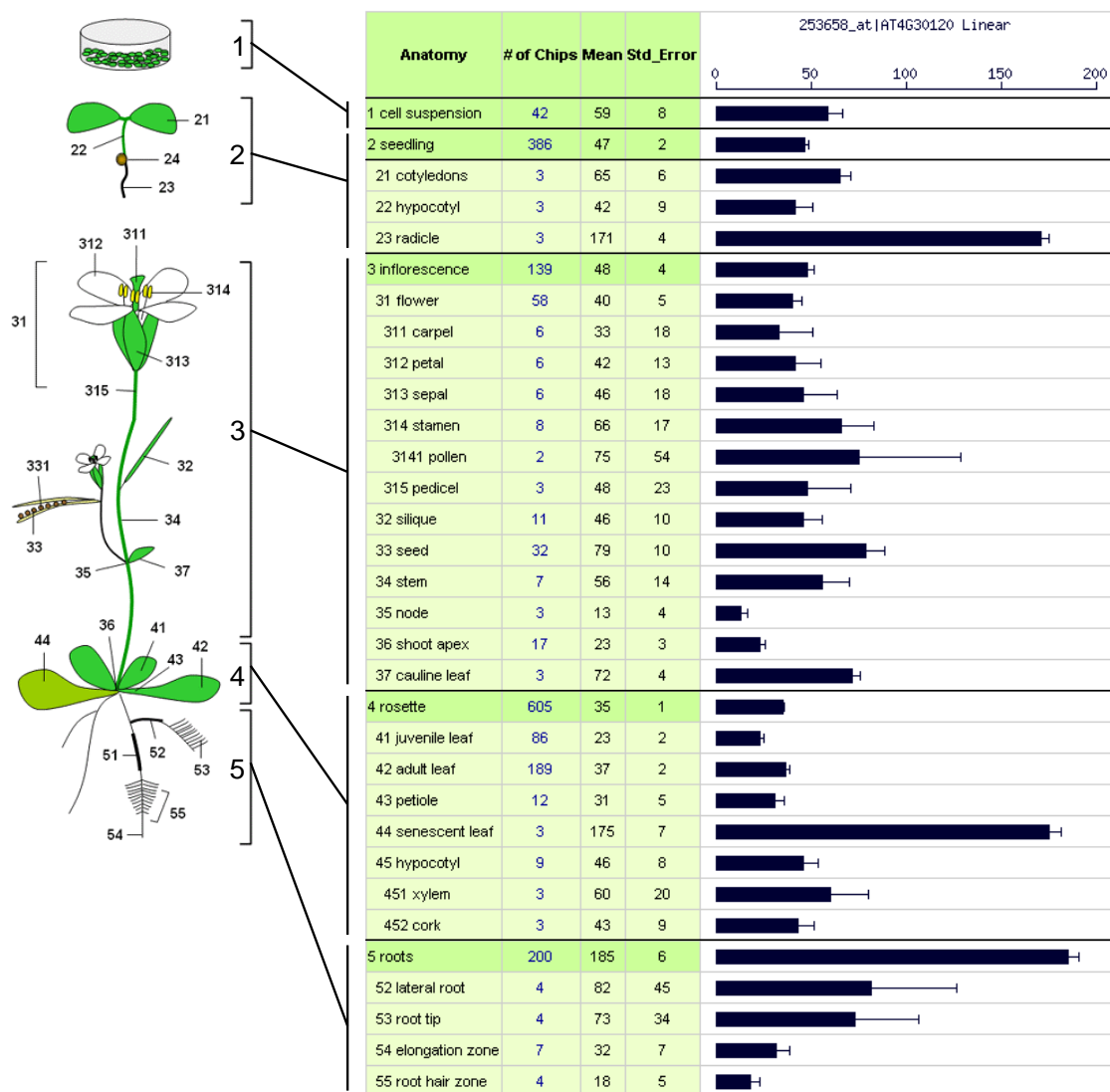


Figure 4.15: Expression pattern of *AtHMA3* determined by the GeneAtlas function in the Genevestigator Database (genevestigator.ehz.ch; Zimmermann *et al.*, 2004).

The table lists relative expression values for five main plant organ or cell groups and corresponding subgroups. Each of the five main groups contains all chip data from the subgroups in addition to their own. For example, the organ “root” (main group) contains all chips hybridised with RNA extracted from whole roots as well as from individual or a combination of specific root tissues (subgroups) such as root hairs, root tip, etc. In contrast, the subgroups (e.g. “root tip”) contain data from chips hybridised with cRNA made from the respective subgroup only. Values are given as the average and the standard error of each group. The number of chips per group is indicated.

of *AtHMA5* and *AtHMA7* (*RAN1*) to a post-Golgi-compartment membrane and a role in Cu compartmentalisation and detoxification (Alonso *et al.*, 1999; Hirayama and Alonso, 2000; Woeste and Kieber, 2000; Lin and Culotta, 1995; Lin *et al.*, 1997; Andrés-Colás *et al.*, 2006) (see page 21 in the *Introduction* Section). The expression patterns of the three close homologs of the Zn/Cd/Co/Pb - Cluster (see page 23), *AtHMA2*, *AtHMA3* and *AtHMA4* differ from each other. In contrast to the already men-

of *HMA2* is restricted to the pericycle of the specialisation zone (stage 3). A similar expression map was obtained for *HMA4* but with an additional expression in the stele. The expression of *HMA1* is also highest in the specialisation zones, especially in cells of the pericycle and the stele (Figure 4.17 A).

Similar to *HMA2* and *HMA4*, *HMA5* is predominantly expressed in pericycle cells of the root specialisation zone. *HMA7* transcript is also elevated in the specialisation zone, particularly in cells of the pericycle and the endodermis. In contrast to other *HMA*s, the expression of *HMA6* is highest in the root cap and decreases towards mature root tissue (Figure 4.17 A).

It should be noted that the maximum signal intensities obtained for *HMA3* are very low compared to the other *HMA* genes, and thus, increasing the influence of errors on the expression values of *HMA3*. It remains to be investigated if plants of the C24 accession also feature a single-basepair deletion as reported for the Columbia accession (Hussain *et al.*, 2004) that could help to explain the low signal intensities as an effect of the suspected non-sense mediated mRNA decay (Maquat, 2002).

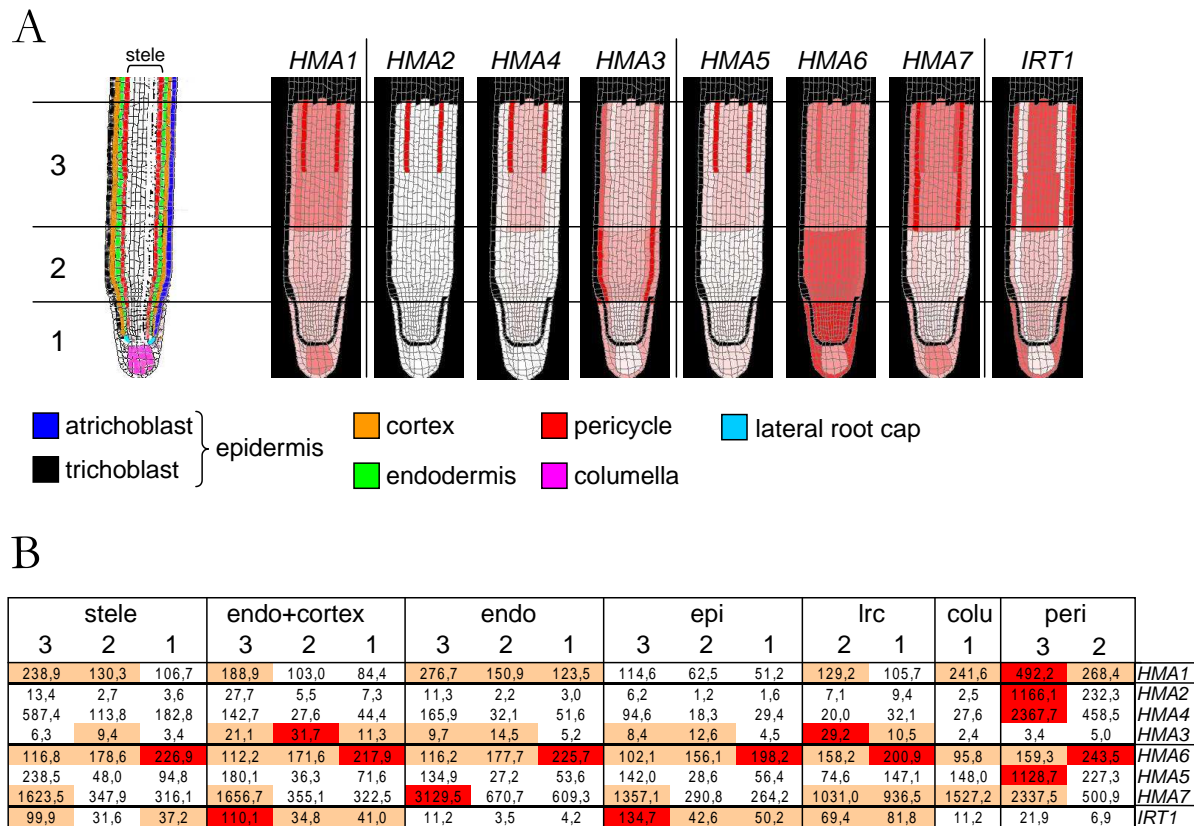


Figure 4.17: Comparison of expression patterns of *HMA1* to *HMA7* at three developmental root stages as determined by digital *in-situ* expression mapping at the AREX database (arexdb.org; Birnbaum *et al.*, 2003).

A: The Scheme illustrates the different analysed root tissue types and progressive developmental stages. The relative expression levels of *HMA1* to *HMA7* was determined in cells from the inner stele (stele), the pericycle (peri), the endodermis (endo), the endodermis plus cortex (endo+cortex), the epidermal atrichoblast cells (epi), the lateral root cap (Lrc) and the columella (colu). Moreover, gene expression data was obtained from three progressive developmental stages (stage 1, 2 and 3) characterised by the following features: stage 1, where root tip reached its full diameter (root cap); stage 2, where cells begin longitudinal expansion; stage 3, where root hairs were fully elongated. For each selected gene, a root expression map is given. Dark red correlates to a high expression level.

B: Average values from the 17 subzones are shown. Shades of red represents relative expression levels and a dark red indicates a high expression level. Please note that the shades of red only correlate to the relative expression values of the same gene and cannot be used to compare different gene expression levels.

IRT1 expression is included for later discussion. At the time of query, *AtHMA8* was not present in the data-base.

2.2 Quantitative real-time RT-PCR

2.2.1 Expression analysis of *HMA3* in different ecotypes

Transcript levels of *HMA3* in the *A. thaliana* ecotypes Ws and Col-0 as well as in *A. halleri* Lan3.1 were compared to each other under low and high zinc conditions (Figure 4.18). The purpose of these experiments was to ensure that the reported differential expression of *HMA3* between *A. halleri* and *A. thaliana* is also observed when *A. halleri* plants are compared to plants of the *A. thaliana* ecotype Wassilewskija (Ws). This was necessary because of a frameshift mutation in the *AtHMA3* coding sequence of the Columbia accession (see Section 1.1.4 on page 66).

To analyse the expression of *HMA* genes, *Arabidopsis* plants were hydroponically grown in 0.25-strength Hoagland medium (*Materials and Methods* Section 8.2.2 on page 53). In addition, plants from the *A. thaliana* accession Brunn (Br-0) were included in the experiment. The Br-0 ecotype served as an additional control. Furthermore, root length growth experiments suggested a higher tolerance of the accession Br-0 toward Zn (I. Talke, group of Ute Krämer; personal communication). Br-0 was used to test whether the higher tolerance correlates with altered *HMA3* transcript levels. Besides the transcript levels of *HMA3*, the transcript levels of *HMA1*, *2* and *4* were determined as well to investigate the expression pattern of these *HMA3* related genes in other accessions of *A. thaliana*.

It was confirmed that that *HMA3* transcript levels are higher in shoots of *A. halleri* compared to *A. thaliana*, and that transcript levels are similar in roots of both species (Figure 4.18 C and Becher *et al.*, 2004). *HMA3* transcript levels were upregulated by high zinc concentrations in *A. thaliana* but not in *A. halleri*. Thus, the differences in *HMA3* transcript levels between *A. halleri* and *A. thaliana* were confirmed also in an accession harbouring a functional *HMA3* gene. But when transcript levels among the different ecotypes were compared, it was noteworthy that in shoots of the Columbia ecotype, virtually no *HMA3* transcript was present and that root transcript levels were about 4- to 7-fold lower compared to the Ws and Br-0 ecotypes. Transcript levels of *HMA1*, *2* and *4* were similar in all accessions and differed as expected from expression pattern of *HMA3* (Figure 4.18 A, B and D).

2.2.2 Copy-specific expression analysis of *AbHMA3*

As described previously, the genome of *A. halleri* contains more than one copy of *HMA3* (section 1.1 on page 58). By amplifying genomic *AbHMA3* sequences from different BAC clones and genomic DNA from two different accessions, two distinct *AbHMA3* sequences were found, *AbHMA3-1* and *AbHMA3-2* (Figure 4.4 on page 65). The knowledge of characteristic sequence differences between *AbHMA3-1* and *AbHMA3-2* allowed the design of copy-specific primer pairs. To analyse transcript levels in a copy-specific manner, primers had to be designed on distinguishing features in exon sequences. Of the five copy-specific features that were determined in exon regions of *AbHMA3* (Table 4.2 on page 64) only one was suitable to design specific real-time RT-PCR primers. The designed primers, BAC7-1F and BAC6-2F, were based on the GGT/ACC substitution in exon I (*Appendix* Section, Figure A.3).

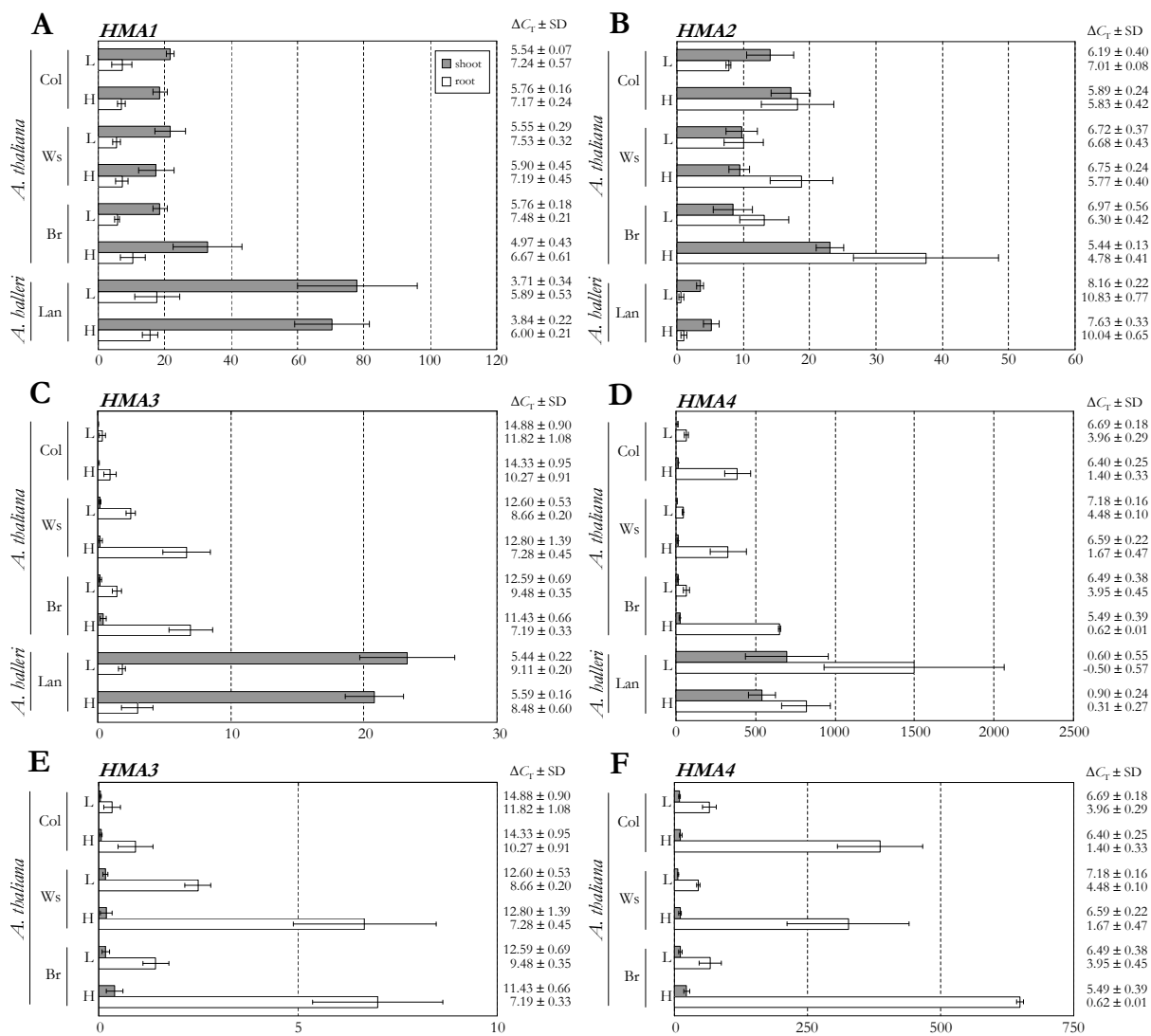


Figure 4.18: Expression analysis of *HMA1* to *HMA4* in different accessions of *A. halleri* and *A. thaliana* using real-time RT-PCR.

Relative transcript levels were determined in shoots (green) and roots (yellow) of hydroponically grown six-week-old plants after a four-day exposure to low (L; no added $ZnSO_4$) and high (H; $100 \mu M ZnSO_4$ for *A. thaliana*; $300 \mu M ZnSO_4$ for *A. halleri*) Zn concentrations. For a better representation, transcript levels of *HMA3* and *HMA4* in *A. thaliana* are shown in the subfigures E and F, respectively. The given values are mean relative transcript levels based on the expression of the constitutive control gene *EF1 α* and are based on at least three technical replicates for each treatment comprising three individual plants each. The *EF1 α* primers exhibited an average C_T value of 19.17 ± 1.71 between different cDNAs.

Col, Columbia; Ws, Wassilewskija; Br, Brunn; Lan, Langelsheim

Both primers contained the distinctive three nucleotides at their 3'-end. Another forward primer for the unspecific detection of *AbHMA3* (USP-F) annealed 16 bp upstream. The corresponding reverse primer, USP-R, hybridised 149 bp downstream of USP-F and was not copy-specific. The cDNA was obtained from the experiment described above (see page 92).

As expected, the unspecific primer pair was able to amplify *AbHMA3* from all templates (see Figure 4.19 B). The *AbHMA3-2* specific primer pair led to a detectable signal on DNA of BAC No.6

that is known to contain a *AbHMA3-2* sequence and on cloned genomic *AbHMA3-2* from the *A. halleri* individual Lan3. On cloned cDNA and genomic DNA of *AbHMA3-1*, only the use of the *AbHMA3-1* specific primer pair successfully amplified a fragment. The results suggested a high specificity of the *AbHMA3-1* and *AbHMA3-2* primer pairs.

Interestingly, both copies, *AbHMA3-1* and *AbHMA3-2*, were detected on DNA of BAC clone No.7 with primer pairs specific to *AbHMA3-1* and *AbHMA3-2*, respectively (Figure 4.19 B). The C_T for the *AbHMA3-2* signal on BAC No.7 was about two cycles higher than for total *AbHMA3*, and the C_T for the *AbHMA3-1* signal on BAC No.7 was about one cycle lower than for *AbHMA3-2*. One (1) cycle difference reflects a doubled (2^1) amount of *AbHMA3* template. Under consideration of primer specific reaction efficiencies, the values correlate with an 1:2 ratio of *AbHMA3-2* and *AbHMA3-1* signal intensities, respectively. Based on this observation, it appears that BAC No.7 could contain one copy of an *AbHMA3-2*-like sequence and two copies of *AbHMA3-1*-like sequences. However, the difference of only one amplification cycle between different primer pairs might be too small for a confident conclusion about the exact number of *AbHMA3* copies on BAC No.7. Moreover, Southern hybridisation data only supports a total number of two *AbHMA3* copies on BAC No.7 (see Figure 4.3 on page 62). The putative fourth copy of *AbHMA3* on BAC No.7 is called *AbHMA3-4*.

To analyse the copy-specific expression of *AbHMA3* in *A. halleri* the primer pairs were applied to the cDNA samples from roots and shoots exposed to different metal treatments. In shoots of *A. halleri*, the *AbHMA3-1* specific primer pair resulted in similar constitutively high transcript levels than the use of unspecific *AbHMA3* primers. Virtually no expression of *AbHMA3-2*-like genes including *AbHMA3-4* was detected (Figure 4.19 A).

The same was observed for roots of *A. halleri* treated with 300 μ M Zn. But the relative transcript levels in roots were about 10 times lower than in shoots (Figure 4.19 A). Interestingly, *AbHMA3-2*-like expression was detected only in roots of plants grown at low Zn supply. Transcript levels of *AbHMA3-1* and *AbHMA3-2/AbHMA3-4* were each about the half of total *AbHMA3* transcript level. In roots of *A. halleri*, however, total *HMA3* transcript levels were no higher than in *A. thaliana*.

AbHMA3 transcript levels are increased in roots of six-week-old *A. halleri* plants after exposure to Cu for 2 and 8 hours (I. Talke, group of Ute Krämer; personal communication). The cDNA samples of that experiment were included in the experiment described here. In contrast to the obtained data after exposure to Zn (Figure 4.19 A), an 8-hour treatment with Cu increased the expression of *AbHMA3-2/AbHMA3-4* by a factor of 10 whereas *AbHMA3-1* transcript levels doubled at most (Figure 4.19 C). The transcript levels of both copies add up to approximately the total determined *AbHMA3* transcript level.

In conclusion, the constitutively high transcript levels of *HMA3* in *A. halleri* originate mainly from an *AbHMA3-1* related sequence rather than from an *AbHMA3-2*-like gene copy including *AbHMA3-4*. But *AbHMA3-2/AbHMA3-4* expression is increased by high Cu concentrations, and this observation might indicate a specific role of *AbHMA3-2*-like genes in the response of *A. halleri* to altered Cu con-

centrations. The fourth *AbHMA3* gene copy (*AbHMA3-4*) that is related to *AbHMA3-2* was detected on BAC clone No.7.

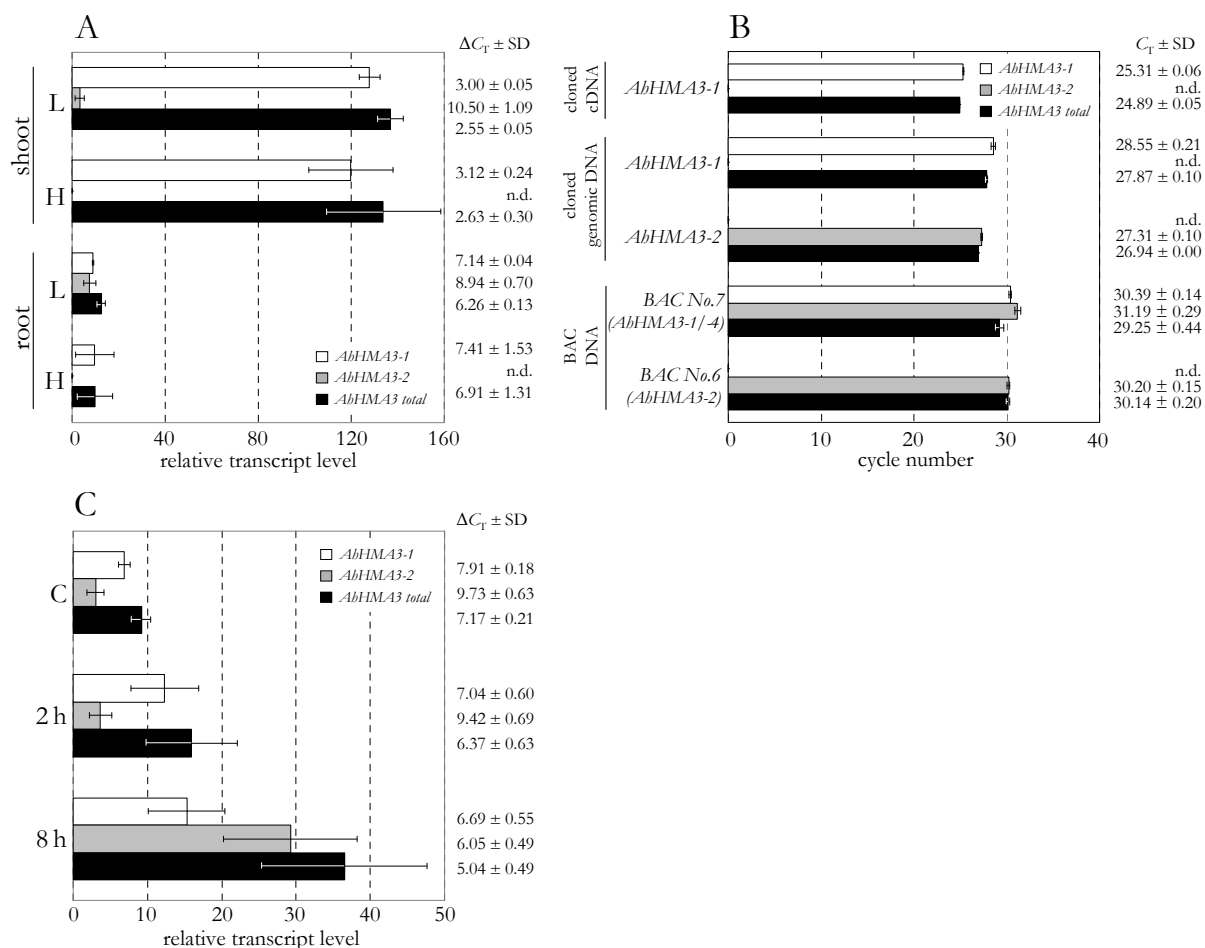


Figure 4.19: Copy-specific expression analysis of *AhHMA3* using real-time RT-PCR.

(A) Relative transcript levels were determined in shoots and roots of hydroponically grown six-week-old plants after a four-day exposure to low (L; no added ZnSO_4) and high (H; $300 \mu\text{M ZnSO}_4$) Zn concentrations. The given values are mean relative transcript levels normalised to the constitutive control gene *EF1 α* and are based on at least three technical replicates for each treatment comprising three individual plants each. The calculation includes the reaction efficiencies (R_{eff}) and is calculated as described on page 41. The *EF1 α* primers exhibited an average C_T value of 19.61 ± 1.07 between different cDNAs.

(B) Detection of *AhHMA3* copies on BAC plasmid DNA of BAC clone No.7, thought to contain the *AhHMA3-1* copy and on BAC clone No.6, containing the *AhHMA3-2* copy. Cloned genomic DNA of *AhHMA3-1* (from *A. halleri* accession Lan5) and *AhHMA3-2* (from *A. halleri* accession Lan3) as well as cloned *AhHMA3-1* cDNA served as control templates^a. Please note that the given values are not relative transcript levels but cycle numbers (C_T) at which the amount of PCR product reached a set threshold.

(C) Relative transcript levels were analysed in roots of six-week-old *A. halleri* plants after different times of exposure to Cu. The *EF1 α* primers exhibited an average C_T value of 18.58 ± 0.51 between different cDNAs. For calculations see (A) above.

C, control, no extra Cu added; 2 h, two hours; 8 h, eight hours

^aThe template DNA was diluted by a factor of 10^6 to 10^8 to match the expected concentration of *HMA3* cDNA in the total cDNA samples used to determine the *AbHMA3* transcript level. The required final concentration of the control template was estimated as follows: The amount of $1.5 \mu\text{g}$ total mRNA was used to synthesise cDNA. The cDNA was dissolved in a volume of $20 \mu\text{l}$ resulting in a concentration of about $0.075 \mu\text{g}$. For the real-time RT-PCR, only $0.08 \mu\text{l}$ of a 1:100 dilution was used in a volume of $4 \mu\text{l}$ per $10 \mu\text{l}$ reaction. Hence, 0.015 ng of cDNA per reaction was used. Assuming that the *AbHMA3* transcript occurs once among 1000 transcripts, the expected concentration of *AbHMA3* cDNA should be about $0.015 \text{ pg}/\mu\text{l}$ reaction.

2.3 Summary - Analysis of *HMA3* expression in *Arabidopsis*

In silico analysis of Affymetrix Arabidopsis GeneChip® data showed highest expression levels of *HMA3* in root tissues of one-week-old seedlings and three-week-old *A. thaliana* plants, and in senescent leaves. Furthermore, the expression patterns of the three *HMA3* homologs *HMA1*, *HMA2* and *HMA4* are distinct. *Digital in-situ* mapping of the expression of *HMA3* in Arabidopsis roots also revealed a unique expression pattern. Contrary to other *HMA* transcripts, it appears to be predominantly expressed in the root cortex and low in the root cap zone.

A reported polymorphism in *AtHMA3* that likely results in a nonfunctional protein in the Columbia accession of *A. thaliana* but not in the Wassilewskija accession was confirmed in plants used in this study. Using real-time RT-PCR, it was shown that the reported differential expression of *HMA3* in *A. halleri* and *A. thaliana* is also observed when *A. halleri* plants are compared with plants of the *A. thaliana* ecotype Wassilewskija.

Based on specific sequence differences, it was possible to determine the specific expression level of *AbHMA3-1*-like *HMA3* gene copies and *AbHMA3-2*-like *HMA3* gene copies in roots and shoots of *A. halleri* plants that were exposed to low and high concentrations of Zn. Transcript levels of *AbHMA3-1*-like genes are constitutively high in shoots of *A. halleri*, and they are approximately equivalent to the total of *AbHMA3* transcript levels. *AbHMA3-2*-like transcript levels are no higher than *AtHMA3* transcript levels under most conditions in roots. Hence, the constitutively high *HMA3* transcript levels in *A. halleri* originate mainly from *AbHMA3-1* related genes rather than from *AbHMA3-2*-like gene copies.

The determination of *AbHMA3* transcript levels in roots of *A. halleri* plants that were exposed to Cu revealed the presence of both transcripts, *AbHMA3-1*-like and *AbHMA3-2*-like. The *AbHMA3-2*-like transcript levels were increased by Cu, and this might point to a specific role of a *AbHMA3-2*-like genes in the response of *A. halleri* to altered Cu concentrations. A fourth *AbHMA3* gene copy (*AbHMA3-4*) related to *AbHMA3-2* was detected on BAC clone No.7.

The data suggest that *AbHMA3-2* and *AbHMA3-4* are unlikely to play a major role in mediating Zn hypertolerance and hyperaccumulation in *A. halleri* because their expression levels are no higher than in *A. thaliana*.

Chapter 5

Cloning and characterisation of *HMA3* promoter regions

What is the cause of the observed differential expression of *HMA3* in *A. halleri* and *A. thaliana*? As discovered by Becher *et al.* (2004) and described in this work (Figure 2.1 on page 28 and Figure 4.18 on page 93), *AbHMA3-1*-like transcript levels are constitutively high in shoots of *A. halleri*, whereas in *A. thaliana*, *HMA3* is predominantly expressed in roots. The reported data was the motivation to investigate the cause of the observed differences in the relative transcript levels and its regulation.

A multitude of mechanisms to regulate the expression of genes exists in eukaryotic organisms (Riechmann, 2002; Taiz and Zeiger, 2002). Each step from gene *via* transcript to protein can be regulated. At the genomic level, the copy number of a gene, chromatin condensation/decondensation and DNA methylation can affect the transcript level. Later on, at the level of transcription, the mRNA synthesis is carried out by RNA polymerases that require general transcription factors to initiate the transcription at the correct start site. In addition, the transcription is modulated by *cis*-acting sequences and specific transcription factors. Subsequently, posttranscriptional processes can alter the amount of mRNA. Eukaryotic genes consist of exons and non-coding intron sequences. From the transcribed pre-mRNA introns are excised, and exons are spliced together. This splicing process may be regulated as well. The export of completely processed mRNA can also be regulated. Furthermore, the stability or turnover rate of mRNA influences the gene expression and depends on physiological conditions.

The form of gene regulation in eukaryotic organisms that acts at the level of transcription has been most intensely studied so far. The aim of this chapter was to analyse the activity and regulation of the promoter of *AbHMA3* and to compare this to the promoter of *AtHMA3*.

1 Cloning and characterisation of the promoter *pAbHMA3-1* and *pAtHMA3*

At the beginning of this work, no sequence information on the 5'- and 3'-regions outside the *AbHMA3* coding sequences was available. In *A. thaliana*, the next gene (AGI number: At4g30130) starts approximately 1.9 kbp upstream of *HMA3* and is oriented in the opposite direction. By assuming a similar genomic organisation in *A. halleri*, a primer pair was designed based on the known sequence of *HMA3* from *A. thaliana*. The forward primer annealed downstream of the transcriptional start of the next gene upstream of *HMA3*, At4g30130, and the reverse primer bound downstream of the initiation codon of *HMA3*. The primer pair successfully amplified a fragment of about 2.2 kbp and 1.9 kbp from genomic DNA of *A. halleri* and *A. thaliana*, respectively. After cloning into pCR2.1TOPO® and sequencing, it was confirmed that the fragments contained a promoter region that is related to the 5' region of *HMA3*. The full length fragments will be referred to as *pAbHMA3-1* and *pAtHMA3*.

There are differences between the nucleotide sequences of the promoter regions from *A. halleri* and *A. thaliana*. Both regions share an overall 68.7 % identity, and the *A. halleri* region is about 300 bp longer (Figure 5.1). The difference in length is mainly caused by several insertions in the *A. halleri* promoter sequence within the first 800 bp upstream of the transcriptional start of *AbHMA3*.

For further promoter analyses, *promoter-GUS* fusions with truncated fragments of these promoter regions were generated (Figure 5.1). The small-sized fragment contained the first 200 bp upstream of the transcriptional start of *HMA3*, a region that shares about 89.1 % identity between *A. halleri* and *A. thaliana*. Additionally, a middle-sized promoter fragment was chosen to contain the first 700 bp and 500 bp of the cloned *HMA3* promoter from *A. halleri* and *A. thaliana*, respectively.

1.1 Pattern of β -glucuronidase (GUS) activity under control of *pAtHMA3* and *pAbHMA3-1* in *A.thaliana*

To analyse the activities of the cloned promoter fragments, they were subcloned from the pCR2.1-TOPO® vector into a pBi101 vector¹ using the *Xba*I and *Hind*III restriction sites in both plasmids. The cloning procedures generated *pHMA3-GUS* fusion constructs that were used to transform *A. thaliana* plants.

The GUS activity was analysed in T1 and T2 plants of 19 lines containing the *pAbHMA3-1-GUS* and 9 lines bearing the *pAtHMA3-1-GUS* construct (Figure 5.2). According to the observed GUS activity, the *HMA3* promoters from *A. halleri* and *A. thaliana* were mainly active in the vascular bundles of the roots (Figure 5.2 A, B and F, G), in the filaments of flowers and young seeds inside siliques (Figure 5.2 D, E and I, K). Weak GUS activity was detected in the vascular bundles of young leaves of seedlings (Figure 5.2 C and H). No activity was observed in the stem, in young and old rosette leaves and in cauline leaves. The predominant GUS activity in root tissue reflects the obtained *in silico*

¹Depending on the required reading frame, pBi101.1, pBi101.2 or pBi101.3 was used.

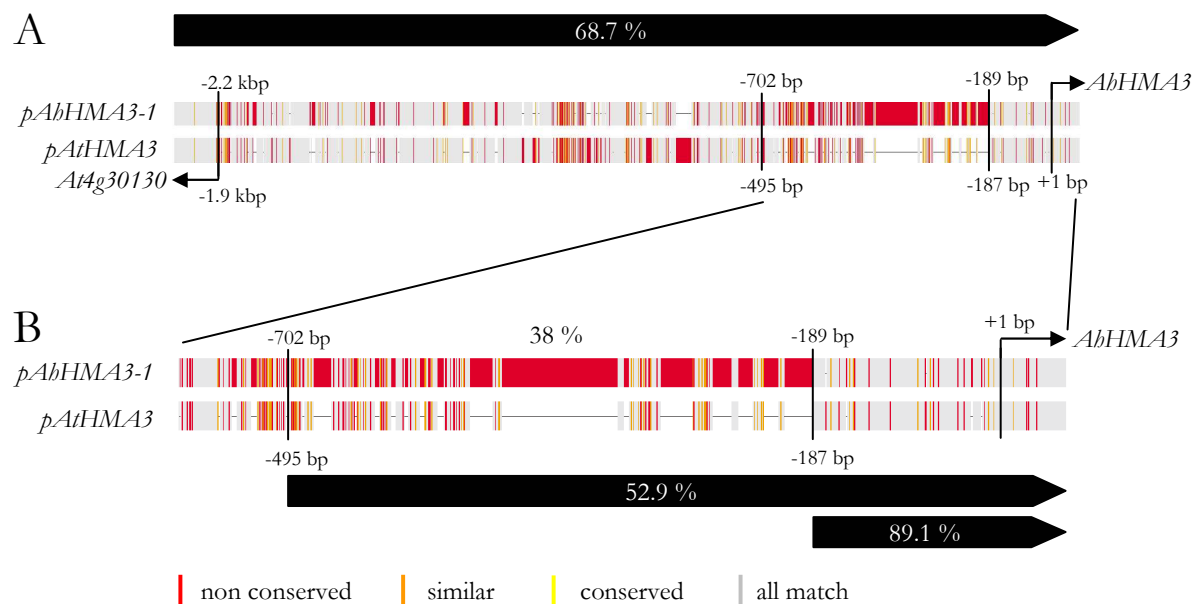


Figure 5.1: Schematic comparison of *HMA3* promoter regions from *A. halleri* and *A. thaliana*.

Shown is the alignment fingerprint of the cloned promoter fragments *pAhHMA3-1* and *pAtHMA3* (A). Scheme B zooms into the first 800/500 bp upstream of the transcriptional start of *HMA3*. The given numbers on top and bottom of each profile indicate the distance relative to the transcriptional start of *HMA3* that is marked with “+1”. The position of the transcriptional start is based on the annotated gene sequence of *AtHMA3* (AGI number: At4g30120) obtained from the *TIGR A. thaliana* database (www.tigr.org). Black filled arrow bars represent the cloned promoter fragments. Inscribed are the percent identities between *A. halleri* and *A. thaliana* fragments.

Percent identity was calculated by using GeneStream Align (xylian.igh.cnrs.fr; Pearson *et al.*, 1997). The alignment file was produced using the *MEGA* application version 3.1 (Kumar *et al.*, 2004, default parameters) and the fingerprint was generated using *TeXshade* (Beitz, 2000a). Nucleotide positions are shaded as follows: ■ all match (100% identical nucleotides), ■ conserved (more than 50% identity); ■ similar (less than 50% identity but all are purine or pyrimidine nucleotides); ■ non conserved (less than 50% and mixed purine/pyrimidine)

data for *HMA3* transcript levels in *A. thaliana* from the Geneinvestigator database (see page 88). A visibly strong GUS activity in senescent leaves as suggested by the *in silico* data was, however, not detected. Considering the data derived from the AREX database that showed highest *AtHMA3* transcript levels in the root cortex and not in vascular bundles (see page 91), a histochemical detection of GUS activity in root cross section of *pHMA3-GUS* lines is suggested to obtain a more precise localisation of GUS activity. The use of a fluorogenic substrate like $C_{12}FDGlcU^2$ is recommended for higher sensitivity and precision.

Only the *A. thaliana* promoter (*pAtHMA3*) of *HMA3* appeared to be active in the root tips (Figure 5.2 B). That is in agreement with *in silico* data from the AREX database that showed low *AtHMA3* transcript levels in the root cap. GUS activity staining of root tips was never obtained in *A. thaliana* transformed with an *A. halleri HMA3 promoter-GUS* reporter construct (*pAhHMA3-1*, Figure 5.2 G). This indicated that in *A. thaliana pAhHMA3-1* is regulated differently in root tips compared to

² $C_{12}FDGlcU$, a lipophilic analog of fluorescein di- β -D-glucuronic acid containing a 12-carbon aliphatic chain (Naleway *et al.*, 1991).

pAtHMA3. Furthermore it shows that *pAbHMA3-1* alone is not sufficient to overexpress the GUS gene in *A. thaliana* shoots, despite high *AbHMA3-1* related transcript levels in shoots of *A. halleri*. This could mean that the following other factors may account for the observed high *HMA3* transcript levels in *A. halleri* (see Figure 4.18):

- transcription factor(s) specific to *A. halleri*
- regulatory elements located outside the cloned promoter affecting transcript levels of *HMA3*
- the promoter of another *AbHMA3* copy
- differential transcript stability of *AtHMA3* and *AbHMA3-1* transcripts in leaves

In order to investigate this further, it was necessary to transform *A. halleri* plants with the *promoter-GUS* reporter constructs. Originally, this was intended to be done in cooperation with the group of Prof. Choi in South Korea. Unfortunately, the received plants were not transgenic. Afterwards the *A. halleri* transformation system established by Ina Talke was used (see *Materials and Methods* Section 8.1.3 on page 51).

1.1.1 GUS activity in *pHMA3-GUS* lines of *A. halleri*

Root pieces of *A. halleri* were transformed with the *pAtHMA3-GUS* and *pAbHMA3-1-GUS* constructs as described (page 51). The first transformation resulted in 6 regenerated plants from 2 independent calli for the *pAtHMA3-GUS* construct and 4 regenerated plants from 2 independent calli for the *pAbHMA3-1-GUS* construct. Regenerated putative transgenic *A. halleri* plants were tested for GUS activity. None of the regenerated plants showed any GUS activity.

A second transformation of *A. halleri* root pieces resulted in one additional line containing the *pAbHMA3-1* reporter construct. No GUS activity was observed in shoots or roots of regenerated plants of this line.

1.2 Regulation of *HMA3* promoter activity in *A.thaliana*

1.2.1 Quantitative analysis of GUS activity in *pHMA3-GUS* lines

Once homozygous, single-insertion *A. thaliana* lines were available in the T3 generation, the inducibility of the promoter by different concentrations of Zn was tested (Figure 5.4). Homozygous, single-insertion lines were selected by segregation analysis of kanamycin resistance as described in the *Materials and Methods* Section 8.3.2 on page 55. Metal responses were measured by a quantitative GUS assay using 4-methylumbelliferyl β -D-glucuronide (4-MUG) as substrate and compared to transcript levels in untransformed plants analysed by real-time RT-PCR.

GUS activity in roots of *pAbHMA3-1-GUS* and *pAtHMA3-GUS* lines The activity of the GUS enzyme in different *promoter-GUS* lines transformed with identical constructs can vary. It is useful to select a few representative lines. Therefore the enzyme activity in all available *pAtHMA3-GUS* and *pAbHMA3-1-GUS* lines (homozygous T3 generation) was tested and compared. This was done through the fluorometric detection of 4-MU, the product in the GUS catalysed turnover of the substrate 4-MUG (see page 47).

The following independent lines were tested: Nine *pAtHMA3-GUS* lines, twelve *pAbHMA3-1a-GUS* lines and seven *pAbHMA3-1b-GUS* lines³. The lines were germinated and grown on vertical agarose plates containing AMOZ medium supplemented with 0.5% (w/v) sucrose and kanamycin. After 4 days, the seedlings were transferred to 0.5-strength Hoagland medium containing 1 μM ZnSO_4 . Eight days later the seedlings were harvested, pooled, and protein extracts were prepared for the 4-MUG assay.

The GUS activity in lines carrying the same construct varies to a great extent (up to factor 25 for *pAtHMA3-GUS*, factor 30 for *pAbHMA3-1a-GUS* and factor 9.5 for *pAbHMA3-1b-GUS*; Figure 5.3 A). For a better comparison and to reduce the influence of outliers on the average GUS activity, the median was calculated. For *pAbHMA3-1* it was 1.65 times higher than for *pAtHMA3*. Because the GUS activities might not follow a normal distribution, a non-parametric test was performed to test whether the medians are equal or not. Excluding outliers, a statistically significant difference was found according to a non-parametric Mann-Whitney test for two independent samples (Figure 5.3 B). As representative lines, *pAtHMA3* 5.1, 11a.2, and 12a.1; *pAbHMA3-1a* 10.3, 3a.2, and *pAbHMA3-1b* 2.1 were chosen.

Exposure to a high zinc concentration The experimental data described in section 2.2.1 on page 92 suggested an upregulation of *HMA3* transcript levels in roots of *A. thaliana* in the presence of high zinc concentrations, when compared to controls. In contrast, Becher *et al.* (2004) reported a more pronounced upregulation of *HMA3* transcript levels in roots of *A. halleri* than in roots of *A. thaliana* (page 28; Figure 2.1 B).

In order to test if the promoter of *HMA3* is inducible after exposure to higher Zn concentrations, a quantitative GUS activity assay was conducted (see page 47).

As shown in Figure 5.4, virtually no GUS activity was detectable in shoots of *A. halleri* and *A. thaliana*. In roots, the GUS activity was detectable after growth under control and high Zn conditions. In contrast to previously described data of GUS activities under control conditions (page 103; Figure 1.2.1 on page 106), no significant differences were found between the GUS activities of *pAbHMA3-1* and *pAtHMA3* lines. Roots of seedlings that were transferred to plates containing a high Zn concentration exhibited a 2.7-fold (median based) increased GUS activity compared to seedlings

³*pAbHMA3-1a* and *pAbHMA3-1b* are independently cloned promoter fragments of *pAbHMA3-1* that differ by a few single base pairs

maintained at control Zn concentrations. The measured GUS activities correlated approximately with the visually observed intensities of blue staining after a X-Glc GUS activity assay (data shown as boxed strip in Figure 5.4).

Is the GUS activity induced by a physiological Fe deficiency caused by an excess of Zn? It is known that a high Zn level causes a physiological Fe deficiency in seedlings due to competitive effects between Zn and Fe ions (Woolhouse, 1983). In a microarray study, Colangelo and Gueriot (2004) reported an increase in root *HMA3* transcript levels under Fe deficient conditions. These observations raised the question whether the *HMA3* promoter actively responds to a physiological Fe deficiency caused by an excess of Zn.

In a first attempt to answer this question, the induction of the GUS activity in the lines describe above by Zn was analysed in the presence of control concentrations of Fe or an Fe oversupply. Following the same experimental set-up as described before (page 103), seedlings of selected *pAtHMA3-GUS* and *pAbHMA3-1-GUS* lines were transferred to 0.5-strength Hoagland medium containing 5 μM Fe-HBED and 1 μM ZnSO_4 or a non-toxic high concentration of 30 μM ZnSO_4 . Furthermore, the seedlings were in parallel transferred to a second set of low and high Zn media plates that contained 150 μM Fe-HBED. The chelator N,N'-di-(2-hydroxybenzoyl)-ethylenediamine-N,N'-diacetate (HBED) is highly specific to Fe^{3+} ions and was used to provide the oversupply of iron in soluble form.

As had been observed before, the GUS enzyme activity was induced when seedlings were grown on higher Zn concentrations (Figure 5.5). In *pAtHMA3-GUS* lines the GUS activity was induced about 8.1-fold, and in *pAbHMA3-1-GUS* lines showed a 20.4-fold increased GUS activity. The *A. halleri* promoter caused a 2.5-fold higher GUS activity than the *A. thaliana* promoter. However, due to the high variability and the small sample size, the difference between the *A. halleri* and *A. thaliana* promoter was not statistically significant.

On plates containing the same low and high Zn concentration but an oversupply of Fe, the measured GUS activity did not statistically differ between control and high Zn conditions and between *pAbHMA3-1-GUS* and *pAtHMA3-GUS* lines. The GUS activity remained low in seedlings grown in the presence of 150 μM Fe-HBED. In conclusion, high Fe supply suppressed the Zn-induced increase in GUS activity in *pAbHMA3-1-GUS* and *pAtHMA3-GUS* lines.

1.2.2 Quantitative analysis of *pHMA3-GUS* activity in protoplasts

Instead of transforming whole plants, an alternative method to compare the GUS activity under control of different cloned promoter fragments is the transient expression of *promoter-reporter* constructs in protoplasts of *A. thaliana* (see *Materials and Methods* Section 8.1.1 on page 50). Results of this experiment for different *pHMA3-GUS* constructs are shown in the next section on page 112.

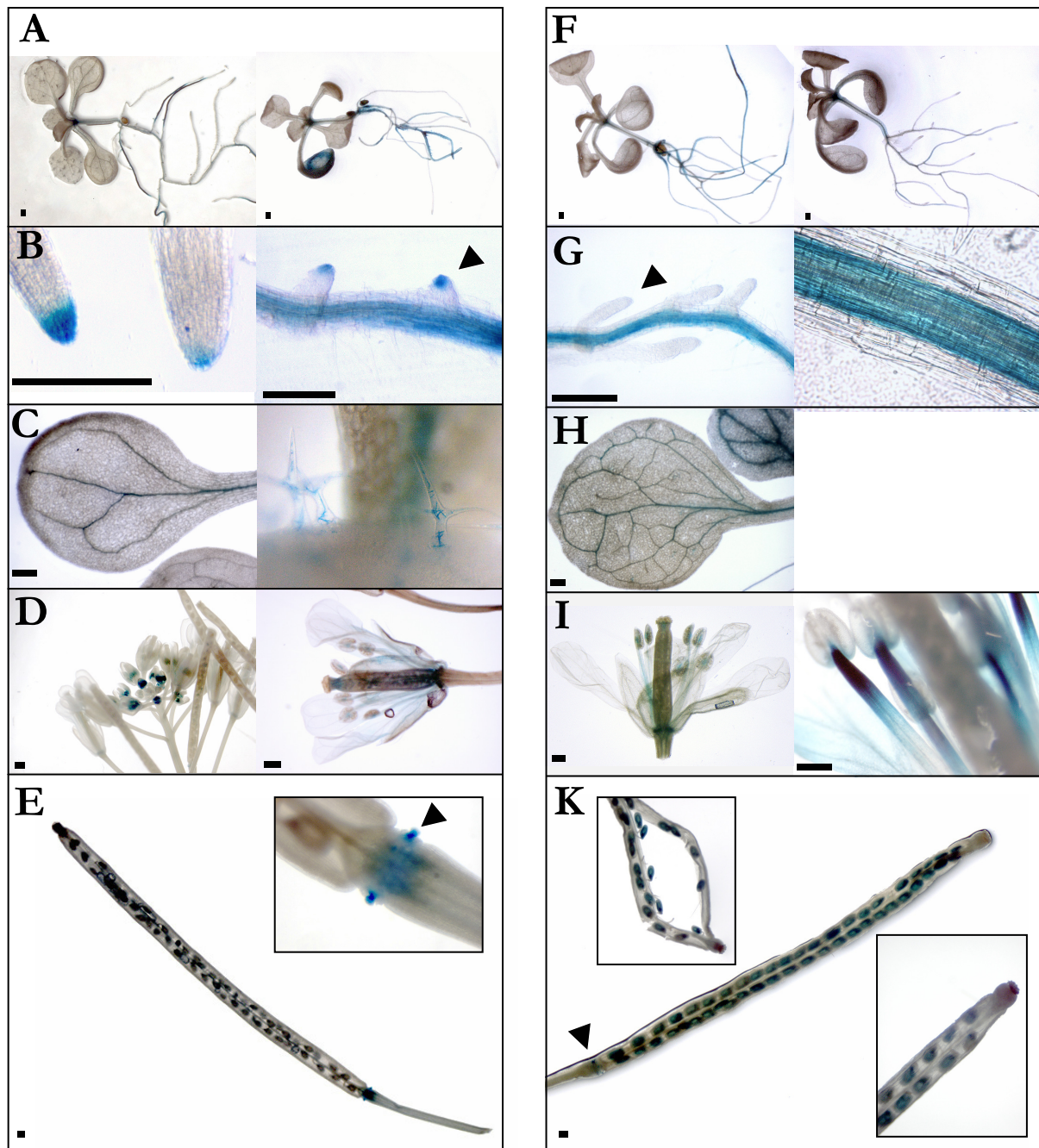


Figure 5.2: Histochemical detection of GUS activity in seedlings transformed with reporter gene constructs for *pAhHMA3-1* and *pAtHMA3*.

The images shown are representative of 19 transgenic lines for *pAhHMA3-1* and 9 transgenic lines of *pAtHMA3-1*.

A to E: *HMA3* promoter from *A. thaliana*, *pAtHMA3-1*

F to K: *HMA3* promoter from *A. halleri*, *pAhHMA3-1*

(A, F: seedling, 12 days after germination; B, G: roots, C, H: leaves and trichomes; D, I: inflorescences, flowers; E, K: siliques)

The black scale bar represents 0.5 mm.

Transgenic seedlings were germinated and grown on vertical agarose plates containing AMOZ medium supplemented with 0.5% (w/v) sucrose and kanamycin. Four days after transfer, tissues were harvested for histochemical detection of GUS activity.

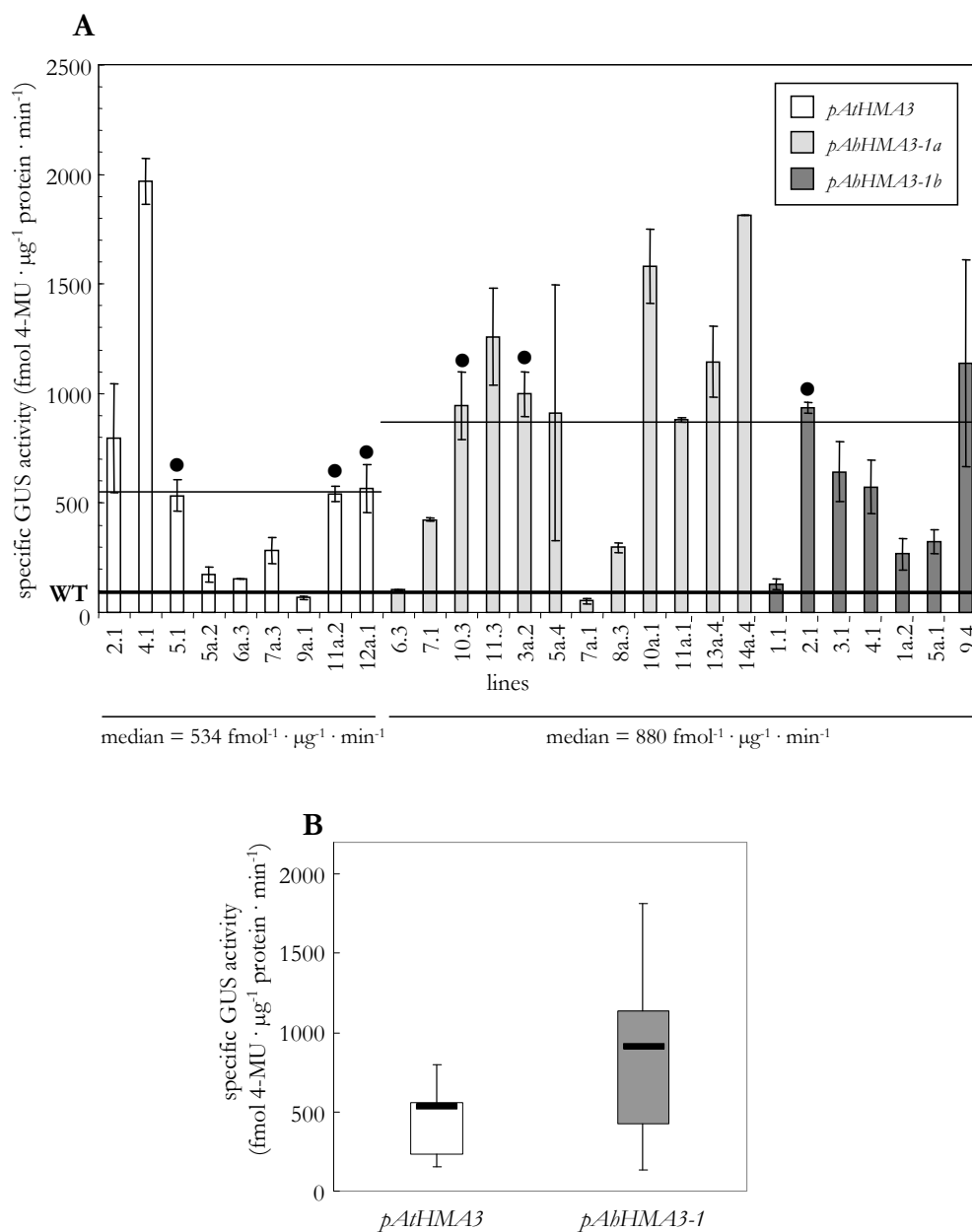


Figure 5.3: GUS activity in roots of *pAtHMA3-GUS* and *pAhHMA3-1-GUS* lines.

A: GUS activity in protein extracts from roots of homozygous transgenic lines transformed with the *pAtHMA3-GUS*, *pAhHMA3-1a-GUS* and *pAhHMA3-1b-GUS* constructs. Values are arithmetic means (\pm SD) of the amount of the fluorescent reaction product 4-MU (4-methylumbelliferone) normalised to total protein amount and reaction time.

Seedlings (homozygous, T3 generation) were germinated and grown on vertical agarose plates containing AMOZ medium supplemented with 0.5% (w/v) sucrose and kanamycin. Four-day old seedlings were transferred on 0.5-strength Hoagland medium containing $1 \mu\text{M ZnSO}_4$ or a non-toxic high concentration of $30 \mu\text{M ZnSO}_4$. After 8 days, roots of seedlings were harvested and protein extracted for the enzyme assay and for the quantification of total protein.

The background GUS activity determined in the wild type (WT) is represented as continuous thick black line. Each datapoint is the arithmetic mean of two independent biological replicates, each consisting of the roots pooled from 5 to 7 seedlings. For each protein extract, 2 to 4 measurement repeats were performed for GUS enzyme activity determination. Black dots mark the lines that were selected for further experiments. Below the diagram the geometric mean (median) for all *pAtHMA3-GUS* and *pAhHMA3-1-GUS* lines is given.

B: A box plot of the measured GUS activities shown in diagram A. The box represents the interquartile range, the thick black line inside marks the median. Upper and lower whiskers indicate the maximal and minimal value in each data set. A statistically significant difference ($P < 0.05$.) was found according to a non-parametric Mann-Whitney test for two independent samples excluding outliers.

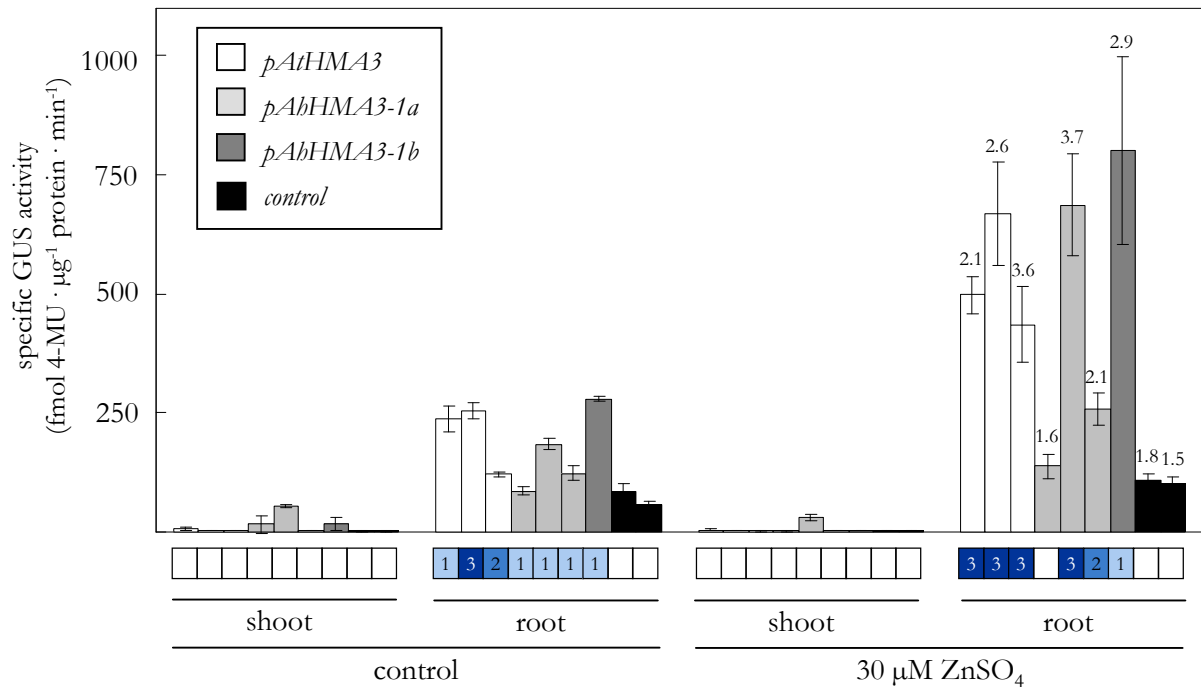


Figure 5.4: GUS activity under control and zinc extrasupply conditions.

GUS activity in protein extracts from roots and shoots of homozygous transgenic lines transformed with the *pAtHMA3-GUS* and *pAhHMA3-1-GUS* constructs. Values are arithmetic means (\pm SD) of the amount of the fluorescent reaction product 4-MU (4-methylumbelliferone) normalised to total protein amount and reaction time.

Seedlings (homozygous, T3 generation) were germinated and grown on vertical agarose plates containing AMOZ medium supplemented with 0.5% (w/v) sucrose and kanamycin. Four-day old seedlings were transferred on control 0.5-strength Hoagland medium ($5 \mu\text{M}$ Fe-HBED, $1 \mu\text{M}$ ZnSO_4), or Hoagland medium containing $30 \mu\text{M}$ ZnSO_4 , and seedlings were harvested after eight additional days. Protein was extracted for the enzyme assay and for the quantification of total protein.

Each datapoint is the arithmetic mean of two independent biological replicates, each consisting of the roots or shoots pooled from 5 to 7 seedlings. For each protein extract, 2 to 4 measurement repeats were performed for GUS enzyme activity determination. The fold-induction in GUS activity in each *promoter-GUS* line is given above the corresponding column. The following lines were used (from left to right): *pAtHMA3-GUS* 5.1, 11a.2, and 12a.1; *pAhHMA3-1a-GUS* 10.3, 3a.2, and 11a.1; *pAhHMA3-1b-GUS* 2.1. The boxed strip below the diagram contains the visually observed intensity of blue staining after a X-Glc GUS activity assay. The strength is given on a scale from weak (1) to strong (3).

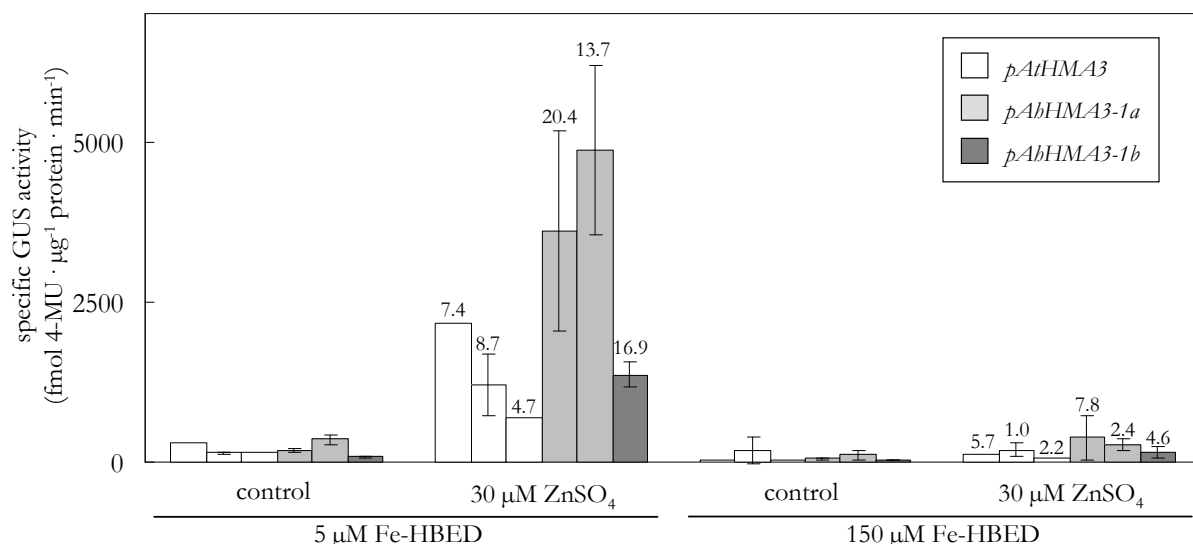


Figure 5.5: GUS activity under control and zinc/iron extrasupply conditions.

GUS activity in protein extracts from roots of homozygous transgenic lines transformed with the *pAtHMA3-GUS* and *pAhHMA3-1-GUS* constructs. Values are arithmetic means (\pm SD) of the amount of the fluorescent reaction product 4-MU (4-methylumbelliferone) normalised to total protein amount and reaction time.

Seedlings (homozygous, T3 generation) were germinated and grown on vertical agarose plates containing AMOZ medium supplemented with 0.5% (w/v) sucrose and kanamycin. Four-day old seedlings were transferred on 0.5-strength Hoagland medium containing either 1 μ M ZnSO₄ or 30 μ M ZnSO₄ supplied with either 5 μ M Fe-HBED or 150 μ M Fe-HBED.

Each datapoint is the arithmetic mean of two independent biological replicates, each consisting of the roots pooled from 5 to 7 seedlings. For the *pAtHMA3-GUS* lines 5.1 and 12a.1 that are the first two of the three analysed *pAtHMA3-GUS* lines, only 1 biological sample was measured. For each protein extract, two measurement repeats were performed for GUS enzyme activity determination. The fold-induction in GUS activity in each *promoter-GUS* line compared to the control is given above the corresponding column.

2 Cloning and characterisation of a second *AbHMA3* promoter, *pAbHMA3-2*

Based on the analysis of *HMA3* at the genomic and mRNA level (see page 58), it became obvious that the genome of *A. halleri* encodes at least 2 and possibly 3 or 4 copies of *AbHMA3*. The observations that there might be more than one *AbHMA3* copy in the genome of *A. halleri* demonstrated the possibility of having cloned a cDNA or a promoter that is not linked to the high expression of *AbHMA3* found in the AFFYMETRIX Arabidopsis GeneChip® experiments. Therefore it was important to obtain sequence information of the other copies of *AbHMA3* and the corresponding promoter regions.

2.1 Obtaining additional *AbHMA3* promoter sequences from a BAC library

An inverse PCR approach was chosen to obtain additional promoter sequence information from BAC clones. The method includes the digestion of BAC plasmid DNA. This is followed by self-ligation of the resulting DNA fragments to form circled DNA rings. DNA rings containing *AbHMA3* fragments can be amplified using two *AbHMA3* specific primers with opposite orientation (for further details see page 39). The successful amplification of an *AbHMA3* specific fragment that contains a sufficiently large promoter sequence fragment depends on the size of the initial DNA fragment in the digested BAC DNA. An approach to find enzymes that produce *AbHMA3* specific DNA fragments of suitable sizes is Southern hybridisation (page 60). It is advisable to choose enzymes that do not produce blunt ends. This would strongly reduce the ligation efficiency. To obtain fragments including parts of the promoter sequence, the detection was done using a ³²P-labeled 126 base pair fragment from the 5'-end of *AbHMA3*.

2.1.1 Inverse PCR

Ligation products of five digested BAC-clones (No.1, 3, 5, 6, and 8; Table 4.1 on page 60) showed a PCR product. After cloning into pCR2.1TOPO® and sequencing, only 2 (No.5 and 6) of these were confirmed to possess a part of the 5'-*AbHMA3* coding sequence and a corresponding promoter region. The full length fragments will be referred to as *pAbHMA3-2*. Both clones were identical but differed from the known *HMA3* promoter region of *A. halleri* and *A. thaliana*, *pAbHMA3-1* and *pAtHMA3*. Based on the new sequence information it was attempted to amplify the corresponding region from genomic DNA of *A. halleri*. This approach was unsuccessful with two alternative primer pairs (P50 F / P50.1 F; Table 3.3 on page 37, *Materials and Methods* Section). Individuals from two *A. halleri* accessions were pooled to make the BAC-library (see *Section 1.1.2* on page 59). Therefore there could be some sequence variations that cause inefficient primer annealing when genomic DNA of the Langelshiem (Lan) accession of *A. halleri* is used. In order to quickly analyse the activity

of the newly cloned promoter it was subcloned from the BAC clone into a binary vector for the transformation of *A. thaliana* plants.

As described before, BAC clone No.6 contains the *AbHMA3-2* copy, and real-time RT-PCR analyses have shown that *AbHMA3-2* does not contribute to the constitutively high *AbHMA3* transcript levels in shoots of *A. halleri*. Nevertheless, the increase of *AbHMA3-2* transcript levels after exposure to Cu might point to a different regulation and a distinct role of *AbHMA3-2* in the metal homeostasis of *A. halleri* compared to *AbHMA3-1* and is worth further investigations.

Sequence comparison The obtained *AbHMA3* promoter sequence from BAC clones No.5 and No.6 is about 1 kbp in size. The promoter fragments *pAbHMA3-1* and *pAbHMA3-2* share an overall 53.5% identity (Figure 5.6). Only the first 73 bp upstream of the transcriptional start of *AbHMA3* show a high similarity (98.9% identity). The promoter fragment *pAbHMA3-2* is 46.5% identical to *pAtHMA3* of *A. thaliana*.

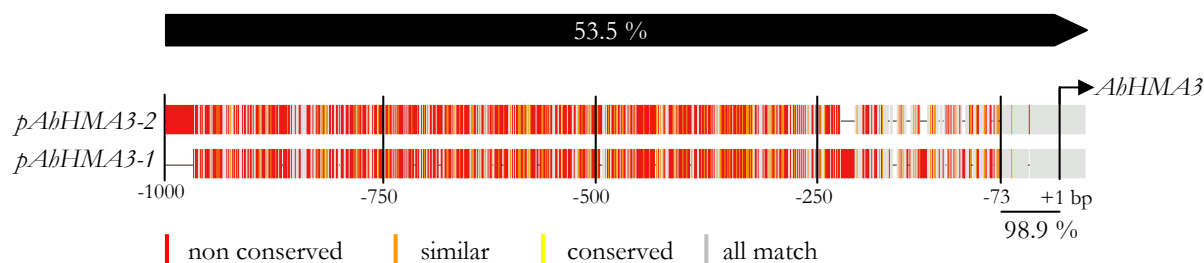


Figure 5.6: Schematic comparison of *AbHMA3* promoter regions from *A. halleri*.

Shown is the alignment fingerprint of the cloned promoter fragments *pAbHMA3-1* and *pAbHMA3-2*. The given numbers below indicate the distance relative to the transcriptional start of *AbHMA3* that is marked with “+1”. The position of the transcriptional start is based on the annotated gene sequence of *AtHMA3* (AGI number: At4g30120) obtained from the *TIGR A. thaliana* database (www.tigr.org). The black filled arrow bar represents the cloned promoter fragments. Inscribed in the arrow bars are the percent identities between both fragments. Percent identity was calculated by using GeneStream Align (xylian.igh.cnrs.fr; Pearson *et al.*, 1997). The alignment file was produced using the *MEGA* application version 3.1 (Kumar *et al.*, 2004, default parameters) and the fingerprint was generated using *TEXshade* (Beitz, 2000a). Nucleotide positions are shaded as follows: ■ all match (100% identical nucleotides), ■ conserved (more than 50% identity); ■ similar (less than 50% identity but all are purine or pyrimidine nucleotides); ■ non conserved (less than 50% and mixed purine/pyrimidine)

2.2 GUS activity of the second *AbHMA3* promoter, *pAbHMA3-2*

The cloned promoter fragment *pAbHMA3-2* was subcloned from the pCR2.1TOPO[®] vector into the pBi101 vector using the *Xba*I and *Hind*III restriction sites in both plasmids. The cloning procedures generated a *pAbHMA3-2-GUS* fusion construct. Transformed seedlings were cultivated for seed production. Twelve of 26 T1 plants produced T2 seeds that showed a 3:1 segregation ratio on selective medium.

2.2.1 GUS activity after exposure to CuSO_4

It has been shown that a *A. halleri HMA3* transcript levels, especially transcript levels of *HMA3-2* might be inducible by the presence of Cu in the medium (page 96, Figure 4.19 C). Therefore seedlings of 12 selected T2 lines were grown under analogous conditions as described before but using $5\ \mu\text{M}$ and $20\ \mu\text{M}$ of CuSO_4 instead of $30\ \mu\text{M}$ ZnSO_4 . The seedlings were histochemically stained for GUS activity 1 day and 4 days after transfer to control and Cu supplied plates.

No obvious difference in the GUS activity or its distribution could be detected between plants that were grown on control plates and plates with additional CuSO_4 . The observed GUS activity seemed to decrease slightly in plants that were exposed to Cu for four days. This observation contrasts the increased *AbHMA3-2*-like transcript levels that were detected after an eight-hour-treatment of hydroponically grown *A. halleri* plants (see Figure 4.19 on page 96). However, due to the different experimental set-ups and used plant species, it is difficult to compare both experiments. In a first approach, future investigations should either investigate *AbHMA3-2* transcript levels after a four-day CuSO_4 treatment or GUS activities in transgenic *pAtHMA3-2* lines after an eight-hour exposure to CuSO_4 . However, the *AbHMA3-2*-like *AbHMA3-4* gene copy that was detected on DNA of BAC clone No.7 might be the gene for which transcript levels are increased in response to Cu. Thus, the promoter of *AbHMA3-4* and not of *AbHMA3-2* could be Cu-responsive and should be considered to be cloned as well.

GUS activity was almost exclusively restricted to the roots (Figure 5.7 A, C, and D). It appears that the GUS enzyme was primarily active in trichoblastic epidermis cells and root hairs (Figure 5.7 C and D). Single seedlings of two lines (*pAhHMA3-2-GUS* 3a, 5a) showed GUS activity at the base of developing rosette leaves and might not be representative (Figure 5.7 A and B).

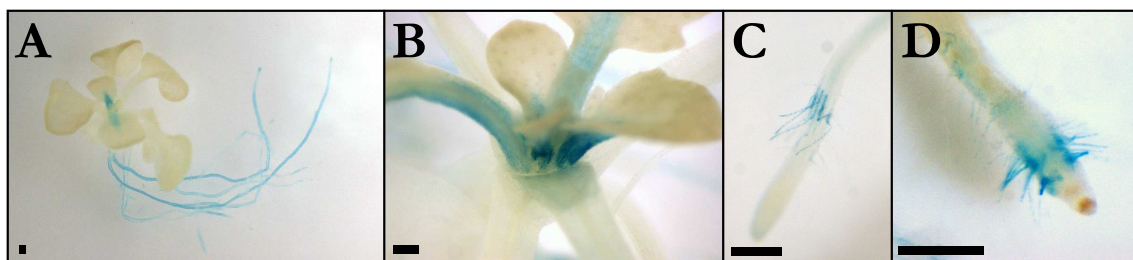


Figure 5.7: Histochemical detection of GUS activity in Arabidopsis seedlings transformed with a GUS reporter gene construct for the *pAhHMA3-2* promoter fragment.

The images A, C, and D are representative of 12 transgenic lines for *pAhHMA3-2*. GUS activity in rosette leaves (B) was observed only single seedlings of two lines (*pAhHMA3-2-GUS* 3a, 5a).

(A: seedling, 12 days after germination; B: basal rosette zone; C, D: roots)

The black scale bar represents 0.5 mm.

Seedlings (T2 generation) were germinated and grown on vertical agarose plates containing AMOZ medium supplemented with 0.5% (w/v) sucrose and kanamycin. Four-day old seedlings were transferred on 0.5-strength Hoagland medium containing control, $5\ \mu\text{M}$ CuSO_4 , or $20\ \mu\text{M}$ CuSO_4 . One and four days after transfer, tissues were harvested for histochemical detection of GUS activity.

2.2.2 GUS activity in *pAbHMA3-2-GUS* lines of *A. halleri*

Pieces of *A. halleri* roots were transformed with the *pAtHMA3-2-GUS* construct as described (page 51). Root pieces from a first transformation did not produce calli. Later, a second transformation resulted in one putative transgenic line. The regenerated *A. halleri* plants were tested for GUS activity. The plants did not show any GUS activity in shoot tissue. The root tissue displayed a visually weak GUS activity similar to the described observations for *A. thaliana* plants transformed with the *pAbHMA3-2-GUS* construct (page 110).

2.3 Quantitative analysis of GUS activity in protoplasts transiently transfected with *pHMA3-GUS* constructs

As an alternative method to compare the GUS activity under control of different, cloned promoter fragments, protoplasts of *A. thaliana* were transiently transformed with the *promoter-GUS* constructs (see *Material and methods* Section on page 50).

The protoplast transformations and fluorescent measurements were performed by Marc Hanikenne (postdoctoral researcher, group of Dr. Ute Krämer). The obtained data is given in Figure 5.8. In protoplasts, the overall GUS activities determined in protoplasts transformed with the *pAtHMA3* and *pAbHMA3-1* promoter fragment constructs did not differ significantly. The average GUS activities in protoplasts transformed with the *pAbHMA3-2* promoter construct was about 2.6 times higher than for the *pAtHMA3* or *pAbHMA3-1* promoter constructs. However, due to the high standard deviations, the difference was not statistically significant according to a non-parametric Mann-Whitney test ($P < 0.05$).

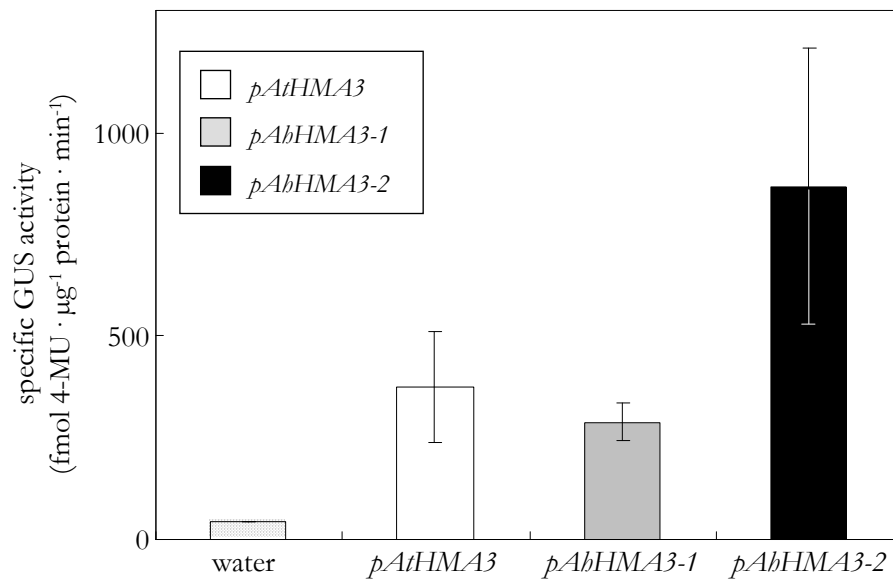


Figure 5.8: GUS activity in *A. thaliana* protoplasts transiently transformed with reporter constructs containing various *HMA3* promoter fragments.

Activity of GUS in total protein extracts from protoplast of *A. thaliana* transformed with the *pAtHMA3-GUS*, *pAhHMA3-1-GUS* and *pAhHMA3-2-GUS* constructs. Values are arithmetic means (\pm SD) of the amount of the fluorescent reaction product 4-MU (4-methylumbelliferone) normalised to total protein amount and reaction time. Each datapoint is the arithmetic mean of two biological replicates.

3 Summary - Cloning and characterisation of *HMA3* promoter regions

GUS reporter fusions were generated for two different *HMA3* promoter regions from *A. halleri* (*pAbHMA3-1* and *pAbHMA3-2*) and the *HMA3* promoter from *A. thaliana* (*pAtHMA3*).

The promoter region *pAbHMA3-1* is more similar to the *HMA3* promoter of *A. thaliana*. In *A. thaliana* transformed with *pAbHMA3-1-GUS* or with *pAtHMA3-GUS*, GUS activity was detected predominantly in the vascular bundles of the roots, in filaments of flowers and young seeds inside siliques. A weak GUS activity was sometimes observed in vascular bundles of young seedling leaves. No activity was detected in the stem, in young and old rosette leaves and in cauline leaves. Only in *A. thaliana HMA3 promoter-GUS* lines, GUS activity was detected in root tips. A quantitative enzyme activity assay revealed a slightly higher GUS activity under control of the *pAbHMA3-1* promoter than controlled by the *A. thaliana* promoter. In *pAbHMA3-1* and *pAtHMA3* lines, GUS activity was inducible by a high non-toxic Zn concentration in the root media. The induction of GUS activity by Zn was suppressed by an non-toxic oversupply of Fe. Putatively transformed *A. halleri* plants did not display any GUS activity.

The *pAbHMA3-2* promoter fragment was cloned from an *A. halleri* BAC library and shows very low similarity to the cloned *pAbHMA3-1* and *pAtHMA3* promoter fragments. T2 seedlings displayed GUS activity primarily in trichoblast epidermis cells and root hairs. In a few plants, GUS enzyme activity was detected at the base of developing rosette leaves and in vascular bundles of young rosette leaves. The exposure to different concentrations of Cu did not affect histochemically detectable GUS activity in contrast to real-time RT-PCR results shown earlier, which suggested that *AbHMA3-2*-like transcript levels increase in response to Cu. Regenerated, supposedly transgenic *A. halleri* plants transformed with a *pAbHMA3-2-GUS* construct showed GUS activity in roots similar to the described GUS activity found in transgenic *A. thaliana pAbHMA3-1-GUS* and *pAtHMA3-GUS* lines.

The activities of all three *promoter-GUS* constructs in protoplasts of *A. thaliana* were similar.

In conclusion, neither the *pAbHMA3-1-GUS* nor the *pAbHMA3-2-GUS* constructs generated high GUS activities in shoots of transgenic *A. thaliana* or *A. halleri* plants or in transiently transfected protoplasts. Therefore, it is unlikely that the cloned promoter fragments are responsible for the high expression of *HMA3* in shoots of *A. halleri*. It is proposed that regulatory elements outside the cloned promoter regions cause the constitutively high expression of an *AbHMA3-1* related gene copy. A possible element could be a characteristic insertion within the first intron of *AbHMA3-1* that does not occur in *AbHMA3-2*. *Promoter-GUS* constructs including the first intron of *AbHMA3-1* or *AbHMA3-2* should be generated in order to compare the resulting transgenic plants with previously generated transformants for *promoter-GUS* constructs. The influence of the intron on the expression of *AbHMA3* can be determined in this way.

It is also possible that the unknown promoter of the mentioned *AbHMA3-3* copy drives the high expression of *AbHMA3* in *A. halleri*. Future investigations should therefore focus on the cloning the

AbHMA3-3 gene and its promoter for further analyses. In addition, it is important to determine the exact number of *HMA3* gene copies in the genome of *A. balleri* and to obtain promoter sequence information from all gene copies.

Part IV

Discussion

Chapter 6

Discussion

1 Basic characteristics of metal homeostasis, hypertolerance and - accumulation

Metal homeostasis in plants is maintained by a rather complex, strictly regulated network of homeostasis factors to sustain the required metal concentrations. The network has to accomplish several major tasks as follows.

1. The mobilisation of metals in the rhizosphere (by secretion of chelators or organic acids)
2. The uptake of chelated or hydrated free metal ions from soil or the apoplast into the root symplasm by metal transporters in the plasma membrane of cells
3. The distribution of metals inside the plant including:
 - (a) translocation of metals from roots to shoots involving xylem loading in the root and unloading, e. g. in the shoot
 - (b) distribution of metals between suitable cells and subcellular compartments (e. g. transport into the vacuole by tonoplast-located transporters); this also involves the detoxification of metals by export to the apoplast, cell wall binding, chelation in the cytoplasm or vacuolar sequestration.

Metal hyperaccumulating plants possess an adapted metal homeostasis network with some characteristics common to several hyperaccumulator species in which hyperaccumulation is likely to have evolved independently (Clemens, 2001; Clemens *et al.*, 2002b; Krämer, 2005b; Peer *et al.*, 2005; Yang *et al.*, 2005):

- Efficient systems for enhanced metal uptake and root-to-shoot-translocation (Clemens *et al.*, 2002b; Yang *et al.*, 2005)
- A shoot:root ratio of metal concentrations usually above unity (Baker, 1981; Baker *et al.*, 1994; Krämer *et al.*, 1996; Dahmani-Muller *et al.*, 2000; White *et al.*, 2002; Macnair, 2003; Becher *et al.*, 2004; Weber *et al.*, 2004; Elbaz *et al.*, 2006)

- An enhanced vacuolar sequestration of metals in leave tissues (Vazquez *et al.*, 1994; Verkleij *et al.*, 1998; Küpper *et al.*, 1999; Chardonnens *et al.*, 1999; Neumann and zur Nieden, 2001)
- A constitutively high expression of metal homeostasis genes, especially of members of the ZIP, HMA, MTP and nicotianamine synthase families (Pence *et al.*, 2000; Persans *et al.*, 2001; Assunção *et al.*, 2001; Dräger *et al.*, 2004; Papoyan and Kochian, 2004; global transcriptional profiling: Becher *et al.*, 2004; Weber *et al.*, 2004)

2 What is the role of *HMA3* and its encoded protein in hypertolerance and -accumulation in *A. halleri*?

2.1 *HMA3* mediates enhanced Zn(Cd) tolerance in metal-sensitive yeast mutant strains

The encoded protein of one *HMA3* gene copy of *A. halleri*, *AbHMA3-1*, was found to partially complement the zinc-sensitive but not the cobalt-sensitive phenotype of the $\Delta zrc1 \Delta cot1$ *S. cerevisiae* double mutant. Furthermore, a minimal complementation of the cadmium-sensitive YYA4 strain was observed. This data suggests a function of *AbHMA3* in the detoxification of Zn and Cd. Experiments with a *AbHMA3* protein mutated at its functionally essential phosphorylation site, revealed that the observed complementation is based on active transport and not on chelation of the ions by the *HMA3* protein.

Despite a close resemblance to cobalt in terms of hydrated ionic radius, zinc is chemically more related to cadmium. Hence, like several other Zn transporters, the *AbHMA3* protein appears to transport both Zn and Cd¹. Moreover, the expression of the homologous Arabidopsis P-type IB ATPases *AtHMA2* and *AtHMA4* in wildtype and metal-sensitive yeast strains has shown a similar dual metal specificity. In mutants of *S. cerevisiae*, *AtHMA4* and *AbHMA4* conferred a comparably enhanced tolerance to Zn (Mills *et al.*, 2003, 2005; Verret *et al.*, 2005; Talke *et al.*, 2006) and Cd (Talke *et al.*, 2006), and *AtHMA4* a slight tolerance to Pb (Mills *et al.*, 2005; Verret *et al.*, 2005). In contrast, an elevated sensitivity to Co was observed in *AtHMA4* expressing yeast cells (Verret *et al.*, 2005). The *HMA4* homolog in the Zn hyperaccumulator *T. caerulescens*, *TcHMA4*, mediates Cd detoxification when expressed in wildtype yeast cells (Papoyan and Kochian, 2004). The complementation of a zinc-sensitive yeast mutant was, unfortunately, not tested in that study.

In 2004, *AtHMA2* was reported by Eren and Argüello (2004) to transport Zn²⁺ and Cd²⁺ and to be activated by Zn²⁺ and Cd²⁺, and to a much lesser degree by Pb²⁺ > Cu²⁺ = Co²⁺ ≥ Cu⁺ ≥ Ni²⁺ >> Fe²⁺ and ≥ Mn²⁺.

A previous publication of Gravot *et al.* (2004) reported that the expression of *AtHMA3* in metal sensitive *S. cerevisiae* mutants slightly increases tolerance to Cd and Pb, but surprisingly not to Zn. This observation is in contrast to the data reported in this study for *AbHMA3* (see *Results* Section

¹However, the specific transport of Zn and not Cd appears to be possible as has been demonstrated for the CDF protein family members *At/PtdMTP1* and *AtMTP3* when heterologously expressed in yeast (Blaudez *et al.*, 2003; Desbrosses-Fonrouge *et al.*, 2005; Arrivault *et al.*, 2006).

1.2.1 on page 76). The proteins that are encoded by *AtHMA3* and *AbHMA3* are identical in 93.3% of their amino acids and share a similarity of 96.2%. None of the known essential and conserved peptide motifs are affected by the amino acid differences. Considering the potential Zn and Cd binding amino acids cysteine, histidine, aspartate, and glutamate, only nine amino acid positions are different between *AbHMA3* and *AtHMA3*. The *AbHMA3*-1 sequence carries an Asp₂₀₉Asn in the N-terminal domain, an Asn₁₆₂Asp in the 3rd MSH, a Glu₂₀₆Asp, His₂₀₉Leu, and an Asp₂₆₀Glu in the small cytoplasmic loop, a His₄₁₇Pro, Ser₄₃₁Cys, and Glu₅₈₅Asp substitution as well as a deleted -₄₉₅Asp in the large cytoplasmic loop and a Ser₇₄₇Cys substitution in the C-terminal domain when compared to the corresponding residues in the *AtHMA3* protein. Compared to other homologous HMA2, HMA3, and HMA4 sequences from *A. thaliana*, *O. sativa* and *T. caerulescens*, only the His₂₀₉Leu substitution appears anomalous. At that position a glutamic acid (Glu, E) is common in 5 of 7 compared sequences. Extensive alignment studies of Argüello (2003) support the idea that amino acids located in the the MSHs VI, VII, and VIII provide metal specificity of P-type IB ATPases. None of the mentioned amino acid differences between *AbHMA3* and *AtHMA3* occur in the putative metal specificity defining regions (see *Appendix* Section 2, Figure 2 on page 76).

Thus, based on the amino acid composition and published experimental data for other closely related HMA proteins, it is difficult to understand why *AtHMA3* only complements the cadmium-sensitive phenotype (Gravot *et al.*, 2004) and *AbHMA3* predominantly the zinc-sensitive phenotype of corresponding yeast mutants. One possible explanation might be that Gravot *et al.* (2004) used the less zinc-sensitive *S. cerevisiae* strain $\Delta zrc1$. In this study, the strain $\Delta zrc1 \Delta cot1$ exhibits a higher sensitivity to Zn than the $\Delta zrc1$ yeast mutant. In case *AtHMA3* has only a small capacity for Zn detoxification in yeast cells, the effect on the Zn-sensitive phenotype might not have been observable in the $\Delta zrc1$ yeast mutant.

Based on the presented data in the *Results* Section 1.2.1 (page 76), it appears that *AbHMA3* from *A. halleri* expressed in yeast confers higher levels of tolerance to Zn²⁺ than to Cd²⁺, and not to Co²⁺. This is somewhat different from the broader metal selectivity of the related P-type IB ATPases HMA2 and HMA4 (Eren and Argüello, 2004; Papoyan and Kochian, 2004; Mills *et al.*, 2005; Verret *et al.*, 2005; Talke *et al.*, 2006) and might indicate a distinct role of HMA3 confined primarily to Zn homeostasis.

2.1.1 Model of Zn detoxification by *AbHMA3* and its regulation

The detoxification of excess Zn(Cd) in yeast cells could be mediated by an active efflux of Zn(Cd) into the surrounding media or by sequestration in the vacuole. Besides a tendency to higher intracellular Zn content of HMA3 expressing yeast mutants that would have indicated a vacuolar Zn import, the Zinc accumulation assays did not help to differentiate significantly between an internal sequestration or a zinc efflux out of the cell (see *Materials and Methods* Section 1.2.1 on page 79).

The observed effect of complementation of the metal-sensitive yeast phenotypes was weak for Cd and only partial for Zn. One could expect a more effective complementation since, according to its

predicted function, HMA3 is a protein that actively pumps ions across a membrane. There are at least three possible explanations:

1. *AbHMA3* does not properly function when expressed in yeast
2. yeast cells only make very small amounts of *AbHMA3*
3. *AbHMA3* mislocalises/misfolds in yeast cells

Most interesting is the consideration of possibility No.1. When HMA3 homologous proteins are aligned, all known HMAs of *Arabidopsis* spec. and *Oryza sativa* (Rice) feature a long C-terminal domain. For comparison, most prokaryotic P-type IB ATPases end directly after the last (8th) MSH (see Figure 2 in the *Appendix* Section on page H).

Furthermore, the HMA3s of *A. thaliana* and *A. halleri* contain a putative 14-3-3 binding motif at the C-terminal cytoplasmic domain (*AtHMA3*: RASTSSP; *AbHMA3*: RASSSP; consensus: RSX_pSXP (mode 1) or RXXX_pSXP (mode 2); where _p indicates the phosphorylated amino acid, Dougherty and Morrison, 2004). 14-3-3 proteins are known to be involved in the regulation of several enzymes. Could the C-terminal domain of HMA3 possess a regulatory function? An example for such a regulation exists already. In *A. thaliana* protons are pumped across the plasma membrane from the cytoplasm to the plant cell exterior by the P-type IIIA ATPase AHA2 (see *Introduction* Section 6.3 on page 18). In order to activate the proton pumping, a membrane bound protein-kinase phosphorylates the threonine in a YTV motif at the C-terminal end of AHA2. Subsequently an unspecified 14-3-3 protein can bind and activates the pumping mechanism by displacing the C-terminal domain (Palmgren *et al.*, 1991). Although the 14-3-3 binding motif in AHA2 differs from the motif found in HMA3, one could imagine a similar mechanism for HMA3. In addition, a Zn(Cd/Cu) inducible promoter of the 14-3-3 protein isoform 20R from *Solanum tuberosum* (potato) supports that idea (Aksamit *et al.*, 2005).

To test the influence of the C-terminus on the activity of the protein, a truncated version of *AbHMA3* cDNA was expressed in both the zinc- and the cadmium-sensitive yeast mutant. The truncated cDNA encodes a *AbHMA3* variant equivalent to homologous bacterial P-type IB ATPases that lack a prolonged C-terminal domain. The expression of this truncated *AbHMA3* did not affect the metal-sensitive phenotype of the used yeast mutants and thus, indicated that the C-terminal domain is required for the transport function of *AbHMA3*. Unless the truncated *AbHMA3* protein is unstable when expressed in yeast, there are several explanations for this observation. Considering the potential regulation of HMA3 by 14-3-3 proteins, it could be that the binding or the release of a 14-3-3 protein to or from the C-terminus is required for the activation of its transport activity. However, since the deletion of the C-terminal domain did inactivate *AbHMA3*, it can be excluded that the C-terminal domain inhibits the transport function by a simple blocking of internal metal binding sites. It is more likely that an interaction of the C-terminus with other parts of the protein is important for the transport function of *AbHMA3*. This model is still compatible with an involvement of 14-3-3-binding to the C-terminus.

It is also possible that the cytoplasmic N- and C-terminal domains act as metallochaperones to facilitate the acquisition of Zn(Cd) ions for subsequent transport. Considering the femtomolar concentration range of free zinc in the cell (Outten and O'Halloran, 2001), a metallochaperone function of the cytoplasmic C-terminal domain could provide the needed high affinity to Zn (Cd) ions and would increase the Zn(Cd) concentration in the immediate vicinity of the *cis* side of the transporter. Banerjee *et al.* (2003) and Haney *et al.* (2005) suggested similar ideas for the ATP-binding-cassette (ABC) transporter subunit ZnuA from *Synechocystis* 6803 and for CDF transporters, respectively. The delivery of metal ions to the protein is probably mediated by independent metallochaperones. Andrés-Colás *et al.* (2006) suggested an interaction of *AtHMA5*, a putative copper pumping P-type ATPase, with an ATX1-like Cu-chaperone of *A. thaliana* after conducting yeast two-hybrid experiments (see *Introduction* Section on page 11 and page 23). To date, only Cu and Ni metallochaperones are described but the existence of yet unidentified chaperones for Zn and Fe is expected (Clemens, 2001; Clemens *et al.*, 2002b). Eren and Argüello (2004) could show that the presence of cysteine in the medium is important to achieve the highest Zn²⁺ transporting activity of HMA2 indicating that cysteine-bound Zn enhances the HMA2 mediated Zn transport activity.

Nevertheless, the handing over of metal ions from a ligand to the HMA3 protein might be supported by the cytoplasmic terminal domains that could subsequently funnel the metal ions to the transport acting site of HMA3. Zinc binding amino acids common in known zinc-binding motifs like cysteine (C), histidine (H), glutamate (E), and aspartate (D) in the N- (*AbHMA3*: 2 C, 0 H, 7 E, 4 D) and C-terminal (*AbHMA3*: 3 C, 0 H, 7 E, 3 D) cytoplasmic domains could be involved in binding the Zn (Cd) ions during the funneling process (see Figure 2 in the *Appendix* Section on page H).

Outlook Further work is needed to clarify the role of 14-3-3 proteins or other interacting proteins in the activity HMA3 by deletion or mutation of the putative 14-3-3 binding motif at the C-terminus of HMA3. A first approach should focus on codons encoding amino acids that can get phosphorylated because of a free hydroxyl group: serine (S), threonine (Y) and tyrosine (T). Regarding the putative 14-3-3 binding motif in *AbHMA3* (RASSSP), a successive substitution of the serines for alanine followed by the expression in metal-sensitive yeast mutant strains could provide a better understanding of the role of that particular peptide motif in *AbHMA3*.

Interestingly, the phytotoxin fusicoccin from the fungus *Fusicoccum amygdali* (Graniti, 1962) renders the interaction of 14-3-3 proteins with the previously mentioned H⁺-ATPase AHA2 almost irreversible and thus activates it permanently (Jahn *et al.*, 1997; Fuglsang *et al.*, 1999; Svanlid *et al.*, 1999). Hence, the incubation of HMA3 expressing yeast mutants with fusicoccin and their ability to detoxify Zn could contribute to understanding the function of the C-terminus of HMA3.

Considering that HMA3 is a plant protein, there is the danger that HMA3 is only partially active in yeast because the binding of yeast 14-3-3 proteins to HMA3 may be of low affinity, or because HMA3 cannot efficiently be phosphorylated by yeast kinases. One possibility to cope with the po-

tential lack of phosphorylation in yeast is to mimic the phosphorylation by substitution of the serine for aspartic acid. This is based on the indication that the significance of phosphorylation is the introduction of a negative charge at the site of 14-3-3-protein interaction. This strategy has been used successfully for the plastid glutamine synthetase of *Medicago trunculata* that contains a 14-3-3 binding motif (RTIS_pKP) similar to that of HMA3 (Lima *et al.*, 2006). The mimicking of phosphorylation has also been used to analyse the interaction of 14-3-3 proteins with Raf-1, a human mitogen-activated protein (MAP) kinase kinase kinase that regulates cell proliferation and differentiation (Carey *et al.*, 2003). It should be noted that Raf-1 activity is inhibited by Zn²⁺ and that its N-terminal domain interacts with the *C. elegans* CDF-1 protein and its human homolog ZnT-1. It has been suggested that these CDF proteins promote Raf-1 activity by removing the Zn²⁺ ions (Jirakulaporn and Muslin, 2004). I therefore propose that mutants of *AbHMA3* should be generated with a serine→aspartic acid (S→D) substitution at the putative 14-3-3 binding motif (RASSSP). The *AbHMA3* variants should be tested in metal-sensitive yeast mutants for their ability to mediate enhanced tolerance to Zn (Cd) in comparison to the wildtype *AbHMA3* protein.

To overcome the lack of Arabidopsis 14-3-3 proteins in *S. cerevisiae*, HMA3 could be coexpressed with each of the 13 Arabidopsis 14-3-3 proteins in metal-sensitive yeast mutants. As mentioned above, Aksamit *et al.* (2005) described that the promoter of the 14-3-3 protein isoform 20R of potato is inducible by Zn (Cd/Cu). The 20R isoform is most similar to the 14-3-3 protein isoform GRF01² (At1g78300) from *A. thaliana*. As *HMA3* expression is constitutively high in *A. halleri* compared to *A. thaliana* one could expect a higher 14-3-3 transcript level in *A. halleri* in case of interaction. The AFFYMETRIX Arabidopsis GeneChip[®] data (obtained from Ina Talke, group of Ute Krämer) does not show a significant difference in relative transcript abundance of *GRF01* between *A. thaliana* and *A. halleri*. The only conspicuous 14-3-3 transcript of the data set belongs to *GRF11* (At1g34760). It is about 4 times more abundant in shoots and about 3 times more abundant in roots of *A. halleri* than in *A. thaliana*. Moreover, like *HMA3*, *GRF11* appears to be transcriptionally regulated by FIT1, a bHLH transcription factor that possesses an important function in the regulation of the iron uptake response (Colangelo and Guerinot, 2004; see also page 130). Based on these facts, I suggest to choose first the GRF01 and GRF11 14-3-3 protein isoforms for a coexpression with *HMA3* in metal-sensitive yeast mutants.

2.2 The role of HMA3 in metal homeostasis of *A. thaliana* and *A. halleri*

2.2.1 Functional redundancy of HMA2, HMA4 and HMA3 in *A. thaliana*

The sister proteins of HMA3, HMA2 (Eren and Argüello, 2004) and HMA4 (Mills *et al.*, 2003, 2005; Verret *et al.*, 2005; Talke *et al.*, 2006), have also been described as Zn transporting P-type ATPases. They belong to the same homology cluster as HMA3. Hence, the thought of an at least partial

²GRF means *gene regulatory factor*.

functional redundancy is obvious. One way to answer this question is the comparison of *AtHMA* expression patterns found in this and other studies.

In silico inquiries showed that the general expression patterns of *AtHMA2*, *AtHMA4*, and *AtHMA3* are distinct. While *AtHMA2* and *AtHMA4* are predominantly expressed in shoot tissues, *AtHMA3* transcript is primarily detected in roots and senescent leaves of *A. thaliana*.

A more detailed look at expression levels in roots by *digital in-situ* mapping revealed a similar expression pattern of *HMA2* and *HMA4*, both primarily expressed in pericycle cells of mature roots. In contrast, *HMA3* appears to be expressed mainly in the cortex of developing and mature roots.

The microarray data have only been partially confirmed by real-time RT-PCR analysis of transcript levels so far. In this context, it has to be noted that in general the microarray signal intensities for *HMA3* are very low and thus, more susceptible to errors. Real-time RT-PCR data in this study showed that *AtHMA2* transcript is equally present in shoots and roots, and both, *AtHMA4* and *AtHMA3* transcripts are predominantly expressed in the roots of *A. thaliana*.

Whereas the results of the *in silico* query of microarray data are consistent with the functional redundancy of *AtHMA4* and *AtHMA2*, the real-time RT-PCR rather suggest that *AtHMA4* and *AtHMA3* might be functionally redundant. A look at published experimental data might exclude one or the other possibility:

Both *AtHMA2* and *AtHMA4* have been shown to localise to the plasma membrane (Hussain *et al.*, 2004; Verret *et al.*, 2004). Looking at *pAtHMA2-GUS* and *pAtHMA4-GUS* lines, Hussain *et al.* (2004) observed GUS activity in the vascular tissue of roots, stems, and leaves indicating a similar localisation and hence, pointing to a potential functional redundancy of *HMA2* and *HMA4*. This is supported by the observation that only the *hma2 hma4* double mutant, whereas neither of the two single mutants displayed an obvious phenotype.

In this study, *pAtHMA3-GUS* lines also showed GUS activity in vascular tissue but almost exclusively in roots, and not in shoots. This is in contrast to the *digital in-situ* microarray data that indicated a localisation within the root cortex (see *Results* Section 4.17 Figure 4.17). It remains unknown whether the microarray data are misleading due to the low signal intensities, or whether the observed GUS activity does not correlate with the distribution of *AtHMA3* transcript in the root. The latter might be caused by unknown *cis*-acting regulatory elements not incorporated in the reporter construct used here, which may modify the tissue-specific activity of the *AtHMA3* promoter.

Gravot *et al.* (2004) reported the localisation of *AtHMA3* to the vacuolar membrane of yeast, although the provided evidence is not convincing due to a fuzzy intravacuolar GFP signal. Since *AtHMA3* is a membrane protein, vacuolar localisation is expected to be associated with a GFP signal in the periphery of the vacuole, i. e. the vacuolar membrane. Such a signal was not observed by Gravot *et al.* (2004). Available algorithms to predict the localisation of HMA3 *in silico* do not provide conclusive data. In case *AtHMA3* is expressed in the root cortex as suggested by querying the AREX database (see *Results* Section, Figure 4.17 on page 91) and localised to the vacuolar membrane it may

share functional redundancy with *AtMTP3*, a vacuolar Zn transporter (Arrivault *et al.*, 2006).

In *A. thaliana* lines containing a *pMDC83-AbHMA3:GFP* construct, no GFP signal could be detected. There are many possible reasons for this. For example, it is known that GFP fused membrane proteins can aggregate and precipitate in the cell as non-fluorescent inclusion bodies when expressed in large quantities (Heim *et al.*, 1994; Crameri *et al.*, 1996). The remaining fluorescent soluble fusion proteins cannot be seen using a standard microscope. It has been shown that in such a case often a weak GFP signal is still detectable using a confocal laser scanning microscope (Freitag *et al.*, 2004). That, however, did not help to detect a fluorescent signal in *AbHMA3:GFP* lines in this study. Considering the expression under the control of the 35S promoter, it is unlikely that the GFP fusion protein fluoresces below the detection limit because it is not densely localised or expressed at a very low level (CLONTECH Laboratories, Inc., 1999).

It is more plausible to assume that the GFP fused HMA3 protein is unstable, gets misfolded and is rapidly degraded. To minimise interference with N- or C-terminal targeting signals, the GFP reporter protein could be fused internally between amino acids of the large cytoplasmic loop of *AbHMA3* as has been demonstrated for other proteins (Tian *et al.*, 2004; Harashima and Heitman, 2005). However, this attempt might prove to be challenging considering previously described toxicity of *HMA3* containing plasmids in *E. coli* (see *Results* Section on page 79 and 86).

Although not described for P-type ATPases, but known for RING finger, zinc finger, and zinc cluster domains, zinc plays an critical structural role and could also be important for the stabilisation and correct folding of HMA3. Indirectly, the activity of transcriptional regulatory proteins often containing the mentioned motifs depends on zinc (Freemont, 1993; Böhm *et al.*, 1997; Takatsujii, 1998, 1999; Krishna *et al.*, 2003). Nevertheless, the adding of extra zinc to the growth medium did not enhance a potential fluorescence signal.

AtHMA3* has no essential role in *A. thaliana During the course of this study, Hussain *et al.* (2004) showed that the *A. thaliana* wildtype of the Columbia accession is already a natural knockout for *AtHMA3* due to a single base pair deletion leading to a subsequent truncation of the encoded *AtHMA3*. The single base pair deletion does not occur in plants of the accession Wassilewskija. The truncated *AtHMA3* lacks about 30% of its original length including large parts of its cytoplasmic domain and the last two membrane spanning helices (MSHs). This polymorphism was confirmed by sequencing *AtHMA3* from Columbia and Wassilewskija plants used in this study and is also supported by real-time RT-PCR data. Compared to Ws, a lower *AtHMA3* expression level in plants of the Columbia accession probably reflects a nonsense-mediated mRNA decay (Maquat, 2002). An *AtHMA3* knockout line in the Ws background showed no apparent phenotype under control and Zn-depleted growth conditions adding an additional argument for a non-essential role of *HMA3* in *A. thaliana* (Hussain *et al.*, 2004). However, an extensive analysis of Zn or Cd uptake and accumulation is missing and thus, it can not be excluded that, even in the absence of a visible phenotype, *hma3* mutations may influence Zn and/or

Cd localisation in the Ws background (Hussain *et al.*, 2004).

Conclusion Taken together, the data obtained here, support an at least functional redundancy for HMA2 and HMA4 in *A. thaliana*. Based on *pAtHMA3-GUS* reporter lines and real-time RT-PCR data it cannot be excluded that *AtHMA3* is functionally redundant with *AtHMA2* and *AtHMA4* in roots of *A. thaliana*. Moreover, *in silico* microarray data support a possible functional redundancy with *AtMTP3*. A nucleotide polymorphism in the *AtHMA3* gene renders the encoded protein non-functional in the Columbia accession of *A. thaliana*, and this is a circumstantial evidence against an essential functional importance for zinc homeostasis in *A. thaliana*.

2.2.2 The role of HMA3 in *A. halleri*

Assuming a redundant function of *HMA3* in *A. thaliana*, why is *HMA3* so highly expressed in shoots of *A. halleri*? Does it play an important role in the zinc hyperaccumulation and tolerance in *A. halleri*?

Several mechanisms can contribute to the observed constitutive high transcript levels of *AbHMA3* that have been shown to be approximately 135-fold increased in shoots of *A. halleri* compared to shoots of *A. thaliana* (see *Introduction* Section, Figure 2.1 on page 28 and *Results* Section, Figure 4.18 on page 93). At the genomic level, the copy number of a gene, chromatin condensation/decondensation and DNA methylation can affect the transcript level. Later on at the level of transcription, the pre-mRNA synthesis is carried out by RNA polymerases that require general transcription factors to initiate the transcription at the correct start site. In addition, the transcription is modulated by *cis*-acting sequences and specific transcription factors. Subsequently, posttranscriptional processes can alter the amount of mRNA. Eukaryotic genes consist of exons and non-coding intron sequences. From the transcribed pre-mRNA, introns are excised, and exons are spliced together. This splicing process may be regulated as well. Furthermore, the stability or turnover rate of mRNA influences the transcript level and can be subject to regulation depending on physiological conditions (Riechmann, 2002; Taiz and Zeiger, 2002). It remains to be investigated if high *HMA3* transcript levels in shoots of *A. halleri* correlate with high HMA3 protein levels.

HMA3 occurs in several copies in the *A. halleri* genome *HMA3* occurs in at least four copies in the genome of *A. halleri*, named *AbHMA3-1*, *AbHMA3-2*, *AbHMA3-3*, and *AbHMA3-4* as shown by genomic DNA blots, BAC clone analyses, real-time RT-PCR, RACE experiments, and the cloning of genomic *HMA3* sequences in this study (see *Results* Section 1.1.7 on page 75). Sequence analysis of cloned *HMA3* copies did not reveal new restriction sites that could be responsible for additional bands on DNA gel blots.

The presence of multiple copies of metal homeostasis genes in metal-tolerant organisms is not unknown. Beside *HMA3*, at least five other metal homeostasis genes occur in several copies in *A. halleri*. Dräger *et al.* (2004) reported at least three genomic copies of *MTP1*, a gene for which there are consti-

tutively high transcript levels, in *A. halleri*. They encode almost identical proteins of the CDF family and mediate the sequestration of Zn in the cell vacuole. Only two of the three identified *MTP1* copies contribute to the high transcript levels and, unlike the third copy, these two copies co-segregate with Zn tolerance in the back-cross 1 generation of a cross between the zinc-tolerant species *A. halleri* and the zinc-sensitive species *Arabidopsis lyrata* (*A. lyrata*). According to Talke *et al.* (2006), the genome of *A. halleri* contains also multiple copies of the putative metal homeostasis genes *ZIP3*, *ZIP6*, *ZIP9*, and *HMA4*, all of which are expressed at higher levels in *A. halleri* than in *A. thaliana*. Other highly expressed candidate genes like *ZIP10*, *IRT3*, *PHT1;4* and *PDI1* are likely to occur in single copies, and so do even some of the genes that showed a substantially higher transcript level in *A. halleri* than in *A. thaliana* (*FRD3*, *ZIP4* and *MTP8*; Talke *et al.*, 2006). Consequently, an increase in genomic copy number is likely to contribute to high transcript levels for some candidate genes for metal hyperaccumulation and metal hypertolerance in *A. halleri*, but not for all of them.

Published data of van Hoof *et al.* (2001) suggested that the observed increased transcription of *metallothionein type 2b* (*SvMt2b*) in roots and shoots of a copper-tolerant ecotype of maiden's tears (*Silene vulgaris*) results from a tandem repeat of the gene. In yeast, a tandem repeat of the metallothionein gene *CUP1* has been described in cadmium-resistant (Tohoyama *et al.*, 1996) and copper-resistant strains (Fogel *et al.*, 1983; Tohoyama *et al.*, 1992). Also in hepatoma cell cultures and in flies, metallothionein gene duplications correlate with increased resistance to copper (Durnam and Palmiter, 1987; Maroni *et al.*, 1987; Czaja *et al.*, 1991).

Other examples for the clustering of multiple gene copies or closely related genes at loci come from the field of plant pathogen and parasite resistance (Martin *et al.*, 1993; Jones *et al.*, 1994; Ernst *et al.*, 2002).

Actually, gene duplication appears to be a common phenomenon as it provides quickly fresh raw material for evolution that can be utilised, e. g. directly to increase gene expression or indirectly for a long-term remodeling of the gene's function and regulation after both copies have sufficiently diverged (Kondrashov *et al.*, 2002; Otto and Yong, 2002).

One might think that the source of gene duplications in *A. halleri* is apparently reflected by its chromosome number ($n=8$ diploid) compared to *A. thaliana* ($n=5$ diploid), and that a genome duplication in the *Arabidopsis* lineage at the separation of *A. halleri* and *A. thaliana* about 3.8 to 5.8 Myr ago (Koch *et al.*, 2001) may have provided the basis for the evolution of the hyperaccumulation trait in *A. halleri*. But the $n=5$ genome of *A. thaliana* is actually an anomaly within its tribe Sisymbrieae of the Brassicaceae and a chromosomal number of 8 is believed to be the ancestral state (Koch *et al.*, 1999; Yogeewaran *et al.*, 2005). The genome reduction in *A. thaliana* is probably the result of chromosomal fusions rather than eliminations as suggested by two mapping studies that compared the *A. thaliana* genome with the *Capsella* genome (Boivin *et al.*, 2004) and the *A. lyrata* genome (Kuittinen *et al.*, 2004). These results indicate that the amplification of metal homeostasis genes in *A. halleri* more likely originated from inner-chromosomal or other duplication events. Considering the close homology be-

tween cloned *AbHMA3* variants (see *Results* Section 4.2 on page 64), the *AbHMA3* duplication events occurred very recently (< 5 Myr ago), probably after the divergence of *A. thaliana* and *A. halleri*, and maybe even after the separation from the zinc-sensitive non-hyperaccumulating *A. lyrata* branch (< 3 Myr ago, see *Introduction* Section 4.1, Figure 1.1).

Further studies should therefore investigate the copy number of the *HMA3* gene in other zinc-sensitive non-hyperaccumulating species of the *Sisymbrieae* tribe like *Capsella rubella* or the *A. halleri* sister species *A. lyrata*. The data could help to shed light on the origin of the *HMA3* gene copy number amplification and its importance for zinc hyperaccumulation.

Several gene copies do not explain the constitutively high expression of *AbHMA3* In summary, the occurrence of several gene copies might contribute to the elevated expression of *HMA3* in *A. halleri* by providing additional *AbHMA3* transcript. But it can neither explain its constitutively high expression, nor the altered primary localisation of *HMA3* transcript to the shoot compared to the root-dominant expression in *A. thaliana*. These properties, which are characteristic for the expression of *AbHMA3* in *A. halleri*, should originate from another, regulatory cause than from a sheer gene amplification.

The cloned promoter regions of *AbHMA3-1* and *AbHMA3-2* are not responsible for the constitutively high expression of *HMA3* in shoots of *A. halleri* The observed constitutively high expression of *HMA3* in *A. halleri* was the starting point for its selection as an interesting candidate gene that might be involved in zinc homeostasis in *A. halleri*. In eukaryotic organisms, the expression of a gene depends primarily on the activity of its promoter. Hence, the activity and regulation of the promoters of *AbHMA3* was analysed and compared to the promoter of *AtHMA3*.

The copy-specific analysis of transcript levels revealed that virtually all *AbHMA3* transcript derives from an *AbHMA3-1* rather than an *AbHMA3-2* related gene sequence. Based on cloned 5'-RACE products and promoter sequences, and on PCR analysis of BAC DNA, *AbHMA3-1* is associated with the promoter *pAbHMA3-1* (see *Results* Section 1.1 on page 58). Therefore *pAbHMA3-1* is the promoter that should be highly active in shoots of *A. halleri*. However, as described in the *Results* Section 5 beginning on page 99, none of the two cloned promoter fragments of *AbHMA3* from *A. halleri*, *pAbHMA3-1* or *pAbHMA3-2* were highly active in shoot tissue of *A. thaliana*. One possible explanation is a different regulation of the *A. halleri* promoter fragments in *A. thaliana*. *A. halleri* specific transcription factors could trigger a shoot specific expression in *A. halleri*. However, transformed *A. halleri* plants did not display a high activity of the *pAbHMA3-1* or the *pAbHMA3-2* promoter in shoots, if any at all. It is unlikely that the two cloned promoter fragments are responsible for the high expression of *HMA3* in shoots of *A. halleri*.

Are there additional *AbHMA3* promoters? Previously described results that suggest the presence of a third and a fourth *HMA3* gene copy in the genome of *A. halleri* evoke another possible

explanation: the existence of yet unknown promoter sequences of *AbHMA3* (see *Results* Section 1.1.7 on page 75).

A third promoter sequence supposedly correlating with a yet unknown *AbHMA3-3* coding sequence is expected in the DNA of the BAC No.2, 3, and 8 (*AbHMA3-1*: BAC No.1 and 7; *AbHMA3-2*: BAC No.4, 5, and 6; see *Results* Section 1.1 on page 58, Figure 4.1, 4.2, and 4.7). A fourth promoter is expected upstream of the *AbHMA3-4* gene copy on BAC No.1 and BAC No.7. *AbHMA3-4* was specifically detected by an *AbHMA3-2* specific primer pair while *AbHMA3-1* specific primers suggested the presence of an *AbHMA3-1* copy on BAC No.7 (see Figure 4.19 B on page 96 in the *Results* Section 2.2.2). This finding is supported by Southern hybridisation data showing two *HMA3* specific signals on restricted BAC No.7 DNA and the related BAC No.1 DNA. The detection of *AbHMA3-4* by primers specific to *AbHMA3-2* renders it a questionable source of the constitutively highly expressed *AbHMA3-1* related transcript in *A. halleri*. Therefore, its promoter should not be a primary target for further investigations.

Future experiments should aim at first for the cloning of *AbHMA3-3* genomic sequences from the DNA of the three BAC clones mentioned. In a first approach, the *AbHMA3-1* and *AbHMA3-2* specific primers that were mentioned above could be used to quickly detect *AbHMA3-1/-2*-like sequences on the BAC clone DNA. If *AbHMA3-3* is responsible for the high *AbHMA3* transcript levels, then it must contain sequence regions that are nearly identical to the used *AbHMA3-1* specific primers as shown by copy-specific expression analysis. If the sequence of *AbHMA3-3* differs from *AbHMA3-1* in the region specific to the *AbHMA3-1* primers, then *AbHMA3-3* does probably not encode the highly expressed *AbHMA3* copy. Consequently, in the latter case the promoter of *AbHMA3-3* would not be a primary target for further investigations.

In case the sequence of *AbHMA3-3* is similar to *AbHMA3-1*, *AbHMA3-3* specific sequences need to be found that distinguish *AbHMA3-3* from other *AbHMA3* copies. This might prove to be impossible taking into account that only one sequence difference between *AbHMA3-1* and *AbHMA3-2* was suitable for real-time RT-PCR, and that this difference is predicted not to occur between *AbHMA3-3* and *AbHMA3-1* in case that *AbHMA3-3* is highly expressed in *A. halleri*. Considering the high risk that it is not possible to distinguish between the transcripts of *AbHMA3-1* and possibly *AbHMA3-1*-like *AbHMA3-3*, the *pAbHMA3-3* promoter should be cloned for the analysis of its activity using reporter gene fusions. In a first attempt, the inverse PCR on DNA of the BAC clones No.2, 3, and 8 that was mentioned in the *Results* Section on page 109 could be repeated. If the approach fails, one could try to directly subclone and sequence a *AbHMA3-3* containing BAC DNA fragment.

***AbHMA3-2* expression is increased in response to Cu** Interestingly, data obtained by Ina Talke (postdoctoral researcher, group of Ute Krämer) indicated an increase of *AbHMA3* expression in *A. halleri* roots after exposure to Cu for 2 and 8 hours. This work's copy-specific analysis of *AbHMA3* expression showed that predominantly *AbHMA3-2* contributes to the copper-inducible por-

tion of *AbHMA3* transcript levels (see Figure 4.19 in the *Results* Section on page 96). This might point to a different regulation and a distinct role of *AbHMA3-2* in the metal homeostasis of *A. halleri* compared to *AbHMA3-1*. However, considering the close similarity of the *AbHMA3-1* and *AbHMA3-2* coding sequences and the differences in the biophysical properties of monovalent Cu ions thought to be present in the cytoplasm and divalent Zn ions, it is unlikely that *AbHMA3-2* transports copper ions. Actually, *AbHMA3-2* transcript levels could be co-regulated and enhanced indirectly in response to increased Cu concentrations. The uptake of monovalent copper ions from the soil is thought to be accomplished by the high affinity copper transporter COPT1, a member of the Ctr copper transporter family that does not transport zinc (Sancenon *et al.*, 2004, 2003; Puig and Thiele, 2002). *AtZIP4* encoding a putative Zn^{2+} uptake system has been shown to transport not only zinc but also copper when expressed in yeast cells (Wintz *et al.*, 2003). *AbZIP4* is highly expressed in roots of *A. halleri* compared to *A. thaliana* (Becher *et al.*, 2004; Weber *et al.*, 2004; Talke *et al.*, 2006). However, *AbZIP4* transcript levels were suppressed in *A. halleri* in response to high copper concentrations (Talke *et al.*, 2006). Therefore, it is possible that high soil copper concentrations could affect intracellular zinc concentrations in roots of *A. halleri*. This would consequently affect the regulation of genes involved in Zn homeostasis, e. g. *AbHMA3-2*.

Some copper binding cellular compounds, like glutathione, are known to have a broader metal specificity and also bind zinc. Thus, the increased chelation of Cu ions in response to high intracellular copper concentrations could probably affect the pool of available Zn binding sites by competitive zinc displacement. On the one hand this could temporarily increase intracellular free Zn concentrations or intracellular Zn availabilities. On the other hand Cu treatment could reduce the availability of zinc ions by competitively inhibiting Zn uptake and therefore generate an intracellular lack of zinc. In both cases, the zinc homeostasis, e. g. including the Zn/Cu stoichiometry, has to be adjusted, and *AbHMA3-2* could play a role in this.

Regulation of *AbHMA3-1* in response to a physiological Fe deficiency? Due to competitive effects between Zn^{2+} and Fe^{2+} ions (Woolhouse, 1983), a high Zn level causes a physiological Fe deficiency in seedlings. Moreover, *Arabidopsis* exhibits a high uptake of Zn into the root under Fe deficient conditions (Vert *et al.*, 2003; Ute Krämer and Ina Talke, unpublished data). It is the result of the action of IRT1, a plasma membrane transporter of the ZRT / IRT protein family (see *Introduction* Section 5.2.1 on page 12). IRT1 usually imports Fe under Fe deficient conditions, but it can also transport Mn, Zn, Cd, and Co into the root symplasm of root epidermis and cortical cells (Marschner and Rohmold, 1994; Robinson *et al.*, 1999).

Experiments with *pAbHMA3-1-GUS* plants revealed that the Zn induced increase in promoter activity of *AbHMA3-1* is suppressed by supplying excess Fe (see Figure 5.5 in the *Results* Section on page 108). This observation indicates that the induction of *AbHMA3-1* expression by an oversupply of Zn depends on a physiological Fe deficiency. Data from Colangelo and Guerinot (2004) support these

findings by describing an induction of *HMA3* expression under Fe deficient conditions in *A. thaliana*.

In *A. thaliana* FIT1, a bHLH transcription factor, plays a major role in the regulation of the iron deficiency response. The microarray based analysis of a *fit1-1* Arabidopsis mutant line revealed that the expression of at least 40 % of the deficiency-induced iron-regulated genes directly depend on FIT1 (Colangelo and Gueriot, 2004). The occurrence of *AtHMA3* among those genes provides a further hint that its expression is coupled to the Fe status of the plant. This is similar to the transcriptional regulation of the vacuolar Zn transporter *AtMTP3* (Arrivault *et al.*, 2006).

Alternative explanation for a high shoot *AbHMA3* expression Regulatory elements inside intron sequences can affect the transcriptional control of a gene. *Cis*-regulatory sequences have been described in the second intron of the floral homeotic gene *AGAMOUS* (Sieburth and Meyerowitz, 1997; Busch *et al.*, 1999; Deyholos and Sieburth, 2000; Hong *et al.*, 2003).

Another interesting example comes from the analysis of the expression of the Arabidopsis profilin gene family. These genes encode small actin-binding proteins that regulate cellular dynamics of the actin cytoskeleton. *PRF1*, *PRF2*, and *PRF3* are expressed in vegetative tissues whereas *PRF4* and *PRF5* are expressed in pollen. Jeong *et al.* (2006) demonstrated by *promoter-GUS* fusions that the first intron of *PRF2*, located inside the coding region, is required for strong and constitutive gene expression. The *PRF2* promoter without the first intron was only active in vascular bundles.

The comparison of genomic sequences of *AbHMA3-1*, *AbHMA3-2* and *AtHMA3* uncovered an *AbHMA3-1* specific 29 bp insertion inside the first intron that is located within the coding region of the gene (see *Results* Section 1.1.3 on page 61). With regard to the mentioned examples, it is possible that this difference reflects distinct roles of the first introns in the regulation of *AbHMA3-1* and *AbHMA3-2* transcription. The first intron of *AbHMA3-1* could enhance the activity of its promoter and alter the expression pattern. This may result in a strong constitutive expression primarily in the shoot. However, an *in silico* database search did neither reveal a known regulatory motif inside the 29 bp insertion nor sequence similarities to the mentioned first intron of *PRF2* or a gene that is constitutively highly expressed. Future experiments should focus on the fusion of the GUS reporter gene with the promoter of *AbHMA3-1* and *AbHMA3-2* including their first introns.

Epigenetic silencing mechanisms Epigenetic silencing mechanisms could also be a cause of the differential expression of *HMA3* in *A. thaliana* and *A. halleri*. In the past few years, it became increasingly evident that small non-coding RNAs (20-25 nt) play an important regulatory role. These molecules can target and degrade homologous mRNA or prevent mRNA translation (Jones-Rhoades *et al.*, 2006; Vaucheret, 2006; Valencia-Sánchez *et al.*, 2006; Meins *et al.*, 2005). The ever increasing number of mRNAs that are targeted by small RNAs rises the question if *HMA3* transcript levels in *A. thaliana* might be influenced by small RNAs as well. A novel sequencing approach, MPSS (massively parallel signature sequencing) (Brenner *et al.*, 2000), provided the tool for the in-depth profiling

of the small RNA pool. A query to the Arabidopsis Small RNA MPSS Database (mpss.udel.edu, Lu *et al.*, 2005; Nakano *et al.*, 2006) did not retrieve any potential small RNA signatures associated with the genomic sequence of *AtHMA3* or the intergenic region upstream of *AtHMA3*. Thus, in *A. thaliana* small RNAs might not be involved in the regulation of *AtHMA3* expression.

At this point, it is noteworthy to mention that some studies suggest that the presence of multiple gene copies can trigger post-transcriptional gene silencing if the transcript level exceeds a certain threshold level (Hobbs *et al.*, 1993; Jorgensen *et al.*, 1996; Schubert *et al.*, 2004). However, high *HMA3* expression is observed in *A. halleri* that appears to contain at least four *HMA3* gene copies. This might support the idea that not all *AbHMA3* gene copies contribute to the high transcript levels.

2.2.3 Potential functions of *HMA3* in metal homeostasis

What is the potential function of *HMA3* considering experimental results and published data as well as other described components involved in Zn homeostasis? A better understanding is achieved by following the path of Zn from the soil into upper shoot tissues of *A. halleri*.

The uptake of Zn from soil into the root symplasm is likely to be carried out by plasma membrane transporters of the ZRT/IRT transporter family (see *Introduction* Section 5.2.1 on page 12), especially by ZIP1, ZIP4 and under Fe-deficient conditions, IRT1 (Grotz *et al.*, 1998; Wintz *et al.*, 2002; Henriques *et al.*, 2002; Varotto *et al.*, 2002; Vert *et al.*, 2002). It is likely that hydrated zinc ions are chelated by low-molecular weight cellular compounds like metallochaperones or nicotianamine (NA). Increasing NA concentrations appear to be able to confer Zn tolerance to yeast cells, and *A. halleri* displays a higher NA concentration than *A. thaliana* (Weber *et al.*, 2004; Trampczynska *et al.*, 2006). The root-to-shoot transport of zinc requires the export of the hydrated or chelated zinc ions from the root symplasm into the apoplastic xylem. Experimental data suggest that HMA2 and HMA4 are involved in this process (Eren and Argüello, 2004; Hussain *et al.*, 2004; Verret *et al.*, 2004). In the shoot, the unloading of the xylem resembles a similar situation as the uptake of ions into the root. The proteins that function as ion importers from the xylem inside the shoot are not known. Considering the apoplastic/symplastic nature of the ion transfer one might speculate that rather ZRT/IRT family members than P-type ATPases might play a role. Inside the symplasm of root and shoot cells, zinc ions are delivered to different cell types by various membrane transporters and moved intercellularly via plasmodesmata or by cellular export and re-uptake from the apoplast. HMA2 and HMA4 appear to play a major role in the cellular zinc efflux from vascular cells (Hussain *et al.*, 2004). Zinc influx could be carried out by members of the ZIP family.

Intracellular targets with a high demand of Zn ions are the cytoplasm and the nucleus containing, for example, Zn finger proteins. Chloroplasts and mitochondria also contain Zn-dependent proteins. To date, the proteins involved in chloroplastic or mitochondrial Zn import are unknown. A few insights into chloroplastic copper import were gained showing the involvement of the three P-type IB ATPases, HMA1, HMA6 and HMA8 (see *Introduction* Section 7.2.3 and 7.1.1 on page 24 and 21;

Shikanai *et al.*, 2003; Abdel-Ghany *et al.*, 2005b; Seigneurin-Berny *et al.*, 2006).

Transporters that are important for the detoxification of excess zinc in the cytoplasm sequester zinc ions by transport into the vacuole or move them into specific cell types, e.g. trichomes or epidermal leaf cells (Brune *et al.*, 1995). A rather housekeeping than a detoxifying function was attributed to *AtMTP1*, a CDF protein that transports zinc into the vacuole of root and leaf cells. It is highly expressed in *A. halleri* and contributes to the zinc hypertolerance (Desbrosses-Fonrouge *et al.*, 2005; Krämer, 2005a; Dräger *et al.*, 2004; Kobae *et al.*, 2004). Another MTP protein, *MTP3*, was found to be upregulated by enhanced symplastic influx of Zn and therefore actively contributes to Zn detoxification in the root (Arrivault *et al.*, 2006).

Considering the mentioned targets and functions of zinc-transporting proteins in *Arabidopsis*, what is the potential role of HMA3? First of all: HMA3 appears to be a nonessential zinc transporter in *A. thaliana* as indicated by the confirmed nonsense mutation in the Columbia accession. The promoter of *AtHMA3* and the homologous promoter of *AbHMA3-1* are both primarily active in the vascular bundle of roots. Hence, both the *AtHMA3* and the *AbHMA3* proteins could share a functional redundancy with the closely related HMA2 and HMA4 zinc transporters in root-localised xylem loading. This could explain the dispensability of HMA3 in zinc homeostasis of *A. thaliana*. However, contrary to the observed promoter activities, *AbHMA3-1* transcript levels are constitutively high not only in roots but also and even more so in shoot tissue of *A. halleri*. Furthermore, the observed minor differences in the quantitative GUS activity conferred by the promoters do not reflect the major differences in *HMA3* transcript levels found by real-time RT-PCR between *A. thaliana* and *A. halleri*. It might be that an *AbHMA3-1* specific feature in the first intron enables a constitutively high expression of *AbHMA3-1*. However, the influence of the first intron is speculative and remains to be demonstrated experimentally. Given that the localisation of expression in the root vasculature is correct nevertheless, *AbHMA3-1* could be largely functionally redundant with HMA2 and HMA4 and could support the xylem loading in roots and the cellular Zn export out of vascular shoot tissue cells. In this case, it may contribute to the efficient root-to-shoot translocation and the generation of a Zn sink in the shoot that is a characteristic of hyperaccumulating plants.

Another possibility to be examined is that the promoter of a putatively *AbHMA3-1* related gene copy, *AbHMA3-3* on BAC clones No.2, 3, and 8, is responsible for the observed high *AbHMA3* expression in *A. halleri*. It cannot be ruled out that in shoots and roots, *AbHMA3-3* is the source of the constitutively high *AbHMA3* transcript levels because it is not known whether the sequence of the transcript of this gene is *AbHMA3-1*-like. Alternatively, *AbHMA3-1* may be expressed in roots and *AbHMA3-3* in shoots and *vice versa*. Without further experimental data, a possibly distinct localisation of the *AbHMA3-3* promoter activity remains speculative. A recent study identified three quantitative trait loci (QTL) regions for Zn tolerance in *A. halleri* (Willems *et al.*, 2007). None of these QTL regions is within regions of the *A. halleri* genome corresponding to the *AtHMA3*-containing fourth chromosome of *A. thaliana*. *AbHMA3-1* appears to be orthologous to *AtHMA3* considering genomic

sequences and promoter regions (see *Results* Section 1.1.3 and 1.1.5 on page 61 and 67). This might indicate that *AbHMA3-1* plays no major role in zinc tolerance in *A. halleri*, and it raises the possibility that the putatively *AbHMA3-1* related *AbHMA3-3* gene copy is the constitutively highly expressed *HMA3* gene in *A. halleri*. However, the authors of Willems *et al.* (2007) believe that their QTL detection power was reduced due to the used small progeny size and the observed segregation distortion. Hence, it is possible that some QTLs, especially minor ones, for Zn tolerance have not been detected.

The constitutively high transcript levels of *HMA3* in *A. halleri* support the idea of a housekeeping function in terms of Zn homeostasis of *A. halleri*. Thus, *AbHMA3* may be part of basic Zn homeostasis mechanisms of *A. halleri* that are involved in Zn hyperaccumulation or tolerance. Besides a conceivable support of the functions of HMA2 and HMA4, *AbHMA3* might play a role in maintaining non-toxic intracellular Zn levels in physiologically important cell types by vacuolar sequestration of Zn ions or by delivery of zinc ions to leaf trichomes, epidermal leaf cells, or mesophyll cells. The vacuolar sequestration of Zn is, however, thought to be carried out by MTP1 as a housekeeping Zn transporter and MTP3 in *A. halleri* and *A. thaliana* (Dräger *et al.*, 2004; Kobae *et al.*, 2004; Desbrosses-Fonrouge *et al.*, 2005; Krämer, 2005a; Arrivault *et al.*, 2006). In *A. halleri*, it has been shown that the base of leaf trichomes and mesophyll cells are the main storage sites for Zn (Küpper *et al.*, 2000; Zhao *et al.*, 2000; Sarret *et al.*, 2002). MTP1 could play a role in the vacuolar sequestration of Zn in mesophyll cells. Yet, it is unknown which proteins are involved in the delivery of Zn to the other mentioned main zinc storage sites. Therefore, *AbHMA3* may also be a potential candidate for the Zn delivery to leaf trichomes.

AbHMA3-2 related gene copies do not contribute significantly to the high *AbHMA3* transcript levels as shown by copy-specific expression analysis. However, its significantly enhanced expression in the presence of increased copper concentrations could point to a function in cellular copper response that is distinct from that of a *AbHMA3-1*-like gene copy, e.g. the maintenance of the Zn/Cu stoichiometry by counteracting the effects of a perturbed intracellular copper level. Hence, an *AbHMA3-2* related protein might be localised to organelles with a high Zn and Cu demand like chloroplasts and mitochondria that contain enzymes like the Cu/Zn superoxiddismutase.

2.3 Conclusions and summary

The results obtained with yeast cells expressing *AbHMA3* are consistent with the P-type IB ATPase HMA3 functioning mainly as a Zn transporter. *AtHMA3* transcripts are predominantly expressed in roots and very low in shoots of *A. thaliana*. A nonsense mutation renders the gene nonfunctional in the Columbia accession of *A. thaliana*. It is highly probable that *AtHMA3* has no essential function in *A. thaliana*, and it may share at least a partial functional redundancy with *AtHMA2* and *AtHMA4* in loading the xylem with Zn.

In *A. halleri*, *HMA3* is constitutively highly expressed and therefore a candidate gene in naturally selected Zn hypertolerance and Zn hyperaccumulation. In contrast to *AtHMA3* from *A. thaliana*, it displays a high activity in the shoot. The genome of *A. halleri* encodes at least four *HMA3* copies, *AbHMA3-1*, *AbHMA3-2*, *AbHMA3-3*, and *AbHMA3-4*. The highly expressed *AbHMA3* gene is either *AbHMA3-1* or *AbHMA3-3*, and it is highly homologous to *AbHMA3-1* and less to *AbHMA3-2*. *AbHMA3-2* related gene copies (*AbHMA3-2* and *AbHMA3-4*) are not highly expressed, but appears to be regulated by excess copper. Although highly speculative, *AbHMA3-2*-like gene copies could have a function in the cellular copper response or in the adjustment of Zn homeostasis to high Cu concentrations.

The promoter of *AbHMA3-1* and a 1 kbp upstream fragment of *AbHMA3-2* do not confer high reporter gene activity in shoots of *A. thaliana* or *A. halleri*, as might have been expected for *AbHMA3-1* based on reported transcript levels. Thus, the cloned promoters cannot account for the high expression in *A. halleri* shoots. However, it remains to be investigated whether distinct intronic features of the *AbHMA3-1* sequence could trigger a constitutively high expression of *AbHMA3* in shoots of *A. halleri* or not.

Experimental data point to the existence of a third copy, *AbHMA3-3*. This copy might contribute to or could even be the single source of the constitutively high *AbHMA3* transcript levels in shoots of *A. halleri*. Given that, its coding sequence has to be almost identical to *AbHMA3-1*.

To date, mainly due to a lack of solid localisation data for the encoded protein, no clear function can be assigned to *AbHMA3*, and the cause of its constitutively high transcript levels remains hidden. If functionally redundant with *AbHMA2* and *AbHMA4* and localised to the plasma membrane, *AbHMA3* might contribute to the efficient translocation of Zn from root to shoot and/or to the cell-to-cell distribution of Zn in the shoot. If localised to the vacuolar membrane, then a role in maintaining a low cytoplasmic zinc concentration by vacuolar zinc sequestration is possible. However, this function has already been described for *AbMTP1*.

In addition, *AbHMA3* might be involved in other functions within the zinc homeostasis network. A possible step is the delivery of zinc ions to the base of leaf trichomes and mesophyll cells that are major zinc storage sites in *A. halleri*.

To clarify its function and role in the Zn homeostasis network of *A. halleri*, future work should focus on a solid localisation of *AbHMA3*. Furthermore, the influence of the third copy, *AbHMA3-3* on

the constitutively high expression of *AbHMA3* needs to be elucidated. The sequence of the *AbHMA3-3* genomic region and an analysis of the activity of the *AbHMA3-3* promoter will be very important.

Part V

Bibliography and indices

Bibliography

- Abdel-Ghany, S. E., Burkhead, J. L., Gogolin, K. A., Andrés-Colás, N., Bodecker, J., Puig, S., Peñarrubia, L., and Pilon, M. (2005a). *AtCCS* is a functional homolog of the yeast copper chaperone Ccs1/Lys7. *FEBS Lett.*, **579**, 2307–2312.
- Abdel-Ghany, S. E., Müller-Moulé, P., Niyogi, K. K., Pilon, M., and Shikanai, T. (2005b). Two P-type ATPases are required for copper delivery in *Arabidopsis thaliana* chloroplasts. *Plant Cell*, **17**, 1233–1251.
- Aksamit, A., Korobczak, A., Skala, J., Lukaszewicz, M., and Szopa, J. (2005). The 14-3-3 gene expression specificity in response to stress is promoter dependent. *Plant Cell Physiol.*, **46**, 1635–1645.
- Al-Shehbaz, I. A. and O’Kane, S. L. (2002). The *Arabidopsis* Book, chapter Taxonomy and phylogeny of *Arabidopsis* (Brassicaceae) (The American Society of Plant Biologists), 1–22.
- Albers, R. (1967). Biochemical aspects of active transport. *Annu. Rev. Biochem.*, **36**, 727–756.
- Alonso, J. M., Hirayama, T., Roman, G., Nourizadeh, S., and Ecker, J. R. (1999). EIN2, a bifunctional transducer of ethylene and stress responses in *Arabidopsis*. *Science*, **284**, 2148–2152.
- Altendorf, K., Gassel, M., Puppe, W., Mollenkamp, T., Zeeck, A., Boddien, C., Fendler, K., Bamberg, E., and Drose, S. (1998). Structure and function of the Kdp-ATPase of *Escherichia coli*. *Acta Physiol. Scand.*, **643**, 137–146.
- Ando, A. and Suzuki, C. (2005). Cooperative function of the CHD5-like protein Mdm39p with a P-type ATPase Spf1p in the maintenance of ER homeostasis in *Saccharomyces cerevisiae*. *Mol. Genet. Genomics*, **273**, 497–506.
- Andrés-Colás, N., Sancenón, V., Rodríguez-Navarro, S., Mayo, S., Thiele, D. J., Ecker, J. R., Puig, S., and Peñarrubia, L. (2006). The *Arabidopsis* heavy metal P-type ATPase HMA5 interacts with metallochaperones and functions in copper detoxification of roots. *Plant J.*, **45**, 225–236.
- Anton, A., Grosse, C., Reissmann, J., Pribyl, T., and Nies, D. H. (1999). Czcd is a heavy metal ion transporter involved in regulation of heavy metal resistance in *Ralstonia sp.* strain CH34. *J. Bacteriol.*, **181**, 6876–6881.
- Arazi, T., Sunkar, R., Kaplan, B., and Fromm, H. (1999). A tobacco plasma membrane calmodulin-binding transporter confers Ni²⁺ tolerance and Pb²⁺ hypersensitivity in transgenic plants. *Plant J.*, **20**, 171–182.
- Argüello, J. M. (2003). Identification of ion-selectivity determinants in heavy-metal transport P (1B)-type ATPases. *J. Membr. Biol.*, **195**, 93–108.
- Arrango, M., Gévaudant, F., Oufattole, M., and Boutry, M. (2003). The plasma membrane proton pump ATPase: the significance of gene subfamilies. *Planta*, **216**, 355–365.
- Arrivault, S. (2005). Functional characterization of *Arabidopsis thaliana* MTP3, a putative metal transport protein of the cation diffusion facilitator (CDF) family. Ph.D. thesis, University of Postdam, Max Planck Institute of Molecular and Plant Physiology.
- Arrivault, S., Senger, T., and Krämer, U. (2006). The *Arabidopsis* metal tolerance protein *AtMTP3* maintains metal homeostasis by mediating Zn exclusion from the shoot under Fe deficiency and Zn oversupply. *Plant J.*, **46**, 861–879.

- Assunção, A. G. L., Da Costa Martins, P., De Folter, S., Vooijs, R., Schat, H., and Aarts, M. G. M. (2001). Elevated expression of metal transporter genes in three accessions of the metal hyperaccumulator *Thlaspi caerulescens*. *Plant Cell Environ.*, **24**, 217–226.
- Auland, M. E., Roufogalis, B. D., Devaux, P. F., and Zachowski, A. (1994). A reconstitution of ATP-dependent aminophospholipid translocation in proteoliposomes. *Proc. Natl. Acad. Sci. U. S. A.*, **91**, 10938–10942.
- Ausubel, F. M., Brent, R., Kingston, R. E., Moore, D. D., Sedman, J. G., Smith, J. A., and Struhl, K. (1993). *Current protocols in molecular biology*. 2nd edition (New York: Green Publishing Associates and John Wiley and Sons Inc.).
- Axelsen, K. B. and Palmgren, M. G. (1998). Evolution of substrate specificities in the P-type ATPase superfamily. *J. Mol. Evol.*, **46**, 84–101.
- Axelsen, K. B. and Palmgren, M. G. (2001). Inventory of the superfamily of P-type ion pumps in *Arabidopsis*. *Plant Physiol.*, **126**, 696–706.
- Baker, A. J. M. (1981). Accumulators and excluders - strategies in the response of plants to heavy metals. *J. Plant Nutr.*, **3**, 643–654.
- Baker, A. J. M. and Brooks, R. R. (1989). Terrestrial higher plants which hyperaccumulate metallic elements - a review of their distribution, ecology and phytochemistry. *Biorecovery*, **1**, 81–126.
- Baker, A. J. M., McGrath, S. P., Reevesand, R. D., and Smith, J. A. C. (2000). *Phytoremediation of contaminated soil and water*, chapter Metal hyperaccumulator plants: a review of the ecology and physiology of a biochemical resource for phytoremediation of metal-polluted soils (Boca-Raton, FL, USA: Lewis Publishers), 85–107.
- Baker, A. J. M., Reeves, R. D., and Hajar, A. S. M. (1994). Heavy metal accumulation and tolerance in British populations of the metallophyte *Thlaspi caerulescens* J. & C. Presl (Brassicaceae). *New Phytol.*, **127**, 61–68.
- Balandin, T. and Castresana, C. (2002). *AtCOX17*, an *Arabidopsis* homolog of the yeast copper chaperone COX17. *Plant Physiol.*, **129**, 1852–1857.
- Banerjee, S., Wei, B., Bhattacharyya-Pakrasi, M., Pakrasi, H. B., and Smith, T. J. (2003). Structural determinants of metal specificity in the zinc transport protein ZnuA from *Synechocystis* 6803. *J. Mol. Biol.*, **333**, 1061–1069.
- Baunsgaard, L., Fuglsang, A. T., Jahn, T., Korthout, H. A., de Boer, A. H., and Palmgren, M. G. (1998). The 14-3-3 proteins associate with the plant plasma membrane H⁺-ATPase to generate a fusicoccin binding complex and a fusicoccin responsive system. *Plant J.*, **13**, 661–671.
- Baxter, I., Tchieu, J., Sussman, M. R., Boutry, M., Palmgren, M. G., Gribskov, M., Harper, J. F., and Axelsen, K. B. (2003). Genomic comparison of P-Type ATPase ion pumps in *Arabidopsis* and rice. *Plant Physiol.*, **132**, 618–628.
- Becher, M., Talke, I. N., Krall, L., and Krämer, U. (2004). Cross-species microarray transcript profiling reveals high constitutive expression of metal homeostasis genes in shoots of the zinc hyperaccumulator *Arabidopsis halleri*. *Plant J.*, **37**, 251–268.
- Beitz, E. (2000a). TeXshade: shading and labeling multiple sequence alignments using LaTeX 2 ϵ . *Bioinformatics*, **16**, 135–139.

- Beitz, E. (2000b). TeXtopo: shaded membrane protein topology plots in LaTeX 2 ϵ . *Bioinformatics*, **16**, 1050–1051.
- Bernard, C., Roosens, N., Czernic, P., Lebrun, M., and Verbruggen, N. (2004). A novel CPx-ATPase from the cadmium hyperaccumulator *Thlaspi caerulescens*. *FEBS Lett.*, **569**, 140–148.
- Bert, V., Bonnin, I., Saumitou-Laprade, P., de Laguérie, P., and Petit, D. (2002). Do *Arabidopsis halleri* from nonmetallicolous populations accumulate zinc and cadmium more effectively than those from metallicolous populations? *New Phytol.*, **155**, 47–57.
- Bert, V., Macnair, M. R., de Laguerie, P., Saumitou-Laprade, P., and Petit, D. (2000). Zinc tolerance and accumulation in metallicolous and nonmetallicolous populations of *Arabidopsis halleri* (Brassicaceae). *New Phytol.*, **146**, 225–233.
- Böhm, S., Frishman, D., and Mewes, H. W. (1997). Variations of the C2H2 zinc finger motif in the yeast genome and classification of yeast zinc finger proteins. *Nucleic Acids Res.*, **25**, 2464–2469.
- Birnbaum, K., Shasha, D. E., Wang, J. Y., Jung, J. W., Lambert, G. M., Galbraith, D. W., and Benfey, P. N. (2003). A gene expression map of the *Arabidopsis* root. *Science*, **302**, 1956–1960.
- Blaudez, D., Kohler, A., Martin, F., Sanders, D., and Chalot, M. (2003). Poplar metal tolerance protein 1 confers zinc tolerance and is an oligomeric vacuolar zinc transporter with an essential leucine zipper motif. *Plant Cell*, **15**, 2911–2928.
- Bloss, T., Clemens, S., and Nies, D. H. (2002). Characterization of the ZAT1p zinc transporter from *Arabidopsis thaliana* in microbial model organisms and reconstituted proteoliposomes. *Planta*, **214**, 783–791.
- Boivin, K., Acarkan, A., Mbulu, R.-S., Clarenz, O., and Schmidt, R. (2004). The *Arabidopsis* genome sequence as a tool for genome analysis in Brassicaceae. A comparison of the *Arabidopsis* and *Capsella rubella* genomes. *Plant Physiol.*, **135**, 735–744.
- Bonza, M. C., Morandini, P., Luoni, L., Geisler, M., Palmgren, M. G., and de Michelis, M. I. (2000). At-ACA8 encodes a plasma membrane-localized calcium-ATPase of *Arabidopsis* with a calmodulin-binding domain at the N-terminus. *Plant Physiol.*, **123**, 1495–1506.
- Bouzayen, M., Felix, G., Latché, A., Pech, J.-C., and Boller, T. (1991). Iron: an essential cofactor for the conversion of 1-aminocyclopropane-1-carboxylic acid to ethylene. *Planta*, **184**, 244–247.
- Bradford, M. M. (1976). A rapid and sensitive method for the quantitation of microgram quantities of protein utilizing the principle of protein-dye binding. *Anal. Biochem.*, **72**, 248–254.
- Brenner, S., Johnson, M., Bridgham, J., Golda, G., Lloyd, D. H., Johnson, D., Luo, S., McCurdy, S., Foy, M., Ewan, M., Roth, R., George, D., Eletr, S., Albrecht, G., Vermaas, E., Williams, S. R., Moon, K., Burcham, T., Pallas, M., DuBridges, R. B., Kirchner, J., Fearon, K., i Mao, J., and Corcoran, K. (2000). Gene expression analysis by massively parallel signature sequencing (MPSS) on microbead arrays. *Nat. Biotechnol.*, **18**, 630–634.
- Brooks, R. R. (1998). Geobotany and hyperaccumulators. In R. R. Brooks, ed., *Plants that hyperaccumulate heavy metals* (Wallingford, UK: CAB International), 55–94.
- Brune, A., Urbach, W., and Dietz, K. J. (1995). Differential toxicity of heavy metals is partly related to a loss of preferential extraplasmic compartmentation: a comparison of Cd-, Mo-, Ni- and Zn-stress. *New Phytol.*, **129**, 403–409.

- Bull, P. C. and Cox, D. W.** (1994). Wilson disease and Menkes disease: new handles on heavy-metal transport. *Trends Genet.*, **10**, 246–252.
- Bull, P. C., Thomas, G. R., Rommens, J. M., Forbes, J. R., and Cox, D. W.** (1993). The Wilson disease gene is a putative copper transporting P-type ATPase similar to the Menkes gene. *Nat. Genet.*, **5**, 327–337.
- Burrman, E. T., Kim, K. T., and Epstein, W.** (1995). Genetic evidence for two sequentially occupied K⁺ binding sites in the Kdp transport ATPase. *J. Biol. Chem.*, **270**, 6678–685.
- Busch, M. A., Bomblies, K., and Weigel, D.** (1999). Activation of a floral homeotic gene in *Arabidopsis*. *Science*, **285**, 585–587.
- Callahan, D. L., Baker, A. J. M., Kolev, S. D., and Wedd, A. G.** (2006). Metal ion ligands in hyperaccumulating plants. *J. Biol. Inorg. Chem.*, **11**, 2–12.
- Camakaris, J., Voskoboinik, I., and Mercer, J. F.** (1999). Molecular mechanisms of copper homeostasis. *Biochem. Biophys. Res. Commun.*, **261**, 225–232.
- Carey, K. D., Watson, R. T., Pessin, J. E., and Stork, P. J. S.** (2003). The requirement of specific membrane domains for Raf-1 phosphorylation and activation. *J. Biol. Chem.*, **278**, 3185–3196.
- Cech, T., Zaug, A., and Grabowski, P.** (1981). *In vitro* splicing of the ribosomal RNA precursors of *Tetrahymena*: involvement of a guanosine nucleotide in the excision of the intervening sequence. *Cell*, **27**, 487–496.
- Chardonens, Koevoets, van Zanten A, Schat, and Verkleij** (1999). Properties of enhanced tonoplast zinc transport in naturally selected zinc-tolerant *Silene vulgaris*. *Plant Physiol.*, **120**, 779–786.
- Chateau, S., Sangwan, R. S., and Sangwan-Norreel, B. S.** (2000). Competence of *Arabidopsis thaliana* genotypes and mutants of *Agrobacterium tumefaciens*-mediated gene transfer: role of phytohormones. *J. Exp. Biol.*, **51**, 1961–1968.
- Chelly, J., Tumer, Z., Tønnesen, T., Petterson, A., Ishikawa Brush, Y., Tommerup, N., Horn, N., and Monaco, A. P.** (1993). Isolation of a candidate gene for Menkes disease that encodes a potential heavy metal binding protein. *Nat. Genet.*, **3**, 14–19.
- Chenna, R., Sugawara, H., Koike, T., Lopez, R., J.Gibson, T., Higgins, D. G., and Thompson, J. D.** (2003). Multiple sequence alignments with the Clustal series of programs. *Nucleic Acids Res.*, **31**, 3497–3500.
- Christen, H. R.** (1988). *Grundlagen der allgemeinen und anorganischen Chemie*. 9th edition (Frankfurt am Main, Germany: Otto Salle Verlag).
- Chvapil, M.** (1973). New aspects in the biological role of zinc: a stabilizer of macromolecules and biological membranes. *Life Sci.*, **13**, 1041–1049.
- Clarke, N. D. and Berg, J. M.** (1998). Zinc fingers in *Caenorhabditis elegans*: finding families and probing pathways. *Science*, **282**, 2018–2022.
- Clemens, S.** (2001). Molecular mechanisms of plant metal tolerance and homeostasis. *Planta*, **212**, 475–486.
- Clemens, S., Bloss, T., Vess, C., Neumann, D., Nies, D. H., and Nieden, U. Z.** (2002a). A transporter in the endoplasmic reticulum of *Schizosaccharomyces pombe* cells mediates zinc storage and differentially affects transition metal tolerance. *J. Biol. Chem.*, **277**, 18215–18221.

- Clemens, S., Kim, E. J., Neumann, D., and Schroeder, J. I. (1999). Tolerance to toxic metals by a gene family of phytochelatin synthases from plants and yeast. *EMBO J.*, **18**, 3325–3333.
- Clemens, S., Palmgren, M. G., and Krämer, U. (2002b). A long way ahead: understanding and engineering plant metal accumulation. *Trends Plant Sci.*, **7**, 309–315.
- CLONTECH Laboratories, Inc. (1999). Living Colors® User Manual. CLONTECH Laboratories, Inc.
- Clough, S. J. and Bent, A. F. (1998). Floral dip: a simplified method for *Agrobacterium*-mediated transformation of *Arabidopsis thaliana*. *Plant J.*, **16**, 735–743.
- Cobbett, C. and Goldsbrough, P. (2002). Phytochelatins and metallothioneins: roles in heavy metal detoxification and homeostasis. *Annu. Rev. Plant Biol.*, **53**, 159–182.
- Cobbett, C. S. (2000). Phytochelatins and their roles in heavy metal detoxification. *Plant Physiol.*, **123**, 825–832.
- Cobbett, C. S., Hussain, D., and Haydon, M. J. (2003). Structural and functional relationships between type 1B heavy metal-transporting P-type ATPases in *Arabidopsis*. *New Phytol.*, **159**, 315–321.
- Colangelo, E. P. and Guerinot, M. L. (2004). The essential basic helix-loop-helix protein FIT1 is required for the iron deficiency response. *Plant Cell*, **16**, 3400–3412.
- Coleman, J. E. (1998). Zinc enzymes. *Curr. Opin. Chem. Biol.*, **2**, 222–234.
- Conklin, D. S., McMAster, J. A., Culbertson, M. R., and Kung, C. (1992). *COT1*, a gene involved in cobalt accumulation in *Saccharomyces cerevisiae*. *Mol. Biol. Cell*, **12**, 3678–3688.
- CPEP (2003). Nuclear Science - A Guide to the Nuclear Science Wall Chart, chapter 10: Origin of the Elements (Contemporary Physics Education Project (CPEP)), 10.1–10.4.
- Cramer, A., Whitehorn, E. A., Tate, E., and Stemmer, W. P. C. (1996). Improved green fluorescent protein by molecular evolution using DNA shuffling. *Nat. Biotechnol.*, **14**, 315–319.
- Cronin, S. R., Rao, R., and Hampton, R. Y. (2002). Cod1p/Spf1p is a P-type ATPase involved in ER function and Ca²⁺ homeostasis. *J. Cell Biol.*, **157**, 1017–1028.
- Curie, C. and Briat, J.-F. (2003). Iron transport and signaling in plants. *Annu. Rev. Plant Biol.*, **54**, 183–206.
- Curie, C., Panaviene, Z., Loulergue, C., Dellaporta, S. L., Briat, J. F., and Walker, E. L. (2001). Maize yellow stripe1 encodes a membrane protein directly involved in Fe(III) uptake. *Nature*, **409**, 346–349.
- Curtis, M. D. and Grossniklaus, U. (2003). A gateway cloning vector set for high-throughput functional analysis of genes in planta. *Plant Physiol.*, **133**, 462–469.
- Czaja, M. J., Weiner, F. R., and Freedman, J. H. (1991). Amplification of the metallothionein-1 and metallothionein-2 genes in copper-resistant hepatoma cells. *J. Cell. Physiol.*, **147**, 434–438.
- Dahmani-Muller, H., van Oort, F., Gélie, B., and Balabane, M. (2000). Strategies of heavy metal uptake by three plant species growing near a metal smelter. *Environ. Pollut.*, **109**, 1–8.
- Daleke, D. L. (2003). Regulation of transbilayer plasma membrane phospholipid asymmetry. *J. Lipid Res.*, **44**, 233–242.

- Danks, D. M. (1989). The metabolic basis of inherited diseases, chapter Disorders of copper transport (McGraw-Hill), 1251–1268.
- Davies, K. (1993). Cloning the Menkes disease gene. *Nat. Genet.*, **361**, 98.
- de Meis, L. and Vianna, A. (1979). Energy Interconversion by the Ca^{2+} -dependent ATPase of the sarcoplasmic reticulum. *Annu. Rev. Biochem.*, **48**, 275–292.
- Decottignies, A. and Goffeau, A. (1997). Complete inventory of the yeast ABC proteins. *Nat. Genet.*, **15**, 137–45.
- Delhaize, E., Kataoka, T., Hebb, D. M., White, R. G., and Ryan, P. R. (2003). Genes encoding proteins of the cation diffusion facilitator family that confer manganese tolerance. *Plant Cell*, **15**, 1131–1142.
- Delhaize, E. and Ryan, P. R. (1995). Aluminium toxicity and tolerance in plants. *Plant Physiol.*, **107**, 315–321.
- Desbrosses-Fonrouge, A.-G., Voigt, K., Schröder, A., Arrivault, S., Thomine, S., and Krämer, U. (2005). *Arabidopsis thaliana* MTP1 is a Zn transporter in the vacuolar membrane which mediates Zn detoxification and drives leaf Zn accumulation. *FEBS Lett.*, **579**, 4165–4174.
- DeWitt, N. D., Hong, B., Sussman, M. R., and Harper, J. F. (1996). Targeting of two *Arabidopsis* H^{+} -ATPase isoforms to the plasma membrane. *Plant Physiol.*, **112**, 833–844.
- Deyholos, M. K. and Sieburth, L. E. (2000). Separable whorl-specific expression and negative regulation by enhancer elements within the *AGAMOUS* second intron. *Plant Cell*, **12**, 1799–1810.
- Dohmen, R. J., Strasser, A. W., Honer, C. B., and Hollenberg, C. (1991). An efficient transformation procedure enabling long-term storage of competent cells of various yeast genera. *Yeast*, **7**, 691–692.
- Dougherty, M. K. and Morrison, D. K. (2004). Unlocking the code of 14-3-3. *J. Cell Sci.*, **117**, 1875–1884.
- Dräger, D. B., Desbrosses-Fonrouge, A.-G., Krach, C., Chardonens, A. N., Meyer, R. C., Saumitou-Laprade, P., and Krämer, U. (2004). Two genes encoding *Arabidopsis halleri* MTP1 metal transport proteins co-segregate with zinc tolerance and account for high MTP1 transcript levels. *Plant J.*, **39**, 425–439.
- Dräger, D. B., Voigt, K., and Krämer, U. (2005). Short transcript-derived fragments from the metal hyperaccumulator model species *Arabidopsis halleri*. *Z. Naturforsch [C]*, **60c**, 172–178.
- Dufour, J. P. and Goffeau, A. (1978). Solubilization by lysolecithin and purification of the plasma membrane ATPase of the yeast *Schizosaccharomyces pombe*. *J. Biol. Chem.*, **253**, 7026–7032.
- Durnam, D. M. and Palmiter, R. D. (1987). Analysis of detoxification of heavy metal ions by mouse metallothionein. *Experientia Suppl.*, **52**, 457–463.
- Eide, D., Broderius, M., Fett, J., and Guerinot, M. L. (1996). A novel iron-regulated metal transporter from plants identified by functional expression in yeast. *Proc. Natl. Acad. Sci. U. S. A.*, **93**, 5624–5628.
- Eide, D. J. (1998). The molecular biology of metal ion transport in *Saccharomyces cerevisiae*. *Annu. Rev. Nutr.*, **18**, 441–469.

- Elbaz, B., Shoshani-Knaani, N., David-Assael, O., Mizrachy-Dagri, T., Mizrahi, K., Saul, H., Brook, E., Berezin, I., and Shaul, O. (2006). High expression in leaves of the zinc hyperaccumulator *Arabidopsis halleri* of *AhMHX*, a homolog of an *Arabidopsis thaliana* vacuolar metal/proton exchanger. *Plant Cell Environ.*, **29**, 1179–1190.
- Elzenga, J. T. (1991). Patch clamping protoplast from vascular plants. *Plant Physiol.*, **97**, 1573–1575.
- Eren, E. and Argüello, J. M. (2004). *Arabidopsis* HMA2, a divalent heavy metal-transporting P(1B)-type ATPase, is involved in cytoplasmic Zn²⁺ homeostasis. *Plant Physiol.*, **136**, 3712–3723.
- Ernst, K., Kumar, A., Kriseleit, D., Kloos, D. U., Phillips, M. S., and Ganai, M. (2002). The broad-spectrum potato cyst nematode resistance gene (*Hero*) from tomato is the only member of a large gene family of *NBS-LRR* genes with an unusual amino acid repeat in the LRR region. *Plant J.*, **31**, 127–136.
- Ernst, W. (1968). Zur Kenntnis der Soziologie und Ökologie der Schwermetallvegetation Großbritanniens. *Bericht der Deutschen Botanischen Gesellschaft*, **81**, 116–124.
- Finney, L. A. and O'Halloran, T. V. (2003). Transition metal speciation in the cell: insights from the chemistry of metal ion receptors. *Science*, **300**, 931–936.
- Fogel, S., Welch, J., and Karin, G. C. M. (1983). Gene amplification in yeast: *CUP1* copy number regulates copper resistance. *Curr. Gen.*, **7**, 347–355.
- Fox, T. C. and Guerinot, M. L. (1998). Molecular biology of cation transport in plants. *Annu. Rev. Plant Physiol. Plant Mol. Biol.*, **49**, 669–696.
- Fraser, C. M., Casjens, S., Huang, W. M., Sutton, G. G., Clayton, R., Lathigra, R., White, O., Ketchum, K. A., Dodson, R., Hickey, E. K., Gwinn, M., Dougherty, B., Tomb, J.-F., Fleischmann, R. D., Richardson, D., Peterson, J., Kerlavage, A. R., Quackenbush, J., Salzberg, S., Hanson, M., van Vugt, R., Palmer, N., Adams, M. D., Gocayne, J., Weidman, J., Utterback, T., Wathley, L., McDonald, L., Artiach, P., Bowman, C., Garland, S., Fujii, C., Cotton, M. D., Horst, K., Roberts, K., Hatch, B., Smith, H. O., and Venter, J. C. (1997). Genomic sequence of a Lyme disease spirochaete, *Borrelia burgdorferi*. *Nature*, **390**, 580–586.
- Freemont, P. S. (1993). The ring finger. a novel protein sequence motif related to the zinc finger. *Ann. N. Y. Acad. Sci.*, **684**, 174–192.
- Freitag, M., Hickey, P. C., Raju, N. B., Selker, E. U., and Read, N. D. (2004). GFP as a tool to analyze the organization, dynamics and function of nuclei and microtubules in *Neurospora crassa*. *Fungal Genet. Biol.*, **41**, 897–910.
- Fuglsang, A. T., Borch, J., Bych, K., Jahn, T. P., Roepstorff, P., and Palmgren, M. G. (2003). The binding site for regulatory 14-3-3 protein in plant plasma membrane H⁺-ATPase: involvement of a region promoting phosphorylation-independent interaction in addition to the phosphorylation-dependent C-terminal end. *J. Biol. Chem.*, **278**, 42266–42272.
- Fuglsang, A. T., Visconti, S., Drumm, K., Jahn, T., Stensballe, A., Mattei, B., Jensen, O. N., Aducci, P., and Palmgren, M. G. (1999). Binding of 14-3-3 protein to the plasma membrane H⁺-ATPase AHA2 involves the three C-terminal residues Tyr(946)-Thr-Val and requires phosphorylation of Thr(947). *J. Biol. Chem.*, **274**, 36774–36780.
- Gaedeke, N., Klein, M., Kolukisaoglu, U., Forestier, C., Muller, A., Ansorge, M., Becker, D., Mamnun, Y., Kuchler, K., Schulz, B., Müller-Röber, B., and Martinoia, E. (2001). The *Arabidopsis thaliana* ABC transporter *AtMRP5* controls root development and stomata movement. *EMBO J.*, **20**, 1875–1887.

- Gaither, L. A. and Eide, D. J. (2001). Eukaryotic zinc transporters and their regulation. *BioMetals*, **14**, 251–270.
- Geisler, M., Axelsen, K. B., Harper, J. F., and Palmgren, M. G. (2000). Molecular aspects of higher plant P-type Ca^{2+} -ATPases. *Biochim. Biophys. Acta*, **1465**, 52–78.
- Geisler, M., Frangne, N., Gomes, E., Martinoia, E., and Palmgren, M. G. (2002). The *ACA4* gene of *Arabidopsis* encodes a vacuolar membrane calcium pump that improves salt tolerance in yeast. *Plant Physiol.*, **124**, 1814–1827.
- Gerencser, G. A. (1996). The chloride pump: a Cl^- -translocating P-type ATPase. *Crit. Rev. Biochem. Mol. Biol.*, **31**, 303–337.
- Gerencser, G. A. and Purushotham, K. R. (1996). Reconstituted Cl^- pump protein: a novel ion (Cl^-)-motive ATPase. *J. Bioenerg. Biomembr.*, **28**, 459–469.
- Gilbert, W. (1986). The RNA world. *Nature*, **319**, 618.
- Gitan, R. S. and Eide, D. J. (2000). Zinc-regulated ubiquitin conjugation signals endocytosis of the yeast ZRT1 zinc transporter. *Biochem. J.*, **346** (Pt 2), 329–336.
- Gitan, R. S., Luo, H., Rodgers, J., Broderius, M., and Eide, D. (1998). Zinc-induced inactivation of the yeast ZRT1 zinc transporter occurs through endocytosis and vacuolar degradation. *J. Biol. Chem.*, **273**, 28617–28624.
- Glerum, D. M., Shtanko, A., and Tzagoloff, A. (1996). Characterization of *COX17*: a gene involved in copper metabolism and assembly of cytochrome oxidase. *J. Biol. Chem.*, **271**, 14504–14509.
- Goldstein, A. L. and McCusker, J. H. (1999). Three new dominant drug resistance cassettes for gene disruption in *Saccharomyces cerevisiae*. *Yeast*, **15**, 1541–1553.
- Gomes, E., Jakobsen, M. K., Axelsen, K. B., Geisler, M., and Palmgren, M. G. (2000). Chilling tolerance in *Arabidopsis* involves ALA1, a member of a new family of putative aminophospholipid translocases. *Plant Cell*, **12**, 2441–2454.
- Graniti, A. (1962). Azione fitotossica di *Fusicoccum amygdali* Del. su mandorlo *Prunus amygdali* St. *Phytopatol. Mediterr.*, **1**, 182–185.
- Gravot, A., Lieutaud, A., Verret, F., Auroy, P., Vavasseur, A., and Richaud, P. (2004). *AtHMA3*, a plant P1B-ATPase, functions as a Cd/Pb transporter in yeast. *FEBS Lett.*, **561**, 22–28.
- Grill, E., Löffler, S., Winnacker, E.-L., and Zenk, M. (1989). Phytochelatins, the heavymetal-binding peptides of plants, are synthesized from glutathione by a specific γ -glutamylcysteine dipeptidyl transpeptidase (phytochelatin synthase). *Proc. Natl. Acad. Sci. U. S. A.*, **86**, 6838–6842.
- Grill, E., Winnacker, E. L., and Zenk, M. H. (1985). Phytochelatins, the principle heavy-metal binding peptides of higher plants. *Science*, **230**, 674–676.
- Grill, E. and Zenk, M. H. (1989). Wie schützen sich Pflanzen vor toxischen Schwermetallen? *Chemie in unserer Zeit*, **23**, 193–199.
- Grosshans, C. A. and Cech, T. R. (1989). Metal ion requirements for sequence-specific endoribonuclease activity of the *Tetrahymena* ribozyme. *Biochemistry*, **25**, 6888–6894.
- Grotz, N., Fox, T., Connolly, E., Park, W., Guerinot, M. L., and Eide, D. (1998). Identification of a family of zinc transporter genes from *Arabidopsis* that respond to zinc deficiency. *Proc. Natl. Acad. Sci. U. S. A.*, **95**, 7220–7224.

- Guerinot, M. L. (2000). The ZIP family of metal transporters. *Biochim. Biophys. Acta*, **1465**, 190–198.
- Guerrier-Takada, C., Gardiner, K., Marsh, T., Pace, N., and Altman, S. (1983). The RNA moiety of ribonuclease P is the catalytic subunit of the enzyme. *Cell*, **35**, 849–857.
- Hall, J. L. and Williams, L. E. (2003). Transition metal transporters in plants. *J. Exp. Bot.*, **54**, 2601–2613.
- Hall, L., Sánchez, R., and Holloway, S. (2000). X-ray crystallographic and analytical ultracentrifugation analyses of truncated and full-length yeast copper chaperone from SOD (LYS7): a dimer-dimer model of LYS7-SOD association and copper delivery. *Biochemistry*, **39**, 3611–3623.
- Hammond, J. P., Bowen, H. C., White, P. J., Mills, V., Pyle, K. A., Baker, A. J. M., Whiting, S. N., May, S. T., and Broadley, M. R. (2006). A comparison of the *Thlaspi caerulescens* and *Thlaspi arvense* shoot transcriptomes. *New Phytol.*, **170**, 239–260.
- Haney, C. J., Grass, G., Franke, S., and Rensing, C. (2005). New developments in the understanding of the cation diffusion facilitator family. *J. Ind. Microbiol. Biotechnol.*, **32**, 215–226.
- Harashima, T. and Heitman, J. (2005). Galpha subunit gpa2 recruits kelch repeat subunits that inhibit receptor-g protein coupling during camp-induced dimorphic transitions in *saccharomyces cerevisiae*. *Mol. Biol. Cell*, **16**, 4557–4571.
- Harper, J. F. (2001). Dissecting calcium oscillators in plant cells. *Trends Plant Sci.*, **6**, 395–397.
- Harper, J. F., Hong, B., Hwang, I., Guo, H. W., Stoddard, R., Huang, J. F., Palmgren, M. G., and Sze, H. (1998). A novel calmodulin-regulated Ca²⁺-ATPase (ACA2) from *Arabidopsis* with an N-terminal autoinhibitory domain. *J. Biol. Chem.*, **273**, 1099–1106.
- Hasselbach, W. and Makinose, M. (1961). Die Calciumpumpe der Erschlaffungsgrana des Muskels und ihre Abhängigkeit von der ATP-Spaltung. *Eur. J. Biochem.*, **333**, 518–528.
- Heim, R., Prasher, D. C., and Tsien, R. (1994). Wavelength mutations and posttranslational autooxidation of green fluorescent protein. *Proc. Natl. Acad. Sci. U. S. A.*, **91**, 12501–12504.
- Hellens, R. P., Edwards, E. A., Leyland, N. R., Bean, S., and Mullineaux, P. (2000). pGreen: a versatile and flexible binary Ti vector for *Agrobacterium*-mediated plant transformation. *Plant Mol. Biol.*, **42**, 819–832.
- Henriques, R., Jasik, J., Klein, M., Martinoia, E., Feller, U., Schell, J., Pais, M. S., and Koncz, C. (2002). Knock-out of *Arabidopsis* metal transporter gene *IRT1* results in iron deficiency accompanied by cell differentiation defects. *Plant Mol. Biol.*, **50**, 587–597.
- Hertogh, B. D., Lantin, A.-C., Baret, P. V., and Goffeau, A. (2004). The archaeal P-type ATPases. *J. Bioenerg. Biomembr.*, **36**, 135–142.
- Heynhold, G. (1842). *Clav. Gen. Fl. Sachsen*, volume 1, chapter *Arabidopsis thaliana* (L.) (Dresden: Verlag von Justus Naumann), 538.
- Higgins, C. (1992). ABC transporters: from microorganisms to man. *Annu. Rev. Cell. Biol.*, **8**, 67–113.
- Higuchi, K., Suzuki, K., Nakanishi, H., Yamaguchi, H., Nishizawa, N., and Mori, S. (1999). Cloning of nicotianamine synthase genes, novel genes involved in the biosynthesis of phyto siderophores. *Plant Physiol.*, **119**, 471–480.

- Himelblau, E., Mira, H., Lin, S.-J., Culotta, V. C., Peñarrubia, L., and Amasino, R. M. (1998). Identification of a functional homolog of the yeast copper-binding gene *ATX* from *Arabidopsis thaliana*. *Plant Physiol.*, **117**, 1227–1234.
- Hiraga, S., Jaffé, A., Ogura, H. M., and Takahashi, H. (1986). F plasmid *ccd* mechanism in *Escherichia coli*. *J. Bacteriol.*, **166**, 100–104.
- Hirayama, T. and Alonso, J. M. (2000). Ethylene captures a metal! Metal ions are involved in ethylene perception and signal transduction. *Plant Cell Physiol.*, **41**, 548–555.
- Hoagland, D. R. and Arnon, D. I. (1938). The water-culture method for growing plants without soil. *Univ. Calif. Agri. Exp. Stn. Cir.*, **347**, 1–32.
- Hobbs, S. L., Warkentin, T. D., and DeLong, C. M. (1993). Transgene copy number can be positively or negatively associated with transgene expression. *Plant Mol. Biol.*, **21**, 17–26.
- Holland, I. B. (2003). *ABC proteins: From Bacteria to Man* (London: Academic Press).
- Hong, B., Ichida, A., Wang, Y., Gens, J. S., Pickard, B. G., and Harper, J. F. (1999). Identification of a calmodulin-regulated Ca^{2+} -ATPase in the endoplasmic reticulum. *Plant Physiol.*, **119**, 1165–1175.
- Hong, R. L., Hamaguchi, L., Busch, M. A., and Weigel, D. (2003). Regulatory elements of the floral homeotic gene *AGAMOUS* identified by phylogenetic footprinting and shadowing. *Plant Cell*, **15**, 1296–1309.
- Horton, H. R., Moran, L. A., Ochs, R. S., Rawn, J. D., and Gray-Scrimgeour, K. (2002). *Principles of Biochemistry*. 3rd edition (Upper Saddle River, NJ, USA: Prentice-Hall/Pearson Education).
- Howden, R., Andersen, C. R., Goldsbrough, P. B., and Cobbett, C. S. (1995a). A cadmium-sensitive, glutathione-deficient mutant of *Arabidopsis thaliana*. *Plant Physiol.*, **107**, 1067–1073.
- Howden, R., Goldsbrough, P. B., Andersen, C. R., and Cobbett, C. S. (1995b). Cadmium-sensitive, *cad1* mutants of *Arabidopsis thaliana* are phytochelatin deficient. *Plant Physiol.*, **107**, 1059–1066.
- Hulo, N., Bairoch, A., Bulliard, V., Cerutti, L., Castro, E. D., Langendijk-Genevaux, P. S., Pagni, M., and Sigrist, C. J. A. (2006). The PROSITE database. *Nucleic Acids Res.*, **34**, D227–D230.
- Hunt, A. G. (1994). Messenger RNA 3' end formation in plants. *Annu. Rev. Plant Physiol. Plant Mol. Biol.*, **45**, 47–60.
- Hussain, D., Haydon, M. J., Wang, Y., Wong, E., Sherson, S. M., Young, J., Camakaris, J., Harper, J. F., and Cobbett, C. S. (2004). P-type ATPase heavy metal transporters with roles in essential zinc homeostasis in *Arabidopsis*. *Plant Cell*, **16**, 1327–1339.
- Invitrogen (2006). pENTRTM directional TOPO[®] cloning kits. Invitrogen, Karlsruhe, Germany, Version G edition.
- Jaffé, A., Ogura, T., and Hiraga, S. (1985). Effects of the *ccd* function of the F plasmid on bacterial growth. *J. Bacteriol.*, **163**, 841–849.
- Jahn, T., Fuglsang, A. T., Olsson, A., Brüntrup, I. M., Collinge, D. B., Volkmann, D., Sommarin, M., Palmgren, M. G., and Larsson, C. (1997). The 14-3-3 protein interacts directly with the C-terminal region of the plant plasma membrane H^{+} -ATPase. *Plant Cell*, **9**, 1805–1814.

- Jefferson, R. A., Kavanagh, T. A., and Bevan, M. W. (1987). GUS fusions: β -glucuronidase as a sensitive and versatile gene fusion marker in higher plants. *EMBO J.*, **6**, 3901–3907.
- Jeong, Y.-M., Mun, J.-H., Lee, I., Woo, J. C., Hong, C. B., and Kim, S.-G. (2006). Distinct roles of the first introns on the expression of Arabidopsis profilin gene family members. *Plant Physiol.*, **140**, 196–209.
- Jiang, R. F., Ma, D. Y., Zhao, F. J., and McGrath, S. P. (2005). Cadmium hyperaccumulation protects *Thlaspi caerulescens* from leaf feeding damage by thrips (*Frankliniella occidentalis*). *New Phytol.*, **167**, 805–814.
- Jirakulaporn, T. and Muslin, A. J. (2004). Cation diffusion facilitator proteins modulate Raf-1 activity. *J. Biol. Chem.*, **279**, 27807–27815.
- Jones, D. A., Thomas, C. M., Hammond-Kosack, K. E., Balint-Kurti, P. J., and Jones, J. D. (1994). Isolation of the tomato *Cf-9* gene for resistance to *Cladosporium fulvum* by transposon tagging. *Science*, **266**, 789–93.
- Jones-Rhoades, M. W., Bartel, D. P., and Bartel, B. (2006). MicroRNAs and their regulatory roles in plants. *Annu. Rev. Plant Biol.*, **57**, 19–53.
- Jorgensen, P., Hakansson, K., and Karlsh, S. (2003). Structure and mechanism of Na,K-ATPase: functional sites and their interactions. *Annu. Rev. Physiol.*, **65**, 817–849.
- Jorgensen, R. A., Cluster, P. D., English, J., Que, Q., and Napoli, C. A. (1996). Chalcone synthase cosuppression phenotypes in petunia flowers: comparison of sense vs. antisense constructs and single-copy vs. complex t-dna sequences. *Plant Mol. Biol.*, **31**, 957–973.
- Kamizono, A., Nishizawa, M., Teranishi, Y., Murata, K., and Kimura, A. (1989). Identification of a gene conferring resistance to zinc and cadmium ions in the yeast *Saccharomyces cerevisiae*. *Mol. Gen. Genet.*, **219**, 161–167.
- Kaplan, J. H. (2002). Biochemistry of Na,K-ATPase. *Annu. Rev. Biochem.*, **71**, 511–535.
- Karimi, M., Inze, D., and Depicker, A. (2002). GATEWAY vectors for *Agrobacterium*-mediated plant transformation. *Trends Plant Sci.*, **7**, 193–195.
- Keilin, D. and Mann, T. (1940). Carbonic anhydrase. Purification and nature of the enzyme. *Biochem. J.*, **34**, 1163–1176.
- Kim, S., Takahashi, M., Higuchi, K., Tsunoda, K., Nakanishi, H., Yoshimura, E., Mori, S., and Nishizawa, N. K. (2005). Increased nicotianamine biosynthesis confers enhanced tolerance of high levels of metals, in particular nickel, to plants. *Plant Cell Physiol.*, **46**, 1809–1818.
- Kobae, Y., Uemura, T., Sato, M. H., Ohnishi, M., Mimura, T., Nakagawa, T., and Maeshima, M. (2004). Zinc transporter of *Arabidopsis thaliana* AtMTP1 is localized to vacuolar membranes and implicated in zinc homeostasis. *Plant Cell Physiol.*, **45**, 1749–1758.
- Kobayashi, T., Nakayama, Y., Itai, R. N., Nakanishi, H., Yoshihara, T., Mori, S., and Nishizawa, N. K. (2003). Identification of novel cis-acting elements, IDE1 and IDE2, of the barley *IDS2* gene promoter conferring iron-deficiency-inducible, root-specific expression in heterogeneous tobacco plants. *Plant J.*, **36**, 780–793.
- Koch, M., Bishop, J., and Mitchell-Olds, T. (1999). Molecular systematics and evolution of *Arabidopsis* and *Arabis*. *Plant Biol.*, **1**, 529–537.

- Koch, M., Haubold, B., and Mitchell-Olds, T. (2001). Molecular systematics of the Brassicaceae: Evidence from coding plastidic matK and nuclear Chs sequences. *Am. J. Bot.*, **88**, 534–544.
- Kochian, L. V. (1993). Zinc in soils and plants, chapter Zinc absorption from hydroponic solutions by plant roots. (Boston/ Dordrecht: Kluwer), 45–57.
- Koike, S., Inoue, H., Mizuno, D., Takahashi, M., Nakanishi, H., Mori, S., and Nishizawa, N. K. (2004). OsYSL2 is a rice metal-nicotianamine transporter that is regulated by iron and expressed in the phloem. *Plant J.*, **39**, 415–24.
- Kondrashov, F. A., Rogozin, I. B., Wolf, Y. I., and Koonin, E. V. (2002). Selection in the evolution of gene duplications. *Genome Biol.*, **3**, 1–9.
- Korshunova, Y. O., Eide, D., Clark, W. G., Guerinot, M. L., and Pakrasi, H. B. (1999). The IRT1 protein from *Arabidopsis thaliana* is a metal transporter with a broad substrate range. *Plant Mol. Biol.*, **40**, 37–44.
- Küpper, H., Lombi, E., Zhao, F. J., and McGrath, S. P. (2000). Cellular compartmentation of cadmium and zinc in relation to other elements in the hyperaccumulator *Arabidopsis halleri*. *Planta*, **212**, 75–84.
- Küpper, H., Zhao, F. J., and McGrath, S. P. (1999). Cellular compartmentation of zinc in leaves of the hyperaccumulator *Thlaspi caerulescens*. *Plant Physiol.*, **119**, 305–312.
- Krishna, S. S., Majumdar, I., and Grishin, N. V. (2003). Structural classification of zinc fingers: survey and summary. *Nucleic Acids Res.*, **31**, 532–550.
- Krämer, U. (2005a). MTP1 mops up excess zinc in Arabidopsis cells. *Trends Plant Sci.*, **10**, 313–315.
- Krämer, U. (2005b). Phytoremediation: novel approaches to cleaning up polluted soils. *Curr. Opin. Biotechnol.*, **16**, 133–141.
- Krämer, U. and Clemens, S. (2005). Functions and homeostasis of zinc, copper, and nickel in plants. *Top. Curr. Gen.*, **14**, 215–271.
- Krämer, U., Cotter-Howells, J. D., Charnock, J. M., Baker, A. J. M., and Smith, J. A. C. (1996). Free histidine as a metal chelator in plants that accumulate nickel. *Nature*, **379**, 635–638.
- Kruger, K. (1982). Self-splicing RNA: autoexcision and autocyclization of the ribosomal RNA intervening sequence of *Tetrahymena*. *Cell*, **31**, 147–157.
- Kühlbrandt, W. (2004). Biology, structure and mechanism of P-type ATPases. *Nat. Rev. Mol. Cell Biol.*, **5**, 282–295.
- Kuittinen, H., de Haan, A. A., Vogl, C., Oikarinen, S., Leppala, J., Koch, M., Mitchell-Olds, T., Langley, C., and Savolainen, O. (2004). Comparing the linkage maps of the close relatives *Aabidopsis lyrata* and *Arabidopsis thaliana*. *Genetics*, **168**, 1575–1584.
- Kumar, S., Tamura, K., and Nei, M. (2004). MEGA3: Integrated software for Molecular Evolutionary Genetics Analysis and sequence alignment. *Brief. Bioinform.*, **5**, 150–163.
- Landy, A. (1989). Dynamic, structural, and regulatory aspects of λ site-specific recombination. *Annu. Rev. Biochem.*, **58**, 913–049.
- Lane, T. W., Saito, M. A., George, G. N., Pickering, I. J., Prince, R. C., and Morel, F. M. M. (2005). Biochemistry: a cadmium enzyme from a marine diatom. *Nature*, **435**, 42.

- Lane, W. T. and Morel, F. M. M. (2000). A biological function for cadmium in marine diatoms. *Proc. Natl. Acad. Sci. U. S. A.*, **97**, 4627–4631.
- Lanquar, V., Lelièvre, F., Bolte, S., Hamès, C., Alcon, C., Neumann, D., Vansuyt, G., Curie, C., Schröder, A., Krämer, U., Barbier-Brygoo, H., and Thomine, S. (2005). Mobilization of vacuolar iron by *AtNRAMP3* and *AtNRAMP4* is essential for seed germination on low iron. *EMBO J.*, **24**, 4041–4051.
- Larsen, P., Degenhardt, J., Tai, C.-Y., Stenzler, L., Howell, S., and Kochian, L. (1998). Aluminum-resistant *Arabidopsis* mutants that exhibit altered patterns of aluminum accumulation and organic acid release from roots. *Plant Physiol.*, **117**, 9–17.
- Lasat, M. M., Pence, N. S., Garvin, D. F., Ebbs, S. D., and Kochian, L. V. (2000). Molecular physiology of zinc transport in the Zn hyperaccumulator *Thlaspi caerulescens*. *J. Exp. Bot.*, **51**, 71–79.
- Lee, A. G. (2002). A calcium pump made visible. *Curr. Opin. Struct. Biol.*, **12**, 547–554.
- Li, Q. Q. and Hunt, A. (1997). The polyadenylation of RNA in plants. *Plant Physiol.*, **115**, 321–325.
- Li, Z. S., Lu, Y. P., Zhen, R. G., Szczypka, M., Thiele, D. J., and Rea, P. A. (1997). A new pathway for vacuolar cadmium sequestration in *Saccharomyces cerevisiae*: YCF1-catalyzed transport of bis(glutathionato)cadmium. *Proc. Natl. Acad. Sci. U. S. A.*, **94**, 42–47.
- Li, Z.-S., Szczypka, M., Lu, Y.-P., Thiele, D. J., and Rea, P. A. (1996). The yeast cadmium factor protein (YCF1) is a vacuolar glutathione S-conjugate pump. *J. Biol. Chem.*, **271**, 6509–6517.
- Liao, M. T., Hedley, M. J., Woolley, D. J., Brooks, R. R., and Nichols, M. A. (2000). Copper uptake and translocation in chicory (*Cichorium intybus* L. cv Grasslands Puna) and tomato (*Lycopersicon esculentum* Mill. Cv Rondy) plants grown in NFT system: II. The role of nicotianamine and histidine in xylem sap copper transport. *Plant Soil*, **223**, 243–252.
- Life technologies (2000). GatewayTM cloning technology. Life technologies, Karlsruhe, Germany, Version 1 edition.
- Lima, L., Seabra, A., Cullimore, P., and Carvalho, H. (2006). Phosphorylation and subsequent interaction with 14-3-3 proteins regulate plastid glutamine synthetase in *Medicago trunculata*. *Planta*, **223**, 558–567.
- Lin, S. J. and Culotta, V. C. (1995). The *ATX1* gene of *Saccharomyces cerevisiae* encodes a small metal homeostasis factor that protects cells against reactive oxygen toxicity. *Proc. Natl. Acad. Sci. U. S. A.*, **92**, 3784–3788.
- Lin, S. J., Pufahl, R. A., Dancis, A., O'Halloran, T. V., and Culotta, V. C. (1997). A role for the *Saccharomyces ATX1* gene in copper trafficking and iron transport. *J. Biol. Chem.*, **272**, 9215–9220.
- Liu, G., Sánchez-Fernández, R., Li, Z. S., and Rea, P. A. (2001). Enhanced multispecificity of *Arabidopsis* vacuolar multidrug resistance-associated protein-type ATP-binding cassette transporter, *AtMRP2*. *J. Biol. Chem.*, **276**, 8648–8656.
- Loke, J. C., Stahlberg, E. A., Strenski, D. G., Haas, B. J., Wood, P. C., and Li, Q. Q. (2005). Compilation of mRNA polyadenylation signals in *Arabidopsis* revealed a new signal element and potential secondary structures. *Plant Physiol.*, **138**, 1457–1468.
- Lombi, E., Zhao, F. J., Dunham, S. J., and McGrath, S. P. (2000). Cadmium accumulation in populations of *Thlaspi caerulescens* and *Thlaspi goesingense*. *New Phytol.*, **145**, 11–20.

- Lu, C., Tej, S. S., Luo, S., Haudenschild, C. D., Meyers, B. C., and Green, P. J. (2005). Elucidation of the small RNA component of the transcriptome. *Science*, **309**, 1567–1569.
- MacDiarmid, C. W., Gaither, A. L., and Eide, D. (2000). Zinc transporters that regulate vacuolar zinc storage in *Saccharomyces cerevisiae*. *EMBO J.*, **19**, 2845–2855.
- Macnair, M. R. (2003). The hyperaccumulation of metals by plants. *Adv. Bot. Res.*, **40**, 64–106.
- Malmström, S., Askerlund, P., and Palmgren, M. (1997). A calmodulin-stimulated Ca^{2+} -ATPase from plant vacuolar membranes with a putative domain at its N-terminus. *FEBS Lett.*, **400**, 324–328.
- Maquat, L. E. (2002). Nonsense-mediated mRNA decay. *Curr. Biol.*, **12**, 196–197.
- Maroni, G., Wise, J., Young, J. E., and Otto, E. (1987). Metallothionein gene duplications and metal tolerance in natural populations of *Drosophila melanogaster*. *Genetics*, **117**, 739–744.
- Marschner, H. (1986). Mineral nutrition of higher plants (London: Academic Press Ltd.).
- Marschner, H. and Rohmold, V. (1994). Strategies of plants for acquisition of iron. *Plant Soil*, **165**, 375–388.
- Martin, G. B., Brommonschenkel, S. H., Chunwongse, J., Frary, A., Ganai, M. W., Spivey, R., Wu, T., Earle, E. D., and Tanksley, S. D. (1993). Map-based cloning of a protein kinase gene conferring disease resistance in tomato. *Science*, **262**, 1432–1436.
- Martinoia, E., Klein, M., Geisler, M., Bovet, L., Forestier, C., Kolukisaoglu, U., Müller-Röber, B., and Schulz, B. (2002). Multifunctionality of plant ABC transporters - more than just detoxifiers. *Planta*, **214**, 345–355.
- Meharg, A. A. (2005). Mechanisms of plant resistance to metal and metalloid ions and potential biotechnological applications. *Plant Soil*, **274**, 163–174.
- Meins, F., Si-Ammour, A., and Blevins, T. (2005). RNA silencing systems and their relevance to plant development. *Annu. Rev. Cell Dev. Biol.*, **21**, 297–318.
- Mendel, G. (1866). Versuche über Pflanzen-Hybriden. *J. Herid.*, **42**, 3–47. Reprinted in 1951.
- Mersereau, M., Pazour, G. J., and Das, A. (1990). Efficient transformation of *Agrobacterium tumefaciens* by electroporation. *Gene*, **90**, 149–151.
- Miki, T., Yoshioka, K., and Horiuchi, T. (1984). Control of cell division by sex factor F in *Escherichia coli*. I. The 42.84-43.6 F segment couples cell division of the host bacteria with replication of plasmid DNA. *J. Mol. Biol.*, **174**, 605–625.
- Mills, R. F., Francini, A., da Rocha, P. S. C. F., Baccarini, P. J., Aylett, M., Krijger, G. C., and Williams, L. E. (2005). The plant P1B-type ATPase *AtHMA4* transports Zn and Cd and plays a role in detoxification of transition metals supplied at elevated levels. *FEBS Lett.*, **579**, 783–791.
- Mills, R. F., Krijger, G. C., Baccarini, P. J., Hall, J. L., and Williams, L. E. (2003). Functional expression of *AtHMA4*, a P1B-type ATPase of the Zn/Co/Cd/Pb subclass. *Plant J.*, **35**, 164–176.
- Minagawa, J. and Takahashi, Y. (2004). Structure, function and assembly of photosystem II and its light-harvesting proteins. *Photosynth. Res.*, **82**, 241–263.
- Minet, M., Dufour, M. E., and Lacroute, F. (1992). Complementation of *Saccharomyces cerevisiae* auxotrophic mutants by *Arabidopsis thaliana* cDNAs. *Plant J.*, **2**, 417–422.

- Morsomme, P., Chami, M., Marco, S., Nader, J., Ketchum, K. A., Goffeau, A., and Rigaud, J.-L. (2002). Characterization of a hyperthermophilic P-type ATPase from *Methanococcus jannaschii* expressed in yeast. *J. Biol. Chem.*, **277**, 29608–29616.
- Mäser, P., Thomine, S., Schroeder, J. I., Ward, J. M., Hirschi, K., Sze, H., Talke, I. N., Amtmann, A., Maathuis, F. J., Sanders, D., Harper, J. F., Tchieu, J., Gribskov, M., Persans, M. W., Salt, D. E., Kim, S. A., and Guerinot, M. L. (2001). Phylogenetic relationships within cation transporter families of *Arabidopsis*. *Plant Physiol.*, **126**, 1646–1667.
- Murashige, T. and Skoog, F. (1962). A revised medium for rapid growth and bioassays with tobacco cultures. *Physiol. Plant.*, **15**, 473–496.
- Murphy, A., Zhou, J. M., Goldsbrough, P. B., and Taiz, L. (1997). Purification and immunological identification of metallothioneins 1 and 2 from *Arabidopsis thaliana*. *Plant Physiol.*, **113**, 1293–1301.
- Mutoh, N. and Hayashi, Y. (1988). Isolation of mutants of *Schizosaccharomyces pombe* unable to synthesize cadystin, small cadmium-binding peptides. *Biochem. Biophys. Res. Commun.*, **151**, 32–39.
- Nakano, M., Nobuta, K., Vemaraju, K., Tej, S. S., Skogen, J. W., and Meyers, B. C. (2006). Plant MPSS databases: signature-based transcriptional resources for analyses of mRNA and small RNA. *Nucleic Acids Res.*, **34**, 731–735.
- Naleway, J. J., Zhang, Y.-Z., Bonnett, H., Galbraith, D. W., and Haugland, R. P. (1991). Detection of GUS gene expression in transformed plant cells with new lipophilic fluorogenic beta-glucuronidase substrate. *J. Cell Biol.*, **115**, 151.
- Neumann, D. and zur Nieden, U. (2001). Silicon and heavy metal tolerance of higher plants. *Phytochemistry*, **56**, 685–92.
- Nies, A., Nies, D., and Silver, S. (1989). Cloning and expression of plasmid genes encoding resistances to chromate and cobalt in *Alcaligenes eutrophus*. *J. Bacteriol.*, **171**, 5065–5070.
- Nies, D. H. (2003). Efflux-mediated heavy metal resistance in prokaryotes. *FEMS Microbiol. Rev.*, **27**, 313–339.
- Nies, D. H. and Silver, S. (1995). Ion efflux systems involved in bacterial metal resistances. *J. Ind. Microbiol.*, **14**, 186–199.
- Nisbet, E. G. and Sleep, N. H. (2001). The habitat and nature of early life. *Nature*, **409**, 1083–1091.
- Novel, N. and Novel, M. (1973). Mutants d'*Escherichia coli* K 12 affectés pour leur croissance sur méthyl-beta-D-glucuronide: localisation of gène de structure de la beta-d-glucuronidase (*uidA*). *Mol. Gen. Genet.*, **120**, 319–335.
- Nriagu, J. (2003). Heavy metals and the origin of life. *J. Phy. IV France*, **107**, 969–974.
- Ochman, H., Ajioka, J. W., Garza, D., and Hartl, D. L. (1990). Inverse polymerase chain reaction. *Nat. Biotechnol.*, **8**, 759–760.
- Ochman, H., Gerber, A. S., and Hartl, D. L. (1988). Genetic applications of an inverse polymerase chain reaction. *Genetics*, **120**, 621–623.
- Odell, J. T., Nagy, F., and Chua, N. H. (1985). Identification of DNA sequences required for activity of the cauliflower mosaic virus 35S promoter. *Nature*, **3**, 810–812.

- Ogura, T. and Hiraga, S. (1983). Mini-F plasmid genes that couple host cell division to plasmid proliferation. *Proc. Natl. Acad. Sci. U. S. A.*, **80**, 4784–4788.
- O’Kane, S. L. J. and Al-Shehbaz, I. A. (1997). A synopsis of *Arabidopsis* (Brassicaceae). *Novon*, **7**, 323–327.
- Okkeri, J., Bencomo, E., Pietilä, M., and Haltia, T. (2002). Introducing Wilson disease mutations into the zinc-transporting P-type ATPase of *Escherichia coli*. The mutation P634L in the ‘hinge’ motif (GDGXNDXP) perturbs the formation of the E2P state. *Eur. J. Biochem.*, **269**, 1579–1586.
- Ortiz, D., Kreppel, L., Speiser, D., Scheel, G., McDonald, G., and Ow, D. (1992). Heavy metal tolerance in the fission yeast requires an ATP-binding cassette-type vacuolar membrane transporter. *EMBO J.*, **11**, 3491–3499.
- Ortiz, D. F., Ruscitti, T., McCue, K. F., and Ow, D. W. (1995). Transport of metal-binding peptides by HMT1, a fission yeast ABC-type vacuolar membrane protein. *J. Biol. Chem.*, **270**, 4721–4728.
- Otegui, M. S., Capp, R., and Staehelin, L. A. (2002). Developing seeds of *Arabidopsis* store different minerals in two types of vacuoles and in the endoplasmic reticulum. *Plant Cell*, **14**, 1311–27.
- Otto, S. P. and Yong, P. (2002). The evolution of gene duplicates. *Adv. Genet.*, **46**, 451–483.
- Outten, C. E. and O’Halloran, T. V. (2001). Femtomolar sensitivity of metalloregulatory proteins controlling zinc homeostasis. *Science*, **292**, 2488–2492.
- Palmgren, M., Sommarin, M., Serrano, R., and Larsson, C. (1991). Identification of an autoinhibitory domain in the C-terminal region of the plant plasma membrane H⁺-ATPase. *J. Biol. Chem.*, **266**, 20470–20475.
- Palmgren, M. G. (2001). Plant plasma membrane H⁺-ATPases: Powerhouses for nutrient uptake. *Annu. Rev. Plant Physiol. Plant Mol. Biol.*, **52**, 817–845.
- Palmgren, M. G. and Axelsen, K. B. (1998). Evolution of P-type ATPases. *Biochim. Biophys. Acta*, **1365**, 37–45.
- Papoyan, A. and Kochian, L. V. (2004). Identification of *Thlaspi caerulescens* genes that may be involved in heavy metal hyperaccumulation and tolerance. Characterization of a novel heavy metal transporting ATPase. *Plant Physiol.*, **136**, 3814–3823.
- Paulsen, I. T. and Saier, M. H. (1997). A novel family of ubiquitous heavy metal ion transport proteins. *J. Membr. Biol.*, **156**, 99–103.
- Pearson, W. R., Wood, T., Zhang, Z., and Miller, W. (1997). Comparison of DNA sequences with protein sequences. *Genomics*, **46**, 24–36.
- Pedersen, P. L. and Carafoli, E. (1987). Ion motive ATPase. I. ubiquity, properties, and significance to cell function. *Trends Biochem. Sci.*, **12**, 146–150.
- Peer, W. A., Baxter, I. R., Richards, E. L., Freeman, J. L., and Murphy, A. S. (2005). Phytoremediation and hyperaccumulator plants. *Top. Curr. Gen.*, **14**, 299–340.
- Pence, N. S., Larsen, P. B., Ebbs, S. D., Letham, D. L., Lasat, M. M., Garvin, D. F., Eide, D., and Kochian, L. V. (2000). The molecular physiology of heavy metal transport in the Zn/Cd hyperaccumulator *Thlaspi caerulescens*. *Proc. Natl. Acad. Sci. U. S. A.*, **97**, 4956–4960.

- Persans, M. W., Nieman, K., and Salt, D. E.** (2001). Functional activity and role of cation-efflux family members in Ni hyperaccumulation in *Thlaspi goesingense*. *Proc. Natl. Acad. Sci. U. S. A.*, **98**, 9995–10000.
- Petit, J. M., Briat, J. F., and Lobréaux, S.** (2001). Structure and differential expression of the four members of the *Arabidopsis thaliana* ferritin gene family. *Biochem. J.*, **359**, 575–582.
- Piccirilli, J. A., Vyle, J. S., Caruthers, M. H., and Cech, T. R.** (1993). Metal ion catalysis in the *Tetrahymena* ribozyme reaction. *Nature*, **361**, 85–88.
- Piper, P., Mahe, Y., Thompson, S., Pandjaitan, R., Holyoak, C., Egner, R., Muhlbauer, M., Coote, P., and Kuchler, K.** (1998). The Pdr12 ABC transporter is required for the development of weak organic acid resistance in yeast. *EMBO J.*, **17**, 4257–4265.
- Pomorski, T., Lombardi, R., Riezman, H., Devaux, P. F., van Meer, G., and Holthius, J. C. M.** (2003). Drs2p-related-type ATPases Dnf1p and Dnf2p are required for phospholipid translocation across the yeast plasma membrane and serve a role in endocytosis. *Mol. Biol. Cell*, **14**, 1240–1254.
- Porter, J. W. G.** (1957). Vitamin B12 and intrinsic factor, chapter Occurrence and biosynthesis of analogues of vitamin B12 (Stuttgart: Enke), 43–54.
- Post, R. L., Hegyvary, C., and Kume, S.** (1972). Activation by adenosine triphosphate in the phosphorylation kinetics of sodium and potassium ion transport adenosine triphosphatase. *J. Biol. Chem.*, **247**, 6530–6540.
- Puig, S. and Thiele, D. J.** (2002). Molecular mechanisms of copper uptake and distribution. *Curr. Opin. Chem. Biol.*, **6**, 171–80.
- Punz, W.** (1995). Metallophytes in the eastern Alps with special emphasis on higher plants growing on calamine and copper localities. *Phyton*, **35**, 295–309.
- Pyle, A. M.** (1996). Metal ions in biological systems: Interactions of metal ions with nucleotides, nucleic acids, and their constituents, volume 32, chapter Role of metal ions in ribozymes (New York - Basel: Dekker, Inc.), 479–520.
- Pyle, A. M.** (2002). Metal ions in the structure and function of RNA. *J. Biol. Inorg. Chem.*, **7**, 679–690.
- Ramakers, C., Ruijter, J. M., Deprez, R. H. L., and Moorman, A. F. M.** (2003). Assumption-free analysis of quantitative real-time polymerase chain reaction (PCR) data. *Neuroscience Lett.*, **339**, 62–66.
- Rasmussen, B.** (2000). Filamentous microfossils in a 3,235-million-year-old volcanogenic massive sulphide deposit. *Nature*, **405**, 676–679.
- Rausser, W. E.** (1995). Phytochelatins and related peptides: structure, biosynthesis, and function. *Plant Physiol.*, **109**, 1141–1149.
- Rausser, W. E.** (1999). Structure and function of metal chelators produced by plants: the case for organic acids, amino acids, phytin, and metallothioneins. *Cell Biochem. Biophys.*, **31**, 19–48.
- Rea, P. A., Li, Z.-S., Lu, Y.-P., and Drozdowicz, Y. M.** (1998). From vacuolar GS-X pumps to multispecific ABC transporters. *Annu. Rev. Plant Physiol. Plant Mol. Biol.*, **49**, 727–760.

- Rea, P. A., Sánchez-Fernández, R., Chen, S., Peng, M., Klein, M., Geisler, M., and Martinoia, E. (2003). ABC proteins: From Bacteria to Man, chapter The plant ABC transporter superfamily: the functions of a few and identities of many. (Academic Press), 335–355.
- Riechmann, J. L. (2002). The Arabidopsis book, chapter Transcriptional regulation: a genomic overview (The American Society of Plant Biologists), 1–46.
- Römheld, V. and Marschner, H. (1986). Evidence for a specific uptake system for iron phytosiderophores in roots of grasses. *Plant Physiol.*, **80**, 175–180.
- Robinson, N. J., Procter, C. M., Connolly, E. L., and Guerinot, M. L. (1999). A ferric-chelate reductase for iron uptake from soils. *Nature*, **397**, 694–697.
- Robinson, N. J., Tommey, A. M., Kuske, C., and Jackson, P. J. (1993). Plant metallothioneins. *Biochem. J.*, **295 (Pt 1)**, 1–10.
- Rosso, M. G., Li, Y., Strizhov, N., Reiss, B., Dekker, K., and Weisshaar, B. (2003). An *Arabidopsis thaliana* T-DNA mutagenized population (GABI-Kat) for flanking sequence tag-based reverse genetics. *Plant Mol. Biol.*, **53**, 247–259.
- Rothnie, H. M. (1996). Plant mRNA 3'-end formation. *Plant Mol. Biol.*, **32**, 43–61.
- Rothnie, H. M., Chen, G., Futterer, J., and Hohn, T. (2001). Polyadenylation in rice tungro bacilliform virus: cis-acting signals and regulation. *J. Virol.*, **75**, 4184–4194.
- Rutherford, A. W. (1989). Photosystem II, the water-splitting enzyme. *TIBS*, **14**, 227–232.
- Rutherford, J. C., Cavet, J. S., and Robinson, N. J. (1999). Cobalt-dependent transcriptional switching by a dual-effector MerR-like protein regulates a cobalt-exporting variant CPx-type ATPase. *J. Biol. Chem.*, **274**, 25827–25832.
- Ryan, P. R., Delhaize, E., and Randall, P. J. (1995a). Characterisation of Al-stimulated efflux of malate from the apices of Al-tolerant wheat roots. *Planta*, **196**, 103–110.
- Ryan, P. R., Delhaize, E., and Randall, P. J. (1995b). Malate efflux from roots apices and tolerance to aluminium are highly correlated in wheat. *Aust. J. Plant Physiol.*, **22**, 531–536.
- Sambrook, J. and Russel, D. W. (2001). *Molecular Cloning - A Laboratory Manual* (Cold Spring Harbor, New York: Cold Spring Harbor Laboratory Press).
- Sancenon, V., Puig, S., Mateu-Andres, I., Dorcey, E., Thiele, D. J., and Penarrubia, L. (2004). The *Arabidopsis* copper transporter COPT1 functions in root elongation and pollen development. *J. Biol. Chem.*, **279**, 15348–15355.
- Sancenon, V., Puig, S., Mira, H., Thiele, D. J., and Penarrubia, L. (2003). Identification of a copper transporter family in *Arabidopsis thaliana*. *Plant Mol. Biol.*, **51**, 577–587.
- Sarret, G., Saumitou-Laprade, P., Bert, V., Proux, O., Hazemann, J.-L., Traverse, A., Marcus, M. A., and Manceau, A. (2002). Forms of zinc accumulated in the hyperaccumulator *Arabidopsis halleri*. *Plant Physiol.*, **130**, 1815–1826.
- Schröter, W., Lautenschläger, K.-H., Bilbrack, H., and Schnabel, A. (1979). *Chemie*, chapter Zink und Zinkverbindungen. 13th edition (Leipzig: VEB Fachbuchverlag), 409.
- Schubert, D., Lechtenberg, B., Forsbach, A., Gils, M., Bahadur, S., and Schmidt, R. (2004). Silencing in Arabidopsis T-DNA transformants: The predominant role of a gene-specific RNA sensing mechanism versus position effects. *Plant Cell*, **16**, 2561–2572.

- Schuldt, A. J., Adams, J. H., Davidson, C. M., Micklem, D. R., Haseloff, J., Johnston, D. S., and Brand, A. H. (1998). Miranda mediates asymmetric protein and RNA localization in the developing nervous system. *Genes Dev.*, **12**, 1847–1857.
- Seigneurin-Berny, D., Gravot, A., Auroy, P., Mazard, C., Kraut, A., Finazzi, G., Grunwald, D., Rappaport, F., Vavasseur, A., Joyard, J., Richaud, P., and Rolland, N. (2006). HMA1, a new Cu-ATPase of the chloroplast envelope, is essential for growth under adverse light conditions. *J. Biol. Chem.*, **281**, 2882–2892.
- Sherman, F., Fink, G. R., and Hicks, J. B. (1986). *Methods in Yeast Genetics* (Cold Spring Harbor, NY, USA: Cold Spring Harbor Press).
- Shikanai, T., Müller-Moulé, P., Munekage, Y., Niyogi, K. K., and Pilon, M. (2003). PAA1, a P-type ATPase of Arabidopsis, functions in copper transport in chloroplasts. *Plant Cell*, **15**, 1333–1346.
- Shuman, S. (1991). Recombination mediated by Vaccinia virus topoisomerase I in *Escherichia coli* is sequence specific. *Proc. Natl. Acad. Sci. U. S. A.*, **88**, 10104–10108.
- Shuman, S. (1994). Novel approach to molecular cloning and polynucleotide synthesis using Vaccinia DNA topoisomerase. *J. Biol. Chem.*, **269**, 32678–32684.
- Sieburth, L. E. and Meyerowitz, E. M. (1997). Molecular dissection of the *AGAMOUS* control region shows that *cis* elements for spatial regulation are located intragenically. *Plant Cell*, **9**, 355–365.
- Silver, S., Nucifora, G., Chu, L., and Misra, T. K. (1989). Bacterial resistance ATPases: primary pumps for exporting toxic cations and anions. *TIBS*, **14**, 76–80.
- Skerra, A. (1994). Use of the tetracycline promoter for the tightly regulated production of a murine antibody fragment in *Escherichia coli*. *Gene*, **151**, 131–135.
- Skou, J. C. (1957). The influence of some cations on an adenosine triphosphatase from peripheral nerves. *Biochim. Biophys. Acta*, **23**, 394–401.
- Solioz, M. and Vulpe, C. (1996). CPx-type ATPases: a class of P-type ATPases that pump heavy metals. *Trends Biochem. Sci.*, **21**, 237–241.
- Southern, E. (1975). Detection of specific sequences among DNA fragments separated by gel electrophoresis. *J. Mol. Biol.*, **98**, 503–517.
- Stabler, S. P. and Allen, R. H. (2004). Vitamin B12 deficiency as a worldwide problem. *Annu. Rev. Nutr.*, **24**, 299–326.
- Steinhauser, D., Usadel, B., Luedemann, A., Thimm, O., and Kopka, J. (2004). CSB.DB: a comprehensive systems-biology database. *Bioinformatics*, **20**, 3647–3651.
- Stephan, U. W., Schmidke, I., Stephan, V. W., and Scholz, G. (1996). The nicotianamine molecule is made-to-measure for complexation of metal micronutrients in plants. *BioMetals*, **9**, 84–90.
- Stephan, U. W. and Scholz, G. (1993). Nicotianamine: mediator of transport of iron and heavy metals in the phloem? *Physiol. Plant.*, **88**, 522–529.
- Stokes, D. L. and Green, N. M. (2003). Structure and function of the calcium pump. *Annu. Rev. Biophys. Biomol. Struct.*, **32**, 445–468.

- Strasburger, E., Noll, F., Schenck, H., and Schimper, A. F. W.** (1991). Lehrbuch der Botanik, chapter IV. Die Nährstoffe und ihr Umsatz in der Pflanze. 33rd edition (Stuttgart, Jena, New York: Gustav Fischer Verlag), 320.
- Suzuki, A. and Knaff, D. B.** (2005). Glutamate synthase: structural, mechanistic and regulatory properties, and a role in the amino acid metabolism. *Photosynth. Res.*, **83**, 191–217.
- Suzuki, C.** (2004). Acidophilic structure and killing mechanism of the *Pichia farinosa* killer toxin SMKT. *Top. Curr. Gen.*, **11**, 189–214.
- Svennelid, F., Olsson, A., Piotrowski, M., Rosenquist, M., Ottman, C., Larsson, C., Oecking, C., and Sommarin, M.** (1999). Phosphorylation of Thr-948 at the C terminus of the plasma membrane H⁺-ATPase creates a binding site for the regulatory 14-3-3 protein. *Plant Cell*, **11**, 2379–2391.
- Taiz, L. and Zeiger, E.** (2002). *Plant Physiology*, chapter 14. Gene expression and signal transduction. 3rd edition (Sunderland, MA, USA: Sinauer Associates, Inc.), 1–30.
- Takahashi, M., Yamaguchi, H., Nakanishi, H., Shioiri, T., Nishizawa, N. K., and Mori, S.** (1999). Cloning two genes for nicotianamine aminotransferase, a critical enzyme in iron acquisition (Strategy II) in graminaceous plants. *Plant Physiol.*, **121**, 947–56.
- Takatsuji, H.** (1998). Zinc-finger transcription factors in plants. *Cell. Mol. Life Sci.*, **54**, 582–596.
- Takatsuji, H.** (1999). Zinc-finger proteins: the classical zinc finger emerges in contemporary plant science. *Plant Mol. Biol.*, **39**, 1073–1078.
- Talke, I. N., Hanikenne, M., and Krämer, U.** (2006). Zn-dependent global transcriptional control, transcriptional de-regulation and higher gene copy number for genes in metal homeostasis of the hyperaccumulator *Arabidopsis halleri*. *Plant Physiol.*, **142**, 148–167.
- Tang, X., Halleck, M. S., Schlegel, R. A., and Williamson, P.** (1996). A subfamily of P-type ATPases with aminophospholipid transporting activity. *Science*, **272**, 1495–1497.
- Tanzi, R. E., Petrukhin, K., Chernov, I., Pellequer, J. L., Wasco, W., Ross, B., Romano, D. M., Parano, E., Pavone, Brzustowicz, L. M., Devoto, M., Peppercorn, J., Bush, A. I., Sternlieb, I., Pirastu, M., Gusella, J. F., Evgrafov, O., Penchaszadeh, G. K., Honig, B., Edelman, I. S., Soares, M. B., Scheinberg, I. H., and Gilliam, T. C.** (1993). The Wilson disease gene is a copper transporting ATPase with homology to the Menkes disease gene. *Nat. Genet.*, **5**, 344–350.
- The Arabidopsis Genome Initiative** (2000). Analysis of the genome sequence of the flowering plant *Arabidopsis thaliana*. *Nature*, **408**, 796–815.
- Thomas, B. and Rothstein, R.** (1989). The genetic control of direct-repeat recombination in *Saccharomyces*: The effect of rad52 and rad1 on mitotic recombination at *GAL10*, a transcriptionally regulated gene. *Genetics*, **123**, 725–738.
- Thomine, S., Lelièvre, F., Debarbieux, E., Schroeder, J. I., and Barbier-Brygoo, H.** (2003). At-NRAMP3, a multispecific vacuolar metal transporter involved in plant responses to iron deficiency. *Plant J.*, **34**, 685–695.
- Thomine, S., Zimmermann, S., Guern, J., and Barbier-Brygoo, H.** (1995). ATP-dependent regulation of an anion channel at the plasma membrane of protoplasts from epidermal cells of *Arabidopsis* hypocotyls. *Plant Cell*, **7**, 2091–2100.

- Tian, G.-W., Mohanty, A., Chary, S. N., Li, S., Paap, B., Drakakaki, G., Kopec, C. D., Li, J., Ehrhardt, D., Jackson, D., Rhee, S. Y., Raikhel, N. V., and Citovsky, V. (2004). High-throughput fluorescent tagging of full-length *Arabidopsis* gene products in planta. *Plant Physiol.*, **135**, 25–38.
- Tohoyama, H., Shiraishi, E., and Amano, S. (1996). Amplification of a gene for metallothionein by tandem repeat in a strain of cadmium-resistant yeast cells. *FEMS Microbiol. Lett.*, **136**, 269–273.
- Tohoyama, H., Tomoyasu, T., and Inouhe, M. (1992). The gene for cadmium metallothionein from a cadmium-resistant yeast appears to be identical to *CUP 1* in a copper-resistant strain. *Curr. Genet.*, **21**, 275–280.
- Towbin, H., Staehelin, T., and Gordon, J. (1979). Electrophoretic transfer of proteins from polyacrylamide gels to nitrocellulose sheets: procedure and some applications. *Proc. Natl. Acad. Sci. U. S. A.*, **46**, 4350–4354.
- Toyoshima, C., Nakasako, M., Nomura, H., and Ogawa, H. (2000). Crystal structure of the calcium pump of sarcoplasmic reticulum at 2.6 Å resolution. *Nature*, **405**, 647–655.
- Tramczynska, A., Böttcher, C., and Clemens, S. (2006). The transition metal chelator nico-tianamine is synthesized by filamentous fungi. *FEBS Lett.*, **580**, 3173–3178.
- Vacchina, V., Mari, S., Czernic, P., Marquès, L., Pianelli, K., Schaumlöffel, D., Lebrun, M., and Lobinski, R. (2003). Speciation of nickel in a hyperaccumulating plant by high-performance liquid chromatography-inductively coupled plasma mass spectrometry and electrospray MS/MS assisted by cloning using yeast complementation. *Anal. Chem.*, **75**, 2740–2745.
- Valencia-Sánchez, M. A., Liu, J., Hannon, G. J., and Parker, R. (2006). Control of translation and mRNA degradation by miRNAs and siRNAs. *Genes Dev.*, **20**, 515–524.
- van der Zaal, B. J., Neuteboom, L. W., Pinas, J. E., Chardonens, A. N., Schat, H., Verkleij, J. A. C., and Hooykaas, P. J. J. (1999). Overexpression of a novel *Arabidopsis* gene related to putative zinc-transporter genes from animals can lead to enhanced zinc resistance and accumulation. *Plant Physiol.*, **119**, 1047–1055.
- van Hoof, N. A., Hassinen, V. H., Hakvoort, H. W., Ballintijn, K. F., Schat, H., Verkleij, J. A., Ernst, W. H. O., Karenlampi, S. O., and Tervahauta, A. I. (2001). Enhanced copper tolerance in *Silene vulgaris* (Moench) Garcke populations from copper mines is associated with increased transcript levels of a 2b-type metallothionein gene. *Plant Physiol.*, **126**, 1519–1526.
- Vandamme, P. and Coenye, T. (2004). Taxonomy of the genus *Cupriavidus*: a tale of lost and found. *Int. J. Syst. Evol. Microbiol.*, **54**, 2285–2289.
- Varotto, C., Maiwald, D., Pesaresi, P., Jahns, P., Salamini, F., and Leister, D. (2002). The metal ion transporter IRT1 is necessary for iron homeostasis and efficient photosynthesis in *Arabidopsis thaliana*. *Plant J.*, **31**, 589–599.
- Vashist, S., Frank, C. G., Jakob, C. A., and Ng, D. T. (2002). Two distinctly localized P-type ATPases collaborate to maintain organelle homeostasis required for glycoprotein processing and quality control. *Mol. Biol. Cell*, **13**, 3955–3966.
- Vatamaniuk, O. K., Mari, S., Lu, Y. P., and Rea, P. A. (1999). *AtPCS1*, a phytochelatin synthase from *Arabidopsis*: Isolation and *in vitro* reconstitution. *Proc. Natl. Acad. Sci. U. S. A.*, **96**, 7110–7115.

- Vaucheret, H. (2006). Post-transcriptional small RNA pathways in plants: mechanisms and regulations. *Genes Dev.*, **20**, 759–771.
- Vazquez, M. D., Poschenrieder, C., Barcelo, J., Baker, A. J. M., Hatton, P., and Cope, G. H. (1994). Compartmentation of zinc in roots and leaves of the zinc hyperaccumulator *Thlaspi caerulescens*. *Bot. Acta*, **107**, 243–250.
- Verkleij, J. A. C., Koevoets, P. L. M., Blake-Kalff, M. M. A., and Chardonens, A. N. (1998). Evidence for an important role of the tonoplast in the mechanism of naturally selected zinc tolerance in *Silene vulgaris*. *J. Plant Physiol.*, **153**, 188–191.
- Verret, F., Gravot, A., Auroy, P., Leonhardt, N., David, P., Nussaume, L., Vavasseur, A., and Richaud, P. (2004). Overexpression of *AtHMA4* enhances root-to-shoot translocation of zinc and cadmium and plant metal tolerance. *FEBS Lett.*, **576**, 306–312.
- Verret, F., Gravot, A., Auroy, P., Preveral, S., Forestier, C., Vavasseur, A., and Richaud, P. (2005). Heavy metal transport by *AtHMA4* involves the N-terminal degenerated metal binding domain and the C-terminal His11 stretch. *FEBS Lett.*, **579**, 1515–1522.
- Vert, G., Briat, J. F., and Curie, C. (2001). *Arabidopsis IRT2* gene encodes a root-periphery iron transporter. *Plant J.*, **26**, 181–189.
- Vert, G., Grotz, N., Dédaldéchamp, F., Gaymard, F., Guerinot, M. L., Briat, J.-F., and Curie, C. (2002). *IRT1*, an *Arabidopsis* transporter essential for iron uptake from the soil and for plant growth. *Plant Cell*, **14**, 1223–1233.
- Vert, G. A., Briat, J.-F., and Curie, C. (2003). Dual regulation of the *Arabidopsis* high-affinity root iron uptake system by local and long-distance signals. *Plant Physiol.*, **132**, 796–804.
- Vögeli-Lange, R. and Wagner, G. J. (1990). Subcellular localization of cadmium and cadmium-binding peptides in tobacco leaves. Implication of a transport function for cadmium-binding peptides. *Plant Physiol.*, **92**, 1086–1093.
- von Wiren, N., Mori, S., Marschner, H., and Romheld, V. (1994). Iron inefficiency in maize mutant *ys1* (*Zea mays* L. cv Yellow-Stripe) is caused by a defect in uptake of iron phytosiderophores. *Plant Physiol.*, **106**, 71–77.
- Vulpe, C., Levinson, B., Whitney, S., Packman, S., and Gitschier, J. (1993). Isolation of a candidate gene for Menkes disease and evidence that it encodes a copper transporting ATPase. *Nat. Genet.*, **3**, 7–13.
- Wald, G. (1964). The Origins Of Life. *Proc. Natl. Acad. Sci. U. S. A.*, **52**, 595–611.
- Weber, M., Harada, E., Vess, C., von Roepenack-Lahaye, E., and Clemens, S. (2004). Comparative microarray analysis of *Arabidopsis thaliana* and *Arabidopsis halleri* roots identifies nicotianamine synthase, a ZIP transporter and other genes as potential metal hyperaccumulation factors. *Plant J.*, **37**, 269–281.
- Wei, J. and Theil, E. C. (2000). Identification and characterization of the iron regulatory element in the ferritin gene of a plant (soybean). *J. Biol. Chem.*, **275**, 17488–17493.
- Weigel, D., Bergelson, J. M., Borevitz, J. O., Gaut, B. S., Nordborg, M., and Wright, S. I. (2006). DOE Community Sequencing Program: Project Proposal, Sequencing the genomes of two *Arabidopsis thaliana* relatives. Technical report, Max Planck Institute for Developmental Biology.

- Weinberg, S. (1993). *The first three minutes* (New York: Basic Books).
- Weinstein, L. B., Jones, B. C. N. M., Cosstick, R., and Cech, T. R. (1997). A second catalytic metal ion in a group I ribozyme. *Nature*, **388**, 805–808.
- White, P. J., Whiting, S. N., Baker, A. J. M., and Broadley, M. R. (2002). Does zinc move apoplastically to the xylem in roots of *Thlaspi caerulescens*? *New Phytol.*, **153**, 201–207.
- Willems, G., Godé, C., Dräger, D. B., Courbot, M., Verbruggen, N., and Saumitou-Laprade, P. (2007). The genetic basis of zinc tolerance in the metallophyte *Arabidopsis halleri* ssp. *halleri* (Brassicaceae): an analysis of quantitative trait loci. *Genetics, in revision*.
- Williams, L. E. and Mills, R. F. (2005). P(1B)-ATPases - an ancient family of transition metal pumps with diverse functions in plants. *Trends Plant Sci.*, **10**, 491–502.
- Williams, L. E., Pittman, J. K., and Hall, J. L. (2000). Emerging mechanisms for heavy metal transport in plants. *Biochim. Biophys. Acta*, **1465**, 104–126.
- Wintz, H., Fox, T., and Vulpe, C. (2002). Responses of plants to iron, zinc and copper deficiencies. *Biochem. Soc. Trans.*, **30**, 766–768.
- Wintz, H., Fox, T., Wu, Y.-Y., Feng, V., Chen, W., Chang, H.-S., Zhu, T., and Vulpe, C. (2003). Expression profiles of *Arabidopsis thaliana* in mineral deficiencies reveal novel transporters involved in metal homeostasis. *J. Biol. Chem.*, **278**, 47644–47653.
- Woeste, K. E. and Kieber, J. J. (2000). A strong loss-of-function mutation in RAN1 results in constitutive activation of the ethylene response pathway as well as a rosette-lethal phenotype. *Plant Cell*, **12**, 443–455.
- Woolhouse, H. W. (1983). Toxicity and tolerance in the responses of plants to metals, volume New Series Vol. 12 C, chapter Physiological Plant Ecology III: Responses to the Chemical and Biological Environment (Berlin: Springer-Verlag), 245–300.
- Wu, Z., Liang, F., Hong, B., Young, J. C., Sussman, M. R., Harper, J. F., and Sze, H. (2002). An endoplasmic reticulum Ca^{2+} / Mn^{2+} pump, ECA1, supports plant growth and confers tolerance to Mn^{2+} stress. *Plant Physiol.*, **130**, 128–137.
- Yang, X., Feng, Y., He, Z., and Stoffella, P. J. (2005). Molecular mechanisms of heavy metal hyperaccumulation and phytoremediation. *J. Trace Elem. Med. Biol.*, **18**, 339–353.
- Yang, Y. W., Lai, K. N., Tai, P. Y., and Li, W. H. (1999a). Rates of nucleotide substitution in angiosperm mitochondrial DNA sequences and dates of divergences between *Brassica* and other angiosperm lineages. *J. Mol. Evol.*, **48**, 597–604.
- Yang, Y. W., Lai, K. N., Tai, P. Y., Ma, D. P., and Li, W. H. (1999b). Molecular phylogenetic studies of *Brassica*, *Rorippa*, *Arabidopsis* and allied genera based on the internal transcribed spacer region of 18S-25S rDNA. *Mol. Phylogenet. Evol.*, **13**, 455–462.
- Yasutake, Y., Watanabe, S., Yao, M., Takada, Y., Fukunaga, N., and Tanaka, I. (2003). Crystal structure of the monomeric isocitrate dehydrogenase in the presence of NADP^+ . *J. Biol. Chem.*, **278**, 36897–36904.
- Yogeeswaran, K., Frary, A., York, T. L., Amenta, A., Lesser, A. H., Nasrallah, J. B., Tanksley, S. D., and Nasrallah, M. E. (2005). Comparative genome analyses of *Arabidopsis* spp.: inferring chromosomal rearrangement events in the evolutionary history of *A. thaliana*. *Genome Res.*, **15**, 505–515.

- Zenk, M. H.** (1996). Heavy metal detoxification in higher plants - a review. *Gene*, **179**, 21–30.
- Zhao, F., Lombi, E., Breedon, T., and McGrath, S.** (2000). Zinc hyperaccumulation and cellular distribution in *Arabidopsis halleri*. *Plant Cell Environ.*, **23**, 507–514.
- Zhao, J., Hyman, L., and Moore, C.** (1999). Formation of mRNA 3' ends in eukaryotes: mechanism, regulation, and interrelationships with other steps in mRNA synthesis. *Microbiol. Mol. Biol. Rev.*, **63**, 405–445.
- Zhou, J. M. and Goldsbrough, P. B.** (1995). Structure, organization and expression of the metallothionein gene family in *Arabidopsis*. *Mol. Gen. Genet.*, **248**, 318–328.
- Zimmermann, P., Hirsch-Hoffmann, M., Hennig, L., and Gruissem, W.** (2004). GENEVESTIGATOR. Arabidopsis Microarray Database and Analysis Toolbox. *Plant Physiol.*, **136**, 2621–2632.

Part VI

Appendices

A Supplementary data

A.1 2D topology model of *AhHMA3*

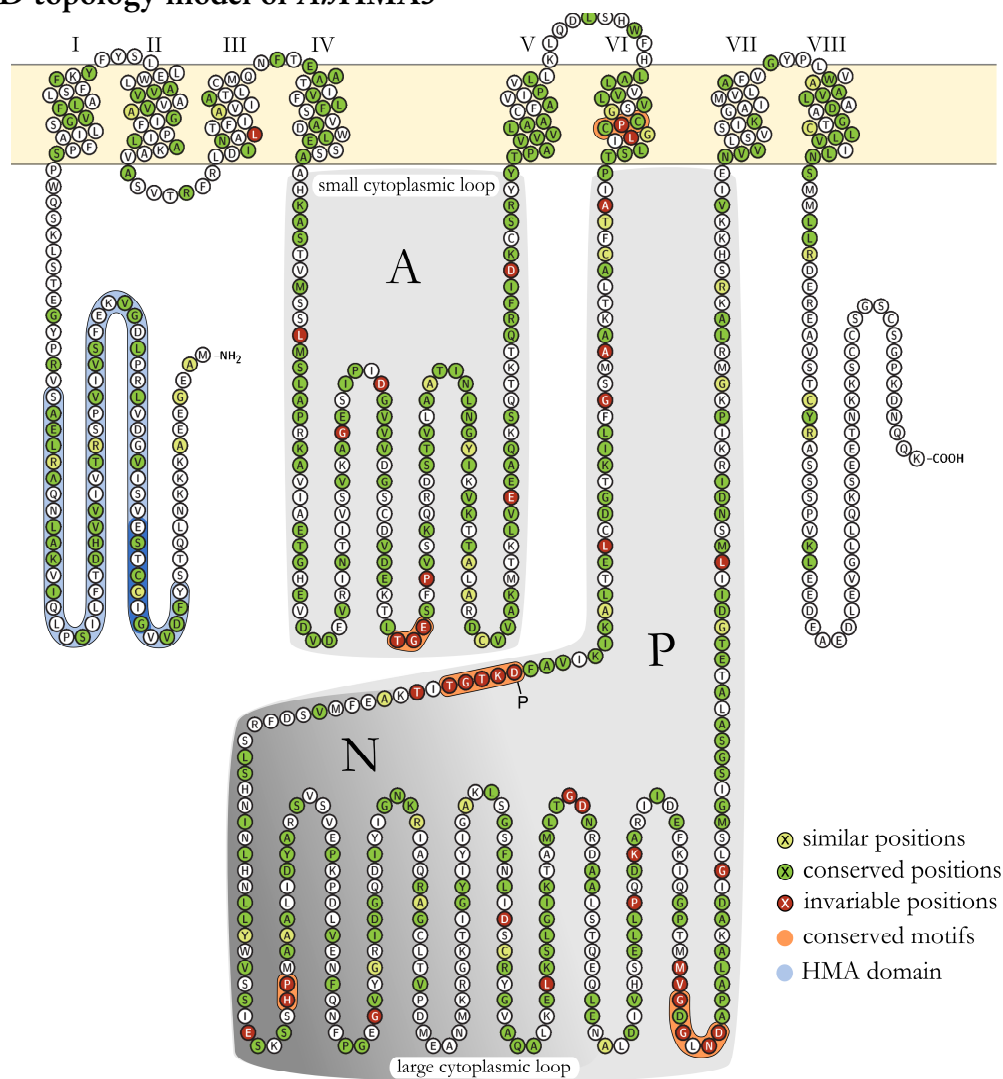


Figure 1: 2D topology model of *AhHMA3*.

P-type IB ATPases possess 8 MSHs with a small cytoplasmic loop between MSH IV and V that forms the phosphatase or actuator (A) domain and a large cytoplasmic loop between MSH VI and VII containing the phosphorylation (P) and the nucleotide binding (N) domain. The large cytoplasmic loop contains the highly conserved **DKTGT** motif, the site of phosphorylation during the reaction cycle. The conserved **HP** and **GDGIND** motifs are of unknown function. The sixth MSH contains a highly conserved **CPx** (Cys-Pro-x) motif.

Membrane spanning helices (MSHs) are labeled with roman numbers from I to VIII. The positions are based upon alignments with *EcZntA*, a bacterial P-type IB ATPase with partially known topology, and transmembrane predictions listed at the *aramemnon*-website (aramemnon.botanik.uni-koeln.de). Conserved protein motifs are framed in red boxes.

The amino acid shading is based on the alignment of 22 plant and one *E. coli* P-type IB ATPases as described in Figure 2 below. The alignment file was produced using the *MEGA* application version 3.1 (Kumar *et al.*, 2004, default parameters) and *TEXshade* (Beitz, 2000a). The 2D representation of *AhHMA3* was drawn with the help of *TEXtopo* (Beitz, 2000b).

GMTcxc / GICC(T/S/E)

HMA motif

A/HMA3 (Ws)	EVSIVGNVLRQVDGVKFSVIVPSRTVIIVVHDTFLISPLQIVKALNQARLEAS	79
A/HMA3	EVSIVGNVLRPDDGVKFSVIVPSRTVIIVVHDTFLISPLQIVKALNQARLEAS	79
A/HMA2	EVPLIENILNSMDGVKFSVIVPSRTVIIVVHDTFLISPLQIVKALNQARLEAS	73
A/HMA4	EYPTIENILNSMDGVKFSVIVPSRTVIIVVHDTFLISPLQIVKALNQARLEAS	83
T/CHMA4	EPLIENILNSMDGVKFSVIVPSRTVIIVVHDTFLISPLQIVKALNQARLEAS	87
O/HMA3	EVALVRLIAPLDGVRVVSIVASRTVIVVHDTAAAPASIVKALNQARLEAS	108
O/HMA2	EYPLVRLIAPLDGVRVVSIVASRTVIVVHDTAAAPASIVKALNQARLEAS	75
A/HMA1	PKTLRLQKPLRLSASLNPPRSIRLRAVEDHHDDHHDDQDDHHHHHHGGCCSVELKA	98
O/HMA1	PPSPGSPILLARRSLPFAFR...AHGDDHHGHHHHHHGGHSHHHHPVHG	66

30 40 50 60 70

GMTcxc

HMA motif

A/HMA3 (Ws)	...VRPYG	84
A/HMA3	...VRPYG	84
A/HMA2	...VRVTC	78
A/HMA4	...VRVTC	88
T/CHMA4	...VRVTC	92
O/HMA3	...VRAYG	113
O/HMA2	...VRAYG	82
A/HMA1	...ESKPKMLFQFAKAIG	114
O/HMA1	...SGGGAAVVRVAKAIG	81

EcZntA
A/HMA8 (PAA2) ...FEAKR...VSG...MGVAENVKWKEMYS... 114
O/HMA8 ...FPSVARGGAASGASDSARKWREMAA... 139
A/HMA6 (PAA1) ...TNCGFQSTPRDLVTENFFKVFETKTK... 177
O/HMA7 ...TTCGYKSNLRDSSKASSQTVFERKMD... 240
BnRAN1 ...TKTQATLVGQFT...GGMTCAA...VNSV... 219
A/HMA7 (RAN1) ...QATLVGQFT...GGMTCAA...VNSV... 215
O/HMA6 ...PKLQNTLSGQF...GGMTCAA...VNSV... 213
O/HMA4 ...QETIAYCRILQK...GMACTS... 194
A/HMA5 ...RSRQVCRIR...GMACTS... 212
ZmQ6JAH7 ...KNILCRHLH...GMACKY... 225
O/HMA5 ...KNILVCRHLH...GMACT... 236
S/Q6JAG2 ...KNILVCRHLH...GMACT... 235
S/Q6JAG3 ...KNVLLCRHLH...GMACKY... 130

80

MSH I

A/HMA3 (Ws)	...ETSLK...SOWP...SPPAIVS...GVL	104
A/HMA3	...ETSLK...SOWP...SPPAIVS...GVL	104
A/HMA2	...ETNFK...KWKW...SPPAVS...GILL	98
A/HMA4	...ETSFK...KWKW...SPPAVS...GILL	108
T/CHMA4	...ETSFK...KWKW...SPPAVS...GILL	112
O/HMA3	...SSGVV...SRNP...SPTVAS...GML	133
O/HMA2	...SEKTI...MKWP...SPTVEL...CGLL	102
A/HMA1	...WVRIAN...VREH...LHCCS...AAMFL	137
O/HMA1	...WADVADAL...REHL...QLCC...ISLGLL	104

EcZntA
A/HMA8 (PAA2) ...QAAE...EPOAS...RLKEN...P...ITL...IVM 137
O/HMA8 ...KKED...L...VSR...R...VAF...AWT...VAL...CCG 164
A/HMA6 (PAA1) ...RKAEL...L...R...GR...VAF...AWT...VAL...CCG 202
O/HMA7 ...DKQAR...L...K...ES...G...RE...L...VAF...AWT...VAL...CCG 265
BnRAN1 ...EKLLQ...K...Q...S...G...RE...L...VAF...AWT...VAL...CCG 268
A/HMA7 (RAN1) ...VLN...EL...DA...Q...V...L...E...G...I...L...T...R...N...G...V...R...F...L...D...R...I...T...G...E...L...V...F...D...E...V...V...S...S...L...V...D...G...E...G...E...G...Y...K...F...K...L...R...V...M...S...P...Y...E...R...L...T... 315
O/HMA6 ...LHTE...V...D...V...D...L...H...D...I...L...K...K...M...E...L...R...Q...F...N...V...L...S...E...A...E...V...F...D...E...V...V...S...S...L...V...D...G...E...G...E...G...Y...K...F...K...L...R...V...M...S...P...Y...E...R...L...T... 311
O/HMA4 ...VSSP...E...D...I...K...I...Q...S...R...L...E...S...V...E...G...V...N...V...E...C...D...T...A...G...Q...T...I...I...A...Y...D...P...R...L...L...I...O...C...Q...D...A...A...Q... 309
A/HMA5 ...ELT...D...E...S...H...K...V...I...E...R...S...L...E...A...L...P...G...V...S...V...E...I...S...H...G...T...D...K...I...S...V...L...Y...K...D...V...T...G...P...R...N...F...I...Q...V...E...S...T...V...F...G...H...S...H...I...K...A...T...I...F...S...E...G...G...V...R...E...S...Q...Q...E...I...K...Y...K...S...L...W...S...L...V...F...I...P...V...F...L... 292
ZmQ6JAH7 ...TILN...E...L...M...I...L...K...S...S...I...Q...A...L...P...G...V...E...N...V...K...F...N...S...E...L...H...K...V...T...S...Y...N...D...H...T...G...P...R...L...I...E...V...I...K...A...A...T...F... 312
O/HMA5 ...LTER...L...T...E...R...L...M...I...L...K...S...S...I...Q...A...L...P...G...V...E...D...V...K...V...D...T...E...L...H...K...V...T...S...Y...N...D...H...T...G...P...R...L...I...E...V...I...K...A...A...T...F... 321
S/Q6JAG2 ...VLDE...T...L...M...I...L...K...S...S...I...Q...A...L...P...G...V...E...N...I...T...F...N...S...E...L...H...K...V...T...S...Y...N...D...H...T...G...P...R...L...I...E...V...I...K...A...A...T...F... 331
S/Q6JAG3 ...VLDE...T...L...M...I...L...K...S...S...I...Q...A...L...P...G...V...E...N...I...T...F...N...S...E...L...H...K...V...T...S...Y...N...D...H...T...G...P...R...L...I...E...V...I...K...A...A...T...F... 226

90 100

MSH I MSH II MSH III

A/HMA3 (Ws)	...VLSF...K...FY...S... 162	...PLEW...L...A...V...A...V...G...F...P...I...L...A...K...A...V...S...V...T...F...R...L...D...I...N...A...T...L...I...A...V...I...A...T...L...C...M...Q...D... 162	...VLSF...K...FY...S... 162
A/HMA3	...VLSF...K...FY...S... 162	...PLEW...L...A...V...A...V...G...F...P...I...L...A...K...A...V...S...V...T...F...R...L...D...I...N...A...T...L...I...A...V...I...A...T...L...C...M...Q...D... 162	...VLSF...K...FY...S... 162
A/HMA2	...LVSF...K...FY...S... 166	...PFR...W...L...A...V...A...V...G...F...P...I...L...A...K...A...V...S...L...A...R...F...R...I...D...I...N...T...V...V...T...V...G...A...T...I...G...M...Q...D... 166	...LVSF...K...FY...S... 166
A/HMA4	...LVSF...K...FY...S... 170	...PLR...W...L...A...V...A...V...G...F...P...I...L...A...K...A...V...S...I...R...R...L...V...D...I...N...T...V...T...V...A...T...L...A...M...O...D... 170	...LVSF...K...FY...S... 170
T/CHMA4	...LVSF...K...FY...S... 170	...PLR...W...L...A...V...A...V...G...F...P...I...L...A...K...A...V...S...I...R...R...L...V...D...I...N...T...V...T...V...A...T...L...A...M...O...D... 170	...LVSF...K...FY...S... 170
O/HMA3	...TAS...F...E...W...L...F...H...P... 191	...P...L...Q...C...L...A...V...A...V...G...A...P...P...V...R...R...G...F...A...A...S...L...S...L...D...I...N...V...I...L...I...A...V...A...G...L...C...L...G...D... 191	...TAS...F...E...W...L...F...H...P... 191
O/HMA2	...VVS...L...E...W...L...F...H...P... 160	...P...L...K...W...F...A...L...A...A...A...G...L...P...P...I...V...L...R...S...I...A...I...R...L...L...D...V...N...I...L...I...A...V...A...G...L...A...L...K...D... 160	...VVS...L...E...W...L...F...H...P... 160
A/HMA1	...AAA...V...C...P...L...A...P... 201	...E...P...Y...I...K...Q...A...N...F...I...G...F...P...L...V...G...V...S...A...L...D...A...L...M...D...I...A...G...K...V...N...I...H...V...M...A...L...A...F...A...S...V...M...G...N... 201	...AAA...V...C...P...L...A...P... 201
O/HMA1	...IAA...C...P...H...I...P...V... 168	...L...N...S...V...R...R...L...Q...A...I...A...V...A...F...L...V...G...V...S...A...L...D...A...L...V...N...I...A...D...G...K...I...N...I...H...V...M...A...L...A...F...A...S...I...M...G...N... 168	...IAA...C...P...H...I...P...V... 168

EcZntA
A/HMA8 (PAA2) ...MAIS...W...L...E...Q...F...N... 200
O/HMA8 ...SHT...S...H...I...L...H...L...G...H...I...A...H...G... 242
A/HMA6 (PAA1) ...SHAT...H...L...S...L...G...H...V...G...H...G...S... 292
O/HMA7 ...GHL...T...H...L...F...L...G...V...N... 337
BnRAN1 ...GHIS...H...L...F...G...V...N... 340
A/HMA7 (RAN1) ...IQVI...C...P...H...I...A...L... 393
O/HMA6 ...IQVI...C...P...H...I...A...L... 389
O/HMA4 ...IRNV...C...P...H...I...F... 388
A/HMA5 ...F...S...H...L...P...H...I...S...P... 371
ZmQ6JAH7 ...TAN...V...M...I...P...G... 391
O/HMA5 ...T...S...M...V...M...I...P...W... 400
S/Q6JAG2 ...T...S...M...V...M...I...P...V... 410
S/Q6JAG3 ...T...S...M...V...M...I...P...W... 305

110 120 130 140 150 160

large cytoplasmic loop

AhHMA3 (Ws) EPKPDIVENFNQFPFEGYGRIDGQD..... IYI GNKRI IAQ	488
AhHMA3 EPKPLVFNQFPFEGYGRIDGQD..... IYI GNKRI IAQ	488
AhHMA2 EPKPEAVEDYQNFPEGYGKIDGKE..... IYI GNKRI IAQ	482
AhHMA4 EPRPEVEDYQNFPEGYGKIDGND..... IYI GNKRI IAQ	492
TcHMA4 EPRSEVEDYQNFPEGYGKIDGNN..... IYI GNKRI IAQ	496
OsHMA3 QMPENVGDRIRYFPEGYEIHGKH..... IYI GNRRTLA	518
OsHMA2 EPKSENVSESKYLVRGFMVKSTEQA..... YILGTRNFVK	486
AhHMA1 SIFVSES.....EYFPGRLTATVNGVK..... TVAEESRRLK	556
OsHMA1 LVAVSES.....ECLPGRGVATLISGVK..... AGNNEDELSK	524
<i>EcZntA</i> AIPTAESQRAIVLGSGLTEAVNGER..... VLTIC	518
AhHMA8 (PAA2) TPETRG.....QLTEPGFGLAEVDGRF..... VAVGSLLEWWS	608
OsHMA8 IPATSG.....QLTEPGFGLAEVDGCL..... VAVGLTDWVH	658
AhHMA6 (PAA1) THKARDGTTEEPGSGAVATMNRRA..... YVGTLEWVK	696
OsHMA7 YLQAKDGSHEEPGSAVATIGERQ..... YVGTLDWLR	700
BtRAN1 GDTSNKVYQ.....NAGWLLDTSDF SALPGKGLCLVNDKL..... IYVGNRRKLS	763
AhHMA7 (RAN1) GETNNKDLQ.....NSGWLLDTSDF SALPGKGLCLVNEKM..... IYVGNRRKLS	765
OsHMA6 KDDIKRKRQQLSQWLLLEVAEFSALPGKGLCLVNGKK..... IYVGNRRLIT	766
OsHMA4 SHSDHIMEKDFEVHFGAGVSNVVEKGL..... IYVGNRRLMQ	736
AhHMA5 EENPAWPEACDFVSIITGKWKATVKGRE..... YLVGNRNLNM	754
ZmQ6JAH7 EGNHMWPEAREISVITGQVKAESVSKS..... YLVGNRGLML	762
OsHMA5 EESHVWTEARDISVITGHGKAKISGRA..... YLVGNRSLFM	773
SbQ6JAG2 EENHIWPEARDISVITGHGKAKVFDKS..... YLVGNRSLFM	772
SbQ6JAG3 EENHIWPEARDISVITGHGKVDVSDKS..... YLVGNRSLFM	678

460 470 480

large cytoplasmic loop

AhHMA3 (Ws)	RACGLTD.NVPDIEATMKRGGKTI..... IYIMGA.KITGSFNLIDGCRVVAQALKLKS.LGKIQAMTLDGNODAAAMSTOQLGNALD	570
AhHMA3	RACGLT.....VPPMAMNMRKGGKTI..... IYIYGA.KISGSFNLIDGCRVVAQALKLKS.LGKIQAMTLDGNODAAAMSTOQLGNALD	568
AhHMA2	RAGCLS.....VPPDIDVDTKGGKTI..... YVYVGE.TIAGVFNLDACRSVVAQAMKLD.LGKIQAMTLDGNODAAAMSTOQLGNALD	562
AhHMA4	RAGCST.....VPEIEVDTKGGKTVG..... YVYVGE.TIAGVFNLDACRSVVAQAMKLD.LGKIQAMTLDGNODAAAMSTOQLGNALD	572
TcHMA4	RAGCST.....VPEIEVDTKGGKTVG..... YVYVGE.TIAGVFNLDACRSVVAQAMKLD.LGKIQAMTLDGNODAAAMSTOQLGNALD	576
OsHMA3	RASSPQ.....STQEMGEMIKGVSTIC..... YVICCG.ELIAGVFNLDACRTGAAEAATRLGS.LGKIQAMTLDGNODAAAMSTOQLGNALD	598
OsHMA2	SFMNRN.....LVTIG..... YVICCNV.ELIAGVFNLDACRTGAAEAATRLGS.LGKIQAMTLDGNODAAAMSTOQLGNALD	556
AhHMA1	ASLGSFEFITSILFKSDESKQIKDAVNASSYKGFV..... HAALYVDQKVTLLHEDQPVPVSGVIAELKSWARLRVMHLLGHSASAWRVAN.AVGTI	651
OsHMA1	ASIGSVYISSLVRSSESEQIKAVKASAFPGFV..... QALVYDQKVTLLHEDQPVPVSGVIAELKSWARLRVMHLLGHSASAWRVAN.AVGTI	619
<i>EcZntA</i>	AAGKHPADAFGLINLELSAGQIVV..... LVVNRD.VLGVVIAAQDITLRADAATAISLINA.LGVGVILIGDPPRAAAATLGEIG.....L	599
AhHMA8 (PAA2)	DRFLKKNDSDDMVKLLSLDLKLSNITSSRSYKSTV..... YVYVGE.EGIIQAATAISDLRQDAEFTWARLOE.KGKRTWLSLREGGAVATVAWVGIKSKS	705
OsHMA8	NRFETKASSTLTDLGNHLEFVSS.SEASSNHSKSVIA..... YVYVGE.EGIIQAATAISDLRQDAEFTWARLOE.KGKRTWLSLREGGAVATVAWVGIKSKS	754
AhHMA6 (PAA1)	RHGATGNSLLALEEHEINNOQSV..... YVIGVFN.TIAAATRFEDKVREDAQQVVENLTR.OGIDVYMLGDKRRAANVAIVSIVGNHNE	778
OsHMA7	RHGVLHN.....PFADGENFGQSV..... YVAVDG.TIAGLIFCFDKLRDSSHQIIDLISK.OGIVSYMLGDKRRAANVAIVSIVGNHNE	779
BtRAN1	ENSIITPDHVEKFEELLESKATGV..... IVAYSG.QLVGVMGVADPLKREAAVVEVGLR.HGVRPIMVTDNRTARAVAK.EVGTIE	845
AhHMA7 (RAN1)	ENAINTPDHVEKFEELLESKATGV..... IVAYNG.KLVGVMGVADPLKREAAVVEVGLR.HGVRPIMVTDNRTARAVAK.EVGTIE	847
OsHMA6	ENGINPEEAESFLVDLELNKATGV..... LVAYDS.ELIGVLSVDDPLKPSAREASISLKS.HNKSIMVTDNRTARAVAK.EVGTIE	848
OsHMA4	EFEVPTSEVEGHMSSETEELARTCV..... LVLAIDR.TICGALSVDDPLKPEAGRAISYLS.MGISSIMVTDNRTARAVAK.EVGTIE	818
AhHMA5	DHKVLPDDAEELLDSEDMATQIG..... LVLSINS.ELIGVLSVDDPLKPSAREASISLKS.HNKSIMVTDNRTARAVAK.EVGTIE	836
ZmQ6JAH7	SSGIGPLEASIELVEEGKARTGT..... IVAVDR.EVAVGIVSVDDPKPNALQVIVSYLS.MNVESIMVTDNRTARAVAK.EVGTIE	844
OsHMA5	TSIGIDTPVEALIEITEEBEKARTGT..... IVAMDQ.EVVGIVSVDDPKPNAREVIVSYLS.MNVESIMVTDNRTARAVAK.EVGTIE	855
SbQ6JAG2	SLSIDTPMEASIELVEENARTGT..... IVAMDQ.EVVGIVSVDDPKPNAREVIVSYLS.MNVESIMVTDNRTARAVAK.EVGTIE	854
SbQ6JAG3	SSGIDTSLAELIEITEEBEKARTGT..... IVALDQ.EVVGIVSVDDPKPNAREVIVSYLS.MNVESIMVTDNRTARAVAK.EVGTIE	760

single base pair deletion

large cytoplasmic loop

AhHMA3 (Ws) I.VHSELPLQDKARIIDDFKIQ..... GPTMVVGGDNDAPALAKADIGISM.....GIS.....GSALATBTGDIILMSND.....IRKIPKGM	644
AhHMA3 I.VHSELPLQDKARIIDDFKIQ..... GPTMVVGGDNDAPALAKADIGISM.....GIS.....GSALATBTGDIILMSND.....IRKIPKGM	642
AhHMA2 I.VRAEELPLQDKRSITIKQKREE..... GPTMVVGGDNDAPALATADIGISM.....GVS.....GSALATBTGDIILMSND.....IRKIPQAI	637
AhHMA4 V.VHGEDLPLQDKRSITIQEFKKE..... GPTMVVGGDNDAPALATADIGISM.....GIS.....GSALATBTGDIILMSND.....IRKIPQAV	646
TcHMA4 V.VHGEDLPLQDKRSITIQEFKKE..... GPTMVVGGDNDAPALANADIGISM.....GIS.....GSALTTOTGHIILMSND.....IRKIPQAI	650
OsHMA3 E.LHSELPLQDKRSITISGKARF..... GPTMVVGGDNDAPALAAADVGVSM.....GIS.....GSAAHMTSHALMSB.....LWRPFAV	673
OsHMA2 E.VHSELPLQDKRSITIQEFKKE..... GPTMVVGGDNDAPALAKADIGISM.....GVS.....GSAAHMTSHALMSB.....LWRPFAV	631
AhHMA1 E.VYCNLQKEDLNHVNNIARE..... GGGLTMYVGGDNDAPALAAATVGVIL.AQR.ASATAVAVADVILLRDN.LTGWFFCV	727
OsHMA1 E.VHCLLPQDKLNKVVAVSREG..... GGGLTMYVGGDNDAPALAAATVGVIL.AQR.ASATAVAVADVILLRDN.LTGWFFCV	695
<i>EcZntA</i> E.FKAGLPLQDKRVKAVTELNQH..... APLVMVGGDNDAPAMKAAATIGAM.P.G.S.....GTDVAIEEADIVLNRNS.....LRGVQML	672
AhHMA8 (PAA2) S.TNYSLPEKRFESLNSLQSS..... GHRVAVGGDNDAPSLAQADVGLAL.KIEA.QENASNAASVILVRNK.....SHVMDAL	781
OsHMA8 N.IKSSLTPHRAKGIITALQGE..... GRRVAVGGDNDAPSLAAADVGVAM.RTNS.KESAASDAASVVLGNR.....LQMMDAL	830
AhHMA6 (PAA1) R.VIAGVLPQDKRKNFVNEQKN..... KKVAVVGGDNDAPALASADVGVAM.GG.....GAGAASVSPVVLGNR.....LTDLMDAM	852
OsHMA7 K.VIAEVLPHKRSFSELOKE..... HKLVAVGGDNDAPALASADVGVAM.GG.....GVGAASDVSVVLGNR.....LQVLDAL	853
BtRAN1 D.VRAEVPQDKRAEIVRSLOKD..... GSTVAVGGDNDSPALAAADVGMAT.GA.....GTDVAIEEADIVLNRNS.....LEDVITAI	919
AhHMA7 (RAN1) D.VRAEVPQDKRAEIVRSLOKD..... GSTVAVGGDNDSPALAAADVGMAT.GA.....GTDVAIEEADIVLNRNS.....LEDVITAI	921
OsHMA6 D.VRAEVPQDKRAEIVRSLOKD..... GSTVAVGGDNDSPALAAADVGMAT.GA.....GTDVAIEEADIVLNRNS.....LEDVITAI	922
OsHMA4 T.VFAEIDPVGKAEKIKDLQMK..... GLTVAVGGDNDSPALAAADVGMAT.GA.....GTDVAIEEADIVLNRNS.....LEDVITAI	892
AhHMA5 S.VIAEAKPQDKRAEKVKELQAA..... GHRVAVGGDNDSPALVADVGMAT.GA.....GTDVAIEEADIVLNRNS.....LEDVITAI	910
ZmQ6JAH7 K.VIAEAKPQDKRAEKVKELQLS..... GRTVAVGGDNDSPALVADVGMAT.GA.....GTDVAIEEADIVLNRNS.....LEDVITAI	918
OsHMA5 N.VIAEAKPQDKRAEKVKELQSA..... GRTVAVGGDNDSPALVADVGMAT.GA.....GTDVAIEEADIVLNRNS.....LEDVITAI	929
SbQ6JAG2 K.VIAEAKPQDKRAEKVKELQLS..... GRTVAVGGDNDSPALVADVGMAT.GA.....GTDVAIEEADIVLNRNS.....LEDVITAI	928
SbQ6JAG3 K.VIAEAKPQDKRAEKVKELQLS..... GRTVAVGGDNDSPALVADVGMAT.GA.....GTDVAIEEADIVLNRNS.....LEDVITAI	834

large cytoplasmic loop MSH VII MSH VIIbite of truncation for shortened AhHMA3 variant putative 14-3-3 motif

AhHMA3 (Ws) h..... RLAKRS.....HKKVIEVVLSVSIKGAIVLFGVGYPLVAAVADAGTCLVILNSMILLRDREAVS.....TCYRSSTSPVLEE.....DEVEDLEV	733
AhHMA3 h..... RLAKRS.....HKKVIEVVLSVSIKGAIVLFGVGYPLVAAVADAGTCLVILNSMILLRDREAVS.....TCYRAS.SSPVLEE.....DEADLEV	730
AhHMA2 h..... KLAKRA.....KRRVVENVISITMKGAILALAFAGHPLVAAVADVGTCLVILNSMILLSDKHKTGN.....KCYRESSTSVLAEKLGDAAGDMEAG	730
AhHMA4 h..... KLAKRA.....RRKVVENVCLSIILKAGIILALAFAGHPLVAAVADVGTCLVIFNSMILLREKKTGN.....KCYRSTSKLNGRLEGGDDVVDLAE	740
TcHMA4 h..... KLAKRA.....QRKVLQNVFISITLKVGLVLAFAAGHPLVAAVADVGTCLVILNSMILLREKDKSKIR.....KCYR.....KKVEGDQGLDLAE	736
OsHMA3 h..... RLAKRA.....RRTRAVNVAGSVAVKAAVLAALAAVPRVLAADVGTCLVILNSMILLREKDKSKIR.....EEWKGAKEGDGACRATARSVLRSLQAASQAPNAADG	770
OsHMA2 h..... RLAKRT.....HRTIVNITFSVITKLAIVGLAFAGHPLVAAVADVGTCLVITMSMILLREKDKSKIR.....KCAASHHGSPKCCSSSHGSHAKNNG	725
AhHMA1 h..... AKSRQT.....TSLVKQVALALISIFLAALPSVLGVPVLLVLLHGGTLLVCSNSVRLNDPDSWS.....WKQDVLHLLNR.....SQEPTSSKNS	814
OsHMA1 h..... AKARQT.....TSLVKQSVALLSICVFAALPSVLGFLPLVLLHGGTLLVCSNSTRALNSPTWS.....WDDTRQLTNSLRKYISSKQLSTSSNY	785
<i>EcZntA</i> h..... ELAQAAT.....HANERQNTIILGLKGFVLTLLGMLGLVLAADTQAVIVTANALRLRRR.....LH.....KSETSKNSL.....	732
AhHMA8 (PAA2) h..... SLAQAAT.....MSKVYQNLANAIYNVISIPVIAAGVLLPQDFAMTFLSGLMALSSIFVNS.....LLIQ.....LH.....QSTEQREDLNSRLN.....	856
OsHMA8 h..... SLAQAAT.....MAKVHQLANAVAYNVAIPVIAAGVLLPQDFAMTFLSGLMALSSIFVNS.....LLIQ.....LHGSF.....QSTEQREDLNSRLN.....	914
AhHMA6 (PAA1) h..... ELSKROT.....MKTVKQLWAFYGVNIVGPIAAGVLLPQDFAMTFLSAGALMGVSSLVGMNS.....LLLR.....YRFFSNRNDKVPKEGKQPHENT.....	943
OsHMA7 h..... ELSKRET.....MRTVKQLWAFYGVNIVGPIAAGVLLPQDFAMTFLSAGALMGVSSLVGMNS.....LFLR.....MRLSS.....RQQPHKQATISDVL	938
BtRAN1 h..... DLSRKT.....LTRRLNYVFAMAYNVVSIPIAAGVFPVLRVQLPVAAGACMALSIVSVVCS.....LLLR.....RYKKB.....RLTTLEITKE.....	999
AhHMA7 (RAN1) h..... DLSRKT.....LTRRLNYVFAMAYNVVSIPIAAGVFPVLRVQLPVAAGACMALSIVSVVCS.....LLLR.....RYKKB.....RLTTLEITKE.....	1001
OsHMA6 h..... DLSRKT.....LFRRLNYVFAMAYNVVSIPIAAGVFPVLRVQLPVAAGACMALSIVSVVCS.....LLLR.....RYKKB.....RLTTLEITKE.....	1002
OsHMA4 h..... DLSRKT.....LSRRLNYVVALGYNVLMGPIAAGVFPVLRVQLPVAAGACMALSIVSVVCS.....LLIQ.....LYKKB.....KLVDEVAAGKNDPDL.....	977
AhHMA5 h..... DLSRKT.....FSRRLNYVVALGYNVLMGPIAAGVFPVLRVQLPVAAGACMALSIVSVVCS.....LLLR.....NYKRP.....KLDHLEITRQIPQVRL.....	995
ZmQ6JAH7 h..... DLSRKA.....FFRRLNYVVALGYNVVGPIAAGVFPVLRVQLPVAAGACMALSIVSVVCS.....LLLR.....YKAP.....KIAGTAKEIITTL.....	1001
OsHMA5 h..... DLSRKT.....FFRRLNYVVALGYNVVGPIAAGVFPVLRVQLPVAAGACMALSIVSVVCS.....LLLR.....YKSP.....KLGTR.....	1002
SbQ6JAG2 h..... DLSRKT.....FFRRLNYVVALGYNVVGPIAAGVFPVLRVQLPVAAGACMALSIVSVVCS.....LLLR.....YKSP.....KFDG.....	1002
SbQ6JAG3 h..... DLSRKT.....FFRRLNYVVALGYNVVGPIAAGVFPVLRVQLPVAAGACMALSIVSVVCS.....LLLR.....YKAP.....KIVGS.....	908

650 660 670 680 690 700 710 720 730

A/HMA3 (Ws)	LLQKSE.....ETS.....KKSCSSG.....CCSGPKD	756
A/HMA3	LLQKSE.....ETS.....KKSCSSG.....CCSGPKD	753
A/HMA2	LLPKISDKHKPGCCGKTQEK...AMKPAKASDDHSHGCC.ETKQKDNVTVVKKSCCAEPV.....DLGHGHDSSCGGDKS	804
A/HMA4	LLTKSNGQCKSSCCGDKKNQENVMMKPSKTSDDHSHGCCGDKKQEKVKLVKDGCCSEKTRKSEGDVMSLSSCKKSSHVKHDLKMKGGSGCCASKN	840
TcHMA4	LLSKS...QCNSSCCGDKKSQEKVMLMRPASKTSSDHLHSGCCGKQEKQESVK.LVKDSCCGEKSRRKPEGDMASLSSCKKS...NNDMKMKGGSSCCASKN	829
O _s HMA3	AAGREQTNGCRCCPKPGMSPHESVVDIRADGERQEERPAEAAVAKCCGGGGEGTRCGASKKPT.....ATVVVAKCCGGGGG	850
O _s HMA2	VSHHCSDPCKSMVSCKESSVARNACHDHHHEHHEEPAHKHSNQHGHCHDHSHGHSNCKEPS.....NQLITNKHACHDHGN	804
A/HMA1	LSSAH.....	819
O _s HMA1	VADAVPL.....	792
<i>Ec</i> ZntA	732
A/HMA8 (PAA2)	856
O _s HMA8	914
A/HMA6 (PAA1)	RWKQSS.....	949
O _s HMA7	PNAAESEKSYPSKWSA.....	954
BnRAN1	999
A/HMA7 (RAN1)	1001
O _s HMA6	1002
O _s HMA4	977
A/HMA5	995
ZmQ6JAH7	1001
O _s HMA5	1002
SbQ6JAG2	1002
SbQ6JAG3	908
	740	750
A/HMA3 (Ws)	NQQK.....	760
A/HMA3	NQQK.....	757
A/HMA2	QPPHQHEVQ.....	813
A/HMA4	EKGKEVVAKSCCEKPKQVSVGDCKSGHCEKKQAEDIVVPVQIIGHALTHVEIQLTKETCKTSCCDSKEKVKETGLLLSSENTPYLEKGVLIKDEGN	940
TcHMA4	EKLKEAVVAKSCCEDKERTEGNVEMQIPNLEKGSQKK.....VGETCKSSCCGDKREKAKETRLLASEDPSYLEK.....EE	901
O _s HMA3	GEGTRCGASKNPATAAVVAKCCSGGGGEGIGCGASKKPT.....	889
O _s HMA2	HWRRYEQSARHPSMNCHEHSTCKEELNALPPTN.....	839
A/HMA1	819
O _s HMA1	792
<i>Ec</i> ZntA	732
A/HMA8 (PAA2)	856
O _s HMA8	914
A/HMA6 (PAA1)	949
O _s HMA7	954
BnRAN1	999
A/HMA7 (RAN1)	1001
O _s HMA6	1002
O _s HMA4	977
A/HMA5	995
ZmQ6JAH7	1001
O _s HMA5	1002
SbQ6JAG2	1002
SbQ6JAG3	908
A/HMA3 (Ws)	760
A/HMA3	757
A/HMA2VQQSCHNKPS.....GLDSGCCGKSSQPPHQHE.....LQKSDHKPISGL	853
A/HMA4	CKSGSENMGTVKQSCHEKGCSDKQ.....TGETTLASEEETDD.....QDCSSGCCVNEGTVKQSF.....EKKHSLVKEKGL	1011
TcHMA4	RQTTEANIVTVKQSCHEKASLDIETGVTCDLKLVCNGIEVGEQDLEKGMKLRGECQKSDCCGDEIPLASEEDSVDCSSGCCGNKEELTQICHEKTC	1001
O _s HMA3ATAVVAKCCGGGGEGTRC.....AASKKPATAAVVAKCCGGGGEGTGCGASKRSPPAEGSCS	947
O _s HMA2DHACHGHEHSHCEEPVALHSTG.....EHACHEHEHEHIHCDEPIGSHCADKHAACHDHEQVHEHHCCD	902
A/HMA1	819
O _s HMA1	792
<i>Ec</i> ZntA	732
A/HMA8 (PAA2)	856
O _s HMA8	914
A/HMA6 (PAA1)	949
O _s HMA7	954
BnRAN1	999
A/HMA7 (RAN1)	1001
O _s HMA6	1002
O _s HMA4	977
A/HMA5	995
ZmQ6JAH7	1001
O _s HMA5	1002
SbQ6JAG2	1002
SbQ6JAG3	908
A/HMA3 (Ws)	760
A/HMA3	757
A/HMA2	DITGG.....PKHEGSSTLVNLGDAKEELKVLVNG.....F	885
A/HMA4	DMETGFCCDARLVCCGNTGEGVKEQCR...LEIKREEHCKSSGCCGEEIQTGETTLVSE...EETESTNCGTGC...VDKKEEVTQTC	1089
TcHMA4	DIVS...CDSLKVCCEGTEVEVREQCDLKKGLQIKNEGQCKSVRCGDEKKTEEITTEEDNLKSESGDDCKSLCCGTGLRQEGSSSLVNVVVESEGESGSSC	1098
O _s HMA3	GGEGGTNGVGRCCTSVKRPTCCDHGAEEVSDSSPETAKDCRNGRCCAKTMNSGEVKG.....	1004
O _s HMA2	EQQTPTADLHPCHDHDNLEVEEVKDCHEAPPHHHHHCHEPHDQVKNDTHPVQEH.....	970
A/HMA1	819
O _s HMA1	792
<i>Ec</i> ZntA	732
A/HMA8 (PAA2)	856
O _s HMA8	914
A/HMA6 (PAA1)	949
O _s HMA7	954
BnRAN1	999
A/HMA7 (RAN1)	1001
O _s HMA6	1002
O _s HMA4	977
A/HMA5	995
ZmQ6JAH7	1001
O _s HMA5	1002
SbQ6JAG2	1002
SbQ6JAG3	908

<i>AhHMA3</i> (Ws)	760
<i>AhHMA3</i>	757
<i>AhHMA2</i>	CSSPADLAITS.....LKVKSDSHCKSNCSRRERC.HHGSNCCRSYAKESCSHDHHTTRAHGVGTLKEIVIE	951
<i>AhHMA4</i>	HEKPA ^h SLVVS ^g ...LEVK ^h DEHCESSHRAV ^h KVET ^h CCKV ^h KIP...EACASKCRDRAKR.HSGKSCCRSYAKELCSHRHHHHHHHHHHVSA...	1172
<i>TcHMA4</i>	CSKEGEIVRVSSQSCASP ^h SDVVLSDLEVKKLEICCKAKKTPEEV ^h RGSKCKETEKRRHHV ^h GKSCCRSYAKEYCSHRHHHHHHHHVGA...	1186
<i>OsHMA3</i>	1004
<i>OsHMA2</i>	HEHHHNEEHKAEDCGHHPKPKDCAPPPTDCISRNCSSNTSKGKDICSSSLHRDHHTS...QASRCCRSYVKCSRPSRSCCSHSIVKLPEIVVE..	1059
<i>AhHMA1</i>	819
<i>OsHMA1</i>	792
<i>EcZntA</i>	732
<i>AhHMA8</i> (PAA2)	856
<i>OsHMA8</i>	914
<i>AhHMA6</i> (PAA1)	949
<i>OsHMA7</i>	954
<i>BtRAN1</i>	999
<i>AhHMA7</i> (RAN1)	1001
<i>OsHMA6</i>	1002
<i>OsHMA4</i>	977
<i>AhHMA5</i>	995
<i>ZmQ6JAH7</i>	1001
<i>OsHMA5</i>	1002
<i>SbQ6JAG2</i>	1002
<i>SbQ6JAG3</i>	908

Figure 2: Sequence alignment of 23 P-type IB ATPases.

The amino acids are given in the one-letter-code. The positions of the last residue in the aligned fragments are listed in the right column. Black boxed lowercase letters (**a** to **h**) on top indicate the eight core segments used to produce the phylogenetic tree in Figure 1.5 on page 22. The core segments are based on analyses of Axelsen and Palmgren (1998). The positions of membrane spanning helices (MSHs) and cytoplasmic loops are given on top and correspond to the amino acid sequence of *AhHMA3*. The positions are based on alignments with *EcZntA*, a bacterial P-type IB ATPase with partially known topology, and transmembrane predictions listed at the *aramemnon*-website (aramemnon.botanik.uni-koeln.de). Conserved protein motifs are framed in black boxes. In the N- and C-terminal domain heavy metal associated motifs are emphasised. The invariant phosphorylated aspartate is labeled with a **P**. Moreover, the site of the premature translational stop codon in the wildtype of the Columbia accession of *A. thaliana* due to a single base pair deletion is marked with an black triangle(▲). The potential Zn and Cd binding amino acids cysteine (C), histidine (H), aspartate (D), and glutamate (E) are shaded in blue in the *AhHMA3* protein sequence.

The alignment file was produced using the *MEGA* application version 3.1 (Kumar *et al.*, 2004, default parameters) and *TEXshade* (Beitz, 2000a).

A.3 Sequence alignment of *HMA3* cDNA sequences

		<i>hma3F (BAC Fb)</i>	
AhHMA3-1(BAC1)	ATGGCGGAAGGTGAAGAGCCCAAGAAGA	GAATTTACAGACAAGTTACTTCGACGTCGTTGGAATCTGCT	70
AhHMA3-1(BAC7)	ATGGCGGAAGGTGAAGAGCCCAAGAAGA	GAATTTACAGACAAGTTACTTCGACGTCGTTGGAATCTGCT	70
AhHMA3-2(BAC6)	ATGGCGGAAGGTGAAGAGCCCAAGAAGA	GAATTTACAGACAAGTTACTTCGACGTCGTTGGAATCTGCT	70
AhHMA3-2(Lan3)	ATGGCGGAAGGTGAAGAGCCCAAGAAGA	GAATTTACAGACAAGTTACTTCGACGTCGTTGGAATCTGCT	70
AhHMA3-1	ATGGCGGAAGGTGAAGAGCCCAAGAAGA	GAATTTACAGACAAGTTACTTCGACGTCGTTGGAATCTGCT	70
AtHMA3(Ws)	ATGGCGGAAGGTGAAGAGTCAAAGAAGA	GAATTTACAGACAAGTTACTTCGACGTCGTTGGAATCTGCT	70
AtHMA3(Co1)	ATGGCGGAAGGTGAAGAGTCAAAGAAGA	GAATTTACAGACAAGTTACTTCGACGTCGTTGGAATCTGCT	70
	10 20 30 40 50 60 70		
	<i>hma3F (BAC Fb)</i>		
	→		
	<i>AbHMA3-1-F (BAC7 F) & AbHMA3-2-F (BAC6 F)</i>		
	→		
AhHMA3-1(BAC1)	GTTCATCGGAGGTTTCTATCGTCCGTGACGTTCTCCGTC	CACTTGACGGCGTCAAAGAATTCTCGTTAT	140
AhHMA3-1(BAC7)	GTTCATCGGAGGTTTCTATCGTCCGTGACGTTCTCCGTC	CACTTGACGGCGTCAAAGAATTCTCGTTAT	140
AhHMA3-2(BAC6)	GTTCATCGGAGGTTTCTATCGTACCACGTTCTCCGTC	CACTTGACGGCGTCAAAGAATTCTCGTTAT	140
AhHMA3-2(Lan3)	GTTCATCGGAGGTTTCTATCGTACCACGTTCTCCGTC	CACTTGACGGCGTCAAAGAATTCTCGTTAT	140
AhHMA3-1	GTTCATCGGAGGTTTCTATCGTCCGTGACGTTCTCCGTC	CACTTGACGGCGTCAAAGAATTCTCGTTAT	140
AtHMA3(Ws)	GTTCATCGGAGGTTTCTATCGTAGGTAAAGTTCACGTTCTCCGTC	AAGTGGACGGCGTTAAAGAATTCTCAGTCAT	140
AtHMA3(Co1)	GTTCATCGGAGGTTTCTATCGTAGGTAAAGTTCACGTTCTCCGTC	AAGTGGACGGCGTTAAAGAATTCTCAGTCAT	140
	80 90 100 110 120 130 140		
AhHMA3-1(BAC1)	CGTCCCTTCTAGAACCCTCATCGTTGTCCATGACACTTT	CTTGATTCTCCGTTCAAATCGTCAAGGCT	210
AhHMA3-1(BAC7)	CGTCCCTTCTAGAACCCTCATCGTTGTCCATGACACTTT	CTTGATTCTCCGTTCAAATCGTCAAGGCT	210
AhHMA3-2(BAC6)	CGTCCCTTCTAGAACCCTCATCGTTGTCCATGACACTTT	CTTGATTCTCCGTTCAAATCGTCAAGGCT	210
AhHMA3-2(Lan3)	CGTCCCTTCTAGAACCCTCATCGTTGTCCATGACACTTT	CTTGATTCTCCGTTCAAATCGTCAAGGCT	210
AhHMA3-1	CGTCCCTTCTAGAACCCTCATCGTTGTCCATGACACTTT	CTTGATTCTCCGTTCAAATCGTCAAGGCT	210
AtHMA3(Ws)	CGTCCCTTCTAGAACCCTCATCGTTGTCCATGACTACTTT	CTTGATTCTCCACTTCAAATCGTCAAGGCT	210
AtHMA3(Co1)	CGTCCCTTCTAGAACCCTCATCGTTGTCCATGACTACTTT	CTTGATTCTCCACTTCAAATCGTCAAGGCT	210
	150 160 170 180 190 200 210		
		←	
		<i>AbHMA3-R (BAC R)</i>	
AhHMA3-1(BAC1)	CTGAATCAAGCAGACTAGAAGCAAGTGTAGACCATA	TGGAGAAACAAGCTTGAAGAGTCAATGGCCAA	280
AhHMA3-1(BAC7)	CTGAATCAAGCAGACTAGAAGCAAGTGTAGACCATA	TGGAGAAACAAGCTTGAAGAGTCAATGGCCAA	280
AhHMA3-2(BAC6)	CTGAATCAAGCAGACTAGAAGCAAGTGTAGACCATA	TGGAGAAACAAGCTTGAAGAGTCAATGGCCAA	280
AhHMA3-2(Lan3)	CTGAATCAAGCAGACTAGAAGCAAGTGTAGACCATA	TGGAGAAACAAGCTTGAAGAGTCAATGGCCAA	280
AhHMA3-1	CTGAATCAAGCAGACTAGAAGCAAGTGTAGACCATA	TGGAGAAACAAGCTTGAAGAGTCAATGGCCAA	280
AtHMA3(Ws)	CTGAATCAAGCAGACTAGAAGCAAGTGTAGACCATA	TGGAGAAACAAGCTTGAAGAGTCAATGGCCAA	280
AtHMA3(Co1)	CTGAATCAAGCAGACTAGAAGCAAGTGTAGACCATA	TGGAGAAACAAGCTTGAAGAGTCAATGGCCAA	280
	220 230 240 250 260 270 280		
AhHMA3-1(BAC1)	GTCCCTTTGCAATAGTTTCTGGTGTATTTCTTGC	TCTCTCCTTCTTCAAATACTTTTATAGTCTGCTTGA	350
AhHMA3-1(BAC7)	GTCCCTTTGCAATAGTTTCTGGTGTATTTCTTGC	TCTCTCCTTCTTCAAATACTTTTATAGTCTGCTTGA	350
AhHMA3-2(BAC6)	GTCCCTTTGCAATAGTTTCTGGTGTATTTCTTGC	TCTCTCCTTCTTCAAATACTTTTATAGTCTGCTTGA	350
AhHMA3-2(Lan3)	GTCCCTTTGCAATAGTTTCTGGTGTATTTCTTGC	TCTCTCCTTCTTCAAATACTTTTATAGTCTGCTTGA	350
AhHMA3-1	GTCCCTTTGCAATAGTTTCTGGTGTATTTCTTGC	TCTCTCCTTCTTCAAATACTTTTATAGTCTGCTTGA	350
AtHMA3(Ws)	GCCCTTTGCAATAGTTTCTGGTGTACTCTAGT	TCTCTCCTTCTTCAAATACTTTTATAGTCTGCTTGA	350
AtHMA3(Co1)	GCCCTTTGCAATAGTTTCTGGTGTACTCTAGT	TCTCTCCTTCTTCAAATACTTTTATAGTCTGCTTGA	350
	290 300 310 320 330 340 350		
AhHMA3-1(BAC1)	ATGGCTCGCTGTTGTTGCCGTGGTGGCCGGGAT	TTCCCCATCCTTGCTAAAGCTGTTGCTTCGGTCACA	420
AhHMA3-1(BAC7)	ATGGCTCGCTGTTGTTGCCGTGGTGGCCGGGAT	TTCCCCATCCTTGCTAAAGCTGTTGCTTCGGTCACA	420
AhHMA3-2(BAC6)	ATGGCTCGCTGTTGTTGCCGTGGTGGCCGGGAT	TTCCCCATCCTTGCTAAAGCTGTTGCTTCGGTCACA	420
AhHMA3-2(Lan3)	ATGGCTCGCTGTTGTTGCCGTGGTGGCCGGGAT	TTCCCCATCCTTGCTAAAGCTGTTGCTTCGGTCACA	420
AhHMA3-1	ATGGCTCGCTGTTGTTGCCGTGGTGGCCGGGAT	TTCCCCATCCTTGCTAAAGCTGTTGCTTCGGTCACA	420
AtHMA3(Ws)	ATGGCTCGCTATTGTTGCCGTGGTGGCTGGAGT	TTCCCCATCCTTGCTAAAGCTGTTGCTTCAGTCACA	420
AtHMA3(Co1)	ATGGCTCGCTATTGTTGCCGTGGTGGCTGGAGT	TTCCCCATCCTTGCTAAAGCTGTTGCTTCAGTCACA	420
	360 370 380 390 400 410 420		
AhHMA3-1(BAC1)	AGGTTTCAGCTTGAATCAACGCTCTCACTTTT	ATTGCTGTGATAGCAACTATGTATGCAGGATTTCA	490
AhHMA3-1(BAC7)	AGGTTTCAGCTTGAATCAACGCTCTCACTTTT	ATTGCTGTGATAGCAACTATGTATGCAGGATTTCA	490
AhHMA3-2(BAC6)	AGGTTTCAGCTTGAATCAACGCTCTCACTTTT	ATTGCTGTGATAGCAACTATGTATGCAGGATTTCA	490
AhHMA3-2(Lan3)	AGGTTTCAGCTTGAATCAACGCTCTCACTTTT	ATTGCTGTGATAGCAACTATGTATGCAGGATTTCA	490
AhHMA3-1	AGGTTTCAGCTTGAATCAACGCTCTCACTTTT	ATTGCTGTGATAGCAACTATGTATGCAGGATTTCA	490
AtHMA3(Ws)	AGGTTTCAGCTTGAATCAACGCTCTCACTCTA	ATTGCTGTGATAGCAACTATGTATGCAGGATTTCA	490
AtHMA3(Co1)	AGGTTTCAGCTTGAATCAACGCTCTCACTCTA	ATTGCTGTGATAGCAACTATGTATGCAGGATTTCA	490
	430 440 450 460 470 480 490		

AhHMA3-1 (BAC1)	CAGAAGCTGC	CAAAATTGTGTTT	CTATTCTCAGTTGCAGATTGGCT	A	GAGTCTAGTGTGCTCATAAGGC	560										
AhHMA3-1 (BAC7)	CAGAAGCTGC	CAAAATTGTGTTT	CTATTCTCAGTTGCAGATTGGCT	A	GAGTCTAGTGTGCTCATAAGGC	560										
AhHMA3-2 (BAC6)	CAGAAGCTGC	CAAAATTGTGTTT	CTATTCTCAGTTGCAGATTGGCT	A	GAGTCTAGTGTGCTCATAAGGC	560										
AhHMA3-2 (Lan3)	CAGAAGCTGC	CAAAATTGTGTTT	CTATTCTCAGTTGCAGATTGGCT	A	GAGTCTAGTGTGCTCATAAGGC	560										
AhHMA3-1	CAGAAGCTGC	CAAAATTGTGTTT	CTATTCTCAGTTGCAGATTGGCT	A	GAGTCTAGTGTGCTCATAAGGC	560										
AtHMA3 (Ws)	CAGAAGCTGC	CAAAATTGTGTTT	CTATTCTCAGTTGCAGATTGGCT	T	GAGTCTAGTGTGCTCATAAGGC	560										
AtHMA3 (Co1)	CAGAAGCTGC	CAAAATTGTGTTT	CTATTCTCAGTTGCAGATTGGCT	T	GAGTCTAGTGTGCTCATAAGGC	560										
	500	510	520	530	540	550										
AhHMA3-1 (BAC1)	AAGCA	AGTAATGTCATCACTGATGAGCTTAGCGCCACG	AAAGGCAGTGAT	A	GCGGA	ACTGGAC	ACGAA	630								
AhHMA3-1 (BAC7)	AAGCA	AGTAATGTCATCACTGATGAGCTTAGCGCCACG	AAAGGCAGTGAT	A	GCGGA	ACTGGAC	ACGAA	630								
AhHMA3-2 (BAC6)	AAGCA	AGTAATGTCATCACTGATGAGCTTAGCGCCACG	AAAGGCAGTGAT	A	GCGGA	ACTGGAC	ACGAA	630								
AhHMA3-2 (Lan3)	AAGCA	AGTAATGTCATCACTGATGAGCTTAGCGCCACG	AAAGGCAGTGAT	A	GCGGA	ACTGGAC	ACGAA	630								
AhHMA3-1	AAGCA	AGTAATGTCATCACTGATGAGCTTAGCGCCACG	AAAGGCAGTGAT	A	GCGGA	ACTGGAC	ACGAA	630								
AtHMA3 (Ws)	AAGCA	AGTAATGTCATCACTGATGAGCTTAGCGCCACG	AAAGGCAGTGAT	C	GCGGA	ACTGGACT	AGAA	630								
AtHMA3 (Co1)	AAGCA	AGTAATGTCATCACTGATGAGCTTAGCGCCACG	AAAGGCAGTGAT	C	GCGGA	ACTGGAC	AGAA	630								
	570	580	590	600	610	620	630									
AhHMA3-1 (BAC1)	GT	C	GATGT	AGATGAGGTT	AGGATCAACAC	AA	TGTTTCAGT	G	AAAGCTGGAGAAA	AGTATA	ACC	GAT	T	GATG	700	
AhHMA3-1 (BAC7)	GT	C	GATGT	AGATGAGGTT	AGGATCAACAC	AA	TGTTTCAGT	G	AAAGCTGGAGAAA	AGTATA	ACC	GAT	T	GATG	700	
AhHMA3-2 (BAC6)	GT	C	GATGT	AGATGAGGTT	AGGATCAACAC	AA	TGTTTCAGT	G	AAAGCTGGAGAAA	AGTATA	ACC	GAT	T	GATG	700	
AhHMA3-2 (Lan3)	GT	C	GATGT	AGATGAGGTT	AGGATCAACAC	AA	TGTTTCAGT	G	AAAGCTGGAGAAA	AGTATA	ACC	GAT	T	GATG	700	
AhHMA3-1	GT	C	GATGT	AGATGAGGTT	AGGATCAACAC	AA	TGTTTCAGT	G	AAAGCTGGAGAAA	AGTATA	ACC	GAT	T	GATG	700	
AtHMA3 (Ws)	GT	T	GATGT	AGATGAGGTT	AGGATCAACAC	CG	TGTTTCAGT	T	AAAGCTGGAGAAA	AGTATA	ACC	GAT	C	GATG	700	
AtHMA3 (Co1)	GT	T	GATGT	AGATGAGGTT	AGGATCAACAC	CG	TGTTTCAGT	T	AAAGCTGGAGAAA	AGTATA	ACC	GAT	C	GATG	700	
	640	650	660	670	680	690	700									
AhHMA3-1 (BAC1)	GAGTTGTGGTGGATGGAAGCTGTGATGT	A	GATGAGAAAA	CATTGACAGGAGA	T	CATTCCCTG	TCTCCAA	770								
AhHMA3-1 (BAC7)	GAGTTGTGGTGGATGGAAGCTGTGATGT	A	GATGAGAAAA	CATTGACAGGAGA	T	CATTCCCTG	TCTCCAA	770								
AhHMA3-2 (BAC6)	GAGTTGTGGTGGATGGAAGCTGTGATGT	A	GATGAGAAAA	CATTGACAGGAGA	T	CATTCCCTG	TCTCCAA	770								
AhHMA3-2 (Lan3)	GAGTTGTGGTGGATGGAAGCTGTGATGT	A	GATGAGAAAA	CATTGACAGGAGA	T	CATTCCCTG	TCTCCAA	770								
AhHMA3-1	GAGTTGTGGTGGATGGAAGCTGTGATGT	A	GATGAGAAAA	CATTGACAGGAGA	T	CATTCCCTG	TCTCCAA	770								
AtHMA3 (Ws)	GAGTTGTGGTGGATGGAAGCTGTGATGT	G	GATGAGAAAA	CATTGACAGGAGA	A	T	CATTCCCTG	TCTCCAA	770							
AtHMA3 (Co1)	GAGTTGTGGTGGATGGAAGCTGTGATGT	G	GATGAGAAAA	CATTGACAGGAGA	A	T	CATTCCCTG	TCTCCAA	770							
	710	720	730	740	750	760	770									
AhHMA3-1 (BAC1)	ACAGAGAGAT	TCAACTGTT	TGGCTGCAACCATAAA	TCTTAATGGTTATATAA	AGGTGAAAAC	TACAGCT	840									
AhHMA3-1 (BAC7)	ACAGAGAGAT	TCAACTGTT	TGGCTGCAACCATAAA	TCTTAATGGTTATATAA	AGGTGAAAAC	TACAGCT	840									
AhHMA3-2 (BAC6)	ACAGAGAGAT	TCAACTGTT	TGGCTGCAACCATAAA	TCTTAATGGTTATATAA	AGGTGAAAAC	TACAGCT	840									
AhHMA3-2 (Lan3)	ACAGAGAGAT	TCAACTGTT	TGGCTGCAACCATAAA	TCTTAATGGTTATATAA	AGGTGAAAAC	TACAGCT	840									
AhHMA3-1	ACAGAGAGAT	TCAACTGTT	TGGCTGCAACCATAAA	TCTTAATGGTTATATAA	AGGTGAAAAC	TACAGCT	840									
AtHMA3 (Ws)	ACAGAGAGAT	TCAACTGTT	ATGGCTGCAACCATAAA	TCTTAATGGTTATATAA	AGGTGAAAAC	TACAGCT	840									
AtHMA3 (Co1)	ACAGAGAGAT	TCAACTGTT	ATGGCTGCAACCATAAA	TCTTAATGGTTATATAA	AGGTGAAAAC	TACAGCT	840									
	780	790	800	810	820	830	840									
AhHMA3-1 (BAC1)	CTA	T	CCCCGG	T	ACTGCGT	AGT	T	GCGAAAA	T	GACTAAGCTTGT	A	GAAGAAGCT	CAAAAAAG	CCAAAC	CAAAA	910
AhHMA3-1 (BAC7)	CTA	T	CCCCGG	T	ACTGCGT	AGT	T	GCGAAAA	T	GACTAAGCTTGT	A	GAAGAAGCT	CAAAAAAG	CCAAAC	CAAAA	910
AhHMA3-2 (BAC6)	CTA	T	CCCCGG	T	ACTGCGT	AGT	T	GCGAAAA	T	GACTAAGCTTGT	A	GAAGAAGCT	CAAAAAAG	CCAAAC	CAAAA	910
AhHMA3-2 (Lan3)	CTA	T	CCCCGG	T	ACTGCGT	AGT	T	GCGAAAA	T	GACTAAGCTTGT	A	GAAGAAGCT	CAAAAAAG	CCAAAC	CAAAA	910
AhHMA3-1	CTA	T	CCCCGG	T	ACTGCGT	AGT	T	GCGAAAA	T	GACTAAGCTTGT	A	GAAGAAGCT	CAAAAAAG	CCAAAC	CAAAA	910
AtHMA3 (Ws)	CTA	T	CCCCGG	T	ACTGCGT	AGT	T	GCGAAAA	T	GACTAAGCTTGT	A	GAAGAAGCT	CAAAAAAG	CCAAAC	CAAAA	910
AtHMA3 (Co1)	CTA	T	CCCCGG	T	ACTGCGT	AGT	T	GCGAAAA	T	GACTAAGCTTGT	A	GAAGAAGCT	CAAAAAAG	CCAAAC	CAAAA	910
	850	860	870	880	890	900	910									
AhHMA3-1 (BAC1)	CTCAAAGGTTTATAGA	T	AAATG	T	TCTCGTACTACACTCCAGCTGTTGT	CGTGT	T	AGCAGCATGTTT	GC	980						
AhHMA3-1 (BAC7)	CTCAAAGGTTTATAGA	T	AAATG	T	TCTCGTACTACACTCCAGCTGTTGT	CGTGT	T	AGCAGCATGTTT	GC	980						
AhHMA3-2 (BAC6)	CTCAAAGGTTTATAGA	T	AAATG	T	TCTCGTACTACACTCCAGCTGTTGT	CGTGT	T	AGCAGCATGTTT	GC	980						
AhHMA3-2 (Lan3)	CTCAAAGGTTTATAGA	T	AAATG	T	TCTCGTACTACACTCCAGCTGTTGT	CGTGT	T	AGCAGCATGTTT	GC	980						
AhHMA3-1	CTCAAAGGTTTATAGA	T	AAATG	T	TCTCGTACTACACTCCAGCTGTTGT	CGTGT	T	AGCAGCATGTTT	GC	980						
AtHMA3 (Ws)	CTCAAAGGTTTATAGA	T	AAATG	T	TCTCGTACTACACTCCAGCTGTTGT	CGTGT	T	AGCAGCATGTTT	GC	980						
AtHMA3 (Co1)	CTCAAAGGTTTATAGA	T	AAATG	T	TCTCGTACTACACTCCAGCTGTTGT	CGTGT	T	AGCAGCATGTTT	GC	980						
	920	930	940	950	960	970	980									
AhHMA3-1 (BAC1)	GGT	GAT	CCCCGTA	T	TGTTAAAG	T	TTCAG	G	ACCCTTAGCCATTGGTTT	CACTTAG	CAC	TGTAGT	GTTAGTA	1050		
AhHMA3-1 (BAC7)	GGT	GAT	CCCCGTA	T	TGTTAAAG	T	TTCAG	G	ACCCTTAGCCATTGGTTT	CACTTAG	CAC	TGTAGT	GTTAGTA	1050		
AhHMA3-2 (BAC6)	GGT	GAT	CCCCGTA	T	TGTTAAAG	T	TTCAG	G	ACCCTTAGCCATTGGTTT	CACTTAG	CAC	TGTAGT	GTTAGTA	1050		
AhHMA3-2 (Lan3)	GGT	GAT	CCCCGTA	T	TGTTAAAG	T	TTCAG	G	ACCCTTAGCCATTGGTTT	CACTTAG	CAC	TGTAGT	GTTAGTA	1050		
AhHMA3-1	GGT	GAT	CCCCGTA	T	TGTTAAAG	T	TTCAG	G	ACCCTTAGCCATTGGTTT	CACTTAG	CAC	TGTAGT	GTTAGTA	1050		
AtHMA3 (Ws)	GGT	AAT	CCCCGTA	T	TGTTAAAG	T	TTCAG	A	ACCCTTAGCCATTGGTTT	CACTTAG	CAC	TGTAGT	GTTAGTA	1050		
AtHMA3 (Co1)	GGT	AAT	CCCCGTA	T	TGTTAAAG	T	TTCAG	A	ACCCTTAGCCATTGGTTT	CACTTAG	CAC	TGTAGT	GTTAGTA	1050		
	990	1000	1010	1020	1030	1040	1050									

AhHMA3-1(BAC1)	AGTGGTTGTCCATGTGGTCTTATCTATCCACACCTGTTGCTACCTTTTGTGCTCTCACTAAGGCAGCCA	1120
AhHMA3-1(BAC7)	AGTGGTTGTCCATGTGGTCTTATCTATCCACACCTGTTGCTACCTTTTGTGCTCTCACTAAGGCAGCCA	1120
AhHMA3-2(BAC6)	AGTGGTTGTCCATGTGGTCTTATCTATCCACACCTGTTGCTACCTTTTGTGCTCTCACTAAGGCAGCCA	1120
AhHMA3-2(Lan3)	AGTGGTTGTCCATGTGGTCTTATCTATCCACACCTGTTGCTACCTTTTGTGCTCTCACTAAGGCAGCCA	1120
AhHMA3-1	AGTGGTTGTCCATGTGGTCTTATCTATCCACACCTATTGCTACCTTTTGTGCTCTCACTAAGGCAGCCA	1120
AtHMA3(Ws)	AGTGGTTGTCCCTGTGGTCTTATCTATCCACACCTGTTGCTACCTTTTGTGCTCTCACTAAGGCAGCCA	1120
AtHMA3(Co1)	AGTGGTTGTCCCTGTGGTCTTATCTATCCACACCTGTTGCTACCTTTTGTGCTCTCACTAAGGCAGCCA	1120
	1060 1070 1080 1090 1100 1110 1120	
AhHMA3-1(BAC1)	TGTCGGGCTTTCTGATCAAAAAGCTGGTATTGTCTAGAGACTCTTGCAAAGATCAAGATTGTTGCTTTTGA	1190
AhHMA3-1(BAC7)	TGTCGGGCTTTCTGATCAAAAAGCTGGTATTGTCTAGAGACTCTTGCAAAGATCAAGATTGTTGCTTTTGA	1190
AhHMA3-2(BAC6)	TGTCGGGCTTTCTGATCAAAAAGCTGGTATTGTCTAGAGACTCTTGCAAAGATCAAGATTGTTGCTTTTGA	1190
AhHMA3-2(Lan3)	TGTCGGGCTTTCTGATCAAAAAGCTGGTATTGTCTAGAGACTCTTGCAAAGATCAAGATTGTTGCTTTTGA	1190
AhHMA3-1	TGTCGGGCTTTCTGATCAAAAAGCTGGTATTGTCTAGAGACTCTTGCAAAGATCAAGATTGTTGCTTTTGA	1190
AtHMA3(Ws)	CGTCAGGCTTTCTGATCAAAAAGCTGGTATTGTCTAGAGACTTGAAGCAAAGATCAAGATTGTTGCTTTTGA	1190
AtHMA3(Co1)	CGTCAGGCTTTCTGATCAAAAAGCTGGTATTGTCTAGAGACTTGAAGCAAAGATCAAGATTGTTGCTTTTGA	1190
	1130 1140 1150 1160 1170 1180 1190	
AhHMA3-1(BAC1)	CAAAACAGGAAGCTATTACAAAGGCTGAGTTCATGGTCTCGGATTTAGGCTCTTTTCTCAATATCAAT	1260
AhHMA3-1(BAC7)	CAAAACAGGAAGCTATTACAAAGGCTGAGTTCATGGTCTCGGATTTAGGCTCTTTTCTCAATATCAAT	1260
AhHMA3-2(BAC6)	CAAAACAGGAAGCTATTACAAAGGCTGAGTTCATGGTCTCGGATTTAGGCTCTTTTCTCAATATCAAT	1260
AhHMA3-2(Lan3)	CAAAACAGGAAGCTATTACAAAGGCTGAGTTCATGGTCTCGGATTTAGGCTCTTTTCTCAATATCAAT	1260
AhHMA3-1	CAAAACAGGAAGCTATTACAAAGGCTGAGTTCATGGTCTCGGATTTAGGCTCTTTTCTCAATATCAAT	1260
AtHMA3(Ws)	CAAAACAGGAAGCTATTACAAAGGCTGAGTTCATGGTCTCGGATTTAGGCTCTTTTCTCAAGTATCAAC	1260
AtHMA3(Co1)	CAAAACAGGAAGCTATTACAAAGGCTGAGTTCATGGTCTCGGATTTAGGCTCTTTTCTCAAGTATCAAC	1260
	1200 1210 1220 1230 1240 1250 1260	
AhHMA3-1(BAC1)	CTGCACAACTTGCTTTACTGGGTCTCAGCATTGAGAGCAAGTCAAGTTCATCCGATGGCAGCGGCGCTTA	1330
AhHMA3-1(BAC7)	CTGCACAACTTGCTTTACTGGGTCTCAGCATTGAGAGCAAGTCAAGTTCATCCGATGGCAGCGGCGCTTA	1330
AhHMA3-2(BAC6)	CTGCACAACTTGCTTTACTGGGTCTCAGCATTGAGAGCAAGTCAAGTTCATCCGATGGCAGCGGCGCTTA	1330
AhHMA3-2(Lan3)	CTGCACAACTTGCTTTACTGGGTCTCAGCATTGAGAGCAAGTCAAGTTCATCCGATGGCAGCGGCGCTTA	1330
AhHMA3-1	CTGCACAACTTGCTTTACTGGGTCTCAGCATTGAGAGCAAGTCAAGTTCATCCGATGGCAGCGGCGCTTA	1330
AtHMA3(Ws)	CTGCACAACTTGCTTTACTGGGTCTCAAGCATTGAGTGAAGTCAAGTTCATCCGATGGCAGCTGGCGCTTA	1330
AtHMA3(Co1)	CTGCACAACTTGCTTTACTGGGTCTCAAGCATTGAGTGAAGTCAAGTTCATCCGATGGCAGCTGGCGCTTA	1330
	1270 1280 1290 1300 1310 1320 1330	
AhHMA3-1(BAC1)	TTGACTATGCAAGATCAGTTTCTGTTGAGCCTAAGCCTGATCTGTTGAGAACTTTCAAACCTTTCCAGG	1400
AhHMA3-1(BAC7)	TTGACTATGCAAGATCAGTTTCTGTTGAGCCTAAGCCTGATCTGTTGAGAACTTTCAAACCTTTCCAGG	1400
AhHMA3-2(BAC6)	TTGACTATGCAAGATCAGTTTCTGTTGAGCCTAAGCCTGATCTGTTGAGAACTTTCAAACCTTTCCAGG	1400
AhHMA3-2(Lan3)	TTGACTATGCAAGATCAGTTTCTGTTGAGCCTAAGCCTGATCTGTTGAGAACTTTCAAACCTTTCCAGG	1400
AhHMA3-1	TTGACTATGCAAGATCAGTTTCTGTTGAGCCTAAGCCTGATCTGTTGAGAACTTTCAAACCTTTCCAGG	1400
AtHMA3(Ws)	TTGACTATGCAAGATCAGTTTCTGTTGAGCCTAAGCCTGATATAGTCTGAGAACTTTCAAGAACTTTCCAGG	1400
AtHMA3(Co1)	TTGACTATGCAAGATCAGTTTCTGTTGAGCCTAAGCCTGATATAGTCTGAGAACTTTCAAGAACTTTCCAGG	1400
	1340 1350 1360 1370 1380 1390 1400	
AhHMA3-1(BAC1)	AGAAGGAGTTTATGGGAGAATAGATGGTCAAGATATCTACATTGGAAACAAAAGAATGTCACAGAGAGCT	1470
AhHMA3-1(BAC7)	AGAAGGAGTTTATGGGAGAATAGATGGTCAAGATATCTACATTGGAAACAAAAGAATGTCACAGAGAGCT	1470
AhHMA3-2(BAC6)	AGAAGGAGTTTATGGGAGAATAGATGGTCAAGATATCTACATTGGAAACAAAAGAATGTCACAGAGAGCT	1470
AhHMA3-2(Lan3)	AGAAGGAGTTTATGGGAGAATAGATGGTCAAGATATCTACATTGGAAACAAAAGAATGTCACAGAGAGCT	1470
AhHMA3-1	AGAAGGAGTTTATGGGAGAATAGATGGTCAAGATATCTACATTGGAAACAAAAGAATGTCACAGAGAGCT	1470
AtHMA3(Ws)	AGAAGGAGTTTATGGGAGAATAGATGGTCAAGATATCTACATTGGAAACAAAAGAATAGCACAGAGAGCT	1470
AtHMA3(Co1)	AGAAGGAGTTTATGGGAGAATAGATGGTCAAGATATCTACATTGGAAACAAAAGAATAGCACAGAGAGCT	1470
	1410 1420 1430 1440 1450 1460 1470	
AhHMA3-1(BAC1)	GGATGCTTAACAG TTCCGGATAT . GAAAGCTAATATGAAGCGAGGTAAGACCATTGGTTACATA	1533
AhHMA3-1(BAC7)	GGATGCTTAACAG TTCCGGATAT . GAAAGCTAATATGAAGCGAGGTAAGACCATTGGTTACATA	1533
AhHMA3-2(BAC6)	GGATGCTTAACAG TTCCGGATAT . GAAAGCTAATATGAAGCGAGGTAAGACCATTGGTTACATA	1533
AhHMA3-2(Lan3)	GGATGCTTAACAG TTCCGGATAT . GAAAGCTAATATGAAGCGAGGTAAGACCATTGGTTACATA	1533
AhHMA3-1	GGATGCTTAACAG TTCCGGATAT . GGAAGCTAATATGAAGCGAGGTAAGACCATTGGTTACATA	1533
AtHMA3(Ws)	GGATGCTTAACAGATAATGTTCCGGATAT . TGAAGCTACTATGAAGCGAGGTAAGACCATTGGTTACATA	1539
AtHMA3(Co1)	GGATGCTTAACAGATAATGTTCCGGATAT . TGAAGCTACTATGAAGCGAGGTAAGACCATTGGTTACATA	1539
	1480 1490 1500 1510 1520 1530	
AhHMA3-1(BAC1)	TACATGGAGCAAAAAGCTG . CCGGAAGTTTCAACCTTATGACGGTTGTCGATATGGGGTTGCTCAAGCTC	1603
AhHMA3-1(BAC7)	TACATGGAGCAAAAAGCTG . CCGGAAGTTTCAACCTTATGACGGTTGTCGATATGGGGTTGCTCAAGCTC	1603
AhHMA3-2(BAC6)	TACATGGAGCAAAAAGCTG . CCGGAAGTTTCAACCTTATGACGGTTGTCGATATGGGGTTGCTCAAGCTC	1603
AhHMA3-2(Lan3)	TACATGGAGCAAAAAGCTG . CCGGAAGTTTCAACCTTATGACGGTTGTCGATATGGGGTTGCTCAAGCTC	1603
AhHMA3-1	TACATGGAGCAAAAAGCTG . CCGGAAGTTTCAACCTTATGACAGTTGTCGATATGGGGTTGCTCAAGCTC	1603
AtHMA3(Ws)	TACATGGGAGCAAAAAGCTG . CCGGAAGTTTCAACCTTITGATGGTTGTCGATATGGGGTTGCTCAAGCTC	1609
AtHMA3(Co1)	TACATGGGAGCAAAAAGCTG . CCGGAAGTTTCAACCTTITGATGGTTGTCGATATGGGGTTGCTCAAGCTC	1609
	1540 1550 1560 1570 1580 1590 1600	

single base pair deletion

AhHMA3-1 (BAC1)	TCAAGGAGCTTAAAGTCTTTAGGAATCAA	AAACTGCAATGCTCACAGGAGATAACC	GAGACGCAGCCCTGTC	1673	
AhHMA3-1 (BAC7)	TCAAGGAGCTTAAAGTCTTTAGGAATCAA	AAACTGCAATGCTCACAGGAGATAACC	GAGACGCAGCCCTGTC	1673	
AhHMA3-2 (BAC6)	TCAAGGAGCTTAAAGTCTTTAGGAATCAA	AAACTGCAATGCTCACAGGAGATAACC	GAGACGCAGCCCTGTC	1673	
AhHMA3-2 (Lan3)	TCAAGGAGCTTAAAGTCTTTAGGAATCAA	AAACTGCAATGCTCACAGGAGATAACC	GAGACGCAGCCCTGTC	1673	
AhHMA3-1	TCAAGGAGCTTAAAGTCTTTAGGAATCAA	AAACTGCAATGCTCACAGGAGATAACC	GAGACGCAGCCCTGTC	1673	
AtHMA3 (Ws)	TAAAGGAACCTCAAATCTTTAGGAATCAA	AAACTGCAATGCTCACAGGAGATAACC	AAGACGCAGCTATGTC	1679	
AtHMA3 (Co1)	TAAAGGAACCTCAAATCTTTAGGAATCAA	AAACTGCAATGCTCACAGGAGATAACC	AAGACGCAGCTATGTC	1678	
	1610 1620 1630 1640 1650 1660 1670				
AhHMA3-1 (BAC1)	TACTCAAGAACAGTTAGAGAATGCTTTGGATATTGTTCACTCTGAACT	CCTTCCACAAGACAAAAGCAAGA	1743		
AhHMA3-1 (BAC7)	TACTCAAGAACAGTTAGAGAATGCTTTGGATATTGTTCACTCTGAACT	CCTTCCACAAGACAAAAGCAAGA	1743		
AhHMA3-2 (BAC6)	TACTCAAGAACAGTTAGAGAATGCTTTGGATATTGTTCACTCTGAACT	CCTTCCACAAGACAAAAGCAAGA	1743		
AhHMA3-2 (Lan3)	TACTCAAGAACAGTTAGAGAATGCTTTGGATATTGTTCACTCTGAACT	CCTTCCACAAGACAAAAGCAAGA	1743		
AhHMA3-1	TACTCAAGAACAGTTAGAGAATGCTTTGGATATTGTTCACTCTGAACT	CCTTCCACAAGACAAAAGCAAGA	1743		
AtHMA3 (Ws)	TACTCAAGAACAGTTAGAGAATGCTTTGGATATTGTTCACTCTGAACT	CCTTCCACAAGACAAAAGCAAGA	1749		
AtHMA3 (Co1)	TACTCAAGAACAGTTAGAGAATGCTTTGGATATTGTTCACTCTGAACT	CCTTCCACAAGACAAAAGCAAGA	1748		
	1680 1690 1700 1710 1720 1730 1740				
AhHMA3-1 (BAC1)	ATCATGATGAAATTC AAGATCCAAGGGCC	TACAATGATGGTAGGAGA	GGGCTTAAACGATGC	CCGGCTT	1813
AhHMA3-1 (BAC7)	ATCATGATGAAATTC AAGATCCAAGGGCC	TACAATGATGGTAGGAGA	GGGCTTAAACGATGC	CCGGCTT	1813
AhHMA3-2 (BAC6)	ATCATGATGAAATTC AAGATCCAAGGGCC	TACAATGATGGTAGGAGA	GGGCTTAAACGATGC	CCGGCTT	1813
AhHMA3-2 (Lan3)	ATCATGATGAAATTC AAGATCCAAGGGCC	TACAATGATGGTAGGAGA	GGGCTTAAACGATGC	CCGGCTT	1813
AhHMA3-1	ATCATGATGAAATTC AAGATCCAAGGGCC	TACAATGATGGTAGGAGA	GGGCTTAAACGATGC	CCGGCTT	1813
AtHMA3 (Ws)	ATCATGATGAAATTC AAGATCCAAGGGCC	TACAATGATGGTAGGAGA	GGGCTTAAACGATGC	CCGGCTT	1819
AtHMA3 (Co1)	ATCATGATGAAATTC AAGATCCAAGGGCC	TACAATGATGGTAGGAGA	GGGCTTAAACGATGC	CCGGCTT	1818
	1750 1760 1770 1780 1790 1800 1810				
AhHMA3-1 (BAC1)	TAGCGAAAGCAGACATTGGCCTTTC	AATGGGGATCTCAGGGTCAGCACTT	GCAACAGAGACAGGAGACAT	1883	
AhHMA3-1 (BAC7)	TAGCGAAAGCAGACATTGGCCTTTC	AATGGGGATCTCAGGGTCAGCACTT	GCAACAGAGACAGGAGACAT	1883	
AhHMA3-2 (BAC6)	TAGCGAAAGCAGACATTGGCCTTTC	AATGGGGATCTCAGGGTCAGCACTT	GCAACAGAGACAGGAGACAT	1883	
AhHMA3-2 (Lan3)	TAGCGAAAGCAGACATTGGCCTTTC	AATGGGGATCTCAGGGTCAGCACTT	GCAACAGAGACAGGAGACAT	1883	
AhHMA3-1	TAGCGAAAGCAGACATTGGCCTTTC	AATGGGGATCTCAGGGTCAGCACTT	GCAACAGAGACAGGAGACAT	1883	
AtHMA3 (Ws)	TAGCGAAAGCAGACATTGGTATATTC	CATGGGGATCTCAGGGTCAGCACTT	GCAACAGAGACAGGAGACAT	1889	
AtHMA3 (Co1)	TAGCGAAAGCAGACATTGGTATATTC	CATGGGGATCTCAGGGTCAGCACTT	GCAACAGAGACAGGAGACAT	1888	
	1820 1830 1840 1850 1860 1870 1880				
AhHMA3-1 (BAC1)	CATTCTTATGTCAAACGATATAAGGAAGAT	CCGAAAGGGATGAGACTAGCGAAGAGA	GTCTATAAGAAA	1953	
AhHMA3-1 (BAC7)	CATTCTTATGTCAAACGATATAAGGAAGAT	CCGAAAGGGATGAGACTAGCGAAGAGA	GTCTATAAGAAA	1953	
AhHMA3-2 (BAC6)	CATTCTTATGTCAAACGATATAAGGAAGAT	CCGAAAGGGATGAGACTAGCGAAGAGA	GTCTATAAGAAA	1953	
AhHMA3-2 (Lan3)	CATTCTTATGTCAAACGATATAAGGAAGAT	CCGAAAGGGATGAGACTAGCGAAGAGA	GTCTATAAGAAA	1953	
AhHMA3-1	CATTCTTATGTCAAACGATATAAGGAAGAT	CCGAAAGGGATGAGACTAGCGAAGAGA	GTCTATAAGAAA	1953	
AtHMA3 (Ws)	CATTCTTATGTCAAACGATATAAGGAAGAT	CCGAAAGGGATGAGACTAGCGAAGAGA	GTCTATAAGAAA	1959	
AtHMA3 (Co1)	CATTCTTATGTCAAACGATATAAGGAAGAT	CCGAAAGGGATGAGACTAGCGAAGAGA	GTCTATAAGAAA	1958	
	1890 1900 1910 1920 1930 1940 1950				
AhHMA3-1 (BAC1)	GTGATTGAGAAATGTGTTTTGCTGTGAGCATA	AAAAGGAGCAATCATGGTTCTTG	GTTTTGTAGGTTACC	2023	
AhHMA3-1 (BAC7)	GTGATTGAGAAATGTGTTTTGCTGTGAGCATA	AAAAGGAGCAATCATGGTTCTTG	GTTTTGTAGGTTACC	2023	
AhHMA3-2 (BAC6)	GTGATTGAGAAATGTGTTTTGCTGTGAGCATA	AAAAGGAGCAATCATGGTTCTTG	GTTTTGTAGGTTACC	2023	
AhHMA3-2 (Lan3)	GTGATTGAGAAATGTGTTTTGCTGTGAGCATA	AAAAGGAGCAATCATGGTTCTTG	GTTTTGTAGGTTACC	2023	
AhHMA3-1	GTGATTGAGAAATGTGTTTTGCTGTGAGCATA	AAAAGGAGCAATCATGGTTCTTG	GTTTTGTAGGTTACC	2023	
AtHMA3 (Ws)	GTGATTGAGAAATGTGTTTTGCTGTGAGCATA	AAAAGGAGCAATCATGGTTCTTG	GTTTTGTAGGTTACC	2029	
AtHMA3 (Co1)	GTGATTGAGAAATGTGTTTTGCTGTGAGCATA	AAAAGGAGCAATCATGGTTCTTG	GTTTTGTAGGTTACC	2028	
	1960 1970 1980 1990 2000 2010 2020				
AhHMA3-1 (BAC1)	CTCTGGTTTGGGCAGCTGTCTTGCAGATGCA	GGAACCTTGTGTTGCTTGTGATACTCAATAGTATGAT	GCT	2093	
AhHMA3-1 (BAC7)	CTCTGGTTTGGGCAGCTGTCTTGCAGATGCA	GGAACCTTGTGTTGCTTGTGATACTCAATAGTATGAT	GCT	2093	
AhHMA3-2 (BAC6)	CTCTGGTTTGGGCAGCTGTCTTGCAGATGCA	GGAACCTTGTGTTGCTTGTGATACTCAATAGTATGAT	GCT	2093	
AhHMA3-2 (Lan3)	CTCTGGTTTGGGCAGCTGTCTTGCAGATGCA	GGAACCTTGTGTTGCTTGTGATACTCAATAGTATGAT	GCT	2093	
AhHMA3-1	CTCTGGTTTGGGCAGCTGTCTTGCAGATGCA	GGAACCTTGTGTTGCTTGTGATACTCAATAGTATGAT	GCT	2093	
AtHMA3 (Ws)	CTCTGGTTTGGGCAGCTGTCTTGCAGATGCA	GGAACCTTGTGTTGCTTGTGATACTCAATAGTATGAT	GCT	2099	
AtHMA3 (Co1)	CTCTGGTTTGGGCAGCTGTCTTGCAGATGCA	GGAACCTTGTGTTGCTTGTGATACTCAATAGTATGAT	GCT	2098	
	2030 2040 2050 2060 2070 2080 2090				
AhHMA3-1 (BAC1)	TCTACGCGATGAGCGTGAAGCCGTGTCTACATGTTACCGT	GCTTCTTCTTCTTCCCGGTGAAA	CCTTGAG	2163	
AhHMA3-1 (BAC7)	TCTACGCGATGAGCGTGAAGCCGTGTCTACATGTTACCGT	GCTTCTTCTTCTTCCCGGTGAAA	CCTTGAG	2163	
AhHMA3-2 (BAC6)	TCTACGCGATGAGCGTGAAGCCGTGTCTACATGTTACCGT	GCTTCTTCTTCTTCCCGGTGAAA	CCTTGAG	2163	
AhHMA3-2 (Lan3)	TCTACGCGATGAGCGTGAAGCCGTGTCTACATGTTACCGT	GCTTCTTCTTCTTCCCGGTGAAA	CCTTGAG	2163	
AhHMA3-1	TCTACGCGATGAGCGTGAAGCCGTGTCTACATGTTACCGT	GCTTCTTCTTCTTCCCGGTGAAA	CCTTGAG	2160	
AtHMA3 (Ws)	TCTACGCGATGAGCGTGAAGCCGTGTCTACATGTTACCGT	GCTTCTTCTTCTTCCCGGTGAAA	CCTTGAG	2169	
AtHMA3 (Co1)	TCTACGCGATGAGCGTGAAGCCGTGTCTACATGTTACCGT	GCTTCTTCTTCTTCCCGGTGAAA	CCTTGAG	2168	
	2100 2110 2120 2130 2140 2150 2160				

AhHMA3-1(BAC1)	GAGGATGAAG	CAGAGGATCTAGAAGT	TGGCTTGGTTCAGAAGA	GTGAGGAGACAA	GTAAAAAGAGTTGTT	2233
AhHMA3-1(BAC7)	GAGGATGAAG	CAGAGGATCTAGAAGT	TGGCTTGGTTCAGAAGA	GTGAGGAGACAA	GTAAAAAGAGTTGTT	2233
AhHMA3-2(BAC6)	GAGGATGAAG	CAGAGGATCTAGAAGT	TGGCTTGGTTCAGAAGA	GTGAGGAGACAA	GTAAAAAGAGTTGTT	2233
AhHMA3-2(Lan3)	GAGGATGAAG	CAGAGGATCTAGAAGT	TGGCTTGGTTCAGAAGA	GTGAGGAGACAA	GTAAAAAGAGTTGTT	2233
AhHMA3-1	GAGGATGAAG	CAGAGGATCTAGAAGT	TGGCTTGGTTCAGAAGA	GTGAGGAGACAA	GTAAAAAGAGTTGTT	2230
AtHMA3(Ws)	GAGGATGAAG	TAGAGGATCTAGAAGT	TGGCTTGGTTCAGAAGA	GTGAGGAGACAA	GTAAAAAGAGTTGTT	2239
AtHMA3(Co1)	GAGGATGAAG	TAGAGGATCTAGAAGT	TGGCTTGGTTCAGAAGA	GTGAGGAGACAA	GTAAAAAGAGTTGTT	2238
	2170	2180	2190	2200	2210	2220
AhHMA3-1(BAC1)	GCTCTGGTT	TTGTAGT	AGC	CCTAAGGACAATCAACAAAAGTGA	2277	
AhHMA3-1(BAC7)	GCTCTGGTT	TTGTAGT	GGC	CCTAAGGACAATCAACAAAAGTGA	2277	
AhHMA3-2(BAC6)	GCTCTGGTT	TTGTAGT	GGC	CCTAAGGACAATCAACAAAAGTGA	2277	
AhHMA3-2(Lan3)	GCTCTGGTT	TTGTAGT	GGC	CCTAAGGACAATCAACAAAAGTGA	2277	
AhHMA3-1	GCTCTGGTT	TTGTAGT	GGC	CCTAAGGACAATCAACAAAAGTGA	2274	
AtHMA3(Ws)	GCTCTGGTT	TTGTAGT	GGC	CCTAAGGACAATCAACAAAAGTGA	2283	
AtHMA3(Co1)	GCTCTGGTT	TTGTAGT	GGC	CCTAAGGACAATCAACAAAAGTGA	2282	
	2240	2250	2260	2270		
	X	X	X	X		
	X	X	X	X		
	X	X	X	X		

X non conserved
X conserved
X all match

Figure 3: Alignment of HMA3 cDNA sequences.

The alignment of different *HMA3* cDNA sequences is shown. Primers that were used for the copy-specific detection of *AhHMA3* variants are labeled as black arrows (→) on top. The site of the single base pair deletion that leads to a premature translational stop codon in the wildtype of the Columbia accession of *A. thaliana* is marked with an black arrow (↓).

The alignment file was produced using the *MEGA* application version 3.1 (Kumar *et al.*, 2004, default parameters) and *TEXshade* (Beitz, 2000a).

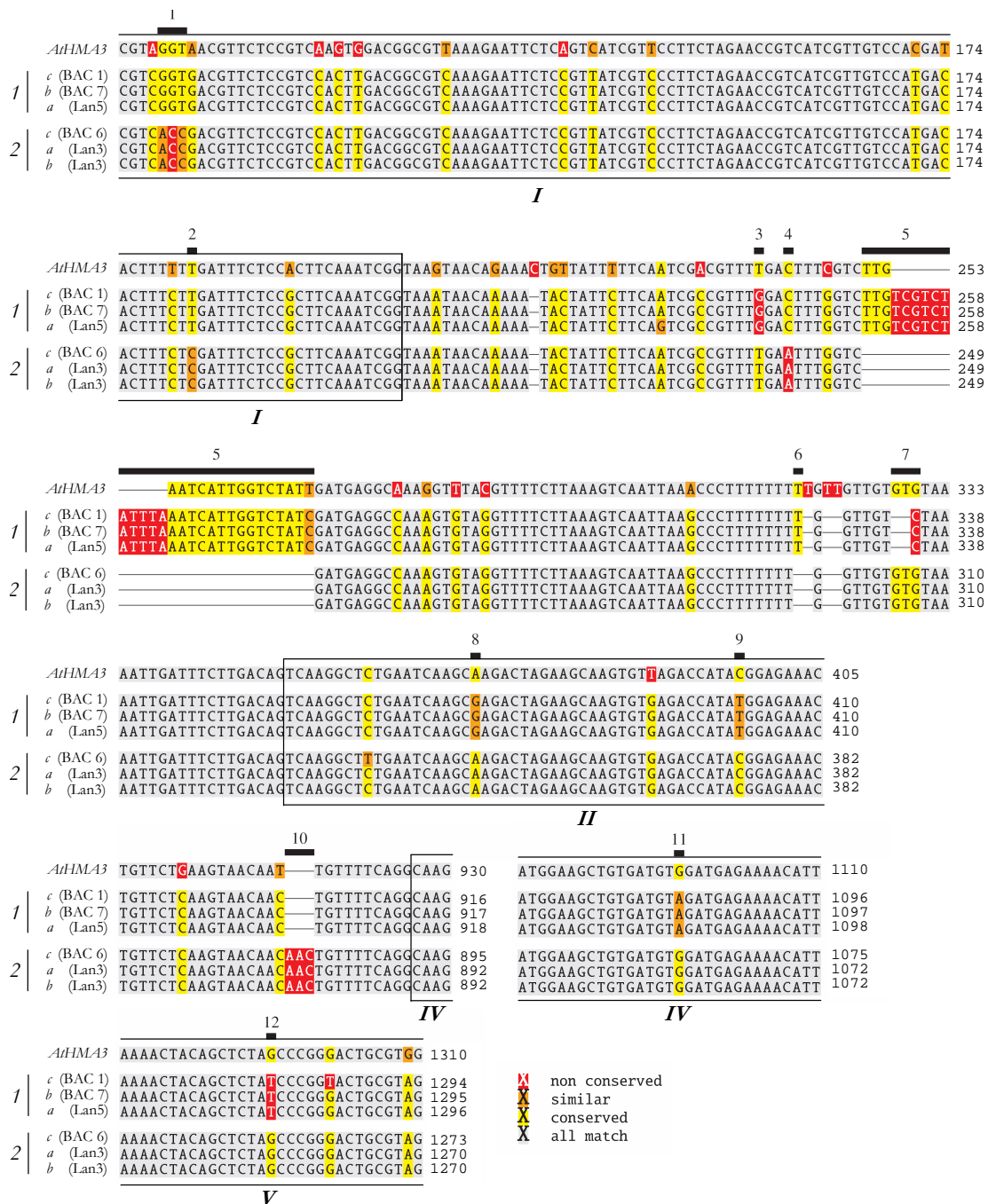


Figure 4: Variant-specific features of genomic *HMA3* sequences.

An alignment of genomic DNA sequences is shown that feature differences specific to *HMA3* variants from *A. halleri*. Genomic sequences of *A. halleri* were obtained from Lan3.1 and Lan5 individuals from the Langelsheim accession and from clones No.1, 6, and 7 of a BAC library (accession Rodacherbrunn and Stutenkamm, Southern Thuringia, *Schiefergebirge*; see Section 1.1.2 on page 59). The *AhHMA3* sequence was amplified by PCR using the primer pair V01 F & V01 R, cloned in the pCR2.1TOPO[®] vector and sequenced. The sequences are compared to the *HMA3* sequence of *A. thaliana*, accession Columbia (AGI number: At4g30120). The *AtHMA3* sequence and its annotated gene structure was obtained from the *TIGR A. thaliana* database (www.tigr.org). The gene structure of *AhHMA3* was determined by comparing genomic sequences with cDNA sequences.

Features that distinguish between *AhHMA3* variants are labeled with numbers on top. Black frames, labeled with roman numbers, mark the exons of *HMA3*. The numbers “1” and “2” at the left side mark the two clearly distinct groups of *AhHMA3* sequences, designated *AhHMA3-1* and *AhHMA3-2*.

The alignment file was produced using the *MEGA* application version 3.1 (Kumar *et al.*, 2004, default parameters) and visualised by *TEXshade* (Beitz, 2000a). Nucleotide positions are shaded as follows: ■ all match (100% identical nucleotides), ■ conserved (more than 50% identity); ■ similar (less than 50% identity but all are purine or pyrimidine nucleotides); ■ non conserved (less than 50% and mixed purine/pyrimidine)

B Eidesstattliche Erklärung

Hiermit erkläre ich, dass ich die vorliegende Arbeit selbständig angefertigt und nur die von mir angegebenen Quellen und Hilfsmittel verwendet habe. Ich versichere ebenfalls, dass diese Arbeit an keiner anderen Einrichtung zur Begutachtung eingereicht wurde.

Potsdam, März 2007

Toni Hoffmann

C Curriculum Vitæ

Personal Information

Name Toni Hoffmann
 Date of Birth March 2nd, 1976
 Nationality German
 Address Nansenstrasse 10
 14471 Potsdam
 Germany
 Phone +49 331 967 96 05
 Email toni.hoffmann@gmail.com

Education

10/2002 - 01/2006 Max-Planck-Institute of Molecular Plant Physiology, Potsdam, Germany
Ph.D. in Biology
 10/1994 - 03/2001 Martin-Luther-University Halle-Wittenberg, Faculty of Biology, Halle/Saale, Germany
Study of Biology
Diplom (Master of Science): 03/2001
 07/1994 Thomas-Müntzer-Gymnasium, Halle/Saale, Germany
Abitur (A-level, Top of the Year)

Research Experience

10/2002 - 01/2006 Max-Planck-Institute of Molecular Plant Physiology, Potsdam, Germany (Supervisor Dr. Ute Krämer)
Ph.D. thesis: "Functional Characterisation of the P-type ATPase HMA3 of *Arabidopsis halleri* (L.) O'KANE and AL'SHEHBAZ and *Arabidopsis thaliana* (L.) HEYNH."
 01/2002 - 09/2002 Centro de Investigación Científica de Yucatán, Unidad de Biotecnología, Mérida, México (Supervisor Dr. Jorge M. Santamaría Fernández)
Research Assistant: "Phytoremediation and Bioadsorption for the Sustainable Use of Water - Use of *Salvinia minima* BAKER for Phytoremediation of Lead and Arsenic"
 09/2001 - 01/2002 Colegio de Postgraduado - Campus San Luis Potosí, Salinas de Hidalgo, México (Supervisor Dr. Adrián R. Quero Carillo)
Research Assistant: "*Bouteloua curtipendula* MICHX. TORR. - Plant Breeding Project; Establishing and Characterisation of the Ecotype Collection and Analysis of the Agamic Complex"
 03/2001 - 09/2001 Martin-Luther-University Halle-Wittenberg, Institute of Microbiology, Halle/ Saale, Germany (Supervisor Prof. Dietrich H. Nies)
Research student: Scholarship holder of the DFG-Graduate-College: "Adaptive Physiological and Biochemical Reactions Caused by Ecological Relevant Substances" (Continuation of research based on Diplom thesis project)
 05/2000 - 03/2001 Martin-Luther-University Halle-Wittenberg, Institute of Microbiology, Halle/ Saale, Germany (Supervisor Prof. Dietrich H. Nies)
Diplom thesis (Master of Science): "Investigation of Heavy Metal Resistance in *Ralstonia metallidurans* CH34 by Two-Dimensional Electrophoresis and Reporter Gene Fusions"

Publications

Articles

Hoffmann, T. and U. Krämer (2007). Studies on the promoter of the P-type IB ATPase HMA3 of *Arabidopsis halleri* and *Arabidopsis thaliana*. in preparation.

Nies, D., G. Rehbein, T. Hoffmann, C. Baumann, and C. Grosse (2006). Paralogs of genes encoding metal resistance proteins in *Cupriavidus metallidurans* strain CH34. *Journal of Molecular Microbiology and Biotechnology* **11**, 82-93.

Hoffmann, T., C. Kutter, and J. M. Santamaría (2004). Capacity of *Salvinia minima* BAKER to tolerate and accumulate As and Pb. *Engineering in Life Sciences* **4**, 61-65.

Große, C., A. Anton, T. Hoffmann, S. Franke, G. Schleuder, and D. H. Nies (2004). Identification of a regulatory pathway that controls the heavy-metal resistance system Czc via promoter *czcNp* in *Ralstonia metallidurans*. *Archives of Microbiology* **182**, 109-118.

Legatzki, A., S. Franke, S. Lucke, T. Hoffmann, A. Anton, D. Neumann, and D. H. Nies (2003). First step towards a quantitative model describing Czc-mediated heavy metal resistance in *Ralstonia metallidurans*. *Biodegradation* **14**, 153-168.

Book chapter

Morales-Nieto, C. R., A. R. Quero-Carrillo, C. Kutter, T. Hoffmann, and L. Miranda-Jiménez (2006). *Bouteloua curtipendula* (MICHX.) TORR. genetic resources potential for arid rangelands recovering in México. submitted as chapter for the book: *Desertificación, retos y oportunidades*. in revision.

April 2, 2007